Phytyl Ester Synthases from *Arabidopsis thaliana* and *Solanum lycopersicum*

Dissertation

zur
Erlangung des Doktorgrades (Dr. rer. nat.)
der
Mathematisch-Naturwissenschaftlichen Fakultät
der
Rheinischen Friedrich-Wilhelms-Universität Bonn

vorgelegt von

Regina Daniela Wehler
aus Wuppertal

Bonn, Dezember 2017

Angefertigt mit Genehmigung der Mathematisch-Naturwissenschaftlichen Fakultät
der Rheinischen Friedrich-Wilhelms-Universität Bonn

1. Gutachter: Prof. Dr. Peter Dörmann
2. Gutachter: Prof. Dr. Frank Hochholdinger
Tag der Promotion: 15.03.2018
Erscheinungsjahr: 2018

Contents

List of Figures

List of Tables

Abbreviations

ACP	acyl carrier protein
APS	ammonium persulfate
AS	acetosyringone
BSA	bovine serum albumine
BSTFA	bis(trimethylsilyl)trifluoroacetamide
cDNA	complementary DNA
CID	collision induced dissociation
CoA	coenzyme A
CTAB	cetyltrimethylammonium bromide
ddH_2O	double deionized water
DEPC	diethyl pyrocarbonate
DGDG	digalactosyldiacylglycerol
DMAPP	dimethylallyl pyrophosphate
DMSO	dimethyl sulfoxide
dNTP	deoxyribonucleotide triphosphates
DOXP	1-deoxy-D-xylulose 5-phosphate
EDTA	ethylenediaminetetraacetic acid
ELT	esterases/lipases/thioesterases
ER	endoplasmic reticulum
EtBr	ethidium bromide
FAFEs	fatty acid farnesyl esters
FAGGEs	fatty acid geranylgeranyl esters
FAMEs	fatty acid methyl esters
FAPEs	fatty acid phytyl esters
FAR	fatty acyl-CoA reductase
FAXEs	fatty acid xanthophyll esters
FAXdEs	fatty acid xanthophyll diesters
FAXmEs	fatty acid xanthophyll monoesters
FAXtEs	fatty acid xanthophyll triesters
FCC	fluorescent chlorophyll catabolite
FID	flame ionisation detector
FPP	farnesyl pyrophosphate

GC	gas chromatography
GGPP	geranylgeranyl pyrophosphate
GGR	geranylgeranyl reductase
GPP	geranyl pyrophosphate
GUS	β-glucuronidase
HEPES	4-(2-hydroxyethyl)-1-piperazineethanesulfonic acid
HMG-CoA	3-hydroxy-3- methyl-glutaryl-CoA
HPLC	high-pressure liquid chromatography
HRP	horseradish peroxidase
IPP	isopentenyl pyrophosphate
IPTG	isopropyl β-D-1-thiogalactopyranoside
I.S.	internal standard
LB	lysogeny broth
MEcPP	2-C-methyl-D-erythritol 2,4-cyclodiphosphate
MEP	methylerythritol phosphate
MES	2-(N-morpholino)ethanesulfonic acid
MGDG	monogalactosyldiacylglycerol
MOI	multiplicity of infection
MOPS	3-(N-morpholino)propanesulfonic acid
MS	mass spectrometry
MSTFA	N-methyl-N-(trimethylsilyl)trifluoroacetamide
MT-J	Micro-Tom-J
m/z	mass-to-charge ratio
NCC	nonfluorescent chlorophyll catabolite
NIST	National Institute of Standards and Technology
NMR	nuclear magnetic resonance spectroscopy
NTC	no template control
OD	optical density
oePES2	PES2 overexpression
P1	passage one
PAGE	polyacrylamide gel electrophoresis
PAO	pheophorbide a oxygenase
PC	phosphatidylcholine
PCR	polymerase chain reaction
PE	phosphatidylethanolamine
PES	phytyl ester synthase
PG	phosphatidylgylcerol
PI	phosphatidylinositol
PPH	pheophytinase
PS	phosphatidylserine
qPCR	quantitative PCR

Q-TOF	quadrupole time-of-flight
RNA	ribonucleic acid
rpm	round per minute
RT	room temperature
RT-PCR	reverse transcription PCR
SD	standard deviation
SDS	sodium dodecyl sulfate
SEs	sterol esters
SPE	solid phase extraction
SQDG	sulfoquinovosyl diacylglycerol
TAE	Tris-acetate-EDTA
TAGs	triacylglycerols
T-DNA	transfer DNA
TEMED	tetramethylethylenediamine
TFA	trifluoroacetic acid
TLC	thin layer chromatography
TMS	trimethylsilyl
Tris	tris(hydroxymethyl)aminomethane
UV	ultra violet
v/v	volume per volume
VLC	very-long-chain
VLC-FAs	very-long-chain fatty acids
WDEs	wax diesters
WEs	wax esters
w/v	weight per volume
X-gal	5-bromo-4-chloro-3-indolyl-β-D-galactopyranoside

Saturated aliphatic acyl chains are abbreviated as CX where X is the number of carbon atoms. Unsaturated aliphatic acyl chains are abbreviated as CX:Y where X is the number of carbon atoms and Y is the number of double bounds.

1 Introduction

The most important biochemical process on earth is photosynthesis, the conversion of light energy into chemical energy. Photosynthesis is conducted by most plants, algae and cyanobacteria, which defines them as photoautotrophic organisms. Oxygenic photoautotrophs use light energy to fix inorganic carbon such as carbon dioxide into organic compounds such as carbohydrates under release of oxygen (Katz and Norris, 1973). In plants and algae, photosynthesis takes place in the chloroplasts. In cyanobacteria the reactions are located to the thylakoid membranes. Chloroplasts are cell organelles that, according to the endosymbiotic theory, are derived from phagocytised cyanobacteria which were not degraded after uptake. Plant chloroplasts contain three membrane systems. The inner and outer envelope membrane and the thylakoid membrane system in the stroma of the chloroplast. All components that are required for photosynthesis are embedded in the thylakoid membranes. The first step of photosynthesis is the absorbance of light energy. To this end, sun light energy is collected in the light-harvesting complexes, which consist of several transmembrane proteins and associated pigments. The associated pigments are mainly chlorophylls, xanthophylls and carotenes. Carotenoids primarily prevent photo-oxidative damage of the chlorophyll, while the chlorophyll molecules absorb the light energy. In addition, the stroma of the chloroplast contains starch granules and plastoglobules (Steinmüller and Tevini, 1985; Tevini and Steinmüller, 1985). Plastoglobules are lipoprotein particles that are separated from the stroma by a membrane lipid monolayer, which is continuous to the stroma facing monolayer of the thylakoid membranes (Austin et al., 2006). By this connection, plastoglobules provide a highly dynamic storage function for proteins and lipids of the thylakoid membranes, serving as lipid storage subcompartments (Austin et al., 2006). The lipids in plastoglobules of chloroplasts include isoprenoids such as prenylquinones (e.g. tocopherol) and neutral lipids such as triacylglycerols (TAGs), fatty acid phytyl esters (FAPEs) and fatty acid xanthophyll esters (FAXEs) (Steinmüller and Tevini, 1985; Tevini and Steinmüller, 1985; Vidi et al., 2006; Gaude et al., 2007). Here, the lipid composition depends on the condition and developmental state. Plastoglobules of green leaves mainly contain TAGs and tocopherols. In contrast, the amount of TAGs declines while FAPEs and FAXEs accumulate in plastoglobules of senescent leaves (Tevini and Steinmüller, 1985; Gaude et al., 2007). Furthermore, plastoglobules of chromoplasts are enriched in free xanthophylls and FAXEs (Lich-

tenthaler, 1970). The proteome of plastoglobules comprises a set of 30 core proteins. Members of this protein group, whose functions have been identified, mainly act on the rearrangement of thylakoid membrane lipids and fatty acids and on the regulation of isoprenoid metabolism. Beyond the core set of proteins, additional proteins are recruited depending on environmental and developmental conditions (van Wijk and Kessler, 2017). The structure, size, and number of plastoglobules are highly dynamic and vary between tissues, during plastid biogenesis or in response to oxidative or chlorotic stress (Austin et al., 2006; van Wijk and Kessler, 2017).

1.1 Isoprenoid Lipids in Plants

1.1.1 Synthesis of Isoprenoid Building Blocks

Prenylquinones (phylloquinone, plastoquinone and tocochromanols), carotenoids and phytol are isoprenoid lipids. All isoprenoids have the same skeleton of one or more C5 isoprene subunits, derived from isopentenyl pyrophosphate (IPP) and its isomer dimethylallyl pyrophosphate (DMAPP) (Wright, 1961). Plants have two different metabolic pathways to synthesise DMAPP and IPP (Lichtenthaler et al., 1997a). The mevalonate pathway is present in all eukaryotes, archaea and some bacteria and is located to the cytosol in plants (Lichtenthaler et al., 1997a). First, two acetyl-CoA molecules are condensed to acetoacetyl-CoA. An additional condensation step with acetyl-CoA leads to the formation of 3-hydroxy-3- methyl-glutaryl-CoA (HMG-CoA) (Ferguson and Rudney, 1959). HMG-CoA is reduced under consumption of NADPH to mevalonate (Durr and Rudney, 1960). Mevalonate is phosphorylated twice by two different kinases under consumption of ATP to yield mevalonate pyrophosphate (Tchen, 1958; Beytia et al., 1970). Decarboxylation of mevalonate pyrophosphate results in IPP (Bloch et al., 1959). IPP can be converted into its isomer DMAPP by the isopentenyl pyrophosphate isomerase (Agranoff et al., 1959).

Plants, most bacteria and some protozoa possess an alternative pathway to synthesise IPP, the so-called methylerythritol phosphate (MEP) or non-mevalonate pathway (Rohmer et al., 1993; Eisenreich et al., 1998). The MEP pathway is localised to the plastids in plants (Lichtenthaler et al., 1997a,b; Schwender et al., 1997). In contrast to the mevalonate pathway, the first step of the MEP pathway is the synthesis of 1-deoxy-D-xylulose 5-phosphate (DOXP) from pyruvate and glyceraldehyde 3-phosphate (Rohmer et al., 1996; Lichtenthaler et al., 1997a). The reduction of DOXP results in the formation of MEP using NADPH as a reducing agent (Takahashi et al., 1998). CDP-methylerythritol is synthesised by reaction of MEP with cytidine triphosphate under the release of diphosphate (Rohdich et al., 1999, 2000). CDP-ME is phosphorylated to CDP-MEP under consumption of ATP (Luttgen et al., 2000; Kuzuyama et al., 2000). In a cyclisation reaction, CDP is released and 2-C-methyl-D-erythritol 2,4-cyclodiphosphate (MEcPP) is formed

(Herz et al., 2000; Takagi et al., 2000). In the end, IPP and DMAPP are generated by 4-hydroxy-3-methylbut-2-enyl diphosphate synthase and reductase using ferredoxin and NADPH, respectively (Hecht et al., 2001; Rohdich et al., 2002). The reductase synthesises both, IPP and DMAPP, in a 5:1 ratio (Rohdich et al., 2002), making an isomerase to produce DMAPP unnecessary. This finding is in accordance with earlier observations which showed that the gene in *E. coli* encoding an isopentenyl diphosphate isomerase is not essential (Hahn et al., 1999). In addition, many bacteria that exclusively use the MEP pathway for isoprenoid synthesis, are devoid of genes encoding an isopentenyl diphosphate isomerase (Rohdich et al., 2001; Cunningham et al., 2000).

1.1.2 Assembly of Isoprenoids

Isoprenoids are a large and diverse group of molecules comprising over 20.000 compounds (Chappell, 1995). The structure varies from simple acyclic molecules to complex ring structures (Chappell, 1995). However, they all have the same skeleton consisting of isoprene units and are derived from the same biosynthetic origin (Gray, 1988). The condensation of two isoprene units, IPP or DMAPP (C5, hemiterpenes), generates geranyl pyrophosphate (GPP), which can be derivatised to linear or cyclic products called monoterpenes (C10) (Figure 1.1). GPP also serves as the substrate for further condensation reactions. Farnesyl diphosphate (FPP) is synthesised by the addition of a third isoprene unit to GPP. Similar to GPP, FPP can also be converted into linear or cyclic products establishing the group of sesquiterpenes (C15). In a third condensation step, geranylgeranyl pyrophosphate (GGPP) is formed by the addition of a C5 unit to FPP. Diterpenes (C20) are linear or cyclic derivates of GGPP. Prominent diterpenes are tocopherol, phylloquinones or phytol. All condensation steps occur in a head-to-tail manner and are catalysed by isoprenyl-PP synthases (Chen et al., 1994; Zhu et al., 1997; Wang and Ohnuma, 2000; Schmidt and Gershenzon, 2007).

In plants, isoprenoids can be classified as primary and secondary metabolites (Chappell, 1995). Examples for primary isoprenoids are sterols, carotenoids, plant hormones (ABA), and prenylquinones (tocopherol, phylloquinone). They play important roles in sustaining the membrane bilayer integrity, in photoprotection, in plant growth, as electron carriers or as antioxidants. On the other hand, some monoterpenes, sesquiterpenes, and diterpenes are referred to as secondary metabolites because they are non-essential for the normal plant development. FPP and GGPP are the main intermediates for the synthesis of cytosolic and plastidial isoprenoids in plants (Bouvier et al., 2005). The enzyme geranylgeranyl reductase (GGR) is responsible for the reduction of GGPP to phytol-PP but can act on the geranylgeranyl moiety of geranylgeranylated chlorophyll as well (Addlesee et al., 1996; Keller et al., 1998; Addlesee and Hunter, 1999). In plastids, GGPP might be the precursor for the phytol side-chain of prenyllipids such as chlorophyll and phylloquinone. However, for tocopherol it had been demonstrated that free phytol is activated twice by two

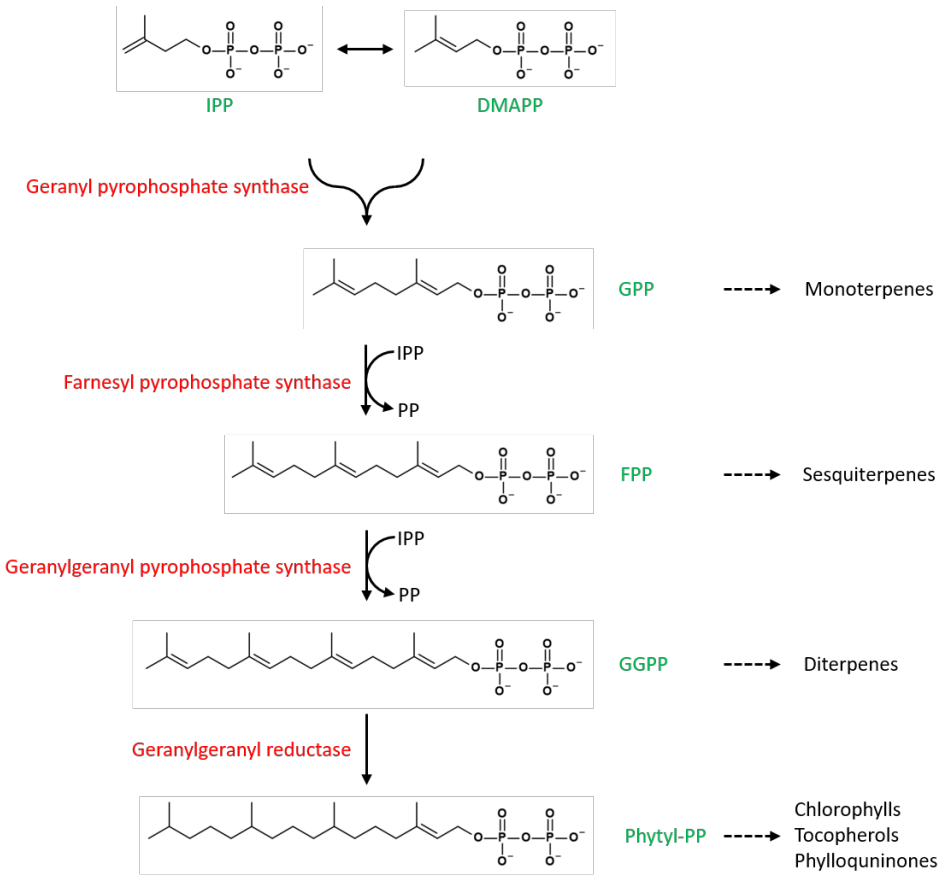

Figure 1.1 – Synthesis of isoprenoids from the subunits isopentenyl pyrophosphate (IPP) and dimethylallyl pyrophosphate (DMAPP). Subsequent condensation steps in a head-to-tail manner lead to the formation of geranyl pyrophosphate (GPP), farnesyl pyrophosphate (FPP) and geranylgeranyl pyrophosphate (GGPP). GGPP is reduced to phytyl pyrophosphate (phytyl-PP) which is incorporated into chlorophylls, tocopherols and phylloquinone as a side chain.

different kinases before it is incorporated into tocopherol (Valentin et al., 2006; vom Dorp et al., 2015).

1.2 Leaf Senescence

The senescence of plant leaves occurs either naturally during plant development or induced by environmental conditions, the latter being reversible until a certain threshold of degradation is reached (Stoddart and Thomas, 1982; Buchanan-Wollaston, 1997). It represents the coordinated disintegration of plant cells in order to remobilise nutrients from leaves to other parts of the plant, which is important for adaptation, survival, and reproduction of the plant (Thomas, 2013). The degradation proceeds in a fixed pattern on structural, metabolic and expression levels (Schippers et al., 2015). On a structural level, Dodge (1970) observed that the chloroplasts are the first organelles that get dismantled upon senescence but are also the last organelles that can be observed in

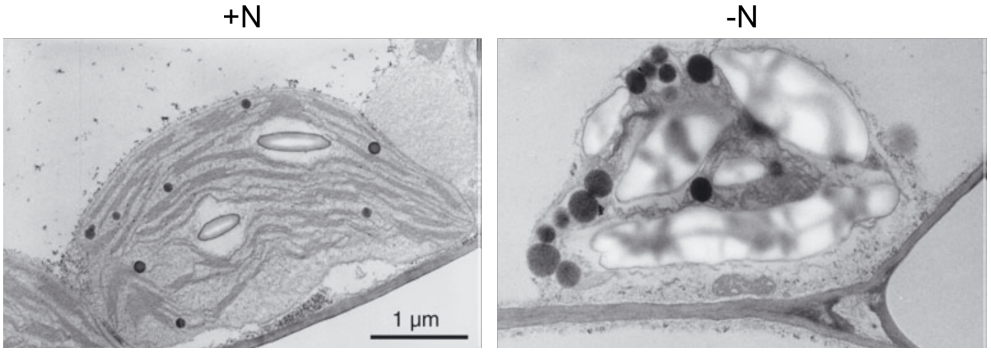

Figure 1.2 – Ultrastructural changes in senescent chloroplasts under nitrogen deficiency. Chloroplasts of green leaves (+N) are packed with thylakoid membranes and contain few starch granules and plastoglobules (black dots). The structure of senescent chloroplasts (-N) show severe changes. The thylakoid membranes are completely disintegrated, starch accumulates in huge crystals and the plastoglobules increase in size and number. Micrographs taken from Gaude et al. (2007).

a senescent plant cell. The chloroplasts of green leaves are packed with thylakoid membranes and contain few starch granules and plastoglobules (Figure 1.2, +N) (Steinmüller and Tevini, 1985; Tevini and Steinmüller, 1985). During leaf senescence, e.g. caused by nitrogen deprivation, chloroplasts undergo severe changes that result in a completely different ultrastructure (Figure 1.2, -N). The shape of the chloroplasts changes, the thylakoid membranes get completely disintegrated, starch crystals accumulates and the plastoglobules increase in size and number (Dodge, 1970; Kaup et al., 2002; Gaude et al., 2007). The correlation of thylakoid degradation and the increase in plastoglobule number and size led to the conclusion that lipids are transferred from the thylakoid membranes to the plastoglobules (Lichtenthaler, 1968; Gepstein, 1988). On a metabolic level, the carbon fixation of photosynthesis is replaced by the catabolism of chlorophyll, proteins, lipids and RNA (Dhindsa et al., 1981; Gan and Amasino, 1997; Lim et al., 2007). Senescence induces changes in gene expression. The majority of highly expressed genes in green leaves, which transcripts are mainly involved in photosynthesis, are down-regulated under senescence (Gepstein, 1988). On the other side, the expression of senescence-associated genes increases in the progress of senescence (Gan and Amasino, 1997; Gepstein et al., 2003). Prominent members of this gene group are proteinases, lipases, nucleases and chlorophyllases (Gepstein et al., 2003).

The drastic structural changes during senescence, especially the disintegration of thylakoid membranes and the accumulation of plastoglobules in the chloroplast, is accompanied by alterations in the chloroplast membrane composition (Ferguson and Simon, 1973; Gepstein, 1988). The amount of total lipids and polar lipids such as monogalactosyldiacylglycerol (MGDG), digalactosyldiacylglycerol (DGDG), phosphatidylgylcerol (PG), phosphatidylethanolamine (PE) and phosphatidylcholine (PC) decreases in senescent tissues (Dalgarn et al., 1979; Koiwai et al., 1981). Simultaneously, an accumulation of neutral lipids, such as free fatty acids, prenyl quinones, toco-

pherol, FAXEs and FAPEs can be observed (Harwood et al., 1982; Tevini and Steinmüller, 1985).

1.3 Breakdown of Chlorophyll

Chlorophyll is the most abundant pigment in the biosphere (Matile et al., 1996). Because of the disappearance of its green colour, the degradation of chlorophyll is the most perceived sign of senescence. As the thylakoid membranes are dismantled during senescence, chlorophyll is degraded concomitantly (Grob and Csupor, 1967). Therefore, the most prominent situation, under which chlorophyll is degraded, is the leaf senescence occurring in autumn. Nevertheless, chlorophyll is also degraded in response to biotic and abiotic stresse, during fruit ripening (Hendry et al., 1987; Hörtensteiner and Kräutler, 2011) and during chlorophyll turnover under normal conditions (Beisel et al., 2010). Analysis of pigments in green and ripe bananas revealed that the total amount of xanthophylls and carotene, which give rise to the yellow colour of ripe fruits, is the same in both green and ripe fruits. However, the chlorophyll which masks the yellow colour in green banana, is degraded until it is completely absent from the ripe fruit (Loesecke, 1929; Gross and Flügel, 1982). In the course of leaf senescence, non-green pigments such as anthocyanins and carotenoids become visible since the degradation of chlorophyll occurs much faster than the degradation of other pigments (Sanger, 1971). Even under normal growth conditions there is a continuous turnover of chlorophyll synthesis and degradation in photosynthetically active leaves (Beisel et al., 2010). During seed maturation, the degradation of chlorophyll at late stages has a direct impact on the seed quality with the amount of retained chlorophyll being inversely related to the germination rate (Jalink et al., 1998).

A well known enzyme involved in chlorophyll degradation is PAO (Figure 1.3), which is conserved in higher plants and is active during leaf senescence and fruit ripening (Hörtensteiner and Kräutler, 2011). Breakdown products of chlorophyll are categorised as fluorescent and non-fluorescent chlorophyll catabolites (FCC and NCC, respectively). The PAO pathway can be divided into two parts. The first part results in the formation of FCCs and is localised to the plastids. The second part takes place in the cytosol and vacuole and leads to the formation of NCCs (Hörtensteiner, 2013). Most FCCs and NCCs are derived from chlorophyll a. Therefore, a two-step reduction of chlorophyll b to chlorophyll a is required prior to degradation. These reactions are catalysed by chlorophyll b reductase and 7-hydroxymethyl chlorophyll a reductase (Horie et al., 2009; Meguro et al., 2011). The first reaction was shown to be essential for the chlorophyll degradation in senescent leaves and during seed maturation (Sato et al., 2009; Nakajima et al., 2012). Subsequently, the Mg^{2+} cation as well as the phytol side chain are removed from the chlorophyll a molecule resulting in the formation of pheophorbide a (Langmeier et al., 1993; Vicentini et al.,

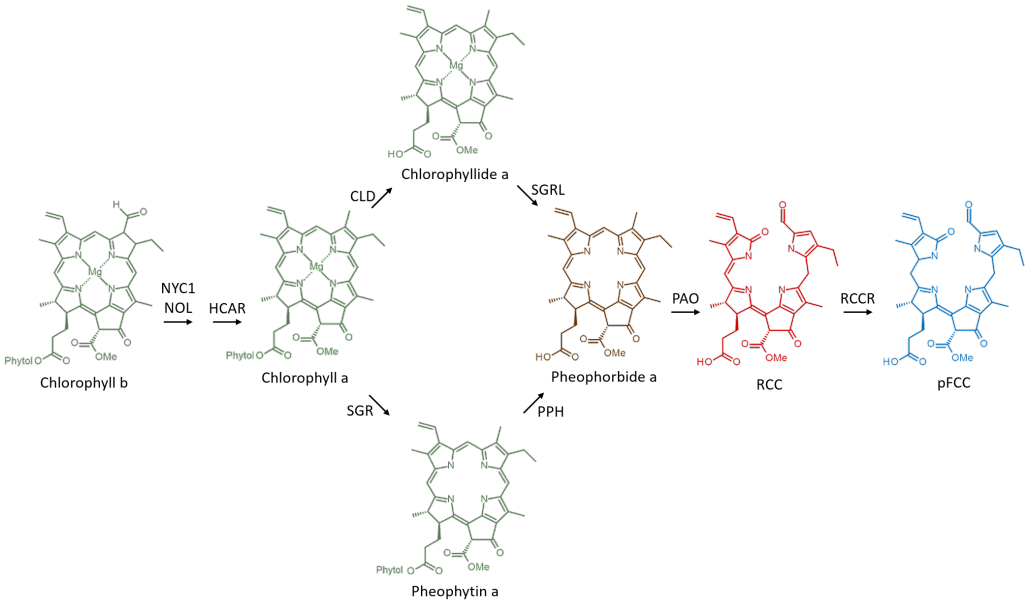

Figure 1.3 – Chlorophyll degradation via the PAO pathway. Chlorophyll b is converted to chlorophyll a by two reducing steps. Subsequently, the central Mg^{2+} cation and the phytol side chain are removed, yielding in pheophorbide a. The opening of the tetrapyrrole ring results in the linear red chlorophyll catabolite (RCC). A primary fluorescent chlorophyll catabolite (pFCC) is formed by reduction. pFCCs are further degraded to non-fluorescent chlorophyll catabolites in several steps. *NYC1* non-yellow colouring 1 (chlorophyll b reductase), *NOL* NYC1-like (chlorophyll b reductase), *HCAR* 7-hydroxymethyl chlorophyll a reductase, *CLD* chlorophyll dephytylase, *SGR* STAY-GREEN (chlorophyll a Mg-dechelatase), *SGRL* STAY-GREEN-LIKE (chlorophyllide a Mg-dechelatase), *PPH* pheophytinase, *PAO* pheophorbide a oxygenase, *RCCR* red chlorophyll catabolite reductase. Schematic modified from Hörtensteiner (2013) and Lin et al. (2016).

1995). For these reactions, two intermediates are identified: chlorophyllide a that lacks the phytol chain but contains a Mg^{2+} cation and pheophytin a that is devoid of Mg^{2+} but still contains a phytol moiety. Thus, for a long time it remained unclear, in which order the reactions of dephytylation and Mg-dechelation take place. Recently, a Mg-dechelatase (SGR) was identified in *A. thaliana* that removes the Mg^{2+} from chlorophyll a, but not from chlorophyll b or chlorophyllide a indicating that Mg-dechelation precedes dephytylation (Shimoda et al., 2016). In accordance, a pheophytinase (PPH) from *A. thaliana* has been characterised that is induced under senescence and that is specific for the dephytylation of pheophytin at least in leaves (Schelbert et al., 2009). The tomato PPH is also responsible for dephytylation of pheophytin in senescent leaves but is not active in chlorophyll degradation during fruit ripening indicating the involvement of other hydrolases (Guyer et al., 2014). In addition, the *A. thaliana* PPH is not essential for chlorophyll degradation during seed development (Zhang et al., 2014). Recently, another chlorophyll dephytylase from *A. thaliana* has been identified that is expressed under non-stress conditions, acts on chlorophyll a and is therefore involved in the steady state turnover of chlorophyll (Lin et al., 2016).

The next step in the PAO pathway is the opening of the chlorin ring of pheophorbide a to

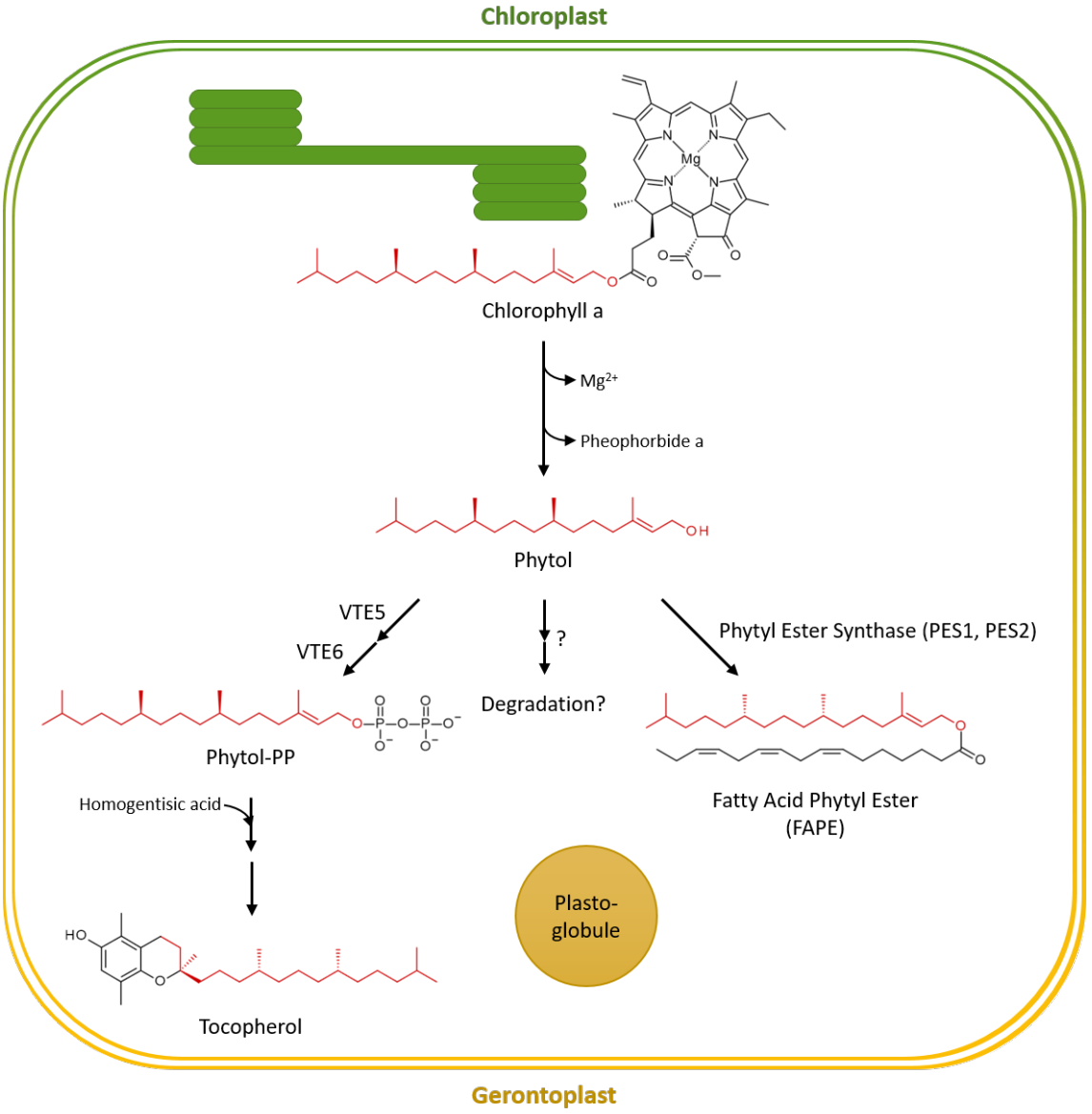

Figure 1.4 – In *A. thaliana* chlorophyll is degraded by removal of the central Mg cation and cleavage of the headgroup from the side chain resulting in the release of phytol and pheophorbide. After two successive phosphorylation steps, which are catalysed by the kinases VTE5 and VTE6, phytol pyrophosphate (phytol-PP) is incorporated into tocopherol. Furthermore, phytol is esterified to fatty acids which yields in fatty acid phytyl esters (FAPE), catalysed by phytyl ester synthases (PES). Tocopherol and FAPEs are stored in the plastoglobules of gerontoplasts. A degradation pathway for phytol in plants is currently presumed but detailed mechanisms remain elusive.

yield red chlorophyll catabolite. This reaction is catalysed by the central enzyme of this pathway, pheophorbide a oxygenase (PAO) (Hörtensteiner et al., 1998; Pružinská et al., 2003; Tanaka et al., 2003). The red chlorophyll catabolite is the first intermediate that lacks the typical green colour due to its linear structure. Red chlorophyll catabolite reductase is required for the formation of primary fluorescent chlorophyll catabolite (Wuthrich et al., 2000). In subsequent reactions, chlorophyll is finally degraded to colourless linear tetrapyrroles (Hörtensteiner and Kräutler, 2011; Hörtensteiner, 2013).

1.4 Processing of Phytol Derived from Chlorophyll Degradation

While the chlorophyllide degradation pathway has been elucidated in detail, much less is known about the fate of the phytol side-chain. Hendry et al. (1987) estimated that each year one billion tons of chlorophyll are degraded, which leads to a massive release of chlorophyll breakdown products including free phytol (Grob and Csupor, 1967). Phytol is cleaved off from the chlorophyll molecule by the action of PPH or chlorophyll dephytylase or other chlorophyll hydrolases (Schelbert et al., 2009; Lin et al., 2016). Although phytol is released from the chlorophyll during senescence, the increase in free phytol is rather low and the amount of total, i.e. bound and free, phytol only slightly decreases (Peisker et al., 1989). These observations indicate that only a small amount of phytol is degraded and that the bulk of phytol is subsequently processed (Figure 1.4). In plants, feeding of radioactively labelled phytol demonstrated the incorporation of phytol into chlorophyll, tocopherol and FAPEs (Ischebeck et al., 2006). In animals, phytol can be degraded by α- and β-oxidation (Wanders et al., 2003).

1.4.1 Incorporation of Phytol into Tocopherol

Tocopherols are a group of isoprenoid lipids that provide protection against oxidative stress by stabilising lipids which improves seed longevity and germination (Kanwischer et al., 2005; Sattler et al., 2004). An accumulation of tocopherols can be observed in response to abiotic stresses (Rise et al., 1989; Wildi and Lütz, 1996; Streb et al., 1998; Bartoli et al., 1999; Munné-Bosch and Alegre, 2000). Tocopherols contain a chromane ring and a hydrophobic phytol side chain. Furuya et al. (1987) demonstrated by incubation of safflower cell cultures with phytol that phytol is used for tocopherol biosynthesis. The condensation of homogentisic acid and phytol yields 2-methyl-6-phytyl-1,4-benzoquinol, the first prenylquinol intermediate in tocopherol biosynthesis (Soll et al., 1980; Marshall et al., 1985). This reaction is catalysed by a membrane-bound homogentisate phytyltransferase that utilises phytol pyrophosphate as a substrate (Collakova and DellaPenna, 2001). Phytol-PP could be derived from GGPP via reduction by GGR, but the flux

through this pathway in leaves is presumably very low. Hence, free phytol needs to be activated by phosphorylation prior to entering the tocopherol biosynthesis pathway (Soll et al., 1980; Collakova and DellaPenna, 2001). Phytol is successively phosphorylated by two different kinases (VTE5 and VTE6) and these reactions are localised to the chloroplast envelope membrane as well (Ischebeck et al., 2006; Valentin et al., 2006; vom Dorp et al., 2015).

In 1989, it was already shown that under senescence, tocopherol levels increase while simultaneously chlorophyll is degraded which suggests a connection of these two processes (Peisker et al., 1989; Rise et al., 1989). The *A. thaliana vte5-1* mutant is defective in tocopherol biosynthesis and exhibits reduced leaf and seed tocopherol contents and an accumulation of free phytol (Valentin et al., 2006). This indicates that phytol which is derived from chlorophyll degradation during seed development is used for tocopherol synthesis in seeds (Goffman et al., 1999; Valentin et al., 2006). During senescence, phytol released from chlorophyll is phosphorylated to phytol phosphate and phytol pyrophosphate and finally incorporated into tocopherol which is then stored in the plastoglobules (Ischebeck et al., 2006).

1.4.2 Esterification of Phytol to Fatty Acids

The first evidence that phytol does not only exist in its free form or bound in the chlorophyll molecule but can also be esterified to fatty acids to form fatty acid phytyl esters (FAPEs) was presented by Grob and Csupor (1967) in senescent leaves of *Acer platanoides*. The connection between chlorophyll degradation, release of phytol and FAPE accumulation in form of transesterification during senescence was concluded by Csupor (1970). The *A. thaliana pao1* mutant is impaired in chlorophyll degradation which leads to a stay-green phenotype (Pružinská et al., 2003). During leaf senescence, this mutant does not accumulate FAPEs which proves that the release of phytol during chlorophyll degradation is essential for FAPE synthesis (Lippold et al., 2012).

FAPEs are detected in dinoflagellates, mosses, bacteria and higher plants (Cranwell et al., 1985, 1990; Buchanan et al., 1996; Rontani et al., 1999; Anderson et al., 1984; Grob and Csupor, 1967; Gellerman et al., 1975; Peisker et al., 1989; Pereira et al., 2002). The *A. thaliana chilling sensitive mutant 1* accumulates FAPEs after exposure to chilling temperatures (Patterson et al., 1993) and in *A. thaliana* wild type FAPE accumulation was observed upon nitrogen deprivation (Gaude et al., 2007), which demonstrates that FAPE synthesis is not only part of the natural leaf senescence but can also occur after stress induction. The major FAPE identified in *A. thaliana* under senescence and nitrogen deprivation is 16:3-phytol (Ischebeck et al., 2006; Gaude et al., 2007). The *A. thaliana act1* mutant is devoid of 16:3 (Kunst et al., 1988) and in accordance to that also contains no 16:3-phytol (Gaude et al., 2007). Interestingly, the missing 16:3-phytol is not replaced by other FAPE

species but the mutation rather leads to a decrease in total FAPE amount (Gaude et al., 2007). This fact demonstrates a high specificity for 16:3-phytol in *A. thaliana* leaves. During the ripening of *A. thaliana* seeds, chlorophyll is completely degraded and concomitantly, FAPEs accumulate (Kanwischer, 2007). The fatty acid distribution of seed FAPEs differs from that of leaves. While FAPEs in leaves contain mainly 16:3, seed FAPEs contain mainly 18:3 and 18:2 and to a lower extent 18:1, 16:3, 16:1 and 16:0 (vom Dorp, 2015).

A. thaliana is a "16:3-plant" which means that it contains high amounts of 16:3 in contrast to "18:3-plants" that lost the ability to produce 16:3 and have therefore 18:3 as the only triunsaturated fatty acid. MGDG is the highest abundant galactolipid in *A. thaliana* and contains the largest proportion of 16:3. Therefore it is reasonable to assume that the fatty acid for 16:3-phytol is derived from MGDG degradation (Ischebeck et al., 2006; Gaude et al., 2007). However, currently there is no *in vitro* evidence available which supports this hypothesis. It was suggested, that FAPEs represent a transient pool for breakdown products of chlorophyll and galactolipids (Gaude et al., 2007). The hypothesis was confirmed by growing plants under nitrogen deprivation and reversing the senescence by transferring the plants back to medium that contains nitrogen. FAPE level increases under nitrogen deficiency and decreases again after returning to full nutrition (Lippold et al., 2012). During chlorotic stress, thylakoid membranes are disintegrated, chlorophyll is degraded, FAPEs accumulate in plastoglobules and as soon as the stress stopped, all processes were inverted (Lippold et al., 2012). This highly dynamic process needs to be tightly regulated (Lippold et al., 2012).

The analysis of further 16:3- and 18:3-plants revealed that potato, a 16:3-plant, contains mainly 18:3-phytol in even higher amounts than compared to 18:3-plants like pumpkin, rice or *Lotus japonicus* with the latter being devoid of 18:3-phytol (Gaude et al., 2007). In addition, *A. thaliana* contains few saturated FAPE species with medium chain lengths from C10 to C16 which might be derived from the plastidial fatty acid *de novo* synthesis (Ischebeck et al., 2006). Because of the two possible sources for fatty acids, different pathways for FAPE synthesis were considered (Gaude et al., 2007). FAPEs in chloroplasts are localised to the plastoglobules as shown by chloroplast isolation followed by membrane fractionation by sucrose gradient centrifugation (Gaude et al., 2007).

The biosynthetic pathway for FAPE synthesis remained unknown for a long time considering that FAPEs are known since the late 1960s. The first indication that *A. thaliana* possesses enzymes to synthesize FAPEs arose by feeding seedlings with phytol (Ischebeck et al., 2006). In addition, the incubation of protein extracts from *A. thaliana* leaves with phytol and acyl-CoA resulted in the production of FAPEs (Ischebeck et al., 2006). Later, two genes from *A. thaliana* were identified that show sequence similarity to wax ester synthases from the *Acinetobacter*- and jojoba-type and

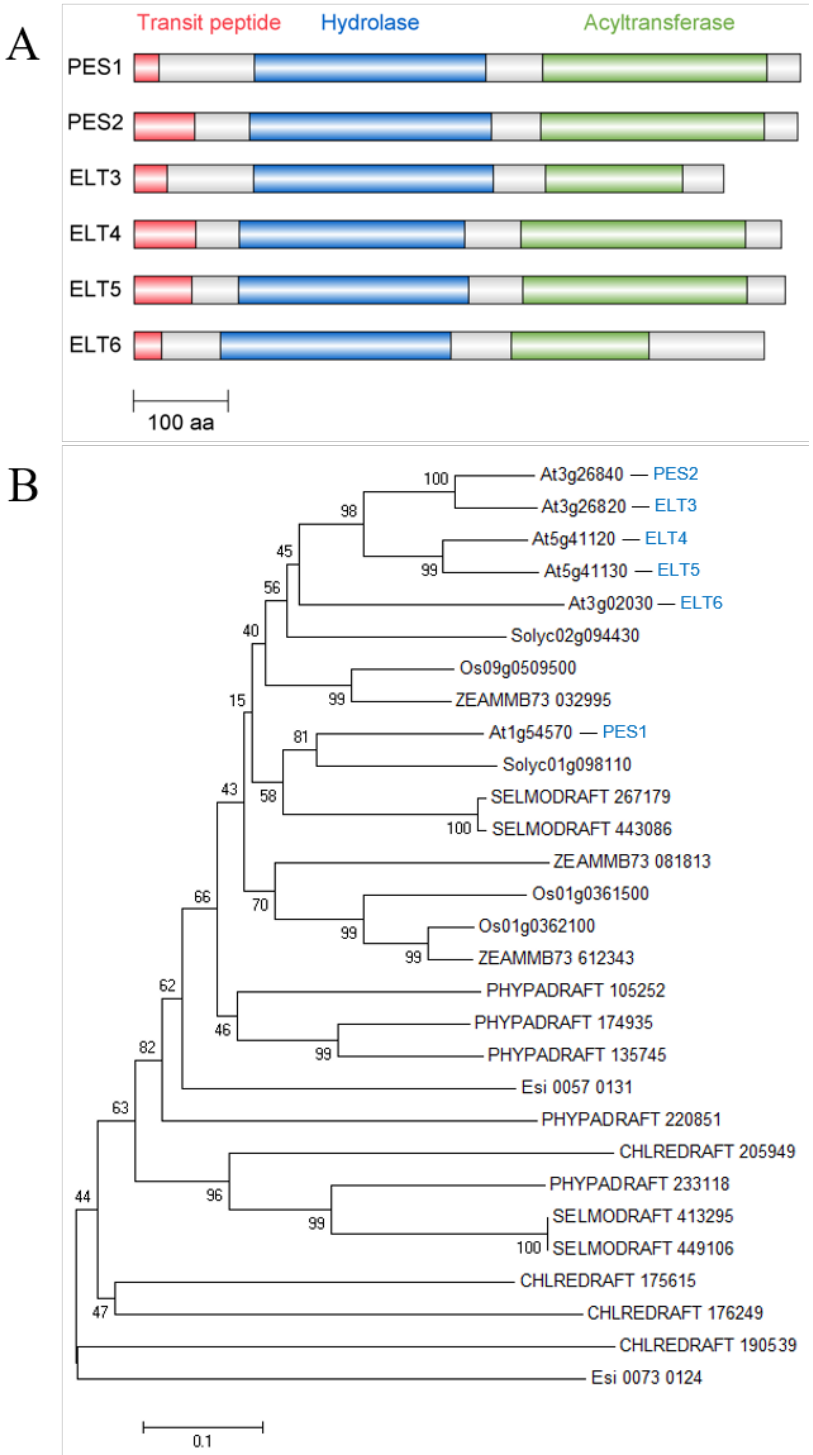

Figure 1.5 – A - Bioinformatic online tools were used to predict functional domains in the sequences of *A. thaliana* ELT proteins. For all members of the ELT family, putative acyltransferase and hydrolase domains were predicted by Pfam 29.0 (Finn et al., 2016) and transit peptides were predicted by ChloroP 1.1 for chloroplast localisation (Emanuelsson et al., 1999). Structures were visualised with IBS 1.0 (Liu et al., 2015). B - Unrooted phylogenetic tree generated by the Neighbour-joining method based on protein sequences from *A. thaliana* (At), *Solanum lycopersicum* (Solyc), *Zea mays* (ZEAM), *Selaginella moellendorffi* (SELMODRAFT), *Oryza sativa* (Os), *Physcomitrella patens* (PHYDRADRAFT), *Ectocarpus siliculosus* (Esi) and *Chlamydomonas reinhardtii* (CHLREDRAFT) (MEGA 5.0). The support values were generated by bootstrapping with 1000 replicates. The horizontal dimension displays the amount of genetic change in amino acid substitutions per site. Phylogenetic tree modified from Lippold et al. (2012).

that are higher expressed during senescence: *Phytyl Ester Synthase 1* (*PES1*) and *Phytyl Ester Synthase 2* (*PES2*) (Lippold et al., 2012). Both PES proteins are localised to the chloroplasts. More particularly, they are found in the proteome of isolated plastoglobules (Vidi et al., 2006; Ytterberg et al., 2006). The disruption of the genes in the *pes1* and *pes2* mutant leads to a decreased FAPE content in green and senescent leaves revealing the phytyl ester synthase activity of both enzymes. The *pes1pes2* double mutant is devoid of 10:0-, 12:0-0, 14:0- and 16:3-phytol, but still contains 16:0-phytol and 18:3-phytol, which indicates the existence of additional phytyl ester synthases in *A. thaliana*. The *pes1pes2* mutant shows no growth retardation under control conditions compared to wild type, but under dark induced senescence the chlorophyll degradation and the thylakoid dismantling is delayed. Although chlorophyll degradation is delayed, *pes1pes2* plants still accumulate free phytol under control conditions and to a higher extent under nitrogen starvation.

The genome of *A. thaliana* contains four additional putative acyltransferases that show sequence similarities to esterases/lipases/thioesterases (ELT) and are therefore designated as *ELT3*, *ELT4*, *ELT5* and *ELT6* (Lippold et al., 2012). *ELT4* and *ELT5* show a high sequence similarity and are closely related to *PES2*, *ELT3* and *ELT6* (Figure 1.5-B). *PES/ELT* genes can only be found in chlorophyll containing, photosynthetic active organisms such as monocotyledons (*Oryza sativa*, *Zea mays*), dicotyledons (*Solanum lycopersicum*), lycophytes (*Selaginella moellendorffi*), mosses (*Physcomitrella patens*), brown algae (*Ectocarpus siliculosus*) and green algae (*Chlamydomonas reinhardtii*) (Lippold et al., 2012). All PES/ELT sequences contain two domains, i.e. a hydrolase and an acyltransferase domain (Figure 1.5-A). Thus, the PES/ELT proteins can putatively hydrolyse an ester linkage and transfer an acyl group to an alcohol acceptor (Lippold et al., 2012). Furthermore they are all predicted to be chloroplast localised. Similarly to PES1 and PES2, ELT4 is found in the proteome of plastoglobules (Lundquist et al., 2012). The expression of *PES1* and *PES2* is upregulated during senescence and nitrogen deprivation (Lippold et al., 2012). The expression of *ELT3* is 8-fold upregulated after pathogen infection of leaves with *Pseudomonas syringae* (Hung et al., 2014). A screening experiment was conducted to find lipases that are involved in the hydrolysis of fatty acids from galactolipids that are used for the synthesis of jasmonic acid after wounding. *ELT3* was a candidate gene but it is not involved in jasmonic acid biosynthesis (Ellinger et al., 2010). The expression and function of *ELT3*, *ELT4*, *ELT5* and *ELT6* are unknown, but taken together it is assumed that at least some of these four ELT enzymes might be involved in phytyl ester synthesis.

1.5 Wax Esters and Wax Diesters

Wax esters (WEs) are structurally similar to FAPEs and consist of fatty alcohols esterified to very-long-chain fatty acids (VLC-FAs). They are components of the plant cuticle. The cuticle is a hydrophobic layer that covers the surfaces of aerial plant organs. The major function of the cuticle is the sealing of tissues and organs to prevent non-stomatal water loss (Riederer and Schreiber, 2001). The cuticle consists of cutin which is embedded in and covered with cuticular waxes (Li-Beisson et al., 2013). Cutin is a polymer of hydroxylated fatty acids and their derivatives which are linked by ester bonds to glycerol backbones. Cuticular waxes consist of VLC-FAs and their derivatives. The synthesis of cuticular waxes starts in the endoplasmic reticulum (ER) of epidermal cells where fatty acids are imported from plastids and elongated to VLC-FAs (Li-Beisson et al., 2013). A fraction of these VLC-FAs ends up directly in the cuticular waxes while the rest is further modified to alkanes, aldehydes, primary and secondary alcohols, ketones and esters (Yeats and Rose, 2013). Primary alcohols are found in their free form in cuticular waxes but also esterified to VLC-FAs to form WEs. In *A. thaliana*, the esterification of primary alcohols to VLC-FAs is catalysed by the bifunctional enzyme WSD1 which shows wax synthase and diacylglycerol acyltransferase activities (WS/DGAT) (Li et al., 2008). After esterification, WEs are transported to the plasma membrane, exported out of the cell and finally end up in the cuticular waxes on the leaf surface (Li-Beisson et al., 2013). The WEs load and composition varies among species and also between different tissues of the same species (Li et al., 2008). WEs of *A. thaliana* comprise total chain lengths of C38 up to C52 (Lai et al., 2007). WEs are not only found in the cuticular wax but also e.g. in the seed oil of the jojoba plant *Simmondsia chinensis* where they serve as carbon and energy storage (Greene and Foster, 1933).

Another type of ester compounds that can be found in the cuticular waxes of some plant species are wax diesters (WDEs) which are composed of an alkanediol and two esterified fatty acids. One of the first reports of WDEs as components of the cuticular waxes goes back to the 1970s where Tulloch (1971) identified α, ω-alkanediol diesters in the leaf wax of wheat. In the following, WDEs were identified in further Poaceae species such as oat and rye (Tulloch, 1973; Tulloch and Hoffman, 1974). The alkanediol backbones of WDEs are also found in their free form as component of the cuticular waxes of *Pinus radiata* needles (Franich et al., 1979), leaves of different *Papaver* species (Jetter et al., 1996), *Osmunda regalis* fonds (Jetter and Riederer, 1999), *Myricaria germanica* leaves (Jetter, 2000), *Pisum sativum* leaves (Wen et al., 2006) and *A. thaliana* stems (Wen and Jetter, 2009). In addition, 1,ω-alkanediols are found in the seed coat polyester of *A. thaliana* seeds (Molina et al., 2006). However, no genes have yet been characterised that are involved in the the synthesis of alkanediols or WDEs.

1.6 Carotenoids

The second most abundant pigments on earth are carotenoids, which are produced by plants and give rise to the yellow to red colours of many fruits, flowers, vegetables, seeds, and senescent leaves (Howitt and Pogson, 2006). Carotenoids comprise a group of more than 750 compounds and have diverse functions (Nisar et al., 2015). They are important components of the photosynthetic complexes in the thylakoid membranes where they have two functions. On the one hand, they absorb light and by that broaden the range of utilised wavelengths which is otherwise restricted by the properties of the chlorophyll molecules. On the other hand, they are important protective compounds that prevent photooxidative damage to the chlorophyll molecules (Howitt and Pogson, 2006). In addition, carotenoids are precursors for the synthesis of phytohormones such as strigolactones and abscisic acid (Cazzonelli and Pogson, 2010). Many plant species accumulate carotenoids in their flower petals to attract pollinators, e.g. *S. lycopersicum* petals are yellow caused by an accumulation of neoxanthin, violaxanthin and to a lesser extent lutein (Galpaz et al., 2006).

1.6.1 Synthesis of Xanthophylls

Carotenoids are tetraterpenoids that consist of eight isoprene subunits and which can be divided into two classes: xanthophylls which contain oxygen and carotenes which are devoid of oxygen. The first committed step in the biosynthesis of carotenoids is the head-to-head condensation of two GGPP moieties catalysed by phytoene synthase (Armstrong, 1994) (Figure 1.6). The resulting intermediate phytoene does not accumulate but is directly processed in four successive desaturation reactions that result in the formation of lycopene (Cunningham and Gantt, 1998). The following cyclisation step is a branching point in the carotenoid biosynthetic pathway where the two branches differ in the cyclic end-groups. On the one side, the cyclisation into β rings at both ends of the lycopene molecule leads to the formation of β-carotene and its derivatives. On the other side, cyclisation into one β and one ε ring yields in α-carotene and its derivatives (Howitt et al., 2007).

Carotenes are the precursors for the synthesis of xanthophylls. In the β, ε branch, the double hydroxylation of α-carotene in successive steps by two different monooxygenases results in the formation of lutein, which is the end product of the β, ε branch. In the β, β branch, one single hydroxylase is responsible for two successive hydroxylations of β-carotene, which leads to the formation of zeaxanthin. Epoxidation of zeaxanthin produces violaxanthin. The end product of the β, β branch is neoxanthin which is derived from violaxanthin (for review on detailed reactions see Howitt and Pogson (2006)).

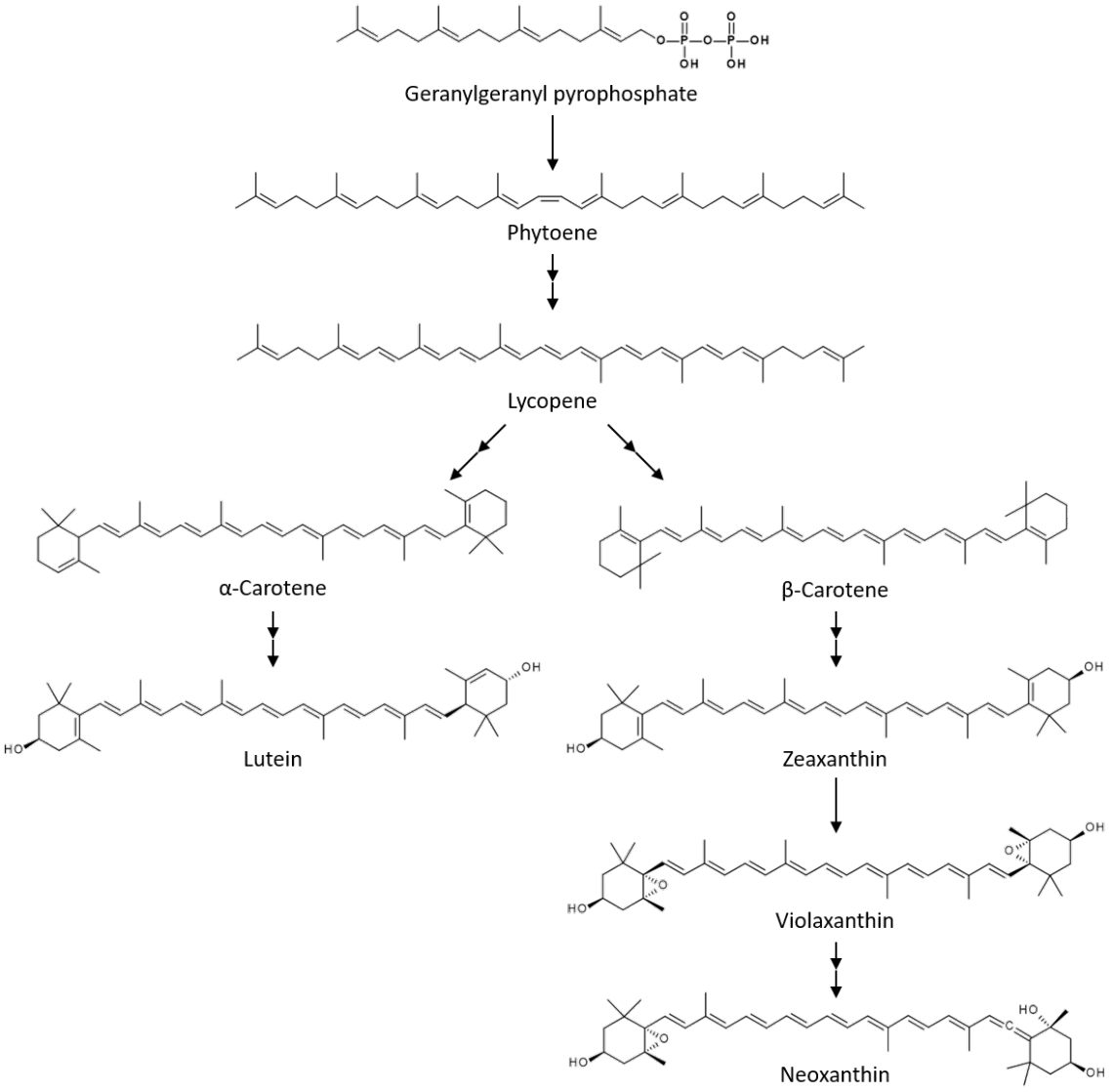

Figure 1.6 – Overview of the xanthophyll biosynthesis. Two molecules of geranylgeranyl pyrophosphate are condensed to phytoene which is further converted into lycopene. Two cyclisations at both ends of lycopene lead to the formation of α-carotene or β-carotene. α-Carotene is hydroxylated to lutein, while hydroxylation of β-carotene yields in zeaxanthin, which is epoxidated to violaxanthin. Neoxanthin is synthesised from violaxanthin. Double arrows indicate multiple steps.

1.6.2 Esterifications of Xanthophylls

In contrast to carotenes, xanthophylls contain hydroxyl groups which can be esterified with fatty acids. Fatty acid xanthophyll esters (FAXEs) have been long known with the probably first reference dating back to the 1920s. Kuhn and Wiegand (1929) extracted the red pigment physalien from *Physalis alkekengi* and *Physalis franchetti* berries. Physalien was later identified as di16:0-zeaxanthin (Kuhn et al., 1930). Over time, esterified xanthophylls were found in fruits, flowers, seeds and algae with examples given in the following paragraphs. The chromophore properties of xanthophylls remain unaffected by esterification. Therefore, it is assumed that esterified xanthophylls have overlapping functions with free xanthophylls, i.e. attraction of animals for pollination and dispersal of fruits and seeds (Hornero-Méndez and Mínguez-Mosquera, 2000). The esterification of free hydroxyl groups with fatty acids increases the lipophilic properties of the xanthophyll which has lead to the conclusion that esterification is a mechanism to sequester xanthophylls in the lipophilic plastoglobules (Hornero-Méndez and Mínguez-Mosquera, 2000). Furthermore, it was suggested that the esterification has a stabilising effect in chromoplasts as the loss of FAXEs leads to an impaired chromoplast development in *S. lycopersicum* (Ariizumi et al., 2014).

FAXEs accumulate in fruits, e.g. in the peel of apples during ripening (Knee, 1972). They have been identified as monoesters of neoxanthin and violaxanthin and as diesters of lutein, violaxanthin and neoxanthin, which are esterified with mainly 16:1 and 18:1 and to a lower extent with 12:0, 14:0 and 18:0 (Knee, 1988). Violaxanthin diesters are also found in the mesocarp of mango but identified as unusual di4:0-violaxanthin (Pott et al., 2003). Another example for xanthophyll esterification during fruit ripening is *Capsicum annuum* (pepper). While non-ripe green pepper fruits only contain free xanthophylls, the xanthophyll content of ripe fruits is composed of equal amounts of free xanthophylls, mono- and diesters (Hornero-Méndez and Mínguez-Mosquera, 2000). Xanthophyll monoesters can also be found in the endosperm of maize kernels (Janick-Buckner et al., 1999). An overview about FAXEs in fruits and vegetables can be found in Bunea et al. (2014).

Furthermore, FAXEs occur in grains, e.g. Mellado-Ortega and Hornero-Méndez (2015) reported mono and diester of lutein with 16:0 and 18:2 in the seeds of *Hordeum chilense*. For *Triticum aestivum* it had been shown that the amount of lutein mono and diester in grains can reach up to 60% of the total carotenoid content depending on the variety (Paznocht et al., 2018).

The green microalgae *Haematococcus pluvialis* only accumulates astaxanthin in its esterified form and the accumulation requires an active synthesis of fatty acids (Schoefs et al., 2001). The overexpression of the *β-carotene oxygenase* gene from *Haematococcus pluvialis* in *A. thaliana* seeds leads to the accumulation of free and esterified ketocarotenoids (Stålberg et al., 2003). *A. thaliana* seeds are normally devoid of FAXEs but the results demonstrate that *A. thaliana* contains enzymes which are able to esterify xanthophylls. In addition, the results indicate that the pro-

duced ketocarotenoids can be more easily esterified than the endogenous carotenoids of *A. thaliana* which remain in their free form. A similar experiment was conducted by overexpression of the *capsanthin/capsorubin synthase* gene from *Capsicum annuum* in leaves of *N. benthamiana* which yielded in the accumulation of free capsanthin in the chloroplasts (Kumagai et al., 1998). In chromoplasts, capsanthin is normally almost totally esterified (Camara and Monéger, 1978). It was concluded, that the esterification of xanthophylls requires the conversion of chloroplasts into chromoplasts (Hornero-Méndez and Mínguez-Mosquera, 2000).

Many plant species with colourful flowers contain esterified xanthophylls in addition to free carotenoids. A well studied plant genus in this context is *Tagetes* (common name: marigold). The petals have a high lutein content and as a consequence, they are a common source for commercially available lutein. The esters are mainly diesters with 14:0 and 16:0, produced during petal development and stored in the plastoglobules of chromoplasts (Gau et al., 1983; Rivas, 1991). Another example for FAXEs containing petals are the yellow petals of *Solanum lycopersicum* (Ariizumi et al., 2014). To increase the accumulation of xanthophylls from the β, β branch, the *S. lycopersicum carotene beta hydroxylase 2* was overexpressed in *S. lycopersicum* wild type plants (D'Ambrosio et al., 2011). The overexpression resulted in the accumulation of free violaxanthin and neoxanthin in leaves, petals and fruits. In addition, the fruits of both, control and overexpression plants, contained FAXEs which shows that not only *S. lycopersicum* petals but also tomato fruit chromoplasts are able to produce and store FAXEs. Goodwin (1980) provides an overview about carotenoid patterns and the occurrence of FAXEs in pollen, anthers and flower petals.

The dismantling of thylakoid membranes and the disintegration of light harvesting complexes during senescence does not only lead to the release of chlorophyll but also of other pigments such as xanthophylls. The first plant species that had been analysed with regard to FAXE formation during senescence were deciduous trees. The esterification of xanthophylls is species dependent, e.g. *Acer platanoides* and *Acer pseudoplatanus* accumulate lutein and violaxanthin esters while *Populus nigra* and *Quercus robur* do not produce FAXEs (Goodwin, 1958; Eichenberger and Grob, 1962, 1963) and in *Populus tremula* lutein and carotene are degraded upon senescence while neoxanthin and violaxanthin are converted into FAXEs (Keskitalo et al., 2005). In addition to the species, FAXE formation is also age dependent. In senescent leaves of 9 year old apple trees three additional FAXEs including unusual neoxanthin triesters appeared that are absent from younger trees (Cardini, 1983). Besides dicots, also monocots produce FAXE during senescence, e.g. *Hordeum vulgare* contains no FAXEs in green leaves, but during senescence 60% of the remaining carotenoids are esterified with 18:3-lutein as the main FAXE species (Young et al., 1991). Upon senescence, chloroplasts are transformed into gerontoplasts. FAXEs, which are produced during senescence, are stored in the plastoglobules of gerontoplasts (Tevini and Stein-

müller, 1985; Biswal, 1995). Because the proteome of plastoglobules contains enzymes involved in carotenoid metabolism, it is assumed that plastoglobules play a key role in synthesis and storage of carotenoids and FAXEs (van Wijk and Kessler, 2017).

Britton (1998) proposed that FAXEs are formed by conventional esterification of acyl-CoAs to the hydroxyl groups but studies on biochemical reactions are not present yet. As mentioned above, the yellow petals of *S. lycopersicum* contain FAXEs. The *pale yellow petal 1* (*pyp1*) mutant of *S. lycopersicum* is characterised by a reduced colouration of its petals (Ariizumi et al., 2014). Analysis of the carotenoid content from *pyp1* petals revealed a complete lack of FAXEs. The underlying mutation is located in a gene that is predicted as a hydrolase/acyltransferase. PYP1 is a homologue of the *A. thaliana* phytyl ester synthase PES1 with 58% identity and 73% similarity in the amino acid sequence (Ariizumi et al., 2014). The results indicate that PYP1 is a xanthophyll ester synthase (Ariizumi et al., 2014).

1.7 Objectives

Chlorophyll is the most abundant pigment in the biosphere and is the molecule that enables plants to utilise light energy. It is subject to a constant turnover of degradation and synthesis in photosynthetic active tissues. Chlorophyll is degraded during leaf senescence but also in response to biotic and abiotic stresses. This process leads to a massive release of chlorophyll breakdown products. The pathway for the degradation of the polar tetrapyrrole headgroup to non-fluorescent catabolites was studied in detail and most of the enzymes involved in the process have been characterised. However, much less is known about the fate of the non-polar phytol side chain. It has been shown that phytol derived from chlorophyll degradation can be incorporated into tocopherols or can be esterified to form fatty acid phytyl esters. Two enzymes from *A. thaliana* have been identified which are highly expressed under senescence and which show phytyl ester synthase activity, PES1 and PES2.

The aim of this project is the further characterisation of PES2 and the characterisation of additional putative phytyl ester synthases from *A. thaliana* and *S. lycopersicum*. Besides PES1 and PES2, the *A. thaliana* genome contains four additional sequences that show sequence similarity to esterases/lipases/thioesterases, *ELT3*, *ELT4*, *ELT5*, and *ELT6*. To investigate their function, the expression in different tissues and under senescence will be analysed as well as the FAPE content in leaves and seeds of mutant lines which will be obtained for all four genes.

The second part of this project is the further characterisation of PES2. PES2 utilises phytol as the fatty acid acceptor, and additional alcohol substrates are unknown. Investigation of other acyltransferases revealed a broader substrate specificity for some enzymes. For example Li et al. (2008)

demonstrated wax ester synthase activity as well as acyl-coenzyme A:diacylglycerol acyltransferase activity for WSD1 from *A. thaliana*. The mouse triacylglycerol synthesis enzyme DGAT1 revealed multiple acyltransferase activities including acyl CoA:monoacylglycerol acyltransferase (MGAT), wax monoester and wax diester synthase, and acyl-CoA:retinol acyltransferase (ARAT) activities (Yen et al., 2005). *Tetrahymena thermophila* possessed acyltransferases that use fatty alcohols, diols, diacylglycerol and isoprenols as substrate (Biester et al., 2012). Furthermore, the expression of PES2 together with a fatty acyl-CoA reductase (FAR) in leaves of *N. benthamiana* resulted in the accumulation of wax esters (Aslan et al., 2014), but it was unclear to which extent PES2 is responsible for the accumulation as it was always expressed with additional enzymes. Considering these studies, PES2 might be able to esterify additional alcohols besides phytol. Further on, it is unknown which fatty acid substrates are used by PES2. The saturated fatty acids derived from fatty acid *de novo* synthesis are bound to acyl carrier protein (ACP), but downstream of *de novo* synthesis, they can also occur esterified to coenzyme A (CoA), in their free form or bound in complex lipids such as membrane lipids. As mentioned before, it was proposed that the 16:3 employed for 16:3-phytol synthesis is derived from MGDG degradation in a way that either PES2 directly hydrolyses the fatty acid from the MGDG molecule or that the fatty acid is released during breakdown and PES2 uses the free 16:3. To investigate these possibilities, PES2 was expressed in *E. coli*, *N. benthamiana* and Sf9 insect cells to produce recombinant proteins for *in vitro* tests. Thus, PES2 might harbour additional unknown functions. To test this, PES2 was expressed in *N. benthamiana* and lipids were analysed.

The putative xanthophyll ester synthase PYP1 from *S. lycopersicum* shows high sequence similarity to PES1 from *A. thaliana*. Therefore, it is likely that PYP1 also possesses phytyl ester synthase activity. To investigate this hypothesis, *pyp1-1* and *pyp1-2* plants are subjected to FAPE analysis.

2 Material and Methods

2.1 Equipment

Autoclave	Systec, Linden (DE)
Balance 770	Kern, Balingen-Frommern (DE)
Balance PG503-S Delta Range	Mettler Toledo, Gießen (DE)
Balance XS205 DualRange	Mettler Toledo, Gießen (DE)
Binocular microscope SZX16	Olympus, Hamburg (DE)
Camera DP72 for microscope	Olympus, Hamburg (DE)
Centrifuge 5810R	Eppendorf, Hamburg (DE)
Centrifuge 5417R	Eppendorf, Hamburg (DE)
Centrifuge 5430	Eppendorf, Hamburg (DE)
Centrifuge Sorvall RC 5C PLUS	Thermo Fisher Scientific, Braunschweig (DE)
Dual fluorescent protein flashlight	NightSea, Bedford (US)
PowerPac Basic electrophoresis power supply	Bio-Rad Laboratories, München (DE)
Freeze dryer Alpha 2-4	Christ, Osterode am Harz (DE)
Gel caster, Mighty small II	GE Healthcare Europe, Freiburg (DE)
Growing cabinet Rumed	Rubarth Apparate, Laatzen (DE)
Heating block	Bioer, Hangzhow (CHN)
Homogeniser HO 4/A	Edmund Bühler, Hechingen (DE)
Homogeniser Precellys 24	PeQlab, Erlangen (DE)
Horizontal electrophoresis chamber	Cti, Idstein (DE)
Incubator, Kelvitron	Thermo Scientific Heraeus, Waltham (US)
Incubation shaker, Multitron 28570	INFORS, Einsbach (DE)
Inverted Microscope Eclipse TE300	Nikon, Düsseldorf (DE)
Magnetic stirrer MR30001	Heidolph Instruments, Schwabach (DE)

Micro pulser electroporator	BioRad Laboratories, München (DE)
Mixer mill MM400	Retsch, Haan (DE)
pH meter inoLab pH Level 1	WTW, Weilheim (DE)
Photometer, Specord 205	Analytik Jena, Jena (DE)
Phytochamber SIMATiC OP17	York International, York (USA)
Real Time PCR System 7300	Applied Biosystems, Thermo Fisher Scientific, Braunschweig (DE)
Rotary evaporator Laborota 4001	Heidolph Instruments, Schwabach (DE)
Sample concentrator	Techne (Bibby Scientific), Stone (GB)
Semi-dry transfer cell Trans-BLOT SD	Bio-Rad Laboratories, München (DE)
Spectrophotometer Nanodrop 1000	PeQlab, Erlangen (DE)
Sterile bench model 1.8	Holten Lamin Air, Allerød (DK)
Synergy Water Purification System	Merck Millipore, Darmstadt (DE)
Thermocycler TPersonel 48	Biometra, Göttingen (DE)
Thermocycler TProfessional 96	Biometra, Göttingen (DE)
Tube Rotator SB3	Stuart, Staffordshire (UK)
Ultracentrifuge Optima L 90K equipped with swing-out rotor SW 28	Beckman Coulter, Krefeld (DE)
UV-transilluminator DP-001 T1A	Vilber Lourmat, Eberhardzell (DE)
Vortex Certomat MV	Braun Biotech, Melsungen (DE)
VortexGenie2	Scientific Industries, Bohemia (USA)
Water bath TW20	Julabo, Seelbach (DE)
Water purification system ELIX 35	Merck Millipore, Darmstadt (DE)
6530 Accurate-mass quadrupole time-of-flight (Q-TOF) LC/MS	Agilent, Böblingen (DE)
7890 gas chromatography (GC) with flame ionisation detector (FID)	Agilent, Böblingen (DE)
7890 gas chromatography (GC) with mass spectrometry (MS)	Agilent, Böblingen (DE)

2.2 Consumables

6-well tissue culture plate	VWR, Darmstadt (DE)
Autosampler vials with inserts and screw caps with PTFE septa	VWR, Darmstadt (DE)

Centrifuge tubes (15 and 20 mL)	Greiner Bio-One, Frickenhausen (DE)
Ceramic beads (1.25–1.6 and 2.0–2.5 mm)	Mühlmeier Mahltechnik, Bärnau (DE)
Chromabond silica columns 60 Å, 45 µm, 500 mg/6 mL and 100 mg/1 mL	Macherey-Nagel, Düren (DE)
CL-XPosurefilm 13 x 18 cm	Thermo Fisher Scientific, Braunschweig (DE)
Culture tube (15.5 x 160 mm)	Schott, Mainz (DE)
Electroporation cuvettes	PeQlab, Erlangen (DE)
Gel blot paper (Whatman, 0.4 mm)	VWR, Darmstadt (DE)
Glass pasteur pipettes (150 and 225 mm)	Brand, Wertheim (DE)
Glass vials with thread (8 mL)	VWR, Darmstadt (DE)
Glass vials with thread (40 mL)	Schmidlin, Neuheim (CH)
Kimtech wipes	Kimberley-Clark, Koblenz (DE)
Leucopore tape (1.25 and 2.5 cm)	Duchefa, Haarlem (NL)
Microcentrifuge tubes (1.5 and 2 mL)	Greiner Bio-One, Frickenhausen (DE)
Microdialysis membranes	Merck Millipore, Darmstadt (DE)
Miracloth	Calbiochem, Merck Millipore, Darmstadt (DE)
Nitrocellulose Blotting Membrane 0.45 µm	Amersham, GE Healthcare Europe, Freiburg (DE)
PCR tubes (0.2 mL)	Brand, Wertheim (DE)
Petri dishes (94 x 16 and 145 x 20 mm)	Greiner Bio-One, Frickenhausen (DE)
Pipette tips 0.5–10 µL	Axygen, Corning, Karlsruhe (DE)
Pipette tips 10–200 µL, 100–1000 µL, 1–5 mL	Greiner Bio-One, Frickenhausen (DE)
Plastic screw caps for 40 mL glass vials	Schmidlin, Neuheim (CH)
Parafilm 10 cm x 38 m	Brand, Wertheim (DE)
Pots for plant cultivation	Pöppelmann, Lohne (DE)
PTFE screw caps for 8 mL glass vials	Schott, Mainz (DE)
Semi-micro cuvettes	Ratiolab, Dreieich (DE)
Soil (type Topf 1.5)	Gebrüder Patzer, Sinntal-Jossa (DE)
Syringe filter, ∅ 30 mm, 0.2 µm	Labomedic, Bonn (DE)
PTFE septa for screw caps (13.3 and 22.4 mm)	Schmidlin, Neuheim (CH)
TLC plates Silica 60 Durasil	Macherey-Nagel, Düren (DE)

Trays for plant cultivation	Pöppelmann, Lohne (DE)
Vermiculite, grain size 2-3 mm	Klemens Rolfs, Siegburg (DE)
Weighing paper	NeoLab, Heidelberg (DE)

2.3 Chemicals

Acetic acid	AppliChem, Darmstadt (DE)
Acetone	VWR, Darmstadt (DE)
Acetosyringone	Sigma-Aldrich, Taufkirchen (DE)
Acrylamide/Bis-acrylamide stock 40% (29:1 v/v)	Carl Roth, Karlsruhe (DE)
Agar	Formedium, Swaffham (UK)
Agarose	PeQLab, Erlangen (DE)
Ammonium acetate	Carl Roth, Karlsruhe (DE)
Ammonium nitrate (NH_4NO_3)	AppliChem, Darmstadt (DE)
Ammonium persulfate (APS)	AppliChem, Darmstadt (DE)
Benzene	AppliChem, Darmstadt (DE)
Boric acid (H_3BO_3)	AppliChem, Darmstadt (DE)
Bovine serum albumin (BSA)	Sigma-Aldrich, Taufkirchen (DE)
Bromophenol blue	Serva, Heidelberg (DE)
Calcium nitrate ($Ca(NO_3)_2$)	AppliChem, Darmstadt (DE)
Cellfectin II	Invitrogen, Thermo Fisher Scientific, Braunschweig (DE)
CHAPS	AppliChem, Darmstadt (DE)
Chloroform ($CHCl_3$)	VWR, Darmstadt (DE)
Cobalt(II) chloride ($CoCl_2$)	Merck Millipore, Darmstadt (DE)
Coenzyme A (CoA)	Sigma-Aldrich, Taufkirchen (DE)
Coomassie Brilliant Blue R250	AppliChem, Darmstadt (DE)
Copper(II) sulfate ($CuSO_4$)	Merck Millipore, Darmstadt (DE)
Dichloromethane	AppliChem, Darmstadt (DE)
Diethyl pyrocarbonate (DEPC)	AppliChem, Darmstadt (DE)
Diethyl ether	Fisher Chemicals, Thermo Fisher Scientific, Braunschweig (DE)
Dimethyl sulfoxide (DMSO)	Sigma-Aldrich, Taufkirchen (DE)
EDTA (ethylenediaminetetraacetic acid)	AppliChem, Darmstadt (DE)

Ethanol	VWR, Darmstadt (DE)
Ethidium bromide	Serva, Heidelberg (DE)
Ethyl chloroformate	Fluka, Sigma-Aldrich, Taufkirchen (DE)
Farnesol	Sigma-Aldrich, Taufkirchen (DE)
Ferric EDTA (Fe-EDTA)	Sigma-Aldrich, Taufkirchen (DE)
Formaldehyde	AppliChem, Darmstadt (DE)
Formamide	Sigma-Aldrich, Taufkirchen (DE)
Formic acid	AppliChem, Darmstadt (DE)
L-Glutamine	Duchefa, Haarlem (NL)
Glycerol	AppliChem, Darmstadt (DE)
Glycine	AppliChem, Darmstadt (DE)
HEPES	AppliChem, Darmstadt (DE)
Heptadecanoic acid	Sigma-Aldrich, Taufkirchen (DE)
1,2-Hexadecanediol	TCI Chemicals, Eschborn (DE)
1,16-Hexadecanediol	TCI Chemicals, Eschborn (DE)
Hexane	Carl Roth, Karlsruhe (DE)
Hydrochloric acid (HCl)	AppliChem, Darmstadt (DE)
IPL-41 Insect Medium	PAN-biotech, Aidenbach (DE)
IPTG	Formedium, Swaffham (UK)
Isopropanol	VWR, Darmstadt (DE)
LB-Broth Lennox low salt	Formedium, Swaffham (UK)
Lipidmix (1000x)	Sigma-Aldrich, Taufkirchen (DE)
Magnesium chloride ($MgCl_2$)	AppliChem, Darmstadt (DE)
Magnesium sulfate ($MgSO_4$)	AppliChem, Darmstadt (DE)
Manganese chloride ($MnCl_2$)	AppliChem, Darmstadt (DE)
MES (2-(N-morpholino)ethanesulfonic acid)	Duchefa, Haarlem (NL)
Methanol	Fisher Chemicals, Thermo Fisher Scientific, Braunschweig (DE)
Monopotassium phosphate (KH_2PO_4)	Carl Roth, Karlsruhe (DE)
MOPS (3-(N-morpholino)propanesulfonic acid)	AppliChem, Darmstadt (DE)
MS salts including vitamins	Duchefa, Haarlem (NL)
MSTFA	Carl Roth, Karlsruhe (DE)
Octadecan-1-ol (18:0ol)	Sigma-Aldrich, Taufkirchen (DE)

Oxalyl chloride	AppliChem, Darmstadt (DE)
Peptone	Formedium, Swaffham (UK)
Percoll	GE Healthcare Europe, Freiburg (DE)
Phosphoric acid (H_3PO_4)	Merck Millipore, Darmstadt (DE)
Phytoagar	Duchefa, Haarlem (NL)
Phytol	Sigma-Aldrich, Taufkirchen (DE)
Pluronic-F68	Sigma-Aldrich, Taufkirchen (DE)
Potassium bicarbonate ($KHCO_3$)	Sigma-Aldrich, Taufkirchen (DE)
Potassium chloride (KCl)	Carl Roth, Karlsruhe (DE)
Potassium hydroxide (KOH)	Merck Millipore, Darmstadt (DE)
Potassium nitrate (KNO_3)	Grüssing, Filsum (DE)
Primuline	Sigma-Aldrich, Taufkirchen (DE)
Pyridine	AppliChem, Darmstadt (DE)
Sarkosyl	Sigma-Aldrich, Taufkirchen (DE)
Silwet Gold	Spiess Urania, Hamburg (DE)
Sodium acetate	Sigma-Aldrich, Taufkirchen (DE)
Sodium azide (NaN_3)	AppliChem, Darmstadt (DE)
Sodium hydrogen carbonate ($NaHCO_3$)	Merck Millipore, Darmstadt (DE)
Sodium chloride (NaCl)	Duchefa, Haarlem (NL)
Sodium dodecyl sulfate (SDS)	AppliChem, Darmstadt (DE)
Sodium hydroxide (NaOH)	VWR, Darmstadt (DE)
Sodium hypochlorite (NaClO)	Carl Roth, Karlsruhe (DE)
Sodium molybdate (Na_2MoO_4)	Merck Millipore, Darmstadt (DE)
Sorbitol	Carl Roth, Karlsruhe (DE)
Stearyl alcohol	Sigma-Aldrich, Taufkirchen (DE)
Sucrose	Duchefa, Haarlem (NL)
TEMED (tetramethylethylenediamine)	Carl Roth, Karlsruhe (DE)
Tetrahydrofuran	Fisher Scientific, Schwerte (DE)
Toluene	VWR, Darmstadt (DE)
Tricine	AppliChem, Darmstadt (DE)
Triethylamine	Acros, Geel (BE)
Trifluoroacetic acid (TFA)	Sigma-Aldrich, Taufkirchen (DE)
Trifluoroacetic anhydride (TFAAH)	Sigma-Aldrich, Taufkirchen (DE)
Tris (tris(hydroxymethyl)aminomethane)	Carl Roth, Karlsruhe (DE)
Triton X-100	Carl Roth, Karlsruhe (DE)

Trizol	Invitrogen, Thermo Fisher Scientific, Braunschweig (DE)
Trypan blue	Sigma-Aldrich, Taufkirchen (DE)
Tween 80	Sigma-Aldrich, Taufkirchen (DE)
Tween 20	Sigma-Aldrich, Taufkirchen (DE)
X-Gal	AppliChem, Darmstadt (DE)
Xylene cyanol FF	Sigma-Aldrich, Taufkirchen (DE)
Yeast extract	Formedium, Swaffham (UK)
Zinc sulfate ($ZnSO_4$)	Merck Millipore, Darmstadt (DE)

2.4 Antibiotics

Ampicillin	Duchefa, Haarlem (NL)
Carbenicillin	Duchefa, Haarlem (NL)
Gentamicin	Duchefa, Haarlem (NL)
Hygromycin B	Duchefa, Haarelm (NL)
Kanamycin	Duchefa, Haarlem (NL)
Penicillin-Streptomycin	Gibco, Thermo Fisher Scientific, Karlsruhe (DE)
Rifampicin	Duchefa, Haarlem (NL)
Spectinomycin	Duchefa, Haarlem (NL)
Streptomycin	Duchefa, Haarlem (NL)
Tetracycline	Duchefa, Haarlem (NL)

2.5 Kits and Enzymes

Ambion TURBO DNA-free Kit	Thermo Fisher Scientific, Karlsruhe (DE)
CloneJET PCR Cloning Kit	Thermo Fisher Scientific, Karlsruhe (DE)
First Strand cDNA Synthesis Kit	Thermo Fisher Scientific, Braunschweig (DE)
High-Speed Plasmid Mini Kit	DNA Cloning Service (DCS), Hamburg (DE)
NucleoSpin Gel and PCR Clean-up Kit	Macherey-Nagel, Düren (DE)
NucleoSpin Plasmid Kit	Macherey-Nagel, Düren (DE)
Total RNA Mini Kit	Geneaid, Taipei (TW)

TURBO DNA-free Kit	Thermo Fisher Scientific, Karlsruhe (DE)
Color Prestained Protein Standard, Broad Range (11–245 kDa)	New England Biolabs, Frankfurt a. M. (DE)
dNTP	DNA cloning service, Hamburg (DE)
EvaGreen QPCR-Mix II	BioBudget, Krefeld (DE)
GeneRuler 1 kb DNA ladder	Thermo Fisher Scientific, Braunschweig (DE)
HisDetector Nickel-HRP Conjugate	Kirkegaard & Perry Laboratories, Wedel (DE)
Lysozyme	Sigma-Aldrich, Taufenkirchen (DE)
PureLink HiPure Plasmid Miniprep Kit	Invitrogen, Thermo Fisher Scientific, Braunschweig (DE)
Q5 High-Fidelity DNA Polymerase	New England Biolabs, Frankfurt a. M. (DE)
Restriction endonucleases	New England Biolabs, Frankfurt a. M. (DE)
Restriction endonucleases	Thermo Fisher Scientific, Braunschweig (DE)
RNase A	Boehringer Mannheim, Roche, Grenzach-Wyhlen (DE)
SuperSignal West Pico Chemiluminescence Substrate	Thermo Fisher Scientific, Braunschweig (DE)
T4 DNA Ligase	Thermo Fisher Scientific, Braunschweig (DE)
T4 DNA Ligase	New England Biolabs, Frankfurt a. M. (DE)
Taq DNA polymerase	DNA Cloning Service, Hamburg (DE)

2.6 Lipid Standards

Birkenöl (mixture of jojoba oil (WEs) and apricot seed oil (TAGs))	Weleda, Arlesheim (CH)
16:0-Cholesterol	Sigma-Aldrich, Taufkirchen (DE)
16:1-Cholesterol	Sigma-Aldrich, Taufkirchen (DE)
18:0-Cholesterol	Sigma-Aldrich, Taufkirchen (DE)
18:1-Cholesterol	Sigma-Aldrich, Taufkirchen (DE)
Pentadecanoic acid (15:0)	Sigma-Aldrich, Taufkirchen (DE)

17:0-Phytol	Synthesised during this work
Tri10:0-TAG	Larodan, Malmö (SE)
Tri11:1-TAG	Synthesised in house
17:0-18:0ol WEs	Synthesised in house

2.7 Vectors

Table 2.7 – Cloning Vectors.

Vector	Target Organism	Selection marker	Reference
pBin-Red-2800	*A. tumefaciens*	Kan	Ed Cahoon, University of Nebraska
pJET1.2	*E. coli* Electroshox	Amp	Thermo Fisher Scientific
pGEM-Teasy	*E. coli* Electroshox	Amp	Promega
pLH6000	*A. tumefaciens* GV2260	Strep/Spec	DNA Cloning Service
pQE-30	*E. coli* M15 pREP4	Amp	Qiagen
pL-nD1cM1-DsRed	*A. tumefaciens* GV2260	Strep/Spec	See below
pFastBac1	*E. coli* DH10Bac	Amp	Invitrogen
pYES2	*S. cerevisae* INVSc1	Uracil	Invitrogen

Table 2.8 – Recombinant plasmids.

Stock	Construct	Protein	Description	Reference
PD532	ev-pQE31	-	Expression in *E. coli*	Qiagen
PD551	U09399	PES2	cDNA clone	ABRC
bn55	pL-PES2	PES2	Expression in plants	See below
bn75	pQE30-PES2oTP	6xHis-PES2oTP	Expression in *E. coli*	See below
bn351	pFastBac1-GUS	GUS	Generation of bacmid	Invitrogen
bn856		P19	Expression in plants	Wood et al. (2009)
bn857	GFiP-pCW49	GFiP	Expression in plants	Wood et al. (2009)
bn858	p35S-tpPES2	PES2	Expression in plants	Aslan et al. (2014)
bn859	p35S-m1PES2	PES2oTP	Expression in plants	See below
bn860	p35S-m2PES2	PES2oTP	Expression in plants	See below
bn1090	pFastBac1-PES2oTP	6xHis-PES2oTP	Generation of bacmid	Chapter 2.12.9

Cloning of pQE30-PES2oTP – The cloning of this construct was carried out by Felix Lippold. PES2 without a predicted signal peptide (PES2oTP, lacking the first 94 amino acids) was amplified by PCR with overhangs for the restriction sites of *Bam*HI and *Kpn*I (primer bn189 and bn190). The cDNA clone U09399 was used as the template. The PCR product was ligated into pGEM-Teasy, resulting in the construct pG-PES2oTP. PES2oTP was released from pG-PES2oTP and pQE-30 was linearised with *Bam*HI and *Kpn*I. PES2oTP was ligated into pQE-30, and pQE30-PES2oTP (Appendix Figure 7.3) was transformed into *E. coli* M15 pREP4 cells.

Cloning of pL-PES2 – The cloning of this construct was carried out by Georg Hölzl and Felix Lippold. PES2 was released from the cDNA clone U09399 with *Eco*RI and *Not*I. pYES2 was linearised with the same enzymes and PES2 was ligated into pYES2. pL-nD1cM1-DsRed was linearised and PES2 was released from PES2-pYES2 with *Bam*HI and *Mlu*I. PES2 was ligated into pL-nD1cM1-DsRed to yield pL-PES2. pL-PES2 (Appendix Figure 7.2) was transformed into *A. tumefaciens* GV2260 cells.

Cloning of pL-nD1cM1-DsRed – The cloning of this construct was carried out by Thomas Geske and Georg Hölzl. pL-nD1cM1-DsRed contains two sets of promoter and terminator within the T-DNA region to transform plants with two genes simultaneously, a gene of interest and the DsRed gene as a marker for transformation. The starting point of cloning was the custom-made construct p35iF2-D1EX1RNAi (DNA Cloning Service), which is an expression vector for gene silencing containing an RNAi construct flanked by a 35S promoter and an OCS terminator. The RNAi was released by digestion with *Bam*HI and *Mlu*I. nD1 (n-terminal part of DGD1) was amplified by PCR with overhangs for the restriction sites of *Bam*HI and *Avr*II (primer PD809 and PD854) from DGD1 cDNA. cM1 (c-terminal part of MGD1) was amplified by PCR with overhangs for the restriction sites of *Avr*II and *Mlu*I (primer PD855 and PD796). Both PCR constructs were cloned into pGEM-Teasy and released with the respective enzymes. nD1 and cM1 were ligated in a single reaction into the linearised p35iF2-D1EX1RNAi vector, resulting in the construct p35-nD1cM1. nD1cM1 including the 35S promoter and the OCS terminator from the vector was released from the vector backbone with *Sfi*I. pLH6000 was linearised with *Sfi*I. The cassette of 35S promoter, nD1cM1 and OCS terminator was ligated into pLH6000 resulting in the construct pL-nD1cM1-Hyg. DsRed including a 35S promoter and NOS terminator was amplified from pBin-Red-2800 by PCR with overhangs for the restriction sites of *Blg*II and *Pme*I (primer bn325 and bn326). The PCR product was ligated into pGEM-Teasy, resulting in the construct pG-DsRed. The entire cassette of 35S promoter, DsRed and NOS terminator was released from pG-DsRed with *Blg*II and *Pme*I and pL-nD1cM1-Hyg (synonymous pLnD1cM1-Hyg) was linearised using the same enzymes. The cassette containing DsRed was ligated into pL-nD1cM1-Hyg resulting in

the construct pL-nD1cM1-DsRed.

Cloning of p35S-m1PES2 – The cloning of this construct was carried out by Per Hofvander. PES2 without a predicted signal peptide (m1PES2, lacking the first 64 amino acids) was amplified by PCR with the two primers mPESattB1 (GGGGACAAGTTTGTACAAAAAAGCAGGCTTCAACAATGGCGAAGGTGGTGGAGAATC) and mPES2attB2 (GGGGACCACTTTGTACAAGAAAGCTGGGTCTTAGAGATCAAACGTTGGAATTTCAG). The plasmid pTrcHis2c harboring the complete sequence of PES2 was used as the template. The fragment was recombined into pDONR221 using BP clonase generating pENTRY-m1PES2. Subsequently the fragment was recombined into pXZP393 using LR clonase generating p35S-m1PES2.

Cloning of p35S-m2PES2 – The cloning of this construct was carried out by Per Hofvander. PES2 without a predicted signal peptide (m2PES2, lacking the first 93 amino acids) was amplified by PCR with the two primers mPES2.2attB1 (GGGGACAAGTTTGTACAAAAAAGCAGGCTTCAACAATGAGAGAGTTCGTCGGAGATGGAG) and mPES2attB2 (GGGGACCACTTTGTACAAGAAAGCTGGGTCTTAGAGATCAAACGTTGGAATTTCAG). The plasmid pTrcHis2c harboring the complete sequence of PES2 was used as the template. The fragment was recombined into pDONR221 using BP clonase generating pENTRY-m2PES2. Subsequently the fragment was recombined into pXZP393 using LR clonase generating p35S-m2PES2.

2.8 Synthetic Oligonucleotides

Synthetic oligonucleotides for PCR analysis were ordered from Integrated DNA Technologies, Leuven (BL). The oligonucleotides are listed in Table 7.11 in the Appendix.

2.9 Sequencing

Sequencing was conducted to confirm the DNA sequence during cloning of expression constructs and to determine the sequence of cDNA derived from mRNA. The quality of sequencing depends highly on the purity of the DNA template. Consequently plasmid DNA or PCR products were purified by kits (NucleoSpin Gel and PCR Clean-up Kit, NucleoSpin Plasmid Kit). Samples were prepared according to the requirements of the sequencing companies, Beckman Coulter Genomics (Takeley, UK) or GATC (Cologne, DE). PCR products were sequenced with gene specific primers. Plasmids were either sequenced with plasmid specific or with gene specific primers (Table 7.11). Results obtained in sequencing files (.abi format) were analysed using FinchTV 1.4.0 (Geospiza, Inc.; Seattle, WA, USA; http://www.geospiza.com). Sequences were aligned with MultAlin (Corpet, 1988).

2.10 Organisms

Agrobacterium tumefaciens

GV3101-pMP90	DNA Cloning Service, Hamburg (DE)

Nicotiana benthamiana

Escherichia coli

Electroshox	Bioline, Luckenwalde (DE)
DH10Bac	Invitrogen, Thermo Fisher Scientific, Braunschweig (DE)
M15 pREP4	Qiagen, Hilden (DE)

Solanum lycopersicum

Micro-Tom-J (MT-J), *pyp1-1*, *pyp1-2*	Ariizumi et al. (2014)

***Spodoptera frugiperda* cells**

Gibco Sf9 cells	Thermo Fisher Scientific, Braunschweig (DE)

Table 2.10 – *A. thaliana* insertion mutant lines.

Mutant	Gene	Mutant line	Ecotype	Origin
pes1pes2	At1g54570 At3g26840	SALK_034549 SALK_071769	Col-0 Col-0	Lippold et al. (2012)
elt3-1	At3g26820	SALK_139280C	Col-0	NASC
elt3-2	At3g26820	pst20507	Ds6-393-19	RIKEN (Ibaraki, JP)
elt4-2	At5g41120	SALK_107487C	Col-0	NASC
elt4-4	At5g41120	GK-319C08	Col-0	NASC
elt5-1	At5g41130	SALK_112407	Col-0	NASC
elt5-4	At5g41130	SALK_005682	Col-0	NASC
elt6-1	At3g02030	SALK_071625C	Col-0	NASC
elt6-2	At3g02030	SAIL_1160_D05	Col-0	NASC

The background ecotype of *A. thaliana* transposon lines provided by the RIKEN Institute is generally Nossen-0 (No-0). However, the genotypes of some donor lines were inconsistent with that of No-0 and all other natural accessions preserved in the resource centre of RIKEN. The parental line of the RIKEN transposon line pst20507 (*elt3-2*) is Ds6-393-19, which belongs to the inconsistent donor lines. Thus the background ecotype of *elt3-2* cannot be identified. The lipid content of Ds6-393-19 was comparable to that of *A. thaliana* ecotype Columbia-0 (Col-0).

Therefore Col-0 plants were used as wild type control for all experiments.

Samples for screening of FAPEs in different plant families were kindly provided by the Crop Garden of the Botanical Garden Bonn. This included leaf samples from the following species: *Capsicum annuum*, *Cyphomandra abutiloides*, *Lycianthes rantonnetii*, *Nicotiana rustica*, *Nicotiana tabacum*, *Physalis peruviana*, *Solanum melongena*. Leaf material from *Oryza sativa* cultivar IR72 was kindly provided by Dr. Lin-Bo Wu (INRES, University of Bonn). Senescent leaves from *Lotus japonicus* ecotype Gifu and *Hordeum vulgare* ecotype Scarlett were kindly provided by Mathias Brands (IMBIO, University of Bonn).

Leaf samples of PEG-treated *A. thaliana* plants for the analysis of FAPEs under drought stress were kindly provided by Victoria Pratzka (IMBIO, University of Bonn).

2.11 Methods for Cultivation and Transformation of Different Organisms

2.11.1 Cultivation of Bacteria

Bacteria were cultivated in liquid as well as on solid LB (lysogeny broth) medium according to Lennox (1955). *E. coli* was incubated at 37 °C whereas *A. tumefaciens* was incubated at 28 °C. The medium contained 20 g L^{-1} LB broth low salt with a pH of 7.2. Liquid cultures were aerated by shaking with 180 rpm. For cultivation on plates, the medium was mixed with 1.5% (w/v) agar. Appropriate antibiotics were added to the medium for selection of positive clones (Table 2.11).

For long term storage of bacteria, 500 µL of overnight cultures were mixed with 500 µL sterile 70% (v/v) glycerol, frozen in liquid nitrogen and stored at -80 °C.

Table 2.11 – Antibiotics used for the selection of plasmid containing *E. coli* and *A. tumefaciens* cells. Antibiotics were prepared as 1000x stocks and dissolved in double deionized water (ddH_2O) unless noted otherwise. Given concentrations are the final concentrations in the medium.

Antibiotics	***E. coli***	***A. tumefaciens***
Ampicillin (Amp)	100 µg mL^{-1}	
Carbenicillin (Carb)	50 µg mL^{-1}	250 µg mL^{-1}
Gentamicin (Gent)	7 µg mL^{-1}	25 µg mL^{-1}
Kanamycin (Kan)	30 µg mL^{-1}	50 µg mL^{-1}
Rifampicin (Rif; in DMSO)		80 µg mL^{-1}
Spectinomycin (Spec)	25 µg mL^{-1}	100 µg mL^{-1}
Streptomycin (Strep)	25 µg mL^{-1}	300 µg mL^{-1}
Tetracycline (Tet; in ethanol)	10 µg mL^{-1}	

2.11.2 Generation and Transformation of Electrocompetent Bacteria

Bacteria were transformed by electroporation. For the preparation of electrocompetent cells 50 mL SOB medium with appropriate antibiotics were inoculated with *E. coli* or *A. tumefaciens* and incubated overnight at 180 rpm and 37 °C or 28 °C, respectively. On the next day 400 mL SOB medium containing antibiotics were inoculated with 20 mL of the overnight culture and incubated until an OD_{600} (optical density at 600 nm) of 0.5–0.7 was reached. Cells were incubated for 30 min on ice and harvested by centrifugation at 4000 *g* and 4 °C for 10 min. Cells were washed subsequently with 400 mL icecold 1 mM HEPES pH 7, 400 mL icecold ddH_2O and 50 mL icecold ddH_2O. Between each step, cells were centrifuged at 4000 *g* and 4 °C for 10 min, the supernatant was discarded and the pellet was resuspended in the next solution. Finally, cells were resuspended in 1–2 mL icecold 10% (v/v) glycerol and aliquots of 50 µL were frozen in liquid nitrogen and stored at -80 °C.

For each transformation, one aliquot of electrocompetent *E. coli* or *A. tumefaciens* cells was thawed on ice and mixed with salt-free 5 µL plasmid DNA or 10 µL of desalted ligation reaction. The mixture was transferred to a precooled electroporation cuvette. After applying a voltage of 1.8 kV, cells were resuspended in 800 µL LB medium without antibiotics and incubated for 40 min at 37 °C (*E. coli*) or for 90 min at 28 °C (*A. tumefaciens*) on a tube rotator. Afterwards, cells were spread on LB plates containing appropriate antibiotics for selection of positive clones.

SOB medium

20 g L^{-1}	Peptone	addition after autoclaving:	
5 g L^{-1}	Yeast extract	2 mL 1 M	$MgSO_4$
0.6 g L^{-1}	NaCl	2 mL 1 M	$MgCl_2$
0.18 g L^{-1}	KCl		

2.11.3 Transformation of Bacteria by Chemical Transformation

E. coli DH10Bac cells were transformed by chemical transformation. 10 µL of chemically competent cells were thawed on ice and transferred to a pre-chilled 1.5 mL reaction tube. 1 ng of pFastBac1 DNA was added to the cells and mixed gently. Cells were incubated on ice for 30 min. Transformation was conducted by heat-shocking the cells for 45 sec at 42 °C. Tubes were immediately placed on ice for 2 min. Cells were resuspended in 300 µL SOB medium and incubated for 4 h at 37 °C on a tube rotator. Afterwards, cells were spread on LB plates containing kanamycin, gentamicin, tetracycline, X-gal and IPTG. Plates were incubated for 48 h at 37 °C and white colonies were picked for further analysis (Chapter 2.12.9).

2.11.4 Feeding of *E. coli* with Different Lipids

E. coli cells that express the phytyl ester synthase PES2 from *A. thaliana* were fed with phytol according to Valentin et al. (2006) with some modifications.

The protein expression was induced at OD_{600} 0.5–0.7 by addition of 1 mM IPTG and cells were incubated overnight at 16 °C and 180 rpm. 50 mL of induced cells were harvested by centrifugation for 15 min at 4000 *g*. The pellet was resuspended in 5 mL LB medium containing appropriate antibiotics, 5 mM phytol and 0.2% (v/v) toluene. The cultures were incubated for 3 h at 30 °C and 180 rpm. Afterwards, the OD_{600} was measured to correlate later the quantified lipids to the cell density. Cells were harvested for 15 min at 4000 *g*. The pellet was washed with water and centrifuged as before. Lipids were extracted from the pellet as described in Chapter 2.13.2.

2.11.5 Cultivation of *A. thaliana*

A. thaliana was cultivated on soil containing 30% (v/v) vermiculite under long day conditions (16 h light/8 h dark) at 20 °C, with 55% humidity and a light intensity of 150 µE. Plants were watered with tap water except for the first irrigation where tap water was mixed with 0.186 % (w/v) boric acid and 0.15 % (v/v) Proplant (Procamocarb hydrochloride, fungicide) (Dr. Stähler). Seeds were sown on soil and seedlings were transplanted two weeks after sowing into five plants per pot.

For nitrogen starvation experiments, *A. thaliana* plants were grown in sterile culture under long day conditions at 22 °C and 120 µE. Seed surfaces were sterilised by incubation in sterilisation solution containing ddH_2O/ethanol/12% sodium hypochlorite (21:25:4, v/v/v) for 20 min under gentle shaking. Seeds were washed three times with ethanol (technical grade) under sterile conditions and subsequently air dried. Sterile seeds were cultivated on MS medium (Murashige and Skoog, 1962) containing 0.4405% (w/v) MS salts including vitamins, 1% (w/v) sucrose and 0.8% (w/v) phytoagar for two weeks. Afterwards plants were transferred to synthetic *A. thaliana* medium either containing nitrogen (+N) or lacking nitrogen (-N) and incubated for further two weeks. For nitrogen deprivation experiments, KNO_3, $Ca(NO_3)_2$, and NH_4NO_3 were replaced with 2.5 mM KCl and 1 mM $CaCl_2$ in the -N medium.

For the screening of transgenic *A. thaliana* plants, seeds were surface sterilised and sown on MS plates containing 15 µg $mL^{-}1$ hygromycin B. Plates were incubated according to Harrison et al. (2006) with two days stratification in the dark at 4 °C followed by incubation at 22 °C for 6 h in the light, two days in the dark and one day in the light. After several days of growth, transgenic, hygromycin resistant plants were identified by an extended hypocotyl.

Synthetic *A. thaliana* medium (Estelle and Somerville, 1987)

0.8% (w/v)	Agarose
1% (w/v)	Sucrose
2.5 mM	KNO_3
1.0 mM	$MgSO_4$
1.0 mM	$Ca(NO_3)_2$
1.0 mM	KH_2PO_4
1.0 mM	NH_4NO_3
25.0 µM	Fe-EDTA
35.0 µM	H_3BO_3
7.0 µM	$MnCl_2$
0.25 µM	$CuSO_4$
0.5 µM	$ZnSO_4$
0.1 µM	Na_2MoO_4
5.0 µM	NaCl
5.0 nM	$CoCl_2$

2.11.6 Stable Transformation of *A. thaliana* by Floral Dipping

Stable expression of genes in *A. thaliana* was conducted by *A. tumefaciens* mediated transformation. To this end, *A. tumefaciens* strains containing the respective binary vectors were grown in 200 mL LB medium containing appropriate antibiotics. Cells were harvested by centrifugation for 20 min at 4000 *g*. Cell pellets were resuspended in dipping solution (tap water with 5% (w/v) sucrose and 0.05% (v/v) Silwet). The *A. tumefaciens* dipping solution was poured into a glass jar. Shoots of 5–6 weeks old *A. thaliana* plants were dipped into the solution for 10 sec, the plants placed horizontally in trays and regenerated for 24 h under low light conditions. Afterwards, the plants were set upright and returned to the phyto chamber where they were grown under normal conditions. Transgenic seeds were selected by fluorescence (DsRed marker) or antibiotic resistance.

2.11.7 Crossing of *A. thaliana* Plants

A. thaliana is a self-fertilising plant. The pistil and stamen mature when petals and sepals are still closed. During flower opening, the stamen grow past the carpel, deliver the mature pollen to the stigma and by that fertilise it. Consequently, very young flowers that are still closed and not yet fertilised, were used for crossing. All other mature siliques, open flowers and buds, that have

already a white tip, from the same inflorescence were removed. The meristem and buds, that were too small for crossing, were removed as well. Normally, 3–5 buds at one inflorescence remained, that had the right size for crossing. Using very fine forceps, the petals, sepals and stamen were carefully removed from the remaining buds without wounding their pistils. Mature stamen from a donor plant were taken and carefully brushed over the stigma of the emasculated flower. Once this was done for all buds at one inflorescence, they were slightly sprayed with tap water, covered in a small piece of plastic wrap and attached to a stick. Buds were checked every day. When an emerging silique was visible, the plastic wrap was removed. Siliques were harvested after 14–21 days into small paper bags, when the silique was yellow but not yet opened.

2.11.8 Feeding Experiment of *A. thaliana* Plantlets with Lipids

For the general assessment of acyltransferase activities in *A. thaliana* mutants, plants were grown in liquid medium containing different alcohol substrates. The method described here is based on protocols from Ischebeck et al. (2006), Lippold et al. (2012) and vom Dorp et al. (2015).

Plants were grown on soil for four weeks as described before (Chapter 2.11.5). For feeding assays, plants were transferred to 20 mL 20 mM MES-KOH buffer (pH 6.5) containing 0.2% (v/v) Tween 20 and 0.1% (v/v) phytol, farnesol, octadecan-1-ol or 1,16-hexadecanediol, or without alcohol as the negative control. After incubation for 24 h under gentle shaking, plants were removed from the buffer, washed with tap water and briefly dried on tissue paper. Roots as well as inflorescences were cut off and the fresh weight of the remaining rosette was determined. The leaf rosettes were frozen in liquid nitrogen and either stored at -80°C or homogenised using the Precellys for subsequent lipid extraction (Chapter 2.13.2).

2.11.9 Cultivation of *N. benthamiana*

N. benthamiana was cultivated on soil containing 30% (v/v) vermiculite under long day conditions (16 h light, 8 h dark) at 25°C, with 60% humidity and a light intensity of 250 µE. The first irrigation water contained 0.186 % (w/v) boric acid and 0.15 % (v/v) Proplant (Dr. Stähler). In the following, plants were watered with tap water. Seeds were sown on soil and seedlings were separated into single pots two weeks after sowing.

2.11.10 Transient Transformation of *N. benthamiana* by Leaf Infiltration

Transient expression of genes after infiltration of *N. benthamiana* leaves with *A. tumefaciens* was conducted according to a modified protocol from Wood et al. (2009).

A. tumefaciens strains harbouring the desired binary vectors were grown in 10 mL LB broth medium with appropriate antibiotics at 28°C and with shaking at 180 rpm for 20 h. Afterwards

100 µM acetosyringone (AS) dissolved in dimethyl sulfoxide (DMSO) were added to the culture and further incubated for 2–3 h to induce virulence genes. Plants were transferred to a well-lit room and watered to stimulate stomata opening. All damaged or old leaves, flowers and shoots were removed. Cells were harvested for 10 min at 4000 *g*. Pellets were gently resuspended by pipetting with a cut tip in 0.5 volume of infiltration medium (5 mM $MgCl_2$, 5 mM MES pH 5.7, 100 µM AS). Cell densities were determined at 600 nm in appropriate dilutions. For infiltration, *A. tumefaciens* strains containing different constructs were mixed with a final concentration of each construct of OD_{600} 0.2. Each mixture contained *A. tumefaciens* harboring constructs with P19, GFP as positive control and the gene of interest. The mixture of P19 and GFP without an additional construct was used as a positive control for expression and as a negative control for enzyme activity. The mixture of *A. tumefaciens* strains was drawn up in a 2 mL syringe without a needle and infiltrated into the bottom side of appropriate leaves with soft counter pressure from a finger on the upper side of the leaf. Gene expression was detected after 4–7 days with a fluorescent lamp (NightSea, Bedford, USA). Leaf areas that displayed a GFP signal were used for lipid extraction (Chapter 2.13.2).

2.11.11 Cultivation of Sf9 Cells

An insect cell culture of the Sf9 cell line infected with baculovirus was used for the heterologous expression of proteins. Sf9 cells were originally established from *Spodoptera frugiperda* ovarian tissue. Cell cultures of the Sf9 cell line were routinely maintained in suspension culture.

Initial cultures were grown from DMSO stocks that had been stored in the vapour phase of liquid nitrogen. Stocks were quickly thawed at 37°C and transferred to 5 mL warm IPL-41 medium. After incubation for 24 h at 28°C and 120 rpm, 5 mL fresh medium were added to the culture. The cell culture was diluted every 2–3 days with fresh medium in a way that the cell number did not drop below 10^5 cells mL^{-1}. Ideally, cultures were diluted at a cell density of 3–4 x 10^6 cells mL^{-1} and diluted to a cell density of 1 x 10^6 cells mL^{-1}. The culture volume was increased stepwise until 100–200 mL cultures were reached. Cultures were maintained routinely for experiments.

IPL-41 Medium

2.463% (w/v)	IPL-41 Insect Medium
	(without L-Glutamine and $NaHCO_3$)
0.4% v/v	Yeast extract
0.1% v/v	Lipidmix (1000x)
1% v/v	Pluronic-F68 (10%)
0.09938% (w/v)	L-Glutamine
0.035% (w/v)	$NaHCO_3$
	pH 6.4 with KOH

	Osmolarity 335 mOsm with NaCl
	Filter sterilised
1% (v/v)	Penicillin-Streptomycin (10,000 U mL^{-1})

Test of Viability

The viability of insect cells was determined by trypan blue staining. Aliquots of 50 µL culture were mixed with 50 µL trypan blue staining solution and incubated for 15 min at room temperature. Cells were counted on a Fuchs-Rosenthal counting chamber with an inverted microscope. Dead cells were differentiated from living cells by their blue staining and counted in a ratio to unstained, viable cells. Cultures were requested to have a viability of at least 95% living cells for transfection and further experiments.

2.11.12 Transfection of Sf9 Cells

Insect cells were transfected with recombinant bacmid to produce baculovirus for the heterologous expression of proteins. The procedure was done according to the Bac-to-Bac Baculovirus Expression System (Invitrogen) manual. Twelve aliquots of 100 µL insect medium without antibiotics were prepared. Six of them were mixed with 8 µL Cellfectin II (Invitrogen) by vortexing, five of them were mixed with 500 ng of bacmid DNA and one aliquot was left without DNA as a negative control. Aliquots of Cellfectin II containing medium were mixed with DNA containing aliquots and incubated for 30 min at room temperature. 8 x 10^5 cells, that were in the log phase (1.5–2.5 x 10^6 cells mL^{-1}) with a greater viability than 95%, were sown in each well of a 6-well tissue culture plate. Plates were kept at room temperature for 15 min to allow the cells to attach to the bottom. The old insect medium (supernatant) was replaced with 2.5 mL of fresh insect medium without antibiotics. The transfection mixture was added dropwise to each well and cells were incubated for 6 h at 27°C. The transfection mixture was removed and replaced with 2 mL of fresh insect medium containing antibiotics. Cells were incubated at 27°C until signs of viral infection were visible. To this end, beginning three days after infection, cells were inspected daily under an inverted microscope. Cells showed characteristic signs of infection such as increased cell size, granular appearance, detachment from the bottom and in the end cell lysis. These signs were visible 72–120 h after transfection. As the budded virus was released into the medium, the passage one (P1) baculovirus stock was harvested by transferring the supernatant into sterile 15 mL tubes. To remove cells and debris, tubes were centrifuged for 5 min at 500 *g*. The supernatant, i.e. the P1 viral stock, was transferred to fresh tubes and stored at 4°C.

2.11.13 Amplification of Baculovirus Stock

The P1 viral stock, harvested after the initial transfection of insect cells with bacmid DNA, is a small-scale low-titre stock. For the expression of recombinant protein, high-titre viral stocks were needed. The amplification of the viral stock was done by infecting the cells with a multiplicity of infection (MOI) of 0.1. MOI gives the ratio of virus particles to cell number. The following equation was used to calculate the required volume of viral stock.

$$Inoculum\ required\ (mL) = \frac{MOI\ (pfu\ cell^{-1}) * number\ of\ cells}{titre\ of\ viral\ stock\ (pfu\ mL^{-1})} \quad (2.1)$$

The titre of the viral stock normally ranges between 1 x 10^6 to 1 x 10^7 pfu mL $^{-1}$. Since the titre was not determined during this study, it was assumed to be in the range of 5 x 10^6 pfu mL $^{-1}$.

The amplification of the baculovirus stock was conducted in 10–20 mL suspension cultures. The required amount of P1 stock was mixed with 2 x 10^6 cells mL $^{-1}$ insect cells and incubated for 72 h at 27°C and 120 rpm. Cultures were harvested by centrifugation for 5 min at 500 x g. The supernatant, i.e. the P2 viral stock, was transferred to a clean tube and stored at 4°C.

2.12 Methods in Molecular Biology

2.12.1 Isolation of Genomic DNA

For isolation of genomic DNA from *A. thaliana*, fresh leaf material was harvested and transferred into 2 mL tubes containing small ceramic beads and 800 µL CTAB buffer. The leaf material was homogenised for 45 sec at 6500 rpm in the Precellys homogeniser. Samples were shortly centrifuged to remove the foam. Subsequently samples were incubated at 65 °C for at least 10 min with shaking at 650 rpm. After addition of 300 µL chloroform and thoroughly vortexing, samples were centrifuged for phase separation at 3000 *g* for 5 min. The aqueous phases were transferred into fresh 1.5 mL tubes and mixed with 600 µL cold isopropanol. DNA was precipitated by incubation on ice for 10 min and harvested at 14000 *g* for 5 min. The DNA pellet was washed with 75% (v/v) ethanol and centrifuged at 14000 *g* for 5 min. DNA was dissolved in 50 µL ddH_2O with 0.5 µL RNase A (8 U mL^{-1}) and incubated at room temperature for 15 min. DNA was quantified by spectrophotometry (NanoDrop) and stored at -20 °C.

CTAB buffer

140 mM	Sorbitol
220 mM	Tris-HCl pH 8.0
22 mM	EDTA
800 mM	NaCl

1% (w/v)	Sarkosyl
0.8% (w/v)	CTAB

2.12.2 Isolation of Plasmid DNA

The isolation of plasmid DNA from *E. coli* was performed by harvesting cells from an overnight culture in 2 mL microcentrifuge tubes for 1 min at 14000 *g*. The pellet was resuspended in 200 µL BF buffer containing 0.1% (w/v) lysozyme. Cells were disrupted by incubation for 1 min at 98 °C and cooled on ice for 2 min. Cell debris was removed by centrifugation for 15 min at 14000 *g*. The supernatant was transferred to a clean microcentrifuge tube and mixed with 400 µL isopropanol and 80 µL 5 M ammonium acetate by inverting the tube several times. The precipitated plasmid DNA was collected by centrifugation at 14000 *g* for 7 min. The pellet was washed with 500 µL 75% (v/v) ethanol and centrifuged for 5 min at 14000 *g*. The plasmid DNA was dried at 55 °C, dissolved in 50 µL ddH_2O containing 0.5 µL RNase A (10 mg mL^{-1} RNase A in ddH_2O) and stored at -20 °C.

BF buffer

8% (w/v)	Sucrose
0.5%	Triton X-100
50 mM	EDTA, pH 8.0
10 mM	Tris-HCl, pH 8.0

Plasmid DNA from *E. coli* used for sequencing required a high purity. Therefore, it was isolated using a plasmid preparation kit (NucleoSpin Plasmid Kit) as specified by the manufacturer.

2.12.3 Isolation of Bacmid DNA

Bacmid DNA was generated and amplified in *E. coli* DH10Bac cells containing the corresponding pFastBac1 construct. Therefore, cells were grown in 10 mL LB medium containing kanamycin, tetracycline and gentamicin at 37°C and 180 rpm. Bacmid DNA was isolated from 10 mL culture using the PureLink HiPure Plasmid Miniprep Kit according to the manufacturer's instructions.

2.12.4 Isolation of RNA

Total RNA was extracted using either the total RNA mini kit according to the manufacturers instructions or with Trizol according to the following protocol. Plant material from *A. thaliana* was harvested into 2 mL microcentrifuge tubes containing small ceramic beads and directly frozen in

liquid nitrogen. The plant tissue was homogenised for 30 sec at 6500 rpm in the Precellys homogeniser and subsequently stored in liquid nitrogen. The homogenate was resuspended in 1 mL Trizol and incubated for 2 min at room temperature. Cell debris was removed by centrifugation at 12000 *g* and 4 °C for 10 min. The supernatant was transferred to a clean microcentrifuge tube and incubated for 5 min at room temperature. 200 µL chloroform were added to the supernatant, mixed by vortexing and incubated for 3 min at room temperature. Phase separation was achieved by centrifugation at 12000 *g* and 4 °C for 15 min. The aqueous upper phase was transferred to a clean microcentrifuge tube, mixed with 500 µL isopropanol and incubated for 10 min at room temperature. RNA was pelleted by centrifugation at 12000 *g* and 4 °C for 10 min. The RNA pellet was washed with 500 µL 80% (v/v) ethanol and centrifuged for 10 min at 10000 *g* and 4 °C. After air drying, RNA was dissolved in 20 µL DEPC treated ddH_2O and stored at -20 °C for shorter periods and at -80 °C for long term storage.

DEPC-ddH_2O

ddH_2O was mixed with 0.1% diethyl pyrocarbonate (DEPC) and incubated over night at 37 °C. Afterwards the DEPC treated ddH_2O (DEPC-ddH_2O) was autoclaved twice to inactivate remaining DEPC.

Removal of Genomic DNA from RNA

Genomic DNA contamination in extracted RNA from *A. thaliana* tissue was removed by incubation with DNase using the Ambion TURBO DNA-free Kit as described by the manufacturer. Afterwards, the RNA quality was examined by formaldehyde gel electrophoresis (Chapter 2.12.13) and quantified by spectrophotometry (Chapter 2.12.5).

2.12.5 Quantification of Nucleic Acids

Nucleic acids were either quantified by spectrophotometry or by agarose gel electrophoresis. For spectrophotometric measurements of nucleic acids the NanoDrop spectrophotometer (PeQlab) was used. 1 µL of aqueous nucleic acid solution was applied to the machine's pedestal. Absorbances at 260 nm (A_{260}) and at 280 nm (A_{280}) were measured. The sample concentration was calculated by the software with the A_{260} value and a modified Beer-Lambert equation. The ratio of absorbance at 260 nm and 280 nm (A_{260}/A_{280}) was used to assess the purity of nucleic acids. A ratio of 1.8 indicated a high purity of DNA whereas a ratio of 2 indicated pure RNA.

For the second method, 1 µL of DNA was loaded on a 1% TAE gel (Chapter 2.12.12). The intensity of the DNA band in the gel was compared to a DNA standard with known concentration to estimate the concentration of the DNA sample.

2.12.6 cDNA Synthesis

DNA-free RNA was transcribed into complementary DNA (cDNA) using the First Strand cDNA Synthesis Kit according to the supplier's instructions. cDNA was synthesised using 500–1000 ng total RNA and oligo dT primers for the reverse transcription reaction. After transcription, the RNA was digested using RNase H. cDNA was stored at -20 °C for shorter periods and at -80 °C for long term storage.

2.12.7 Ligation

Insertion of DNA fragments into linearised plasmids was catalysed by T4 DNA ligase which forms a phosphodiester bond between two DNA strands in an ATP depending reaction. The concentrations of fragment and vector DNA were estimated by agarose gel electrophoresis (Chapter 2.12.12). For optimal ligation efficiency, a molar ratio of vector/insert of 1:3 to 1:5 was used. The ligation was carried out in a 10 µL reaction with 0.5 µL T4 DNA ligase (4000 units/µL) and 1 µL 10x T4 DNA ligase buffer containing ATP. The mixture was incubated for 30 min at room temperature (RT) or at 4 °C overnight.

For transformation into *E. coli* cells by electroporation, it was of importance that salt free plasmid DNA was used. Therefore the ligation reaction was desalted for 1 h on microdialysis membranes floating on ddH_2O in petri dishes.

2.12.8 Digestion of DNA by Restriction Endonucleases

Restriction endonucleases purchased from Thermo Scientific Fisher or New England Biolabs were used according to the supplier's instructions to cleave plasmid DNA. Reactions were set up in a volume of 50 µL. After incubation, fragments were separated by agarose gel electrophoresis (Chapter 2.12.12) and desired fragments were cut out from the gel. DNA was purified from the agarose with the NucleoSpin Gel and PCR Clean-up kit as specified by the manufacturer, eluted with 15–20 µL ddH_2O and stored at -20 °C or directly used.

For test purposes during cloning, plasmid DNA was digested in reactions of 10 µL. Restriction endonucleases were chosen in a way that the plasmid was cleaved at at least two sides, once in the insert and once in the vector backbone. To this end, either two enzymes were chosen that are active under the same reaction conditions or one enzyme was chosen that cuts at least twice.

2.12.9 Generation of Recombinant Bacmid

Recombinant bacmid containing a gene of interest was generated according to the Bac-to-Bac Baculovirus Expression System (Invitrogen) instructions. First, a recombinant pFastBac1 vector had

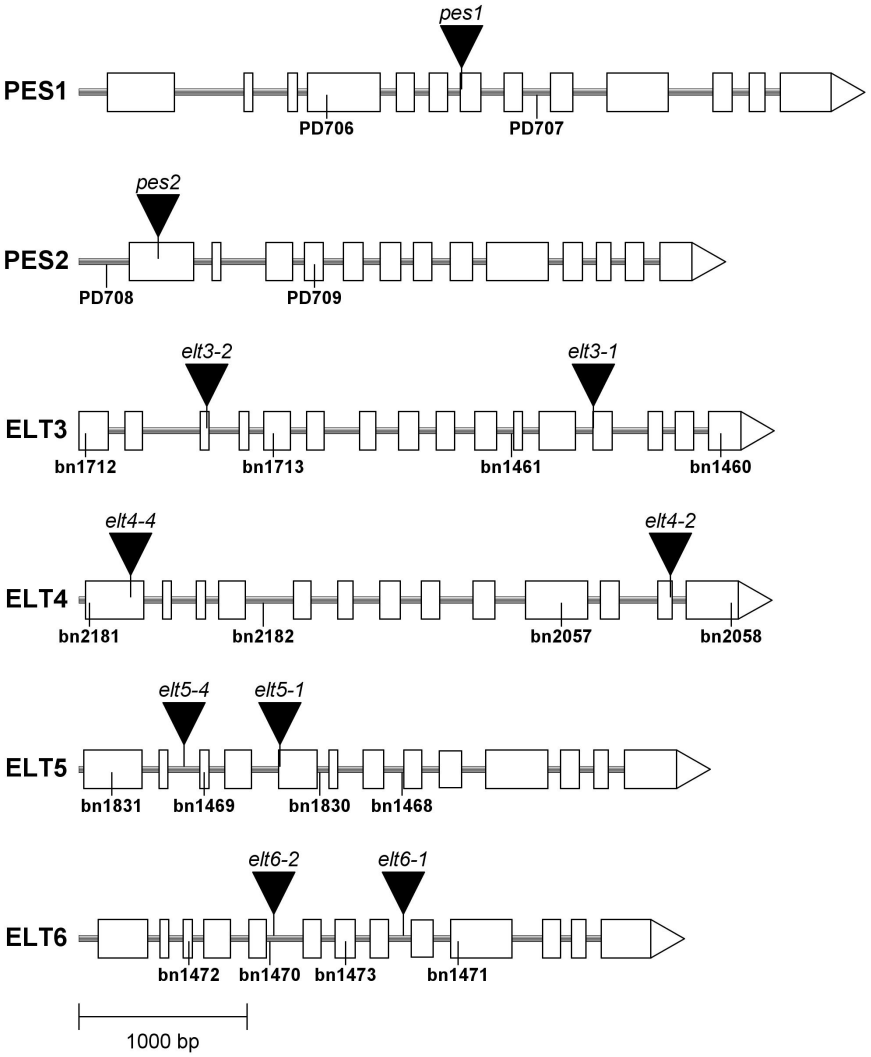

Figure 2.1 – Visualization of the gene structure of *ELT* genes with exons as white boxes and introns indicated by grey bars. Sites of insertions in the different insertion mutant lines are indicated with black triangles and labelled with the mutant designation. Black lines indicate the position of primers used for genotyping of insertion mutant lines. Structures were visualised with IBS 1.0 (Liu et al., 2015).

to be cloned. To this end, PES2 without transit peptide and with an N-terminal polyhistidine-tag (PES2oTP) was released from pQE30-PES2 by digestion with *EcoR*I and *Kpn*I (Chapter 2.12.8). pFastBac1 was linearised using the same enzymes and PES2oTP was ligated into the plasmid (Chapter 2.12.7), resulting in the construct pFastBac1-pES2oTP (Appendix Figure 7.1). pFastBac1-PES2oTP was transformed into electrocompetent *E. coli* Electroshox cells (Chapter 2.11.2). Positive clones were selected for ampicillin resistance. Chemically competent *E. coli* DH10Bac cells were transformed with purified pFastBac1-PES2oTP. Transformants were selected on LB plates containing kanamycin, gentamicin, tetracycline, X-gal and IPTG. White colonies were selected for analysis. DH10Bac cells contained a baculovirus shuttle vector (bacmid) with transposition target sites and a helper plasmid that supplied the cell with transposition proteins. As soon as the cell was transformed with the recombinant plasmid, transposition took place between bacmid and pFastBac1 vector. The successful transposition resulted in the disruption of the LacZα peptide. Consequently, positive clones lost the ability to hydrolyse X-gal, thus they remained as white colonies on medium containing IPTG and X-gal. These colonies were selected and further tested by PCR and digestion with restriction endonucleases (Chapter 2.12.8). Positive bacmid clones were isolated in a large scale and used for the transfection of insect cells (Chapter 2.11.12).

2.12.10 Polymerase Chain Reaction

The amplification of DNA fragments for different purposes was achieved by polymerase chain reaction (PCR). The process consisted in the repetition of a 3-step-cycle: denaturation at 94 °C resulting in single-stranded DNA molecules, annealing at 50–65 °C to allow hybridisation of synthetic oligonucleotides (primer) to the single-strand and elongation at 72 °C using a heat-stable DNA polymerase from *Thermus aquaticus* (*Taq* polymerase) that synthesised a new DNA strand complentary to the single-strand. Following PCR, agarose gel electrophoresis (Chaper 2.12.12) was employed to check the success of the reaction and/or to further purify and process the PCR products.

Genotyping of *A. thaliana* Insertion Mutants

All *A. thaliana* mutants described here were insertion mutants with either a T-DNA or a transposon insertion. These insertions provided the means to screen for mutant alleles by PCR. A combination of three primers was used (Table 2.12): two primers binding up- and downstream of the insertion site in the genome and one primer binding at the border sequence of the insertion (Figure 2.1). PCR products generated from one genomic primer and the insertion primer revealed a mutant allele while the two genomic primers can only produce a product on a wild type allele. Accordingly, a heterozygous mutant would show two different PCR products, one for the mutant allele and one

for the wild type allele, a homozygous mutant would show only PCR products for the mutant allele, while a wild type plant would only have one PCR fragment for the wild type allele.

PCR reaction for genotyping

2 µL DNA
0.2 µL *Taq* polymerase (5 U μL^{-1})
1 µL 10x buffer B
1 µL $MgCl_2$ (25 mM)
1 µL forward primer (10 pmol μL^{-1})
1 µL reverse primer (10 pmol μL^{-1})
1 µL insertion primer (10 pmol μL^{-1})
0.7 µL dNTPs (2 mM each)
ddH_2O ad 10 µL

PCR program for genotyping

95 °C	30 sec	
94 °C	10 sec	x 30
58 °C	30 sec	
72 °C	1.5 min	
72 °C	2 min	
15 °C	5 min	

Table 2.12 – Genotyping of T-DNA or transposon insertion mutants was conducted by PCR analysis on genomic DNA extracted from leaves. PCR reactions contained three primers, two primers binding left (L) or right (R) of the insertion in the genome and one primer binding at the left border (B) of the insertion. Because of indistinguishable fragment sizes, *elt4-2* was genotyped with two PCR reactions containing either L/R or L/B primers.

Mutant	Primer			Fragment Size [bp]		
	Left (L)	Right (R)	Border (B)	L/R	L/B	R/B
pes1	PD706	PD707	bn1832	1275	945	925
pes2	PD708	PD709	bn1832	1284	847	
elt3-1	bn1461	bn1460	bn1832	1265	609	909
elt3-2	bn1712	bn1713	bn126	1146		510
elt4-2	bn2057	bn2058	bn1832	1143	1194	
elt4-4	bn2181	bn2182	bn1920	1210		847
elt5-1	bn1469	bn1468	bn1832	1198	550	880
elt5-4	bn1831	bn1830	bn1832	1258	570	870
elt6-1	bn1470	bn1471	bn1832	1137	752	452
elt6-2	bn1472	bn1473	bn1474	952	735	435

Testing of bacterial colonies for insert-containing plasmids by PCR

After selection of plasmid containing *E. coli* clones with antibiotics, single *E. coli* colonies were used as template for PCR analysis to examine whether the plasmids contain the correct insert. Colonies were picked with pipette tips. Before transfer to the PCR reaction, colonies were dipped on a LB agar plate containing appropriate antibiotics as a reference plate. Plasmid DNA of the colony became available for PCR analysis during the initial heating step at 95 °C. For bacteria containing pJET1.2 constructs, pJET1.2 specific primers binding up- and downstream of the insert were used (bn2020/bn2021). All other constructs were tested with primers binding at the insert of interest.

PCR reaction for colony PCR

	colony as template
0.2 µL	*Taq*-polymerase (5 U μL^{-1})
1 µL	10x buffer B
1 µL	$MgCl_2$ (25 mM)
1 µL	forward primer (10 pmol μL^{-1})
1 µL	reverse primer (10 pmol μL^{-1})
0.7 µL	dNTPs (2 mM each)
	ddH_2O ad 10 µL

PCR program for colony PCR

95 °C	1 min	
94 °C	10 sec	x 30
58 °C	30 sec	
72 °C	2–2.5 min	
72 °C	2 min	
15 °C	5 min	

Amplification of coding sequences for cloning purposes

For the cloning of complete coding sequences from first strand cDNA or from cloned cDNA templates, a thermostable DNA polymerase with 3' - 5' exonuclease activity and low error rate (Q5 DNA polymerase) was used. Afterwards, extraction of PCR products from the agarose gel was conducted with the NucleoSpin Gel and PCR Clean-up kit as specified by the manufacturer. In the last step, DNA was eluted with 15–20 µL ddH_2O. Purified DNA was stored at -20 °C or directly used for ligation (Chapter 2.12.7).

PCR reaction for Q5 DNA polymerase

1 µL	DNA
0.5 µL	Q5 High-Fidelity DNA Polymerase
10 µL	5x Q5 reaction buffer
2.5 µL	forward primer (10 pmol μL^{-1})
2.5 µL	reverse primer (10 pmol μL^{-1})
1 µL	dNTPs (10 mM each)
	ddH_2O ad 50 µL

PCR program for Q5 DNA polymerase

98 °C	30 sec	
98 °C	10 sec	x 30
58 °C	30 sec	
72 °C	1 min	
72 °C	2 min	
4 °C	∞	

2.12.11 Expression Analysis

Semiquantitative RT-PCR

The expression of genes in several plant tissues and under different conditions was analysed by semiquantitative reverse transcription PCR (RT-PCR). Total RNA was isolated (Chapter 2.12.4) and DNA contamination was removed by DNase digestion. Afterwards, RNA was quantified by Nanodrop spectrophotometry and the quality was checked by RNA formaldehyde gel electrophoresis (Chapter 2.12.13). 500–1000 ng of total RNA was used for first strand cDNA synthesis with oligo dT primers. Primers used for RT-PCR were designed such that the length of fragments pro-

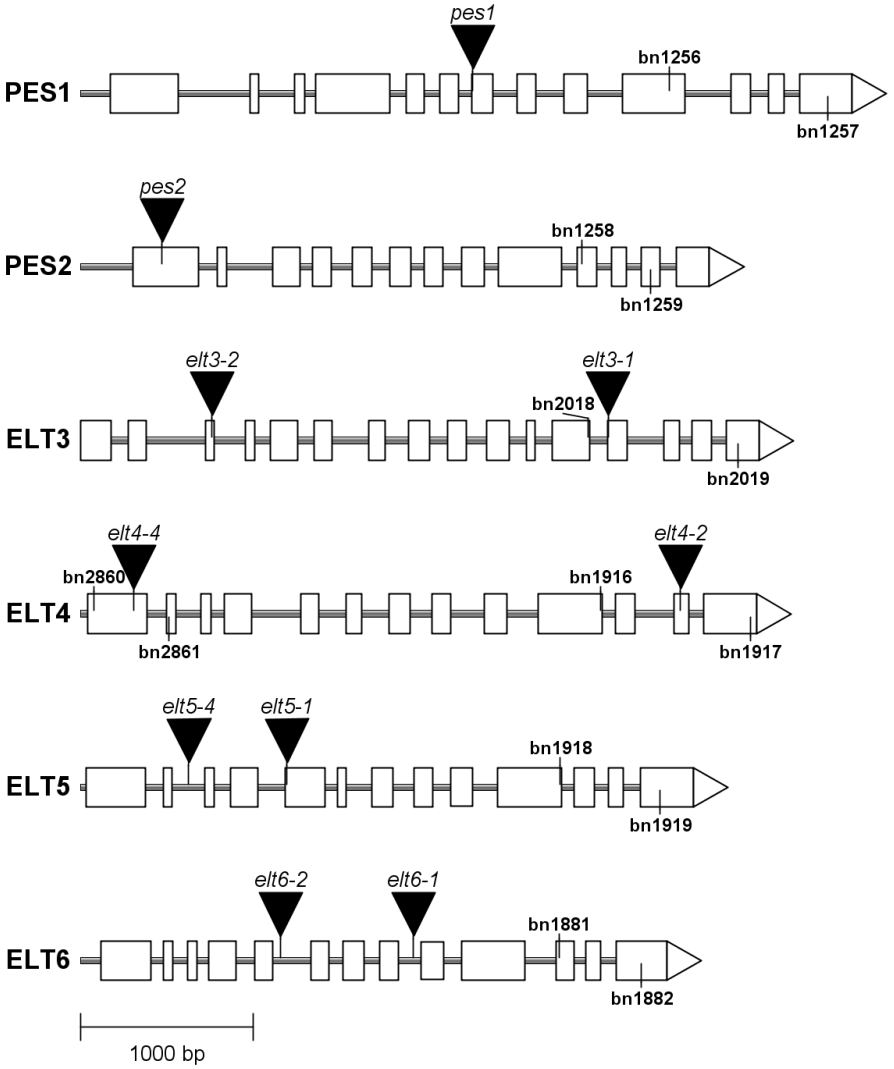

Figure 2.2 – Localisation of primers used for expression analysis. Sites of insertions in the different insertion mutant lines are indicated with black triangles and labelled with the mutant designation. Black lines point to the start of the respective primer with forward primers indicated above and reverse primers below the gene structure. In case of bn1916 and bn1918, the primer spans a splicing site (exon-exon junction). Structures were visualised with IBS 1.0 (Liu et al., 2015).

duced with cDNA as template differs from the fragment length produced with genomic DNA as template. Primer combinations are listed in Table 2.13 and depicted in Figure 2.2. The expression of the housekeeping gene *ACTIN2* (*ACT2*) was used to ensure that equal amounts of cDNA were used for the PCR analysis. *PES1*, *PES2* and *ACT2* were amplified with 30 cycles and *ELT3*, *ELT4*, *ELT5* and *ELT6* with 35 cycles.

PCR reaction for semiquantitative RT-PCR

x µL	cDNA
0.2 µL	*Taq* polymerase (5 U μL^{-1})
1 µL	10x buffer B
1 µL	$MgCl_2$ (25 mM)
1 µL	forward primer (10 pmol μL^{-1})
1 µL	reverse primer (10 pmol μL^{-1})
0.7 µL	dNTPs (2 mM each)
	ddH_2O ad 10 µL

PCR program for genotyping

95 °C	30 sec	
94 °C	10 sec	x 30/35
58 °C	30 sec	
72 °C	45 sec	
72 °C	2 min	
15 °C	5 min	

Table 2.13 – Expression analysis of ELT genes in different tissues was conducted by semi-quantitative RT-PCR.

Gene	Forward Primer	Reverse Primer	Genomic Product	cDNA Product
At1g54570 (PES1)	bn1256	bn1257	941 bp	480 bp
At3g26840 (PES2)	bn1258	bn1259	418 bp	247 bp
At3g26820 (ELT3)	bn2018	bn2019	887 bp	408 bp
At5g41120 (ELT4)	bn1916	bn1917	-	500 bp
At5g41120 (ELT4)	bn2860	bn2861	456 bp	344 bp
At5g41130 (ELT5)	bn1918	bn1919	-	342 bp
At3g02030 (ELT6)	bn1881	bn1882	500 bp	344 bp
At3g18780 (ACT2)	bn1854	bn1855	707 bp	629 bp

Quantitative PCR

The expression of genes was quantified by quantitative PCR (qPCR) with the StepOnePlus Real-Time PCR System (Applied Biosystems). Used primer combinations are listed in Table 2.14. Three technical replicates were employed. The reaction was set up in 20 µL volume. The housekeeping gene *Actin2* (*ACT2*) was used for the calculation of the relative gene expression according to the ΔΔCT method (Livak and Schmittgen, 2001).

PCR reaction for qPCR

4 µL 5x EvaGreen QPCR-Mix II (BioBudget)
5 µL cDNA 1:100 (v/v)
4 µL forward and reverse primer 1:1 (v/v), 2.5 µM each
7 µL ddH_2O

Table 2.14 – Expression analysis of PES2 was conducted by quantitative PCR.

Gene	Forward Primer	Reverse Primer	Product	Reference
At3g26840 (PES2)	bn2948	bn2949	107 bp	Zhang et al. (2014)
At3g18780 (ACT2)	bn2141	bn2142	108 bp	Charrier et al. (2002)

2.12.12 DNA Agarose Gel Electrophoresis

Separation of PCR products or restriction fragments was conducted by DNA agarose gel electrophoresis. To this end, 1% (w/v) agarose was melted in 1x Tris-acetate-EDTA (TAE)-buffer and ethidium bromide (EtBr) was added to a final concentration of 2.5 µg mL^{-1} prior to pouring. DNA samples were mixed with 1/5 vol of 6x loading dye. The GeneRuler 1 kb DNA ladder was used for approximate quantification of fragment sizes. Electrophoresis was carried out at 120 V in 1x TAE buffer. The DNA-EtBr complexes were visualised under UV light at a wavelength of 312 nm.

TAE buffer (50x)

2 M	Tris
1 M	Acetic acid
50 mM	EDTA

6x loading dye

10 mM	Tris-HCl (pH 7.6)
0.03% (w/v)	Bromophenol blue
0.03% (w/v)	Xylene cyanol FF
60% (w/v)	Glycerol
60 mM	EDTA (pH 7.6 adjusted with NaOH)

2.12.13 RNA Formaldehyde Gel Electrophoresis

The quality and quantity of extracted total RNA from plant tissues were analysed by formaldehyde gel electrophoresis prior to first strand cDNA synthesis. To this end, agarose in ddH_2O was melted in the microwave oven and mixed with MOPS buffer, pH 8.0. Formaldehyde was added to the mixture after cooling and the gel was immediately poured. 500–1000 µg total RNA dissolved in water was diluted to a volume of 10 µL with DEPC-ddH_2O and mixed with 2 x RNA sample loading buffer. Prior to loading, the samples were incubated at 65 °C for 10 min to denature the RNA. Electrophoresis was conducted at 90 V for 30 min. The RNA-EtBr complexes were visualised under UV light at a wavelength of 312 nm.

10x MOPS Buffer

0.2 M	MOPS
50 mM	Sodium acetate
10 mM	Na-EDTA

adjusted to pH 7 or pH 8 with NaOH

2x RNA Sample Loading Buffer

65% v/v	Formamide
8% v/v	Formaldehyde
1.3% w/v	1x MOPS, pH 8
54 µL mL^{-1}	Ethidium bromide

Agarose Gel

1.5% (w/v)	Agarose
6% v/v	Formaldehyde

in 1x MOPS, pH 8

RNA Running Buffer

10% (w/v)	Formaldehyde

in 1x MOPS, pH 7

2.12.14 Polyacrylamide Gel Electrophoresis

For the separation of denatured proteins according to their electrophoretic mobility, SDS-polyacrylamide gel electrophoresis (PAGE) was employed (Laemmli, 1970). The binding of SDS to the polypeptide chain provides an even distribution of negative charges that results in a separation by approximate size.

Ammonium persulfate (APS) and tetramethylethylenediamine (TEMED) were added to the separating gel to initiate polymerisation. The gel was directly poured between a glass plate and an alumina plate in a gel caster and overlayed with isopropanol. After polymerisation, which took about 30 min, the isopropanol was removed. Polymerisation of the stacking gel was initiated by addition of APS and TEMED and the gel was loaded on top of the polymerised separating gel. Combs were inserted into the liquid gel to build slots. Protein samples were mixed with 1/3 vol 4x sample loading buffer and incubated for 5 min at 95 °C. 10 µL of protein sample were loaded into one slot. A prestained protein standard was used for approximate quantification of fragment sizes. Electrophoresis was conducted first at 25 mA per mini gel (8 cm x 8 cm) and 200 V until the dye front reached the separating gel. Then the current was increased to 30 mA.

For proteins from bacterial pellets, 1 mL of bacteria culture was harvested by centrifugation for 1 min at 14000 *g* and the supernatant was discarded. The pellet was resuspended in 80 µL OD_{600}^{-1} ddH_2O and 50 µL OD_{600}^{-1} 4x sample buffer were added. Samples were incubated for 5 min at 95 °C prior to loading on the gel.

5x Sample Loading Buffer

500 mM	Tris
10% (w/v)	SDS
50% (v/v)	Glycerol
0.025% (w/v)	Bromophenol blue
5 mM	EDTA
pH 6.9 with HCl	

4 x reducing sample loading buffer was prepared by the addition of 1/8 vol β-mercaptoethanol and 1/8 vol ddH_2O to 5 x sample buffer.

10% Separating Gel

6.25 mL	40% Acrylamide/Bis-acrylamide stock (29:1 v/v)
6.25 mL	1.5 M Tris-HCl pH 8.8
250 µL	10% (w/v) SDS
12.1 mL	ddH_2O
10 µL	TEMED
150 µL	10% (w/v) APS

4% Stacking Gel

1 mL	40% Acrylamide/Bis-acrylamide stock (29:1 v/v)
2.5 mL	0.5 M Tris-HCl pH 6.8
100 µL	10% (w/v) SDS
6.3 mL	ddH_2O
5 µL	TEMED
100 µL	10% (w/v) APS

5x Tank buffer

125 mM	Tris
960 mM	Glycine
0.5% (w/v)	SDS

2.12.15 Coomassie staining

After electrophoresis the stacking gel was cut off from the separating gel, transferred to a glass jar and covered with staining solution. The solution with the gel was heated up in the microwave oven until the boiling point of the staining solution was reached, and then gently shaken for 5 min. The staining solution was removed, the gel washed once with tap water and covered with destaining solution. The gel was again boiled for a short moment in the microwave oven and then gently shaken for 5 min. Afterwards the solution was replaced with fresh destaining solution and again shortly boiled. The destaining procedure was repeated until the desired discolouration was reached.

Staining solution

50% (v/v)	Ethanol
7% (v/v)	Acetic acid
0.252% (w/v)	Coomassie R250

Destaining solution

5% (v/v)	Glycerol
7.5% (v/v)	Acetic acid

2.12.16 Western Blot

For the detection of specific proteins in a complex protein mixture by immunodetection, the proteins were transferred from a polyacrylamide gel to a nitrocellulose membrane by semi-dry blotting. To this end, six blotting papers and a nitrocellulose membrane were cut in the size of the polyacrylamide gel and together with the gel soaked in Towbin transfer buffer for 5 min. Afterwards they were stacked on the anode in the following order: three blotting papers, nitrocellulose membrane, polyacrylamide gel, three blotting papers. The cathode was placed on top. Blotting was conducted at 15 V and 70 mA per mini gel (35 mA for a half mini gel, 4 cm x 8 cm).

Towbin transfer buffer (Towbin et al., 1979)

25 mM	Tris base
192 mM	Glycine
20% (v/v)	Methanol
0.1% (w/v)	SDS

2.12.17 Immunodetection

Immunodetection was used for the specific detection of proteins in a complex protein mixture on a nitrocellulose membrane. For blocking of protein binding sites, the nitrocellulose membrane was incubated in blocking solution (2% bovine serum albumine (BSA) in TBST buffer) for one hour at room temperature with gentle shaking or overnight at 4 °C without shaking. The HisDetector Nickel-HRP Conjugate was diluted 1:10 000 to 1:20 000 in blocking solution, poured onto the membrane and incubated for one hour at room temperature with gentle shaking. Afterwards the membrane was washed three times by incubation for 15 min in TBSTXSB buffer under gentle shaking. For the detection reaction, the substrate for the horseradish peroxidase (HRP) was placed on the membrane. The signal was detected on x-ray film.

TBST buffer

20 mM	Tris-HCl pH 8.0
0.05% (v/v)	Tween 20
150 mM	NaCl

TBSTXSB buffer

10 mM	Tris-HCl
0.9% (w/v)	NaCl
0.02% (w/v)	NaN_3
0.1% (v/v)	Triton X-100
0.05% (w/v)	SDS
0.1% (w/v)	BSA

2.13 Methods in Biochemistry

2.13.1 Chloroplast Isolation

Intact chloroplasts from leaf tissues were isolated according to a protocol modified from Hiltbrunner et al. (2001) and Vidi et al. (2006).

The amount of plant material was adjusted for each plant species. For the isolation of chloroplasts from *S. lycopersicum* cv. Micro-Tom, leaves of six plants were used. For the isolation from infiltrated *N. benthamiana* leaves, a minimal amount of 24 completely infiltrated leaves were used. Prior to isolation, plants were kept in dark for 18 h to minimise the starch content. Starch crystals can disrupt intact chloroplasts during centrifugation steps and therefore the amount of starch should be as low as possible. Leaves were collected into ice cold tap water and incubated in the dark for 20–30 min. Leaves were crushed in 50 mL HB buffer using a homogeniser that is equipped

with wing knives at 15000 rpm for 10 sec. While homogenising, the homogeniser flask was cooled with ice cold water. The mixture was filtered through two layers of Miracloth and centrifuged for 3 min at 2500 rpm and 4 °C. The supernatant was discarded and the pellet was carefully resuspended in 1–2 mL RB buffer using a very soft horsehair brush. A percoll gradient was prepared with 40% and 85% (v/v) percoll in RB buffer. The chloroplast suspension was carefully loaded onto the gradient and centrifuged for 30 min at 2500 *g* and 4 °C using an ultracentrifuge equipped with a swing-out rotor. The 40% percoll phase was removed and intact chloroplasts were harvested from the interphase (1–4 mL). The chloroplast suspension was filled up to 15 mL with RB buffer to wash away the percoll. Chloroplasts were pelleted by centrifugation for 5 min at 4000 *g* and 4 °C. The pellet was resuspended in 1 mL chloroform/methanol/formic acid 1:1:1 (v/v/v), internal standard (I.S.) was added and mixed by vortexing. 1 mL chloroform and 500 µL 1 M KCl/0.2 M H_3PO_4 were added and vortexed. Phases were separated by centrifugation for 5 min at 4000 *g*. The organic phase was dried under air flow and lipids were dissolved in 1 mL chloroform. For the determination of phospho- and galactolipid content, 20 µL lipid extract were mixed with 20 µL standard mix and 160 µL chloroform/methanol/300 mM ammonium acetate (300:600:35, v/v/v). The remaining chloroform extract was dried under air flow and dissolved in hexane prior to solid phase extraction (Chapter 2.13.3).

HB buffer

450 mM	Sorbitol
20 mM	Tricine/KOH pH 8.4
10 mM	EDTA pH 8.5
10 mM	$NaHCO_3$
1 mM	$MnCl_2$

RB buffer

300 mM	Sorbitol
20 mM	Tricine/KOH pH 7.6
2.5 mM	EDTA pH 8.5
5 mM	$MgCl_2$

2.13.2 Preparation of Lipid Extracts

Extraction of Total Lipids

The extraction of lipids used for Q-TOF MS/MS analysis was performed according to a modified protocol from Bligh and Dyer (1959).

Total lipids were extracted from plant leaf material with 50–100 mg fresh weight or 10–20 mg dry weight. Leaves were harvested and boiled in ddH_2O for 20 min to prevent degradation by lipases (Roughan et al., 1978). Lipids were extracted from the leaf material by vortexing in 1 vol chloroform/methanol 1:2 (v/v). I.S. were added except for phospho- and galactolipid standards, which were later added. The lipid extract was transferred to a clean glass vial. The extraction was repeated with 1 vol chloroform/methanol 2:1 (v/v) and 1 vol chloroform. All extracts were combined. The remaining leaf material was dried under a fume hood to determine the dry weight. The crude lipid extract was mixed with 1 vol 1 M KCl/0.2 M H_3PO_4. Phases were separated by centrifugation for 5 min at 2500 *g*. The organic phase was dried under air flow and lipids were dissolved either in hexane prior to solid phase extraction (SPE) (Chapter 2.13.3) or in 200 µL chloroform/methanol/300 mM ammonium acetate (300:600:35, v/v/v) prior to Q-TOF MS/MS analysis (Chapter 2.13.10). For the determination of phospho- and galactolipid content, lipids were dissolved in 1 mL chloroform. 20 µL of lipids dissolved in chloroform were mixed with 20 µL standard mix and 160 µL chloroform/methanol/300 mM ammonium acetate (300:600:35, v/v/v).

Extraction of Non-Polar Lipids

Non-polar lipids such as TAGs, sterol esters (SEs), wax esters (WEs), FAPEs, FAXEs and WDEs were extracted from plant material using a diethyl ether based protocol. To this end, 50–100 mg fresh or 10–20 mg dry plant material or 5–10 mg dry seeds or bacterial pellet obtained by centrifugation were used. Tissues were frozen in liquid nitrogen and disrupted for 30 sec at 6000 rpm in the Precellys homogeniser. 1 nmol I.S. was added. For the quantification of FAPEs and WDEs 17:0-phytol, for the quantification of WEs 17:0-18:0ol, for the quantification of TAGs a mixture of tri10:0- and tri11:0-TAG and for the quantification of SEs a mixture of 16:0-cholesterol, 16:1-cholesterol, 18:0-cholesterol and 18:1-cholesterol was used. Lipids were extracted with 500 µL diethyl ether and 250 µL 1 M KCl/ 0.2 M H_3PO_4. After vortexing, samples were centrifuged for 3 min at 5000 *g* for phase separation. The organic phase was transferred to a clean vial. The extraction with diethyl ether was repeated twice and lipid extracts were combined. The solvent was evaporated and lipids were dissolved either in hexane for SPE (Chapter 2.13.3) or in 200 µL chloroform/methanol/300 mM ammonium acetate 300:665:35 (v/v/v) for Q-TOF MS/MS analysis (Chapter 2.13.10).

2.13.3 Lipid Purification by Solid Phase Extraction

Non-polar ester lipids were purified and enriched by SPE according to vom Dorp et al. (2013) and Tulloch (1973). Silica columns were equilibrated three times with 1 mL hexane. Lipids were

dissolved in hexane and loaded onto the silica column. FAPEs, fatty acid farnesyl esters (FAFEs), SEs and WEs were eluted from the column with 3 x 1 mL hexane/diethyl ether 99:1 (v/v). WDEs were eluted with 3 x 1 mL hexane/diethyl ether 98:2 (v/v) (Tulloch and Hoffman, 1974). TAGs were eluted with 3 x 1 mL 95:5 (v/v) hexane/diethyl ether. Solvents were evaporated under air flow and purified lipids were either dissolved in 200 µL chloroform/methanol/300 mM ammonium acetate 300:665:35 (v/v/v) for Q-TOF analysis or further processed for GC-MS analysis (Chapter 2.13.9).

2.13.4 Thin-Layer Chromatography

Non-polar lipids were separated on Silica 60 Durasil-25 plates with hexane/ diethyl ether/ acetic acid as the mobile phase. For WEs analysis a ratio of 90:10:1 (v/v/v), for TAGs analysis 70:30:1 (v/v/v), and for FAXEs analysis 50:50:1 (v/v/v) was employed. TLC developing tanks were filled with 100 mL of the solvent mixture and solvent vapour was allowed to saturate the tank for at least 10 min prior to developing. The amount of lipid extract corresponding to 10 mg dry weight of plant tissue was dissolved in chloroform, loaded on a line 2 cm above the bottom of the TLC plate and the solvent was evaporated. "Birkenöl" is a mixture of jojoba oil (containing WEs) and apricot seed oil (containing TAGs) and was used as a standard. To this end, the oil was diluted 1:100 (v/v) in chloroform and 10 µL were loaded in one spot on the TLC plate. TLC plates were developed for 50–60 min.

After development, TLC plates were dried and stained with primuline according to White et al. (1998). To this end, a 5% (w/v) stock solution of primuline in water was diluted 100-fold in acetone/water 8:2 (v/v). TLC plates were sprayed evenly with primuline solution using a Preval sprayer. Lipids were visualised under UV-light. For the analysis of FAXEs, TLC plates were not stained as spots were already visible by the yellow colour of the xanthophylls.

For lipid isolation from silica material, lipid spots were scraped off using a razor blade. Silica material was transferred to chloroform/methanol 1:2 (v/v) in a glass vial and sonicated until it was finely dispersed. Afterwards, 1 vol chloroform/methanol 2:1 (v/v), 1 vol chloroform and 1 vol 1 M KCl/0.2 M H_3PO_4 were added and mixed by vortexing. Phase separation was achieved by centrifugation for 5 min at 2500 *g*. The organic phase was transferred to a clean glass vial and dried under air flow. Lipids were either dissolved in 200 µL chloroform/methanol/300 mM ammonium acetate 300:665:35 (v/v/v) for Q-TOF MS/MS analysis (Chapter 2.13.10) or further processed for GC-MS analysis (Chapter 2.13.9).

2.13.5 Synthesis of Fatty Acid Methyl Esters

The fatty acid composition of ester compounds was analysed after formation of their respective methyl esters. With the transesterification reaction, the organic group of an alcohol was replaced by the methyl group of methanol.

Acid Catalysed

Fatty acid methyl esters were synthesised acid-catalysed according to Browse et al. (1986). To this end, up to 8 mL of lipid extract or 5 seeds of *A. thaliana* were mixed with 1 mL 1 N methanolic hydrochloric acid and 5 µg pentadecanoic acid (15:0) as I.S. The mixture was incubated at 80 °C for 20 min (lipid extracts) or 60 min (seeds). After cooling down to room temperature, 1 mL 0.9% sodium chloride and 1 mL hexane were added and mixed by vigorously shaking. Samples were centrifuged for 3 min at 1000 rpm for phase separation. Because fatty acid methyl esters (FAMEs) are soluble in hexane, the hexane phase was transferred to a new glass vial and concentrated under air stream. For short chain FAMEs, which are volatile, samples were not dried completely. FAMEs were dissolved in 100 µL hexane, transferred to autosampler glass vials with inserts and quantified by GC-FID (Chapter 2.13.8).

Base Catalysed

Fatty acid methyl esters from wax diesters were produced by base-catalysed methanolysis. Lipids were dissolved in 1 mL chloroform and mixed with 1 mL 0.6 M methanolic sodium hydroxide. The mixture was incubated at 40 °C for 4 h. After the addition of 750 µL ddH_2O and vigorously shaking, phases were separated by centrifugation for 3 min at 1000 rpm. The lipophilic phase was concentrated under air stream and free alcohols were derivatised in 100 µL BSTFA for 16 h at room temperature or for 30 min at 80 °C. BSTFA was evaporated, lipids were dissolved in 100 µL hexane, transferred to autosampler glass vials with inserts and analysed by GC-MS (Chapter2.13.9).

2.13.6 Chemical Synthesis of Fatty Acid Esters

Via the Formation of Acyl Chlorides

FAPEs, WEs, and 1,16-16:0diol diesters were synthesised according to Gellerman et al. (1975). 0.2 mmol or 0.4 mmol fatty acids for mono or diesters, respectively, were dissolved in 1 mL toluene, mixed with 0.28 mmol oxalyl chloride and incubated for 1.5–2 h at 60–65 °C in a water bath. The solvent, hydrochloric acid and oxalyl chloride were removed under a nitrogen gas stream. Acyl chlorides were dissolved in 1 mL diethyl ether. 0.2 mmol alcohol and 0.25 mL dry

pyridine were added and incubated for 2–3 h at 80 °C. Esters were extracted twice with hexane and applied to a TLC plate (Chapter 2.13.4). Esters were isolated from the TLC plate and eluted from the silica gel with chloroform or hexane. For quantification, esters were transmethylated (Chapter 2.13.5) and FAMEs were measured by GC-FID (Chapter 2.13.8).

Via the Formation of Fatty Acid Anhydrides

1,2-16:0diol diesters were synthesised according to Kanda and Wells (1981), modified by Sten Stymne.

30 µmol alcohol was transferred to a 6 mL screw cap tube and the solvent was evaporated under nitrogen gas. Aliquots of benzene were twice added and evaporated under nitrogen gas to remove residual amounts of water. Water-free alcohols were dissolved in 300 µL trifluoroacetic acid (TFA), the tube was flushed with nitrogen and sealed with a PTFE-packed screw cap.

30 µmol fatty acids were transferred to a clean vial, dissolved in benzene and dried under nitrogen. Aliquots of benzene were twice added and evaporated under nitrogen gas to remove residual amounts of water from the fatty acids. 60 µL trifluoroacetic anhydride was added to the water-free fatty acids, the tube was flushed with nitrogen, sealed with a PTFE-packed screw cap and vortexed continuously for 5 min. Unreacted trifluoroacetic anhydride was removed under a nitrogen stream. The alcohol dissolved in TFA was added to the fatty acid anhydride, the tube was flushed with nitrogen and sealed with a PTFE-packed screw cap. The mixture was vortexed continuously for 5 min.

Solvents were evaporated under a nitrogen gas stream. The synthesised WDEs were dissolved in 2 mL chloroform/methanol 1:1 (v/v) and vortexed. Afterwards 500 µL of 1 M KCl/0.2 M H_3PO_4 were added and mixed by vortexing. Phases were separated by centrifugation for 5 min at 2500 *g*. The chloroform phase was harvested and lipids were separated and purified by TLC (Chapter 2.13.4).

2.13.7 Chemical Synthesis of Acyl-CoA

Acyl-coenzyme A (acyl-CoA) with saturated or unsaturated fatty acids of different chain lengths were synthesised according to a protocol of Sánchez et al. (1973) modified by Sten Stymne.

30 µmol of free fatty acids were transferred to a 6 mL tube with PTFE-sealed screw cap and the solvent was evaporated under a nitrogen gas stream. Aliquots of benzene were twice added and evaporated under a nitrogen gas stream to remove the water from the fatty acids. Fatty acids were dissolved in 500 µL dichloromethane (CH_2Cl_2) and 5 µL triethylamine and the mixture was thoroughly vortexed. The tube was flushed with nitrogen, closed with a PTFE-packed screw cap and incubated for 30 min at room temperature. Afterwards, the tube was cooled down on ice.

3.6 µL of ethyl chloroformate ($ClCOOC_2H_5$) were added and the tube was closed with a PTFE-sealed screw cap. The mixture was vortexed shortly and incubated on ice for 2 h. Afterwards, the solvents were evaporated under a nitrogen gas stream. 1.5 mL tetrahydrofuran was added and precipitations, that had formed, were dispersed by sonication. After centrifugation, the supernatant was transferred to a clean tube with a magnetic stir bar, which was used at a later point (see below). The precipitation, that had been obtained by centrifugation, was mixed with 1 mL tetrahydrofuran. After sonication and centrifugation, the supernatants were combined. The tetrahydrofuran was evaporated under a nitrogen gas stream. The dried mixed anhydrides were dissolved in 300 µL tetrahydrofuran and cooled down on ice.

20 mg CoA (lithium salt) was dissolved in 1 mL ice cold 1 M $KHCO_3$. Immediately after dissolving, the CoA solution was added to the mixed anhydrides dissolved in tetrahydrofuran. The tube was flushed with nitrogen gas and closed with a PTFE-packed screw cap. The reaction was incubated for 90 min at room temperature under rapid stirring with the magnetic stir bar so that the tetrahydrofuran was finely dispersed in the aqueous solution.

Afterwards, the excess tetrahydrofuran was evaporated under nitrogen gas. 2 M HCl was added dropwise to neutralise the solution until the precipitate, which formed upon HCl addition, no longer immediately dissolved. Then one additional last drop was added. Do not add too much HCl, because excess addition of HCl could result in the hydrolysis of acyl-CoAs. Foam that can potentially form can be removed by a short centrifugation. The precipitate was harvested by centrifugation. The pellet was washed two times by resuspending it in 2 mL 0.1 M HCl, sonication and centrifugation. Through the addition of 2 mL diethyl ether to the pellet and a following centrifugation step, unreacted anhydrides and free fatty acids were removed. This washing step was repeated twice. Subsequently, diethyl ether was evaporated under nitrogen gas. Acyl-CoAs were dissolved in ddH_2O and a drop of 1 M $KHCO_3$ was added in case the solution was opaque. Acyl-CoAs were checked for the presence of free fatty acids by TLC (Chapter 2.13.4) and quantified by methylation (Chapter 2.13.5) followed by GC-FID analysis (Chapter 2.13.8). Aliquots of acyl-CoAs were stored in tubes flushed with nitrogen gas at -80 °C.

2.13.8 Gas Chromatography-Flame Ionisation Detection

The quantification of fatty acid containing lipids was conducted by gas chromatography with flame ionisation detector. Prior to analysis, fatty acids were transesterified to methyl esters (Chapter 2.13.5). FAMEs were separated on a Supelco SP-2380 column with an Agilent gas chromatograph with flame ionisation detection. The amount of lipid derived FAMEs was calculated by the ratio of their peak areas to the area of the I.S. methyl pentadecanoate. This method was used to quantify internal standards for lipid measurements, to determine the fatty acid content of seeds and to

investigate the fatty acid composition of FAXEs.

Parameters for GC-FID analysis

gas chromatograph: Agilent 7890 coupled with FID

column: Supelco SP-2380

- length: 25 m
- inside diameter: 0.32 mm
- film thickness: 0.1 µm

carrier gas: Helium

flow rate: 1.2 mL min^{-1}

injection: 2 µL

FID:

- heater: 270°C
- H_2 flow: 30 mL min^{-1}
- air flow: 400 mL min^{-1}

temperature program:

initial	120°C	hold for 2 min
25°C min^{-1}	up to 160°C	
2°C min^{-1}	up to 170°C	
10°C min^{-1}	up to 250°C	hold for 2 min
40°C min^{-1}	down to 120°C	

2.13.9 Gas Chromatography-Mass Spectrometry

The identification of compounds was conducted by GC-MS. Extracted lipids were purified, if necessary, and dried under air flow. In case of free hydroxyl group containing compounds, lipids were dissolved in 50 µL MSTFA and derivatised for 30 min at 80°C. MSTFA was evaporated and lipids were dissolved in 100 µL hexane. Not-derivatised lipids were directly dissolved in hexane. Samples were transferred to autosampler vials with inserts. Lipids were analysed according to Roessner et al. (2000). Compounds were identified based on their mass spectra either with the National Institute of Standards and Technology (NIST) mass spectral library or by comparison to the mass spectra of in-house synthesised standards.

Parameters for GC-MS analysis

gas chromatograph: Agilent 7890

mass spectrometer: Agilent 5975C inert XL MSD

column: Agilent HP-5MS

- length: 30 m
- inside diameter: 0.32 mm
- film thickness: 0.1 μm

carrier gas: Helium

flow rate: 2 mL min^{-1}

injection: 1 μL

temperature program:

initial	70°C	hold for 5 min
5°C min^{-1}	up to 310°C	hold for 1 min
equilibrate	70°C	hold for 6 min

2.13.10 Lipid Analysis by Q-TOF MS/MS

FAFEs, FAPEs, phospho- and galactolipids, SEs, TAGs, WDEs, and WEs were measured by targeted quadrupole-time-of-flight MS/MS (Q-TOF MS/MS). Lipids were extracted and purified as described before (Chapters 2.13.2 and 2.13.3) and dissolved in chloroform/methanol/300 mM ammonium acetate 300:665:35 (v/v/v). Samples were directly infused using an Agilent HPLC-Chip Cube MS interface with a flow rate of 1 μL min^{-1}. The Chip Cube was equipped with an HPLC-Chip that harbours a nano-electrospray tip. This very thin needle gives rise to a fine spray of charged droplets that contain the analyte. Collision induced dissociation (CID) was applied for fragmentation. The collision energy was optimised for each lipid class. Targeted lists with mass-to-charge ratio (m/z) values of the desired lipids were programmed and deployed. Lipid species were quantified either by neutral loss scanning or by product ion scanning, depending on the lipid class. In the course of raw data processing, isotopic correction of intensities was implemented. Quantities were calculated relative to the respective I.S. and related to the weight or cell density of the sample. For the measurement of farnesyl esters and wax diesters, intensities were related to 17:0-phytol. Detailed information about targeted lists, adduct ions, collision energies and type of scanning can be found in the Appendix 7.1.

Parameters for Q-TOF analysis

instrument:	Agilent Series 6530 Accurate Mass Q-TOF LC-MS instrument with Chip Cube source
infusion chip:	FIA Chip II flow injection and infusion
solvent:	chloroform/methanol/300 mM ammonium acetate 300:665:35 (v/v/v)
flow rate:	1 µL min^{-1}
injection:	5 µL
drying gas:	8 L min^{-1} nitrogen
fragmentor voltage:	200 V
gas temperature:	300°C
HPLC-Chip V_{cap}:	1700 V
Scan rate:	1 spectrum sec^{-1}

3 Results

3.1 Characterisation of the ELT Family Proteins

Upon chlorophyll degradation, the released phytol can be esterified with fatty acids to form fatty acid phytyl esters (Grob and Csupor, 1967). The genome of *A. thaliana* contains six sequences that code for putative acyltransferases and that show sequence similarity to esterases, lipases and thioesterases, designated as *ELT* genes (Lippold et al., 2012). Two of these enzymes were identified as Phytyl Ester Synthases, *PES1* (synonymous ELT1) and *PES2* (synonymous ELT2), that catalyse the synthesis of fatty acid phytyl esters and that are highly expressed under senescence. As the remaining members of the ELT family were not characterised yet, one objective of this work was the characterisation of these four genes, *ELT3*, *ELT4*, *ELT5* and *ELT6*.

3.1.1 Expression Analysis of *ELT* Genes in Different Tissues of *A. thaliana*

The expression of *PES1* and *PES2* is highly increased under chlorotic stress such as senescence or nitrogen deprivation (Lippold et al., 2012). To find out whether this is also true for the other four *ELT* genes, their expression was examined in different tissues of soil grown *A. thaliana* Col-0 plants as well as in senescent leaves of soil grown plants and in senescent leaves of plants grown on synthetic medium devoid of nitrogen (-N). Total RNA was extracted and cDNA was generated by reverse transcription. Expression levels were assessed by semi-quantitative RT-PCR. *ACTIN2* (*ACT2*) was used as a housekeeping gene to normalise the amount of cDNA used for PCR.

PES1 and *PES2* show the highest expression in senescent leaves and under nitrogen deprivation (Figure 3.1), as previously reported. In addition, *PES1* is also expressed in the inflorescence. The expression of *ELT3* is increased in plants grown under nitrogen deprivation as compared to the expression in plants grown on complete synthetic medium (+N). *ELT3* is also expressed in senescent leaves from soil grown plants and in inflorescences, but this expression is lower than under -N. *ELT4* is also highly expressed under -N and its expression is slightly increased compared to +N. In addition, *ELT4* is expressed in senescent leaves and in inflorescences. In contrast to the previous genes, the expression of *ELT5* and *ELT6* is not upregulated in senescent leaves or under

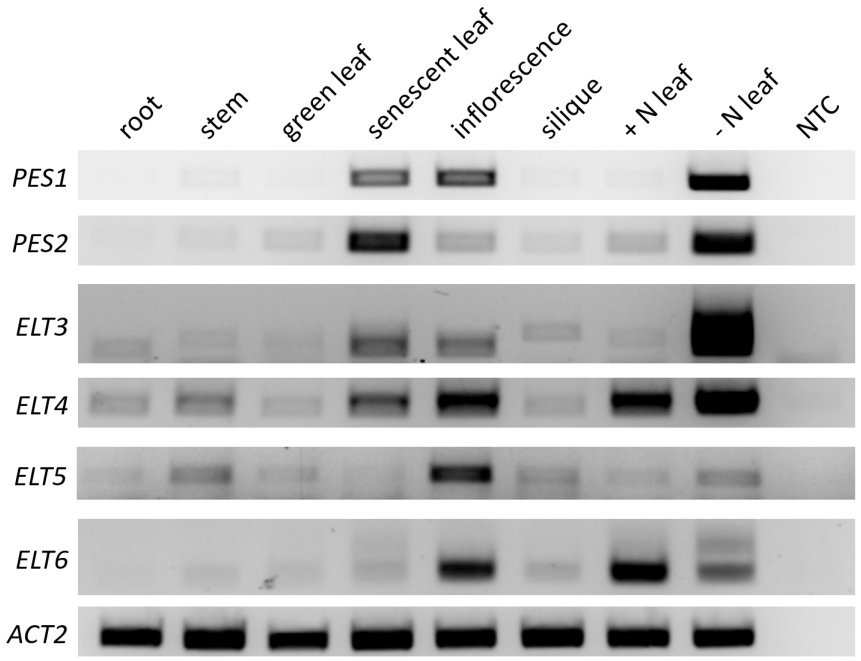

Figure 3.1 – The expression of *ELT* genes in different tissues of *A. thaliana* was analysed by semi-quantitative RT-PCR. Total RNA was isolated from roots, stems, leaves, inflorescences, and siliques of soil grown plants. For -/+N samples, plants were grown on synthetic medium either containing nitrogen sources (+N) or devoid of nitrogen (-N). The "no template control" (NTC) was used as a negative control. RT-PCR products were separated by agarose gel electrophoresis and stained with EtBr.

-N. *ELT5* is mainly expressed in the inflorescences and *ELT6* shows the highest expression in inflorescences and under +N, but not in soil grown green leaves.

3.1.2 Identification of Homozygous Insertion Mutant Lines

The analysis of mutants in which the gene of interest is disrupted, is a common approach to investigate the function of the gene and its product. One mechanism to disrupt a gene is the insertion of DNA. This can be achieved either by *A. tumefaciens* mediated DNA transfer or by transposition with the *Activator (Ac)/Dissociation (Ds)* system from maize. Because the sequence of the insertion fragment is known, the mutation site can be retrieved. As a consequence, the locus of insertion of a mutant plant can be easily sequenced and genotyped by PCR to identify heterozygous and homozygous lines. Two insertion mutant lines for each *ELT* gene were obtained from stock centres (Table 2.10). For *PES1* and *PES2*, a double homozygous mutant, *pes1pes2*, with two T-DNA insertions was already available. Seeds that were received from the seed stock centre were mostly heterozygous. Hence, they had to be propagated and screened for homozygous plants. The genotyping of the two mutant types, T-DNA insertion and transposon insertion, was conducted by PCR with a three primer system. Two primers are gene specific and bind up- and downstream of the insertion site. The third primer is specific for the insertion. Each T-DNA and transposon

collections of *A. thaliana* mutant lines have their own specific insertion fragments. The primer binding in this sequence was located at one of the boarders of the insertion. Figure 2.1 provides an overview of the gene structures of the *ELT* genes with the sites of insertion indicated by black triangles and the binding sites of the gene specific primers.

Seeds obtained from the seed stock centres were germinated and plants were once genotyped with two primers per PCR reaction to confirm the functioning of the primers and the presence of the respective insertion. Routinely, plants were genotyped with the three primer system in a single PCR reaction as described before, except for *elt4-2*. Since *ELT4* and *ELT5* show a very high sequence identity, designing gene-specific primers was complicated. Therefore, it was not possible to design primers which enabled the differentiation of the wild type PCR product from the mutant product by fragment size. Therefore, it was not possible to genotype *elt4-2* with a three primer PCR reaction, but it had to be genotyped with two PCR reactions containing different primer combinations. Homozygous plants were successfully identified for all insertion mutant lines (Figure 3.2). For *elt3-1*, *elt5-1*, *elt5-4*, *elt6-1* and *elt6-2*, PCR products for both primer combinations that included the insertion boarder are obtained. This indicates the existence of two T-DNA copies inserted in tandem where the two T-DNA left boarders are flanked by plant DNA and the right boarders are connected to each other in the centre.

In a null mutation, the disruption of a gene by insertional mutagenesis is expected to lead to the complete loss ("knock-out") of the transcription. Once homozygous insertion mutant plants were identified, the expression of the respective genes was analysed by semi-quantitative RT-PCR and compared to the expression in the wild type Col-0. Tissues for RNA isolation were selected according to the expression analysis of *ELT* genes in different tissues of *A. thaliana* shown above (Chapter 3.1.1-B). Total RNA was isolated from nitrogen deprived leaf material of *pes1pes2*, *elt3-1*, *elt3-2*, *elt4-2* and *elt4-4* and from flowers of *elt5-1*, *elt5-4*, *elt6-1* and *elt6-2* soil grown plants. The locations of the primers are depicted in Figure 2.2. The amount of cDNA used for PCR was adjusted such that the expression of the housekeeping gene *Actin2* (band intensity in the agarose gel) was equal in all samples. In *pes1pes2*, the expression of *PES1* and *PES2* is highly decreased but a small residual expression is left. However, the fragments amplified by RT-PCR localise 3' to the insertion sites in *pes1* and *pes2*. Therefore, the insertions might result in null mutations, but expression of a non-functional truncated sequence comprising the 3' part of the gene might be observed. *elt3-1* and *elt3-2* show no expression of *ELT3*, indicating a complete knock-out of the gene. In *elt4-2*, the T-DNA insertion is located in the 12th exon of *ELT4* (Figure 3.3-A). By using primers that bind close the 3'-end of the cDNA, up- and downstream of the insertion (bn1916/bn1917), no PCR product is obtained, but primers that bind at the 5'-end of the cDNA (bn2860/bn2861) give a product that shows the same intensity as compared to the wild type. In

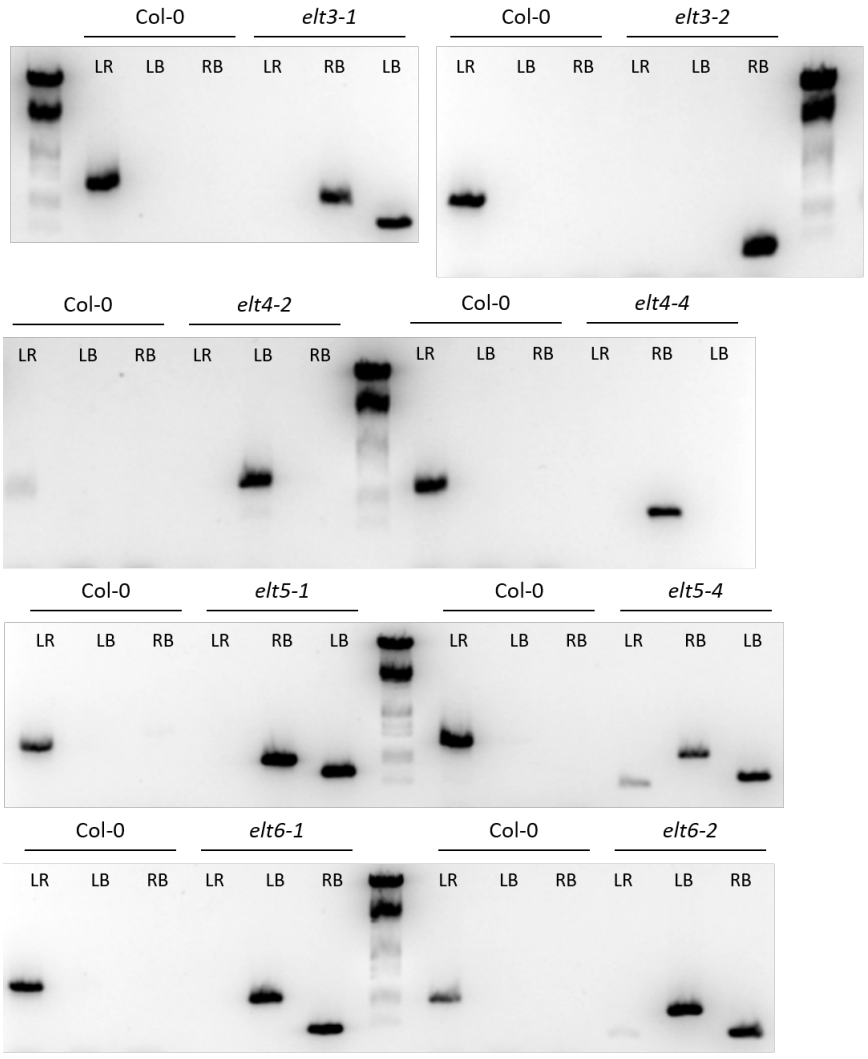

Figure 3.2 – Genotyping of T-DNA or transposon insertion mutants was conducted by PCR analysis of genomic DNA extracted from leaves. As a negative control DNA from *A. thaliana* Col-0 was used. Three primers in different combinations were used: two primers binding upstream (L, left) or downstream (R, right) from the insertion in the genome and one primer binding at the left border (B) of the insertion. Expected fragment sizes are listed in Table 2.12. PCR products were separated by agarose gel electrophoresis and gels were stained with EtBr. The faint bands that are visible with the primer combination LR in the *elt5-4* and *elt6-2* gels are non-specific PCR products.

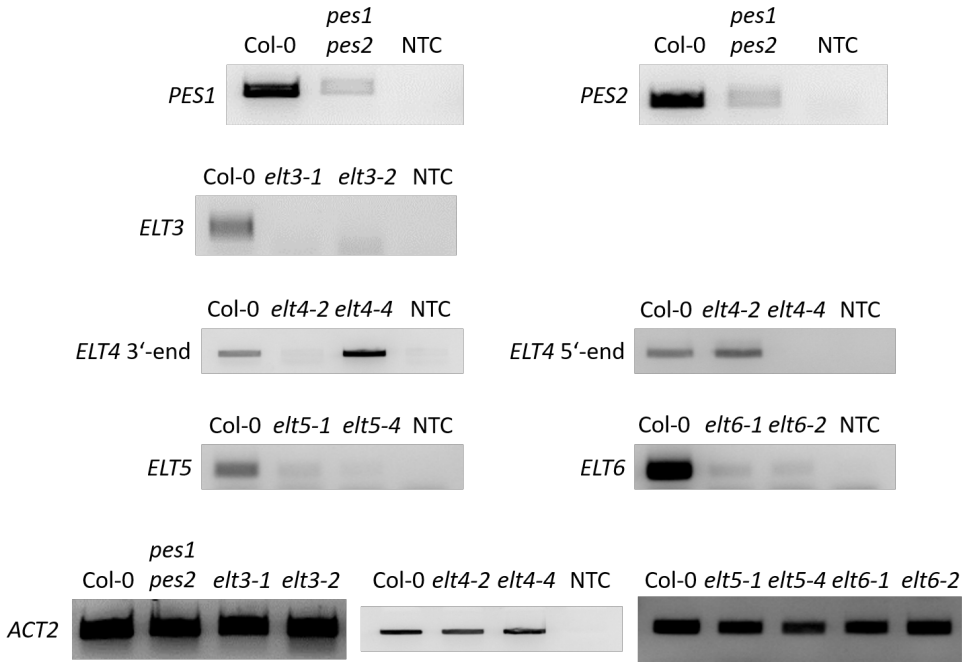

Figure 3.3 – The expression of *ELT* genes in different insertion mutant lines of *A. thaliana* was analysed by semi-quantitative RT-PCR. Total RNA was isolated from nitrogen deprived leaves (*pes1pes2*, *elt3-1*, *elt3-2*, *elt4-2*, *elt4-4*) or flowers (*elt5-1*, *elt5-4*, *elt6-1*, *elt6-2*) of plants grown on plate or soil, respectively. For nitrogen deprived samples, plants were grown on synthetic medium devoid of nitrogen. RT-PCR products were separated by agarose gel electrophoresis and stained with EtBr. The "no template control" (NTC) was used as a negative control. The gene names on the left side of the gels indicate the used primers with exact primer combinations and expected fragment sizes given in Table 2.13. Localisations of primers are depicted in Figure 2.2. For *ELT4* two different primer combinations were used, one binding at the 3'-end of the cDNA and one at the 5'end.

elt4-4 it is the same but vice versa. The T-DNA insertion in *elt4-4* is located in the second exon. 3'-end primers (bn1916/bn1917) generate a PCR product comparable to the wild type, 5'-end primers that bind around the site of insertion produce no product. In *elt5-1*, *elt5-4*, *elt6-1* and *elt6-2* only minor residual expression of *ELT5* or *ELT6*, respectively, is detected. Because similar to *PES1* and *PES2*, the primers are localised close to the 3'-end of the gene, the RT-PCR fragments detected in *elt5-1*, *elt5-4*, *elt6-1* and *6-2* presumably are derived from non-functional, truncated mRNAs.

3.1.3 FAPE Content in Insertion Mutant Lines under Nitrogen Deprivation

Previously, it had been shown that FAPEs accumulate during chlorotic stress, such as nitrogen deprivation, when chlorophyll is degraded (Gaude et al., 2007). Therefore, nitrogen deprivation is employed as a model system to generate chlorotic stress. To answer the question if ELT3, ELT4, ELT5 and ELT6 also have phytyl ester synthase activity, as it was demonstrated for PES1 and PES2 (Lippold et al., 2012), the FAPE content of homozygous mutant lines was examined under nitrogen deprivation. To this end, seeds were germinated and grown for seven days on MS plates. Plants were transferred to fresh medium and incubated for further seven days. Afterwards plants were

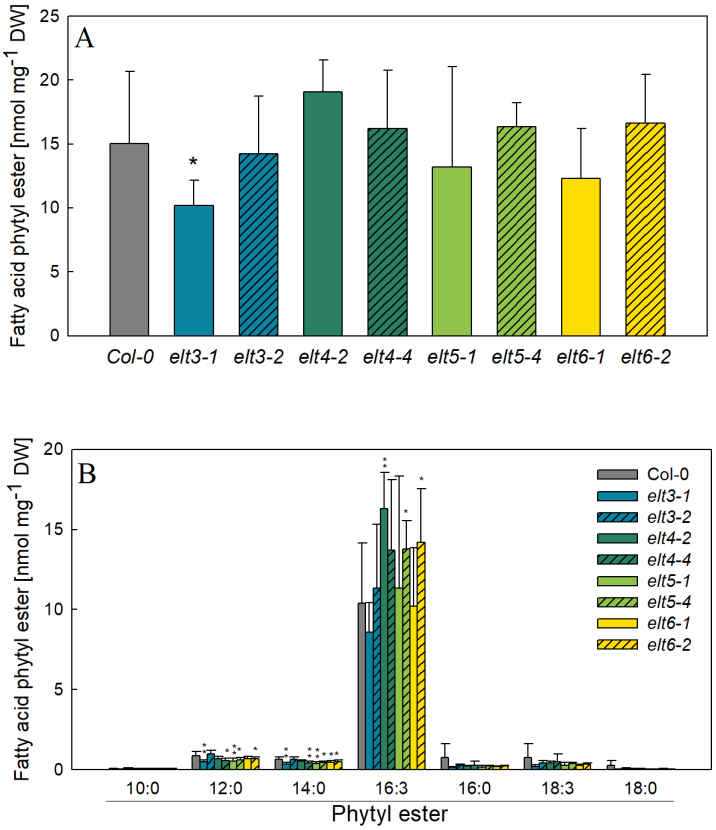

Figure 3.4 – Quantification of the FAPE content in ELT single insertion mutant lines under nitrogen deprivation. Plants were grown on synthetic medium devoid of nitrogen for 14 days. Lipids were isolated, FAPEs purified by SPE and quantified by Q-TOF MS/MS. A – Total FAPE amounts. B – Fatty acid distribution of FAPEs. Bars represent the means of 8–10 replicates with error bars indicating the SD. Significant differences compared to wild type are indicated with ** $P < 0.01$, * $P < 0.05$ according to Student's t-test.

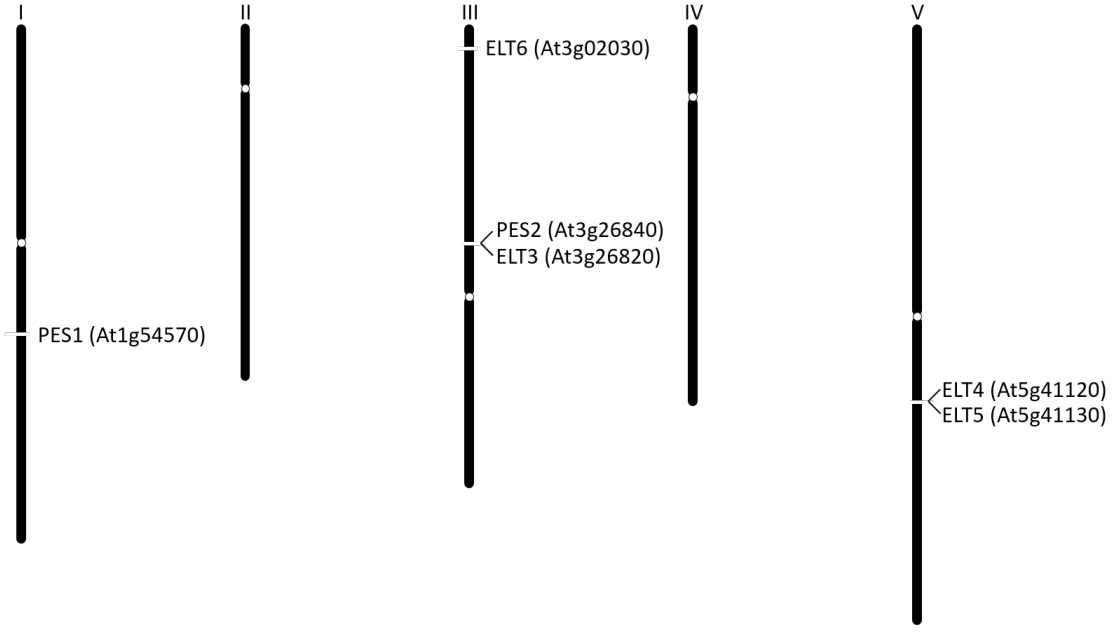

Figure 3.5 – Locations of the six *ELT* genes on the *A. thaliana* chromosomes I to V.

transferred to plates containing synthetic medium devoid of nitrogen (-N) for in total 14–21 days, depending on the visual signs for chlorophyll degradation, i.e. the degreening of the leaves. In between, plants were transferred to fresh medium every seven days. Lipids were isolated from yellow plants, FAPEs were purified by SPE and quantified by Q-TOF MS/MS. The total amount of accumulated FAPEs under nitrogen deprivation ranges between 10 and 15 nmol mg^{-1} DW. The amount of FAPEs in *elt3-1* is reduced in comparison to the wild type but not in the *elt3-2* line. Beside that, there were no significant differences between the *ELT* mutants and wild type (Figure 3.4-A). The fatty acid distribution of FAPEs was similar in all lines, 16:3-phytol was the main FAPE molecular species with lower amounts of 12:0-, 14:0- 16:0 and 18:3-phytol (Figure 3.4-B). The amount of 12:0- or 14:0-phytol was significantly reduced in *elt3-1*, *elt4-4*, *elt5-1*, *elt5-4*, *elt6-1* and *elt6-2* and the amount of 16:3-phytol was increased in *elt4-2*, *elt5-4* and *elt6-2* compared to wild type. Although the differences are significant, there is no strong difference between the absolute amounts of wild type and mutants. These results do not allow the conclusion to be drawn whether the ELT enzymes are phytyl ester synthases.

3.1.4 Generation of Multiple ELT Mutants

The analysis of FAPEs under nitrogen deprivation in single ELT mutant lines showed no differences in comparison to the wild type (Chapter 3.1.3). Possibly the loss of function of one ELT gene is compensated by another ELT gene. To test this hypothesis, multiple mutants were generated by crossing of different mutant plants. For *PES1* and *PES2*, a homozygous double mutant *pes1pes2* was already available (Lippold et al., 2012). This double mutant shows no growth retardation and a strong reduction in FAPEs under control conditions as well as under nitrogen deprivation. It is highly decreased in 12:0-, 14:0- and 16:3-phytol, but still contains 16:0- and 18:3-phytol.

For the generation of additional double and triple mutants, different aspects have to be taken into account. First, the location of the *ELT* genes in the genome of *A. thaliana*. *PES2* and *ELT3* are located in tandem on chromosome 3 (Figure 3.5). *ELT6* is also located on chromosome 3, but further afar from *PES2*/*ELT3*. *ELT4* and *ELT5* are localised in tandem on chromosome 5. *PES1* is located on chromosome 1.

Second, the mechanisms by which the recombination of different alleles can occur. On the one side, interchromosomal recombination takes place, that is the new combination of complete chromosomes from two different parent lines during meiosis. On the other side, during intrachromosomal recombination two different alleles are newly arranged by crossing-over. Interchromosomal recombination occurs with a relative frequency of 50% while intrachromosomal recombination occurs with a relative frequency of 0–50%, depending also on the distance of the two alleles on the chromosome. Taken this into consideration, generating a double mutant with two different mutant

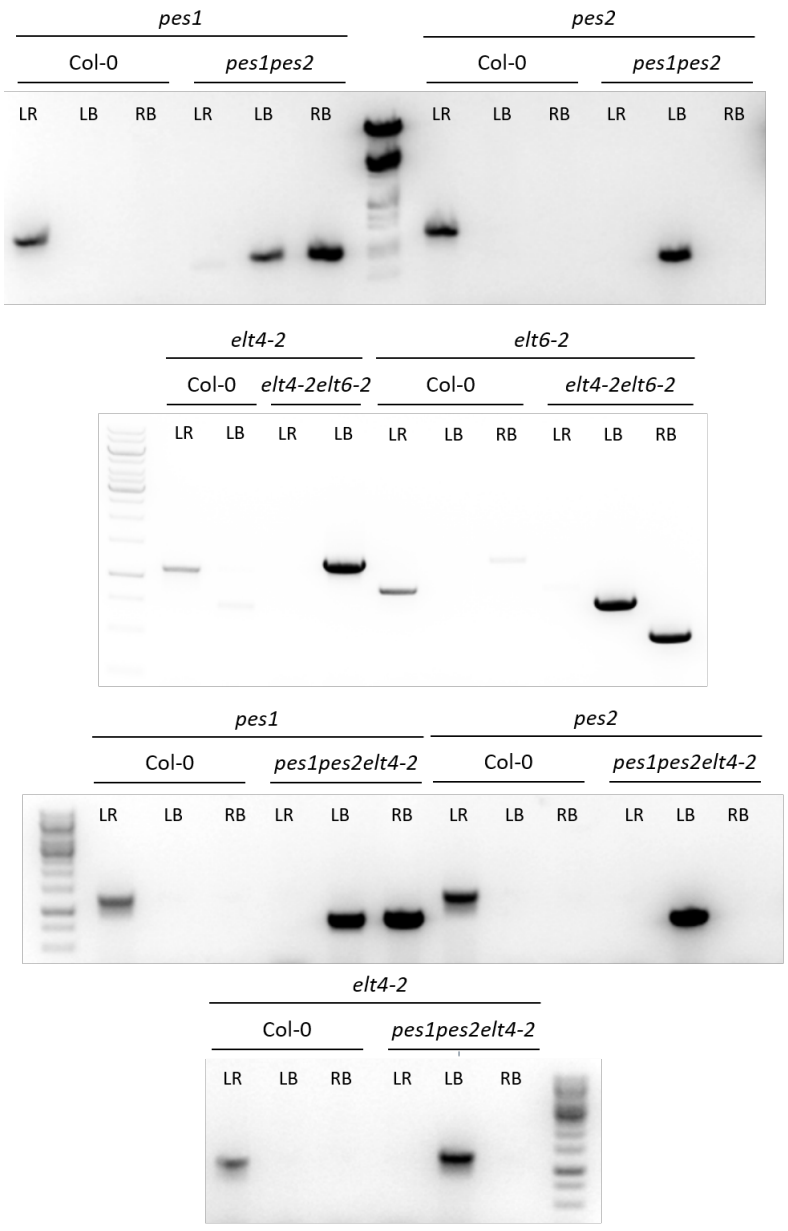

Figure 3.6 – Genotyping of multiple T-DNA insertion mutants was conducted by PCR analyses of genomic DNA extracted from leaves. As a negative control DNA from *A. thaliana* Col-0 plants was used. Three primers in different combinations were used: two primers binding upstream (L, left) or downstream (R, right) from the insertion and one primer binding at the left border (B) of the insertion. PCR products were separated by agarose gel electrophoresis and gels were stained with EtBr. The labelling of the gels indicates the analysed loci, the genotype and the primer combination. Expected fragment sizes and primers are listed in Table 2.12.

alleles that are located close to each other on the same chromosome, by normal plant crossing is not possible as the chance of a crossing-over between these two is nearly zero. In general, because of the higher frequency, interchromosomal recombination should be preferred.

Considering these two aspects, it was decided to cross *pes1pes2* with a mutant line of *ELT4* or *ELT5* to obtain a new triple mutant by interchromosomal recombination. In the end, *elt4-2* was chosen because the expression of *ELT4* is also upregulated under nitrogen deprivation as it is the case for *PES1* and *PES2*, resulting in the triple mutant *pes1pes2elt4*. As *ELT6* is not yet part of a multiple mutant, it was decided to cross *elt4-2* with *elt6-2* to generate the new double mutant *elt4elt6*.

Plants were crossed and the F1 generation as well as the existing *pes1pes2* were genotyped by PCR. In the F1 generation, only *PES1pes1PES2pes2ELT4elt4* and *ELT4eltELT5elt5* genotypes were found which is in accordance with the Mendelian inheritance. For *elt4elt6*, in the F2 generation several double homozygous mutants were identified (Figure 3.6). For the new *pes1pes2elt4* triple mutant, the F2 generation was screened for plants that are homozygous in at least one locus and heterozygous in the other two loci. These plants were then further propagated. In the F3 generation, plants were screened for at least two homozygous loci and one heterozygous locus. One plant was identified that is homozygous for all three mutations (Figure 3.6).

3.1.5 FAPE Content in ELT Multiple Mutants Under Nitrogen Deprivation

The three ELT multiple mutants, *pes1pes2*, *elt4elt6* and *pes1pes2elt4*, were characterised regarding their FAPE content in the leaves of plants grown under nitrogen deprivation. Lipids were isolated, FAPEs purified by SPE and analysed by Q-TOF MS/MS. The amount of FAPEs under nitrogen deprivation in Col-0 is approximately 13 nmol $mg^{-}1$ DW (Figure 3.7-A). *elt4elt6* shows a slight but not significant decrease in FAPE content with 10 nmol $mg^{-}1$ DW. In *pes1pes2* the previously described strong reduction in FAPE content is visible. The additional mutation in *pes1pes2elt4* does not lead to a further decrease in FAPE content in comparison to *pes1pes2*. The *elt4-elt6* double mutant shows no difference in fatty acid composition of FAPEs in comparison to Col-0, where 16:3-phytol is the main FAPE species accompanied with lower amounts of 12:0-, 14:0-, 16:0- and 18:3-phytol. The strong decrease in total FAPE content of *pes1pes2* is due to the loss of 12:0-, 14:0- and 16:3-phytol. 16:0- and 18:3-phytol are slightly increased in comparison to the wild type. In *pes1pes2elt4* no difference could be detected in comparison to *pes1pes2*.

3.1.6 FAPE Content is Decreased in Seeds of ELT Multiple Mutants

Previously, it was shown that FAPEs accumulate in leaves that undergo chlorotic stress (Ischebeck et al., 2006; Gaude et al., 2007). Nevertheless, chlorophyll is not only degraded in response to

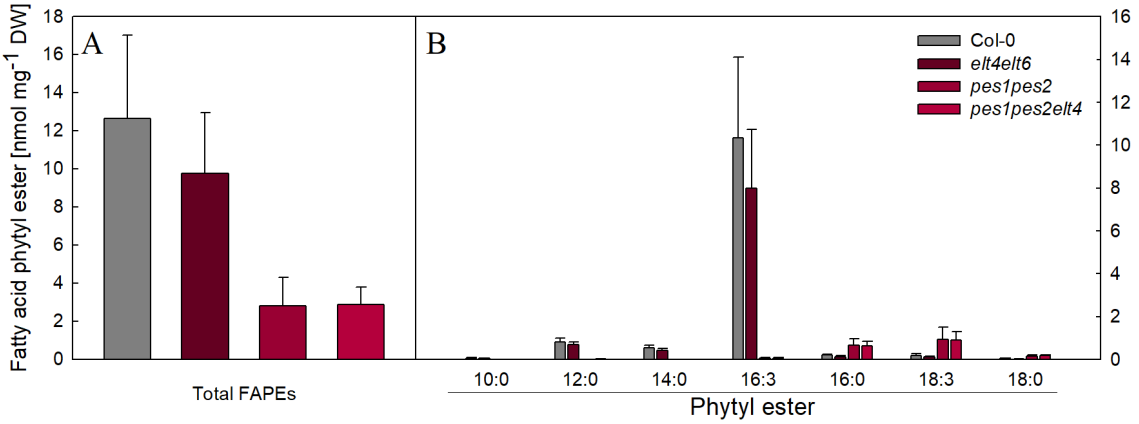

Figure 3.7 – Quantification of the FAPE content in leaves of ELT multiple insertion mutant plants grown under nitrogen deprivation. Lipids were isolated, FAPEs purified by SPE and quantified by Q-TOF MS/MS. A – Total FAPE amounts. B – Fatty acid distribution of FAPEs. Bars represent the means of 4–5 replicates with error bars indicating the SD.

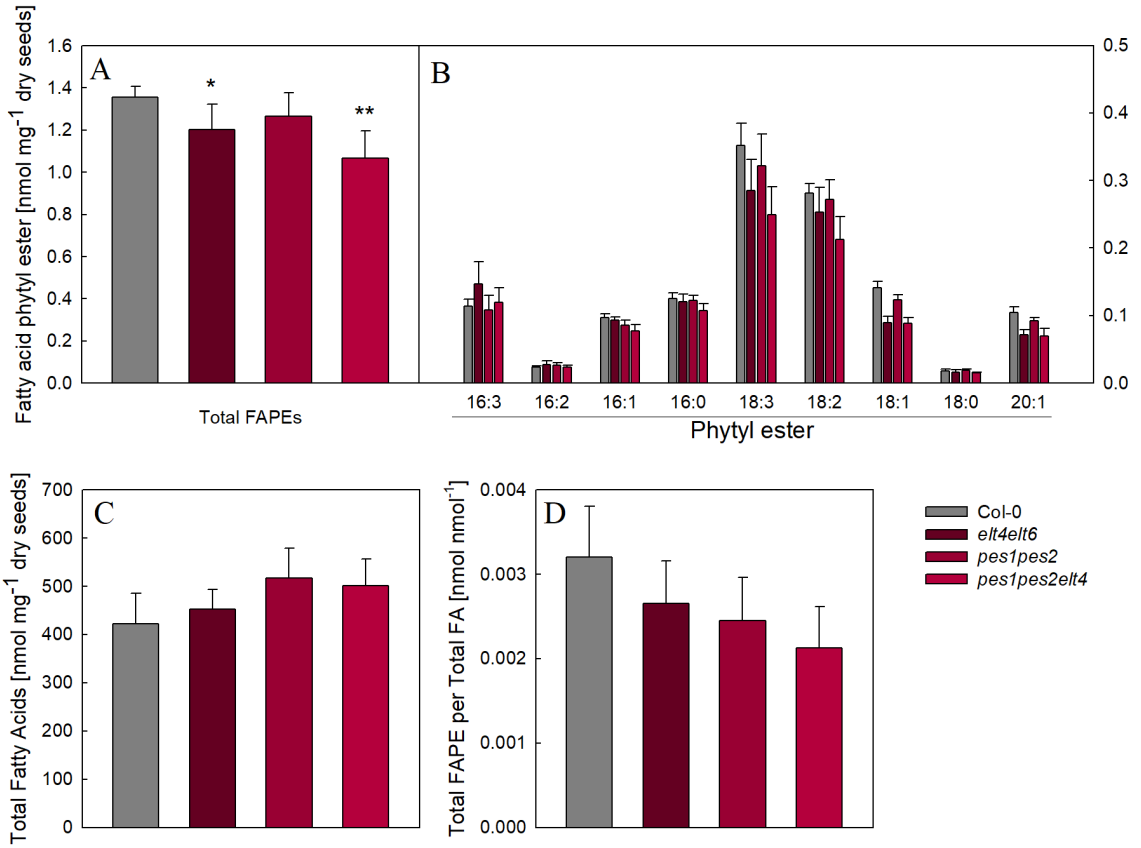

Figure 3.8 – FAPE content in seeds of ELT multiple mutants. Lipids were isolated from homogenised seeds, FAPEs were purified by SPE and quantified by Q-TOF MS/MS. A – Total FAPE amounts. B – Fatty acid distribution of FAPEs. C – Total fatty acids were extracted, transesterified to FAMEs and measured by GC-FID. D – Total FAPE amounts were correlated to total fatty acid amounts. Bars represent the means of 4–5 replicates with error bars indicating the SD. For D the SD was calculated as followed. The SDs of A and C were calculated as percentage of the means, these values were added together resulting in the total SD in percent. The total SD in percent was used for the calculation of the error bars of D. Significant differences compared to wild type are indicated with ** $P < 0.01$ and * $P < 0.05$ according to Student's t-test.

biotic or abiotic stresses but also in the course of the plant life cycle such as during fruit ripening or seed development. Whenever chlorophyll is degraded, it is likely that some of the released phytol is incorporated into FAPEs. Kanwischer (2007) demonstrated that in the course of the first 15 days after anthesis, FAPEs accumulate in the developing seeds. It is not yet known, which enzymes are responsible for the FAPE production in seeds. To investigate the impact of *ELT* genes on seed FAPE accumulation, the FAPE content in ELT multiple mutants was determined. Seeds were homogenised using the Precellys homogeniser and lipids were extracted. FAPEs were purified by SPE and quantified by Q-TOF MS/MS. Col-0 seeds contain around 1.3 nmol FAPEs $mg^{-}1$ dry seeds (Figure 3.8-A). While the amount of FAPEs in *pes1pes2* seeds is similar to that of the wild type, it is decreased by 0.15 nmol $mg^{-}1$ dry seeds in *elt4elt6* and by 0.3 nmol $mg^{-}1$ dry seeds in *pes1pes2elt4* in comparison to the wild type. FAPEs from Col-0 seeds contain mostly 18:3 and 18:2, and smaller amounts of 16:3, 16:2, 16:1, 16:0, 18:1 and 20:1 fatty acids (Figure 3.8-B). Therefore, the fatty acid composition of FAPEs in seeds is strongly different from that of leaves, because seeds accumulate C18 fatty acids (18:3, 18:2) in their FAPEs, while leaves mostly contain 16:3 and lower amounts of 12:0 and 14:0. The reduction in *elt4elt6* and *pes1pes2elt4* can be observed in all FAPE species, in particular 18:3, 18:2, 18:1 and 20:1, but not for 16:3-phytol, which is slightly increased in the two lines.

The reduction in FAPE content could be due to the fact that the seeds in general have a decreased total lipid content. This would be the case, for instance, if the seed development would be affected because of increased stress of the parental plant. If the seeds would have a decreased total lipid content, the FAPE content would not be decreased when related to the total lipid amount. Then the phenotype would not be a reduction in FAPEs but rather a reduction of all lipids. To exclude this possibility, the total fatty acid content of the seeds was determined. Therefore, methyl esters were produced from total seed lipids. FAMEs were quantified by GC-FID. The total fatty acid amount is highest in *pes1pes2* and lowest in Col-0 (Figure 3.8-C). The total FAPE amount was related to total fatty acid amount (Figure 3.8-D). According to this calculation, the FAPE amount is highest in Col-0, decreased in *elt4elt6* and *pes1pes2* and lowest in *pes1pes2elt4*. This result confirms the specific reduction of FAPEs in *elt4elt6* and *pes1pes2elt4* compared to the wild type.

3.1.7 Feeding of ELT Multiple Mutant Plants with Different Alcohols

To investigate the ester synthase activities of the ELT proteins, wild type and ELT multiple mutants were tested by feeding alcohols to the entire plants. To this end, plants were grown on soil for four weeks and than incubated in MES buffer containing 0.2% (v/v) Tween 20 and 0.1% (w/v) either phytol, farnesol, octadecan-1-ol (18:0ol) or hexadecane-1,16-diol (1,16-16:0diol) for 24 h. Afterwards, FAPEs, FAFEs, WEs with 18:0ol and WDEs with 1,16-16:0diol were quantified by

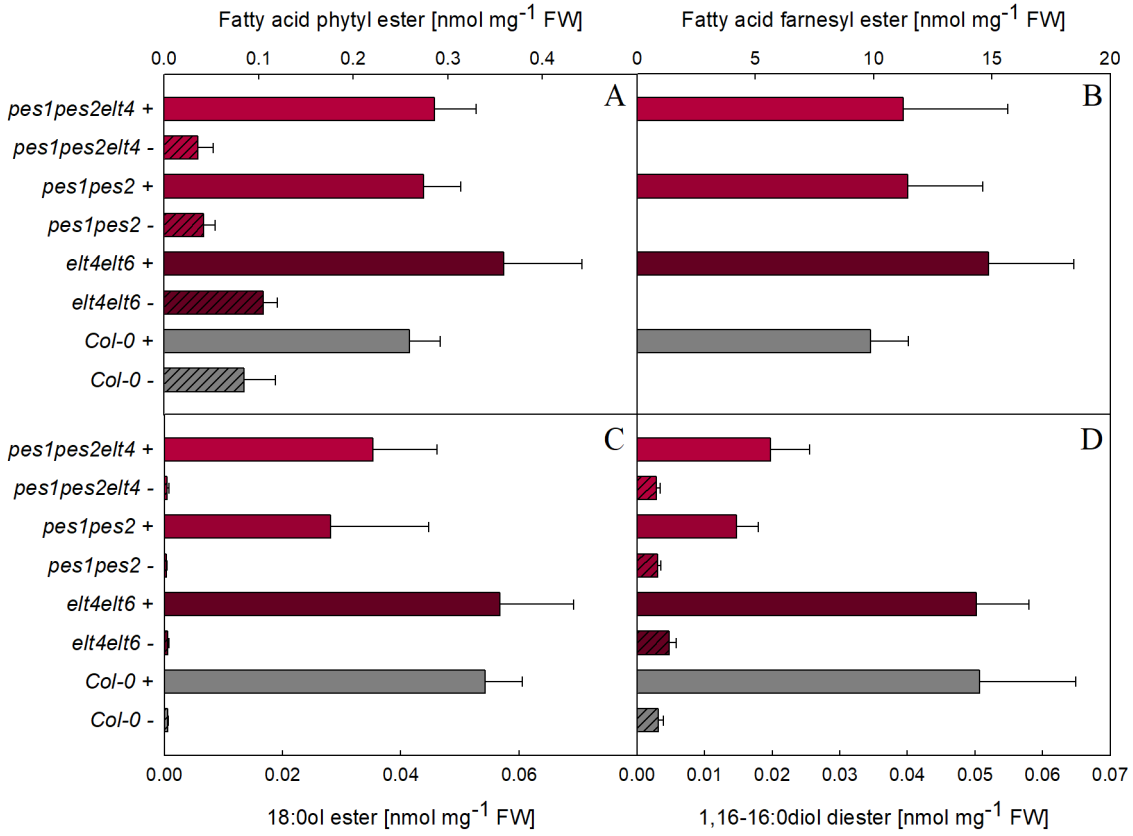

Figure 3.9 – Total ester contents of ELT multiple mutants after feeding of different alcohol substrates. Plants were grown on soil for four weeks and incubated in MES buffer either without (-, bars with pattern) or with (+, solid bars) 0.1% (w/v) phytol (A), farnesol (B), 18:0ol (C) or 1,16-16:0diol (D). Lipids were isolated, purified by SPE and FAPEs, FAFEs, WEs and WDEs were analysed by Q-TOF MS/MS. Bars represent the means of 4–5 replicates with error bars indicating the SD.

Q-TOF MS/MS measurements.

The feeding of all alcohols results in the accumulation of the respective ester products. In Col-0, the feeding of phytol resulted in a 3-fold higher accumulation of FAPEs as compared to control conditions (Figure 3.9-A). Also, under control conditions, the *pes1pes2* and *pes1pes2elt4* plants show a decreased FAPE content in comparison to wild type. This decreased FAPE content is no longer visible after phytol feeding, when the amounts of FAPEs in the mutants are comparable to that of Col-0. This experiment was conducted before in a similar way by Lippold et al. (2012). The feeding of *A. thaliana* plants with phytol led to an accumulation of FAPEs but in *pes1pes2* plantlets the amount of FAPEs after feeding was decreased in comparison to wild type. The decrease resulted from a total loss of 10:0-, 12:0-, 14:0- and 16:3-phytol. The different results can be explained by the different experimental setup. Lippold et al. (2012) only fed phytol without the use of detergents because phytol is already liquid. In this study in addition 18:0ol and 1,16-16:0diol were fed which are solids and therefore Tween 20 was applied to facilitate solubilisation. By the use of Tween 20, also fatty acids were introduced into the experiment. The over excess in fatty

acids might result in additional FAPE synthesis by unspecific acyltransferases besides the specific FAPE synthesis by PES1 and PES2.

FAFEs cannot be detected without feeding of farnesol (Figure 3.9-B). After feeding of farnesol, the accumulation of FAFEs is in general around 40 times higher than the accumulation of FAPEs. The accumulation of FAFEs is 30% higher in *elt4elt6* compared to Col-0. The accumulation of FAFEs in *pes1pes2* and *pes1pes2elt4* is slightly higher than in Col-0. Without feeding of 18:0ol, 18:0ol-WEs are of very low abundance in all genotypes (Figure 3.9-C). The feeding of 18:0ol leads to a 90-fold increase in 18:0ol-WEs in Col-0 and *elt4elt6* but only to a 67-fold increase in *pes1pes2* and *pes1pes2elt4*. WDEs can only be detected as background noise without feeding of 1,16-16:0diol (Figure 3.9-D). The feeding of 1,16-16:0diol leads to a 16 fold increase in WDEs in Col-0. The accumulation of WDEs is decreased in the ELT multiple mutants: by 35% in *elt4elt6*, by 70% in *pes1pes2* and by 57% in *pes1pes2elt4* in comparison to the wild type.

The fatty acid compositions of the produced ester compounds were further analysed. Without feeding, the main fatty acids in FAPEs are 12:0, 14:0 and 16:3 in Col-0 and *elt4elt6* (Figure 3.10-A). *pes1pes2* and *pes1pes2elt4* show the expected decrease in FAPEs with these three fatty acids and a slight increase in 16:0- and 18:3-phytol. FAPEs synthesised after feeding mainly contain 12:0, 14:0, 16:3, 16:0 and 18:3. All these FAPE species increased in all genotypes after feeding except for 16:3 in Col-0 and *elt4elt6*, which did not increase after feeding. After feeding of farnesol, mainly 12:0-farnesol and lower amounts of 14:0- and 16:0-farnesol are produced in all genotypes (Figure 3.10-B). After feeding of 18:0ol, mainly 12:0-18:0ol and also lower amounts of 14:0-18:0ol and 16:0-18:0ol are detected (Figure 3.10-C). This fatty acid distribution represents the fatty acid distribution of Tween 20 which mainly contains 12:0 and lower amounts of 14:0 and 16:0. Total 18:0ol-WEs amounts are decreased in *pes1pes2* and *pes1pes2elt4*. This can be proportionally observed in the three mentioned WE species of 12:0-18:0ol, 14:0-18:0ol and 16:0-18:0ol. The WDE with the highest amount after feeding of 1,16-16:0diol is 12:0-12:0-16:0diol (Figure 3.10-D). In addition, 12:0-14:0-16:0diol, 12:0-16:0-16:0diol and 14:0-14:0-16:0diol are detected above background noise which again represents the fatty acid distribution of Tween 20. The decrease of WDEs in *pes1pes2* and *pes1pes2elt4* is visible in all WDE species.

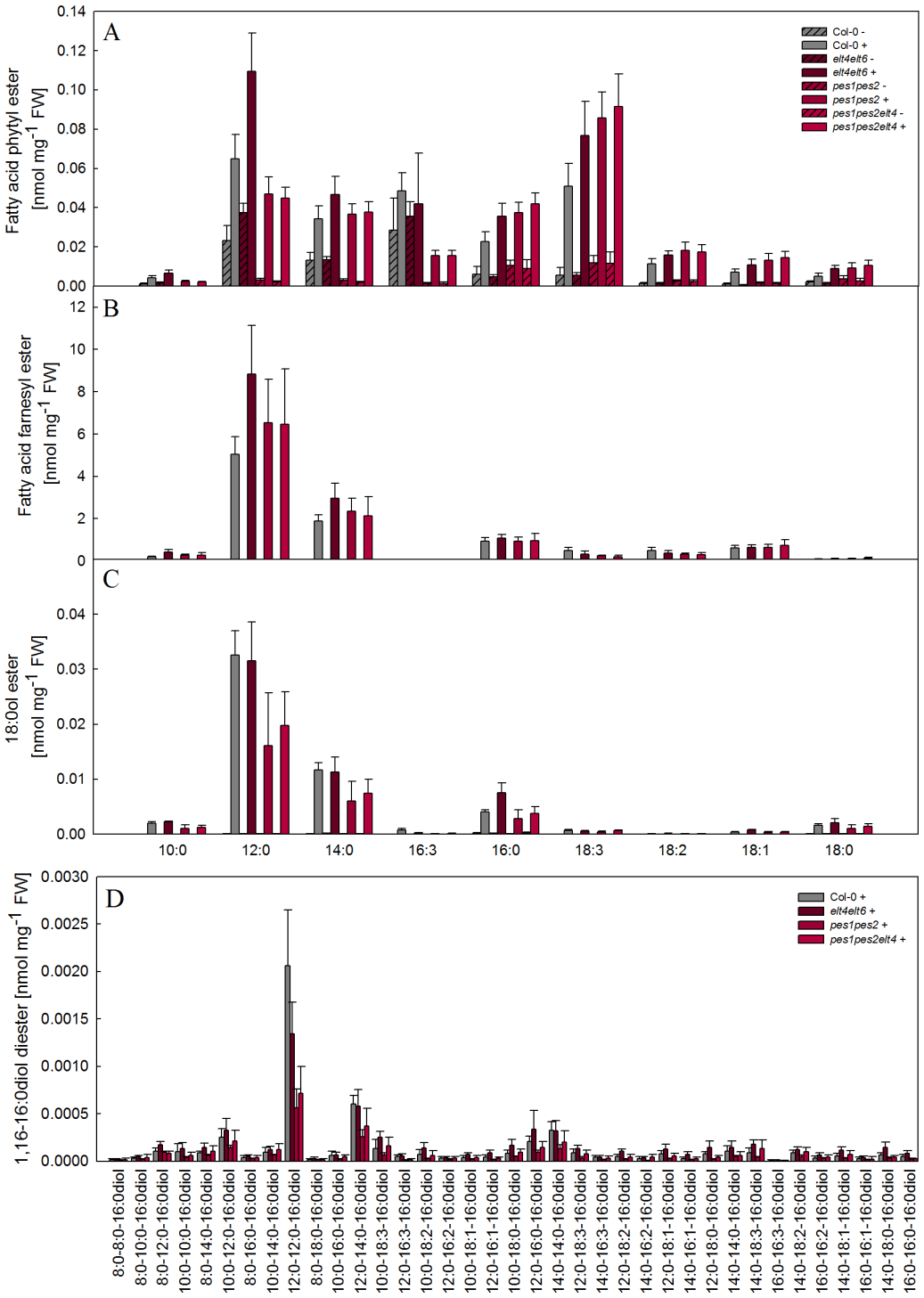

Figure 3.10 – Fatty acid distributions in FAPEs (A), FAFEs (B), WEs (C) and WDEs (D) of ELT multiple mutants after feeding of the respective alcohol substrates. Plants were grown on soil for four weeks and incubated in MES buffer either without (-, bars with pattern) or with (+, solid bars) 0.1% (w/v) phytol (A), farnesol (B), 18:0ol (C) or 1,16-16:0diol (D). For 1,16-16:0diol only the results after feeding are depicted. Lipids were isolated, purified by SPE and esters were analysed by Q-TOF MS/MS. Bars represent the means of 4–5 replicates with error bars indicating the SD.

3.2 Characterisation of PES2

PES2 from *A. thaliana* has been previously identified as a phytyl ester synthase, catalysing the esterification of a fatty acid to a phytol moiety (Lippold et al., 2012). One objective is the further characterisation of PES2 regarding its specificity for fatty acid and alcohol substrates. PES2 contains two enzyme domains, a putative acyltransferase and a hydrolase domain. Thus, the enzyme might be able to not only use free fatty acids but also fatty acids bound to coenzyme A, ACP or other acyl-containing lipids such as membrane lipids as substrates. Under chlorotic stress the thylakoid membranes are disintegrated resulting in the degradation of thylakoid membrane lipids such as MGDG (Gaude et al., 2007). As a consequence, MGDG might serve as an acyl donor for PES2. On the other side, PES2 might also use other alcohols than phytol as fatty acid acceptors. The common method to investigate the substrate specificity of an enzyme is the expression of the target protein in an heterologous host organism, followed by enzyme assays with purified protein or crude protein extracts.

3.2.1 Heterologous Expression of PES2 in *E. coli*

A very common host for the heterologous expression of proteins is the bacterium *E. coli*. This system is used for the expression of PES2 under an IPTG-inducible promoter. PES2 contains a sequence for a putative chloroplast targeting signal. Signal peptides often contain cleavage sites, that are recognised by signal peptidases, and therefore, signal peptides are not part of the active proteins. Because *E. coli* does not contain plastids, the full-length PES2 polypeptide including the signal peptide cannot be targeted and processed correctly. Therefore, PES2 was cloned as a truncated protein without the putative chloroplast targeting signal (first 94 amino acids) into the expression vector pQE-30 (pQE30-PES2oTP, done by Felix Lippold). The expression of PES2oTP was induced at an OD_600 of 0.6 and the protein was expressed for 16 h at 16 °C. The successful expression was confirmed by SDS-PAGE and immunoblotting (Figure 3.11). In the immunoblot, a band is visible that migrates between 58 and 80 kDa and is absent from the empty vector control. The observed size is in agreement with the calculated size of PES2oTP (69 kDa).

The activity of PES2oTP was examined by a phytol feeding assay. *E. coli* cells were cultivated until an OD_600 of 0.6 was reached. The expression of PES2oTP was induced with IPTG and cells were cultivated for 16 h at 16 °C. Afterwards cells were incubated with phytol for 3 h at 30 °C. Lipids were extracted, FAPEs purified by SPE and analysed by Q-TOF MS/MS. The feeding of phytol leads to the accumulation of FAPEs (Figure 3.12). The expression of PES2oTP causes a two-fold higher accumulation of FAPEs than in the empty vector control. These FAPEs contain mainly 16:1, 16:0 and 18:1 fatty acids which are typical for *E. coli*. The relative composition of

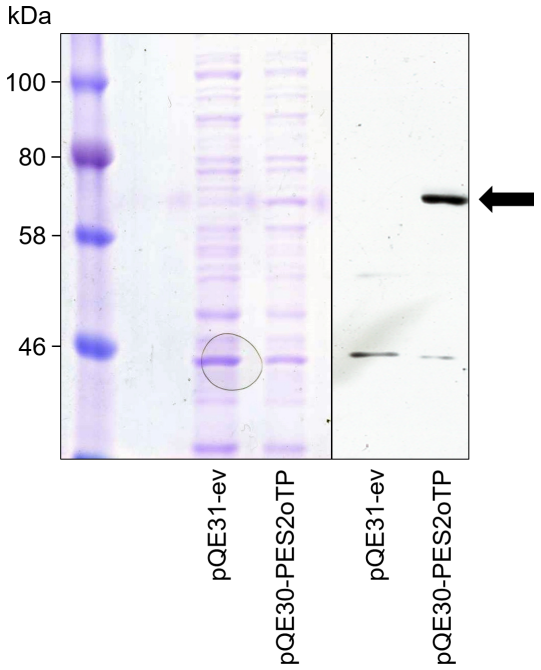

Figure 3.11 – The expression of PES2oTP in *E. coli* was confirmed by SDS-PAGE (left) and immunoblotting (right). The total protein was extracted from induced *E. coli* cells, that contain an empty vector (ev-pQE31) or a PES2oTP expression vector (pQE30-PES2oTP), and was used for SDS-PAGE and Coomassie staining. The proteins were blotted and detected using the His-detector kit. The western blot band at ~65 kDa (arrow) corresponds to the size of PES2oTP carrying an N-terminal His tag (69 kDa). The western blot band at 46 kDa represents a non-specific protein which cross reacted with the His-detector kit. The circle on the SDS-PAGE originated from an air bubble.

FAPE content is the same for PES2oTP and the empty vector control.

This experiment demonstrates that it is possible to express an active PES2oTP protein in *E. coli* cells. For *in vitro* assays, purified proteins or at least a crude protein extract that was extracted from the cell lysate is necessary. To this end, several approaches were conducted. An enzyme assay with crude protein extract was carried out, but no synthesis of FAPEs could be detected with 13:0-CoA and phytol. After the lysis and centrifugation of *E. coli* cells, PES2oTP is mainly found in the pellet. For protein purification by Ni-NTA affinity chromatography, the protein needs to be soluble in the supernatant. To increase the amount of PES2oTP in the supernatant, cells were lysed in the presence of additional detergents (CHAPS, fos-choline-12, dodecyl maltoside, sodium deoxycholate). Nevertheless, none of the detergents lead to an accumulation of PES2oTP in the supernatant as found by western blotting. Finally, attempts were made to purify the small amount of PES2oTP that is located in the supernatant without the use of detergents. The purification resulted in a very low yield of protein. A subsequent enzyme assay with purified protein did not lead to the synthesis of FAPEs, indicating that the enzyme is not active or that its concentration is too low.

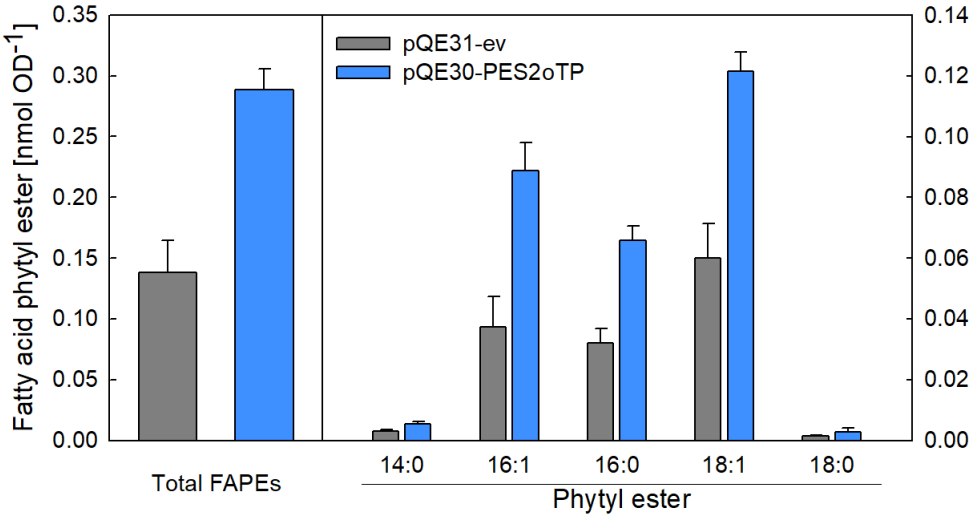

Figure 3.12 – *E. coli* cells that express PES2oTP were incubated with phytol for 3 h. Lipids were extracted, FAPEs were purified by SPE and analysed by Q-TOF MS/MS. The total content of FAPEs was calculated (left) as well as the fatty acid composition of FAPEs (right). Bars represent the means of 4–5 replicates with error bars indicating the SD.

3.2.2 Heterologous Expression of PES2 in *N. benthamiana*

The expression of PES2oTP in *E. coli* resulted in the production of a protein that is active in intact *E. coli* cells but seems to lose activity after disruption of the cells for protein isolation. That is why the expression system was changed to transient expression of PES2 in *N. benthamiana*. Three different constructs were used: tpPES2, containing the PES2 full length ORF including a putative N-terminal chloroplast targeting sequence, and m1PES2/m2PES2, two truncated ORFs lacking the first 64 and 93 N-terminal amino acids, respectively. After expression for seven days in the infiltrated *N. benthamiana* leaves, lipids were isolated, purified by SPE and analysed by Q-TOF-MS/MS. For lipid extraction leaf material was used that showed a fluorescence signal of the co-infiltrated GFP marker. The expression of tpPES2 leads to a seven-fold increase in FAPE content as compared to the control (Figure 3.13-A). The increase of FAPEs containing 12:0, 14:0 and 16:3 is highest, and lower for 10:0-phytol and 16:0-phytol (Figure 3.13-E). The amount of very long-chain FAPEs is unchanged. m1PES2 or m2PES2 infiltrated leaves do not show an accumulation of FAPEs. Furthermore, the contents of WEs, TAGs and SEs were measured by Q-TOF-MS/MS for all three constructs but the measurements revealed no differences compared to the controls which had been infiltrated with P19 and GFP only (Figure 3.13-B, -C and -D, respectively).

Crude protein extract was prepared from *N. benthamiana* leaves expressing tpPES2 and used for *in vitro* enzyme assays. The protein extract was incubated with phytol and 13:0-CoA, but no synthesis of 13:0-phytol could be detected (*data not shown*). Attempts were made to increase the protein activity by adding CHAPS (final concentration 3.75 mM) to the reaction, but the protein was still inactive.

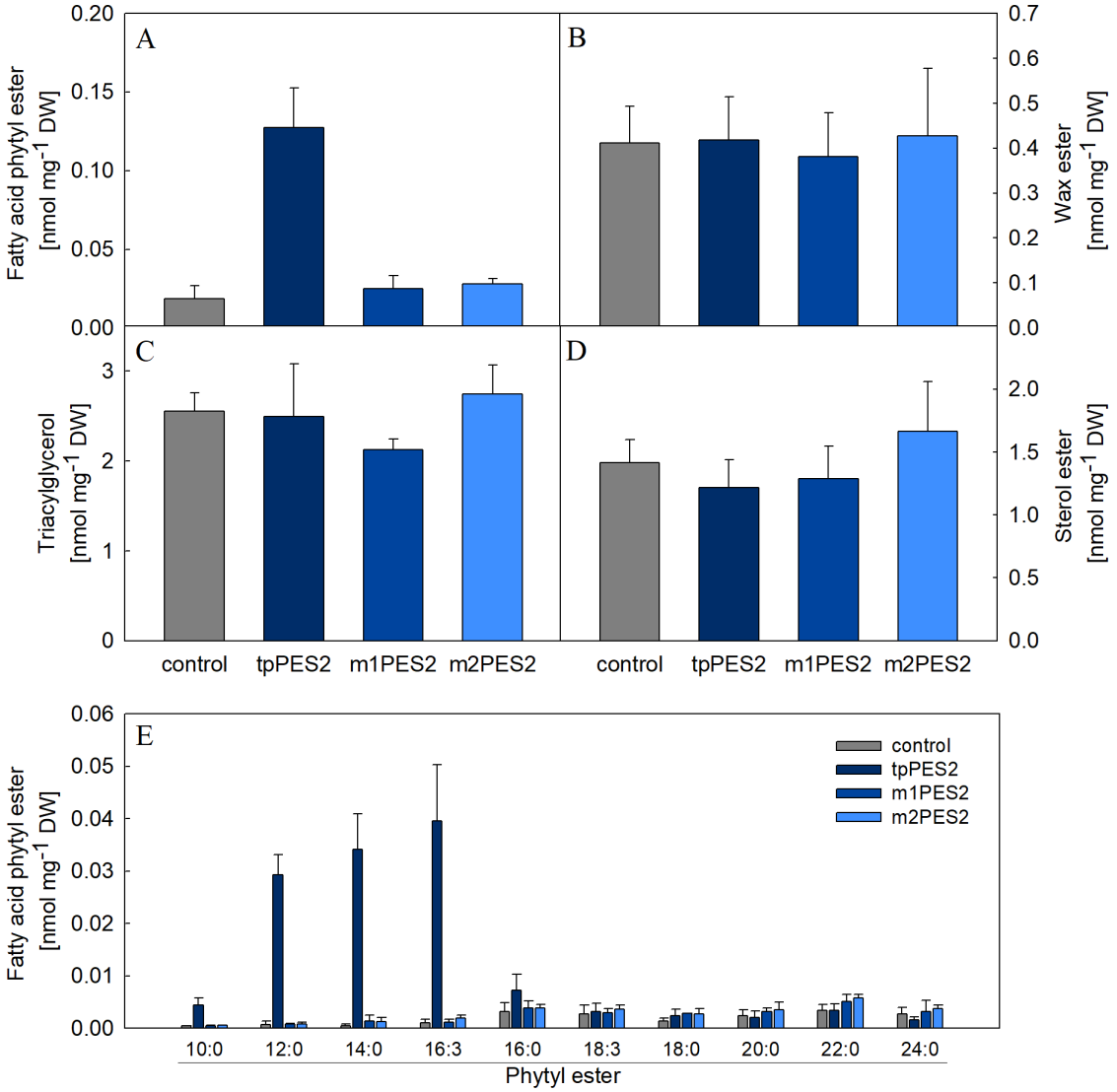

Figure 3.13 – *A. tumefaciens* strains containing different PES2 overexpression constructs were infiltrated into *N. benthamiana* leaves. Lipids were isolated after incubation for seven days and purified by SPE. FAPEs, WEs, TAGs and SEs were measured by Q-TOF-MS/MS. Bars represent the means of five replicates with error bars indicating the SD. tpPES2, full length ORF including its putative N-terminal chloroplast targeting sequence; m1PES2/m2PES2, truncated ORFs lacking the first 64 and 93 N-terminal amino acids, respectively.

3.2.2.1 Accumulation of Additional Lipids Produced by tpPES2

The transient expression in *N. benthamiana* revealed phytyl ester synthase activity of tpPES2 but no activity of m1PES2 or m2PES2. It was possible, that expression of any of these constructs resulted in the production of other non-polar lipids. Therefore, after transient expression of PES2 constructs in *N. benthamiana*, non-polar lipids were separated by TLC. Upon expression of tpPES2, a higher abundance of a band comigrating with the WEs standard was observed on the TLC plate in comparison to the control (Figure 3.14-A). In this TLC solvent system, WEs, SEs and FAPEs comigrate. Therefore, the experiment demonstrated, that FAPEs but not SEs or WEs accumulate in tpPES2 expressing *N. benthamiana* leaves. The intensity of the band co-migrating with WEs in m1PES2 and m2PES2 is comparable to that of the control.

Furthermore, an additional band is visible in tpPES2 that migrates between TAGs and WEs and that is absent from the control, m1PES2 and m2PES2 lipid extracts (Figure 3.14-A, red box). The band from the tpPES2 lipid extract and the corresponding silica in the area of the control were isolated from the TLC plate, lipids were extracted from the silica material and analysed by Q-TOF MS. The total ion chromatogram of the tpPES2 lipids reveals a series of additional lipids absent from the control (Figure 3.14-B). The masses range from m/z 612.5931 up to m/z 724.7183 with the highest abundance at m/z 668.6557. The differences between two successive masses is always 28 mass units, corresponding to the mass of a C_2H_4 unit, which indicates lipids containing aliphatic chains.

All m/z values that are given here and in the following chapters correspond to the calculated masses of the ions. In contrast, all m/z values that are depicted in the presented figures are the measured values. The accuracy of the measured values depends on the quality of the tuning of the Q-TOF instrument.

3.2.2.2 Identification of Additional Lipids Produced in tpPES2 Expressing *N.benthamiana* Leaves as Wax Diesters

The ions with the additional masses observed in the previous experiment were further investigated by Q-TOF MS/MS. To this end, the m/z values were programmed for targeted MS/MS experiments. The voltage for CID was adjusted to 10 V to monitor parental ions and fragment ions simultaneously. Two examples for fragmentation are depicted in Figure 3.15. The main ions for m/z 640.6244 are the parental ion itself and the two fragment ions at m/z 423.4202 and m/z 223.2426. The neutral loss from m/z 640.6244 to m/z 423.4202 is 217.2042. This mass is known from TAG measurements by Q-TOF-MS/MS, where the first neutral loss corresponds to NH_3 and a fatty acid (ammonium acyl adduct). In line with this, 217.2042 is the mass of [12:0+NH_3]. The second neutral loss between m/z 423.4202 and m/z 223.2426 corresponds to

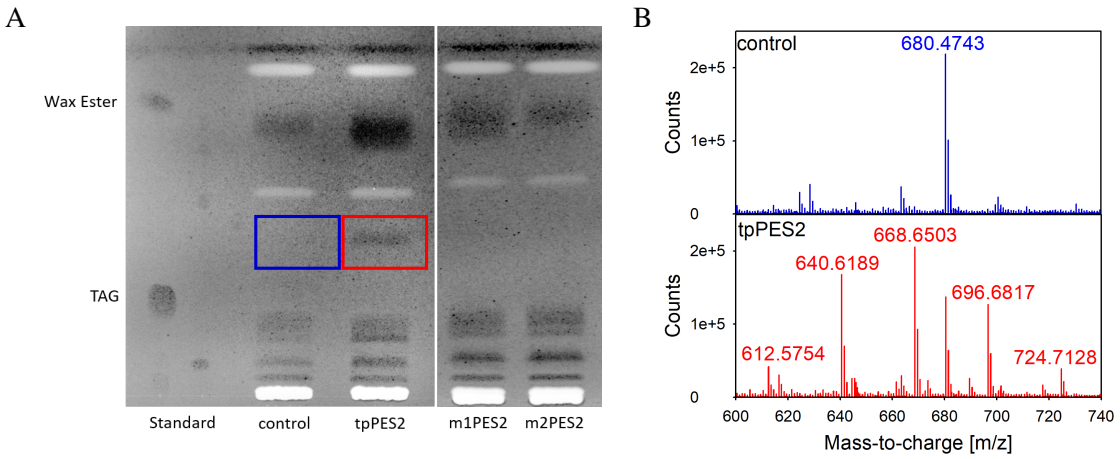

Figure 3.14 – A – Non-polar lipids from *N. benthamiana* leaves expressing tpPES2, m1PES2 or m2PES2 were separated by TLC with hexane/diethyl ether/acetic acid 90:10:1 (v/v/v), stained with primuline and visualised under UV-light. Expression of tpPES2 resulted in the accumulation of an additional lipid band (red box) absent from the control (blue box). B – The silica in the area with the additional lipids and the control area were isolated from the TLC plate, lipids were extracted from the silica and analysed by Q-TOF-MS. The chromatogram shows a series of additional lipids in tpPES2 absent from the control.

200.1776, which is the mass of 12:0 (free fatty acid without NH_3). With a lower abundance, an ion with m/z 201.1855 can be observed, which is the proton adduct ion of 12:0. The neutral loss between m/z 423.4202 and m/z 201.1855 is 222.2348. Considering a proton adduct ion, because the NH_3 group was already lost with the first fatty acid, the m/z 223.2426 fragment ion might be the same molecule as the 222.2348 neutral loss. These masses corresponds to $[C_{16}H_{30} + H]^+$ or $C_{16}H_{30}$, respectively. The two fatty acids that are released from the parental ion upon fragmentation are probably bound via ester bonds. As a consequence, the free backbone has to contain at least two hydroxyl groups. During collision induced dissociation (CID), the fatty acids were both dissociated without the loss of a water molecule. During an esterification reaction, water is released. Thus, to reveal the identity of the backbone, two water molecules have to be added to 222.2348 ($C_{16}H_{30}$). This addition leads to 258.2559 or $C_{16}H_{34}O_2$, which is the mass and the chemical formula of hexadecanediol. In conclusion, the parental ion of m/z 640.6244 was identified as the ammonium adduct of a wax diester (WDEs) consisting of two 12:0 fatty acids esterified to a hexadecanediol backbone. The fragment ion m/z 423.4202 represents the monoester proton adduct ion ($[FA + Diol - H_2O + H]^+$) and the fragment ions m/z 223.2426 and m/z 201.1855 represent the hexadecanediol ($[Diol - 2\,H_2O + H]^+$) and 12:0 ($[FA + H]^+$) proton adduct ions, respectively.

For the parental ion of m/z 668.6557, the main fragments are m/z 451.4515, m/z 423.4202 and m/z 223.2426. The fragmentation pattern is similar to the parental ion of m/z 640.6244 with minor differences. The difference between m/z 668.6557 and m/z 451.4515 corresponds again to the neutral loss of 217.2042 [12:0+NH_3]. In addition, the neutral loss between m/z 668.6557 and

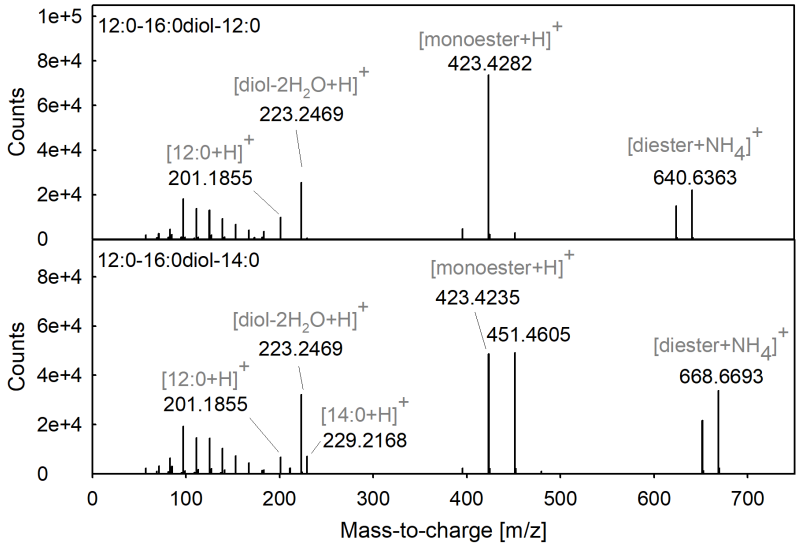

Figure 3.15 – Analysis of the additional lipids produced by tpPES2 after infiltration into *N. benthamiana* leaves by Q-TOF-MS/MS revealed neutral losses and fragment ions of fatty acids, i.e., of 12:0 at m/z 640.6383 or 12:0 and 14:0 at m/z 668.6693. Furthermore, the spectrum displayed the neutral loss of 222.2399 and a fragment ion of m/z 223.2461 indicating that these lipids contain a unique backbone, the diol $C_{16}H_{34}O_2$.

m/z 423.4202 is 245.2355, which corresponds to [14:0+NH_3]. With lower abundance, ions with m/z 201.2855 and m/z 229.2168 are observed that are the proton adduct ions of 12:0 and 14:0, respectively. In addition, the neutral loss and the proton adduct ion of hexadecanediol are present. Taken together, m/z 668.6557 is identified as a WDE composed of 12:0, 14:0 and hexadecanediol. This analysis demonstrated, that the series of additional lipids in tpPES2 infiltrated *N. benthamiana* leaves consists of WDEs with fatty acids of different chain lengths.

3.2.2.3 The Novel WDEs have a Unique Hexadecanediol Backbone

Further experiments were performed to test whether additional diols are involved in the WDE formation. Therefore in-source-fragmentation was enforced by increasing the fragmentor voltage from 200 V to 270 V. Thus, the molecules already fragment during ionisation before they reach the first quadrupole which is used to select specific masses. As a result, monoester ions that were previously detected as fragment ions can be selected as parental ions in a targeted MS/MS approach. Monoester ions are successfully selected with this strategy and further dissociated (Figure 3.16). For each selected monoester ion only one specific fatty acid proton adduct ion [FA + H]$^+$ can be observed, which leads to the conclusion that the series of WDEs contains one unique backbone that is hexadecanediol.

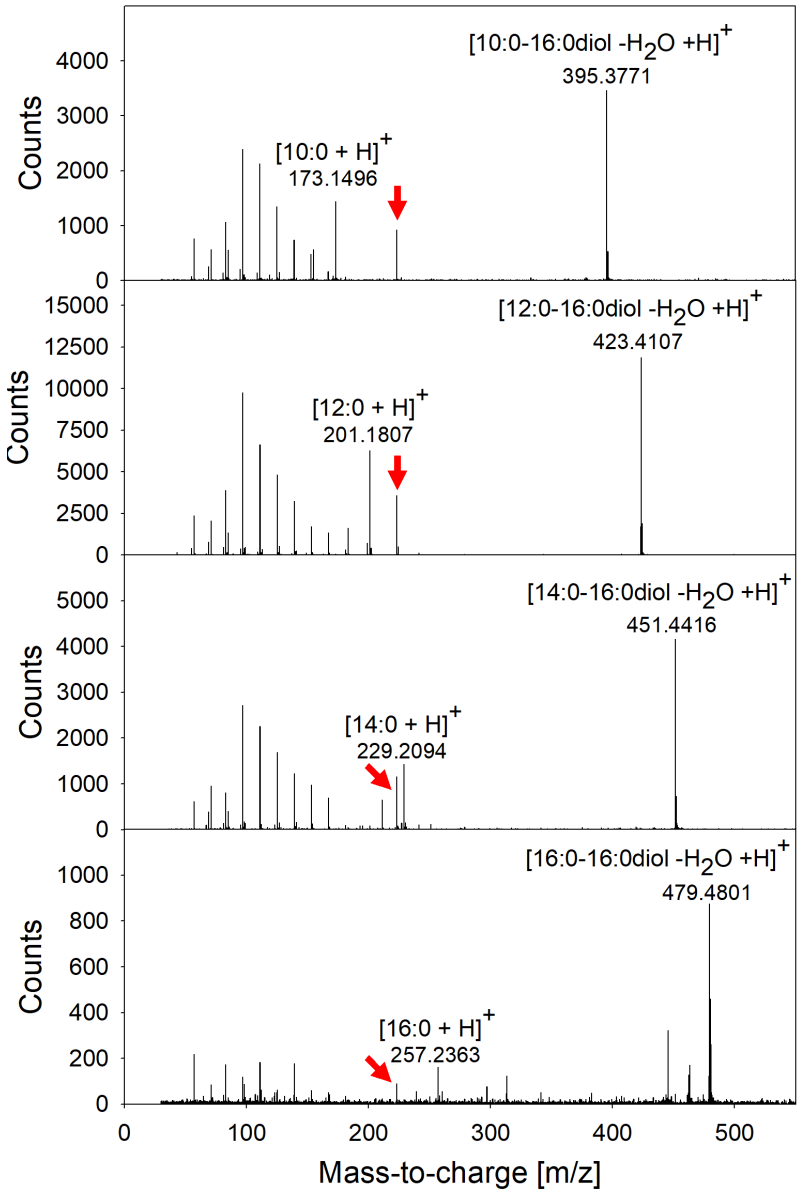

Figure 3.16 – Identification of hexadecanediol as an unique backbone in the WDEs. In-source-fragmentation was enforced by increasing the fragmentor voltage from 200 V to 270 V. Thus, the monoester product ions could be selected in MS/MS experiments as [FA + Diol – H_2O + H]$^+$ ions. Upon dissociation, either a fatty acid product ion [FA + H]$^+$ is formed or the previously mentioned [$C_{16}H_{30}$ + H]$^+$ fragment ion with m/z 223.2426 (indicated by red arrows).

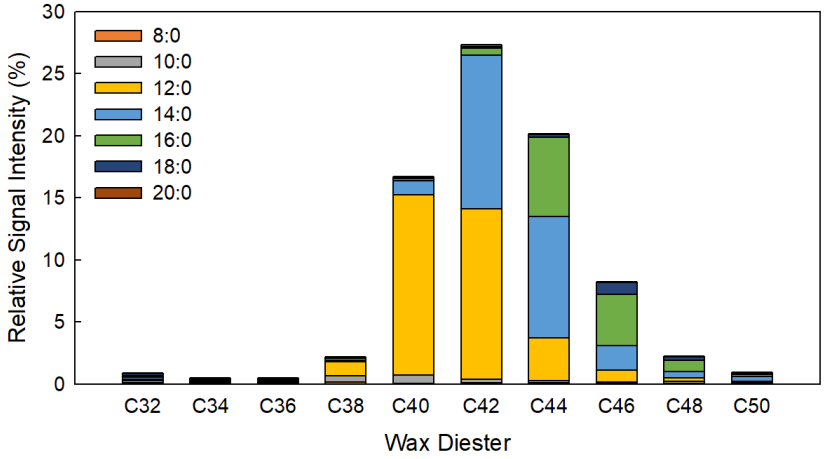

Figure 3.17 – Fatty acid distribution in WDEs of tpPES2 infiltrated *N. benthamiana* leaves. Lipids were isolated, WDEs were purified by SPE and analysed by Q-TOF MS/MS. Fatty acids were quantified by neutral loss scanning for the fragments [FA + NH_3]. Bars represent the values of a single replicate.

3.2.2.4 Analysis of the Fatty Acid Composition in the WDEs

Analysis of the series of additional lipids revealed WDEs that contain hexadecanediol as an unique backbone. The first deployed MS/MS experiment showed, that dissociation of the WDE parental ion leads to a neutral loss of [FA + NH_3] (Chapter 3.2.2.2). This behaviour was utilised to employ neutral loss scanning to obtain an overview of the fatty acid composition of the WDEs. As it is unknown, whether the neutral loss occurs with the same likelihood from the two hydroxyl group positions in the hexadecanediol and whether the fatty acid distribution to the two hydroxyl groups is unspecific, the results of this experiment can only be seen as a rough overview and not as definite results. The three most abundant WDEs are C42, C44 and C40 (Figure 3.17). The most abundant fatty acids are 12:0, followed by 14:0 and 16:0.

The mass of an unsaturated fatty acid is two mass units lower than the mass of its corresponding saturated version with the difference corresponding to two hydrogen atoms. If unsaturated fatty acids would be incorporated into the WDEs, additional masses to the ones detected should be observed, with an m/z value decreased by two, four, six or more, in case that both fatty acids would be unsaturated or that one fatty acid is polyunsaturated. These masses were not detected, indicating that the WDEs only contain saturated fatty acids.

3.2.2.5 Comparison of Plant Derived WDE to Chemically Synthesised WDEs

WDEs typically occur in the sebum of animals or as part of the cuticle of plants. For mouse it was shown that the backbones are 1,2-alkane diols (Ebel et al., 2014). In plants, alkanediols do not belong to the ubiquitous constituents of the cuticle and are more specific for individual plant

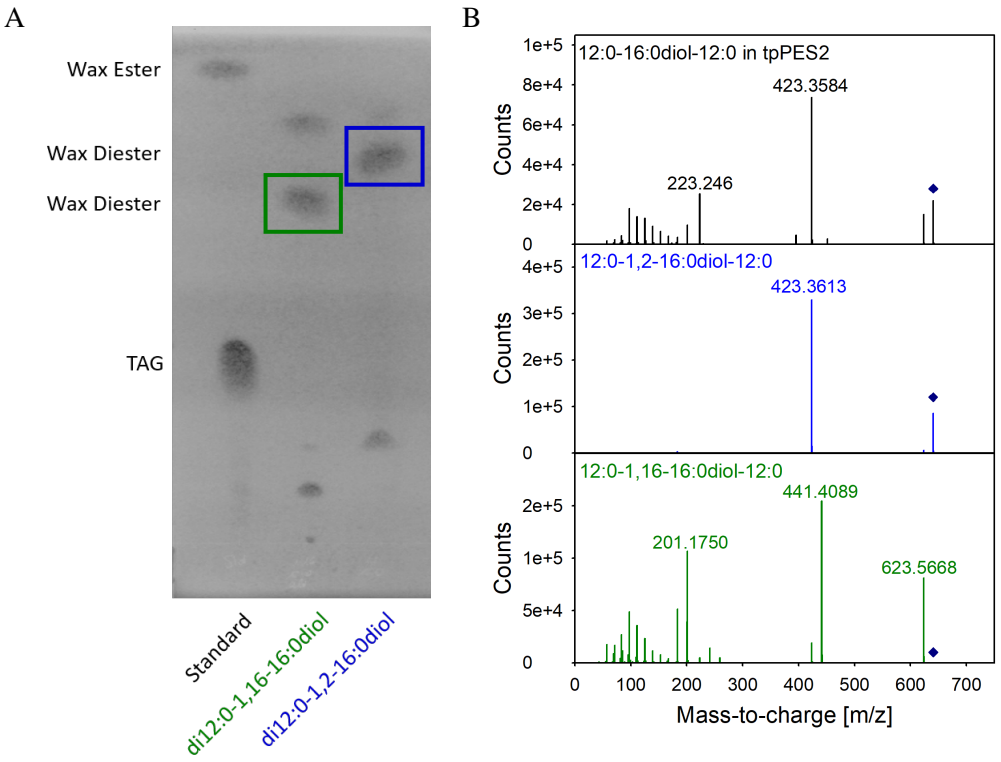

Figure 3.18 – Comparison of plant derived and synthetic WDEs. A – WDEs were synthesised with 12:0 and 1,2-16:0diol or 1,16-16:0diol and purified by TLC which was developed with 90:10:1 (v/v/v) hexane/diethyl ether/acetic and stained with primuline. B – Comparison of mass spectra from m/z 640.6244 generated by Q-TOF MS/MS experiments of WDEs isolated from tpPES2 infiltrated *N. benthamiana* leaves (black), synthetic 1,2-16:0diol diester (blue) and synthetic 1,16-16:0diol diester (green). All three types of WDEs formed ammonium adducts $[M + NH_4]^+$ but differed in fragmentation.

taxa. This also accounts for the chain length and the positions of the hydroxyl groups, which vary between different plant species.

For the identification of the hydroxyl positions in the hexadecanediol backbone, 1,2-hexadecanediol (1,2-16:0diol) and 1,16-hexadecanediol (1,16-16:0diol) standards were purchased. WDEs with 12:0 fatty acids were chemically synthesised and reaction mixtures were separated by TLC (Figure 3.18-A). The chemically synthesised WDEs migrate between WE and TAG standards and have different retention factors. The silica of the bands containing di12:0-1,16-16:0diol and di12:0-1,2-16:0diol was isolated from the TLC plate and lipids were extracted from the silica material. Plant derived di12:0-16:0diol diester and synthetic hexadecanediol diesters were analysed by Q-TOF MS/MS and compared (Figure 3.18-B). All three hexadecanediol diesters ionise as ammonium adducts $[M + NH_4]^+$ with m/z 640.6244. For the plant derived di12:0-16:0diol diester, product ions of 12:0-monoester ($[FA + Diol - H_2O + H]^+$, m/z 423.4202), hexadecanediol (m/z 223.2426) and the fatty acid (m/z 201.1855) are observed, as described before (Chapter 3.2.2.2). The 12:0-monoester product ion m/z 423.4202 can also be found in the di12:0-1,2-

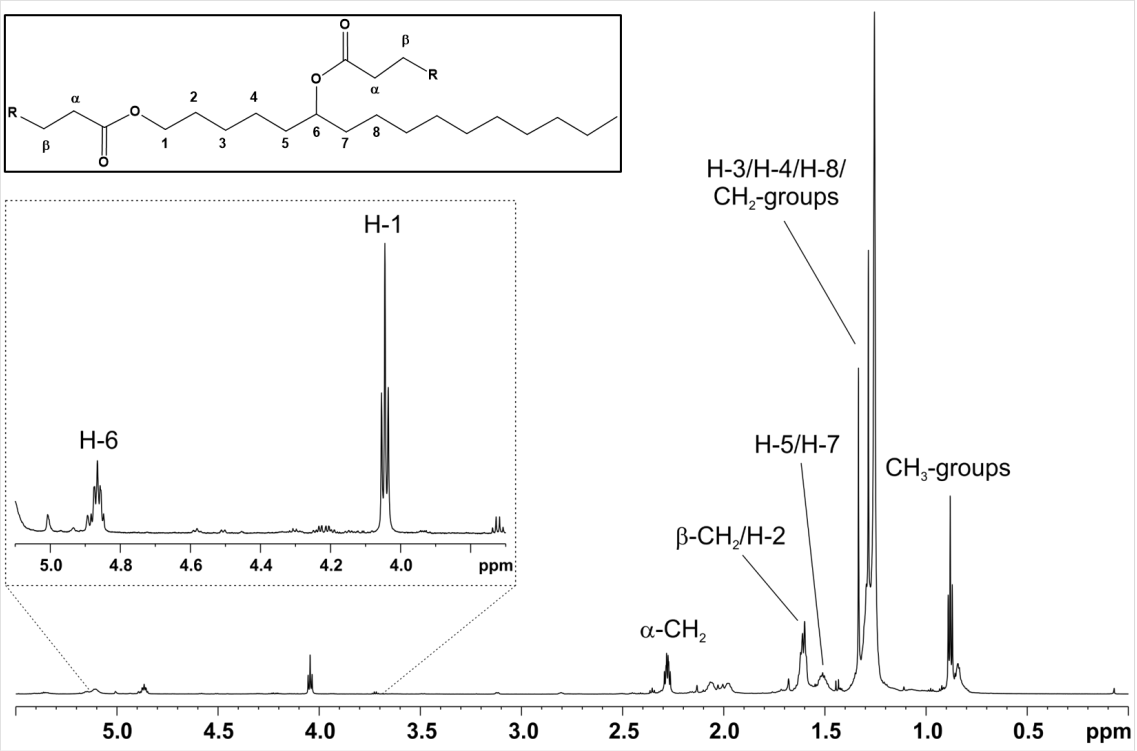

Figure 3.19 – WDEs were isolated and purified from tpPES2 infiltrated *N. benthamiana* leaves and analysed by ^{1}H-NMR, which was conducted by Nicolas Gisch (Forschungszentrum Borstel). NMR results revealed a 1,6-hexadecanediol backbone in the purified WDEs. ^{1}H-NMR and ^{13}HC-NMR data are given in Table 7.10 in the appendix.

16:0diol sample, but no further product ions are detected there. The fragmentation of di12:0-1,16-16:0diol is different from the above described. First, a neutral NH_3 group is lost resulting in the proton adduct m/z 623.5978. The second neutral loss is 12:0 -H_2O resulting in the monoester $[FA + Diol + H]^+$ with m/z 441.4308. In addition, hexadecanediol (m/z 223.2426) and fatty acid (m/z 201.1855) product ions are also observed. Because the fragmentation pattern of the plant derived di12:0-16:0diol esters cannot be retrieved in those of the synthesised WDEs, these results indicate that the plant hexadecanediol backbone is neither 1,2- nor 1,16-hexadecanediol.

3.2.2.6 Structural Elucidation of the Hexadecanediol Backbone

As positional isomers are not distinguishable during direct infusion Q-TOF MS/MS and the analysis and comparison to standards was not meaningful, the exact structure of the hexadecanediol backbone remained unresolved. ^{1}H-NMR was used to elucidate the positions of the hydroxyl groups. WDEs from ~150 infiltrated *N. benthamiana* leaves expressing PES2 were isolated and purified. ^{1}H-NMR and ^{13}HC-NMR analyses were conducted by Nicolas Gisch at the Forschungszentrum Borstel. The NMR results demonstrated that the diol backbone is 1,6-hexadecanediol (^{1}H-NMR results in Figure 3.19, ^{1}H-NMR and ^{13}HC-NMR results in Table 7.10 in the

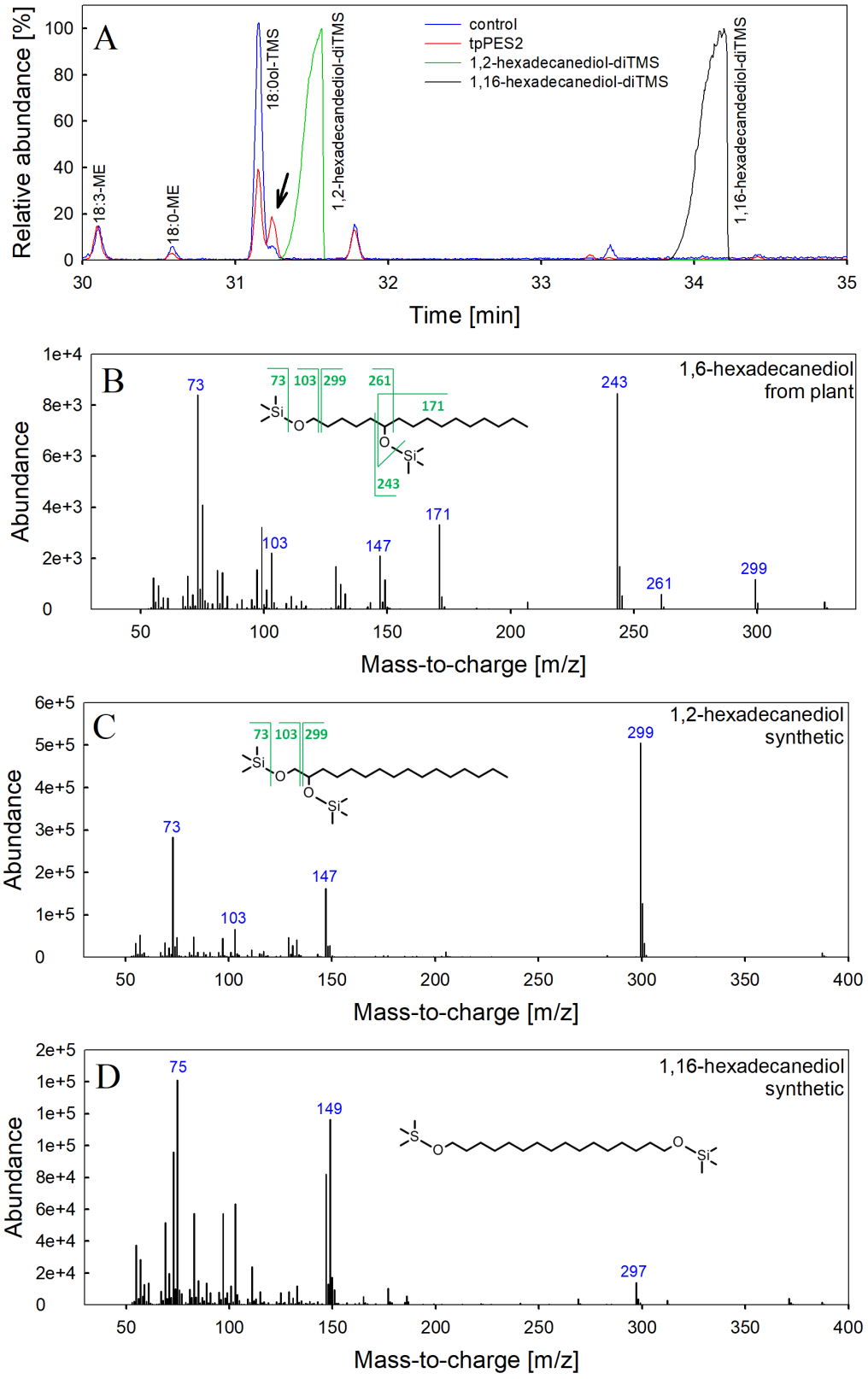

Figure 3.20 – For the structural elucidation of the hexadecanediol backbone, WDEs were isolated and purified from *N. benthamiana* leaves expressing tpPES2 or control leaves, transesterified and derivatised with MSTFA. A – GC-MS chromatogram of 1,2-hexadecanediol-diTMS (green), 1,16-hexadecanediol-diTMS (black) and of lipid extracts from leaves expressing only P19 and GFP (control, blue) or P19, GFP and tpPES2 (tpPES2, red). The black arrow points to the peak that is identified as 1,6-hexadecanediol-diTMS. B – Mass spectrum of plant derived 1,6-hexadecanediol-diTMS. C – Mass spectrum of synthetic 1,2-hexadecanediol-diTMS. D – Mass spectrum of synthetic 1,16-hexadecanediol-diTMS.

appendix).

The NMR result was verified by GC-MS. WDEs purified from *N. benthamiana* were transesterified by methylation and free diols were derivatised by trimethylsilylation prior to analysis. The GC-MS chromatogram of lipids from tpPES2 infiltrated leaves displayed an additional peak with a retention time of 31.25 min that was absent from the control (Figure 3.20-A). The mass spectrum of this peak is shown in Figure 3.20-B. Jetter et al. (1996) listed MS fragments characteristic for primary/secondary alkanediols. The ions with m/z 73 and 75 show the presence of trimethylsilyl (TMS) groups. The fragment m/z 147 is formed by rearrangement when the ion contains at least two TMS groups (Richter and Burlingame, 1968). The occurrence of these three ions proves that the molecule is at least a diol. A hydroxyl group located at the first C-atom is indicated by the fragment m/z 103. These four fragments can be observed in the presented mass spectrum. The position of the secondary hydroxyl group is unravelled by α-fragmentation resulting in the $[C_nH_{2n}OTMS]^+$ fragment (Jetter et al., 1996), with a corresponding m/z 243 for 1,6-hexadecanediol. This fragment is detected as the most abundant ion. In conclusion, the presented GC-MS mass spectrum displays the mass spectra of 1,6-hexadecanediol-diTMS. As a cross-check, Figure 3.20-C and Figure 3.20-D show the mass spectra of the TMS derivatives of 1,2-hexadecanediol and 1,16-hexadecanediol standards, respectively. The fragments of these standards differ from the fragments of the plant derived hexadecanediol TMS derivative. In addition, the retention times of the three hexadecanediol isomers are different. Taken together, the results identify the diol backbone as 1,6-hexadecanediol.

3.2.2.7 Localisation of WDEs in Infiltrated *N. benthamiana* Leaves

Alkanediols are usually found in the cuticle of the plant (Jetter et al., 2006). The synthesis of the cuticle monomers takes place at the ER (see Li-Beisson et al. (2013), Chapter 2.8, for an overview). The WDEs reported here are synthesised by tpPES2 in transiently transformed *N. benthamiana* leaves. PES2 in the construct tpPES2 carries its chloroplast targeting signal, its expression results in FAPE synthesis and therefore, the enzyme is active. On the other hand, the expression of m1PES2 and m2PES2 outside the chloroplast does not result in the accumulation of FAPEs or WDEs (Chapter 3.2.2.1). Therefore, it can be concluded that the WDEs are synthesised in the chloroplast. The question arose, if the WDEs are then stored in the chloroplast or if they are exported, such that they might eventually accumulate in the epicuticular waxes of the cuticle of the leaf. Lipid extracts of infiltrated *N. benthamiana* leaves were prepared by dipping the leaf in chloroform as it is common for the analysis of cuticular waxes. Lipids were analysed by Q-TOF MS and compared to whole leaf lipid extracts (Figure 3.21). Leaf surface lipid extracts are devoid of WDEs, indicating that the WDEs are not found in the epicuticular wax layer.

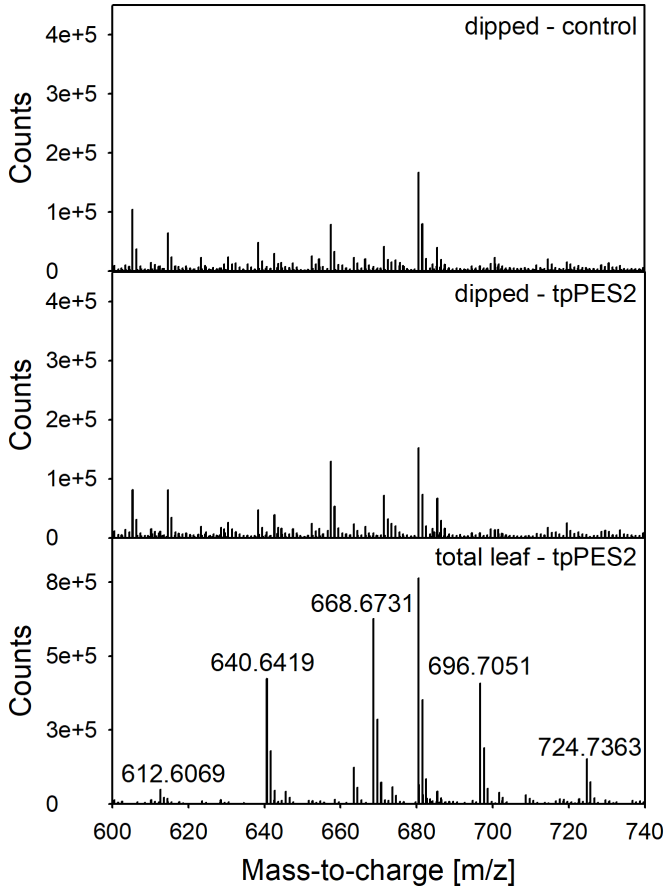

Figure 3.21 – Analysis of leaf surface lipids from tpPES2 infiltrated *N. benthamiana* leaves. Lipid extracts were prepared either by dipping the leaf in chloroform (dipped) or from whole leaf extracts (total leaf). WDEs were purified by SPE. Total ion chromatograms were acquired by Q-TOF MS. Labelled peaks represent WDE masses.

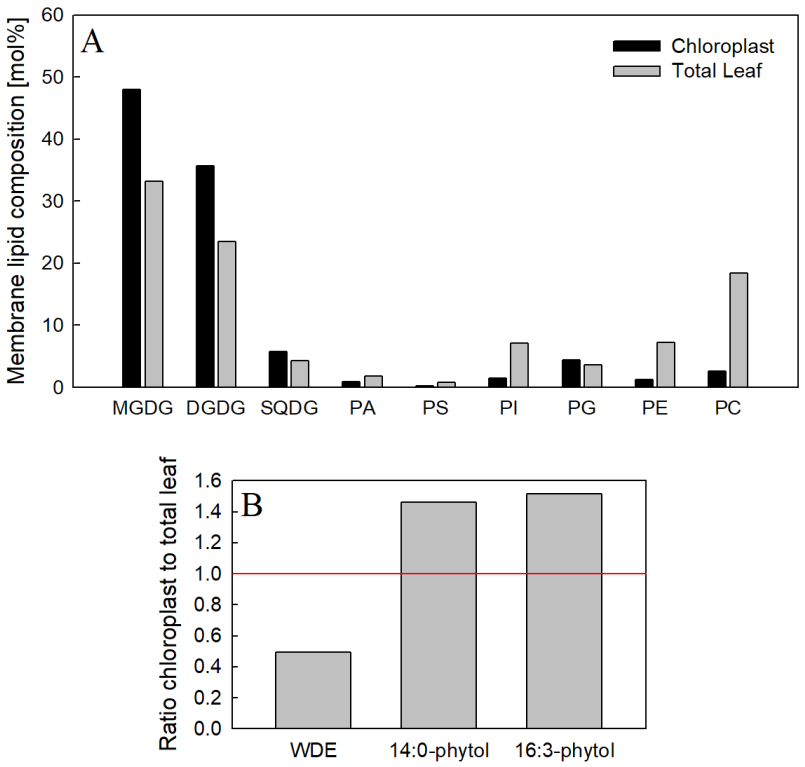

Figure 3.22 – Lipids from isolated intact chloroplasts and from whole leaves of tpPES2 infiltrated *N. benthamiana* were extracted as described before. WDEs and FAPEs were purified by SPE. WDEs, FAPEs, phospho- and galactolipids were quantified by Q-TOF MS/MS. A – Molar composition of phospho- and galactolipids. B – The measured amounts of WDEs, 14:0- and 16:3-phytol were normalised to the total amount of phospho- and galactolipids. These normalised amounts from isolated chloroplasts were then divided by the normalised amounts from total leaves and displayed in the bar chart. Bars represent the values of a single replicate.

To address the question whether WDEs accumulate in the chloroplasts, intact chloroplasts of tpPES2 infiltrated *N. benthamiana* leaves were extracted using centrifugation with a percoll cushion. Lipids were extracted from isolated intact chloroplasts and from total leaf samples of tpPES2 infiltrated leaves. WDEs and FAPEs were purified by SPE. WDEs, FAPEs, phospho- and galactolipids were analysed by Q-TOF MS/MS. First, the distribution of phospho- and galactolipids was analysed (Figure 3.22-A). The total leaf lipid extract mainly consists of MGDG, DGDG, sulfoquinovosyl diacylglycerol (SQDG), phosphatidylinositol (PI), PG, PE and PC. In comparison, the chloroplast lipid extract was nearly devoid of PI, PE and PC and showed an increase in MGDG and DGDG. The enrichment of GLs and the decrease of PI and PE indicates a successful chloroplast isolation containing very little contaminations with other membranes, because under normal conditions GLs are restricted to the plastids and PI and PE are only found in extraplastidial membranes.

The total amount of each quantified phospho- and galactolipid species was summed up to obtain the total amount of phospho- and galactolipids. The ratio of total WDEs, 14:0-phytol or 16:0-

phytol to total phospho- and galactolipids was calculated independently for isolated chloroplasts and total leaf lipids. In a second step, the lipid ratio of isolated chloroplasts to total leaf was calculated. The complete calculation is summed up in Equation 3.1. A final ratio larger than one indicates that the lipid was enriched by chloroplast isolation relative to the other lipids and thus suggests that it is localised in the chloroplast. In contrast, a ratio below one means that the lipid is more abundant in the total leaf extract. Thus, the lipid might not be localised in the chloroplast.

$$Ratio = \frac{\left[\frac{nmol\ lipid\ of\ interest}{nmol\ phospho-\ and\ galactolipids}\right]_{chloroplast}}{\left[\frac{nmol\ lipid\ of\ interest}{nmol\ phospho-\ and\ galactolipids}\right]_{total\ leaf}} \tag{3.1}$$

WDEs and 14:0- and 16:3-phytol from isolated chloroplasts and from total leaf extracts were quantified. As the two FAPEs as well as WDEs are synthesised by tpPES2, they are all synthesised in the chloroplast. The calculation for 14:0- and 16:3-phytol can be seen as a proof of concept, as FAPEs with these chain lengths were previously localised to the plastoglobules of the chloroplasts (Gaude et al., 2007). The ratios for 14:0- and 16:3-phytol are above one, indicating that they were enriched by chloroplast isolation and are therefore likely localised in the chloroplast (Figure 3.22-C). The ratio for WDEs is below one. This means that the total leaf extract contains relatively more WDEs than the isolated chloroplasts. This result suggests that WDEs are produced in the chloroplast, but then exported out of the chloroplast.

3.2.2.8 No Accumulation of WDEs in *A. thaliana* Under Nitrogen Deprivation

WDEs are produced during the heterologous expression of tpPES2 in *N. benthamiana* leaves and in dependence on PES1/PES2 after feeding of 1,16-16:0diol to *A. thaliana* plants (Chapter 3.1.7) which both represent somewhat artificial situations. Thus, the question was raised if PES2 also produces WDEs in *A. thaliana*. To address this question, non-polar lipids of *A. thaliana* Col-0 plants were analysed. Plants were grown on synthetic medium without nitrogen to induce chlorotic stress because PES2 shows the highest expression under senescence. Wild type plants grown on synthetic medium containing nitrogen and *pes1pes2* plants grown on nitrogen deprived medium were used as negative controls because in both cases WDEs might be missing if their synthesis depends on PES2. Non-polar lipids were isolated from leaves and analysed by TLC (Figure 3.23). The two samples from nitrogen deprived plants show an increase in TAGs and FAPEs, the latter comigrate with a WE standard, as expected. No additional band was observed in Col-0 lipid extracts under nitrogen deprivation, indicating that no WDEs in amounts detectable by TLC were produced.

Lipids of *A. thaliana* Col-0 plants overexpressing PES2 (oePES2, Chapter 3.2.4) were extracted from leaves, WDEs were purified by SPE and analysed by Q-TOF MS. No accumulation of WDE

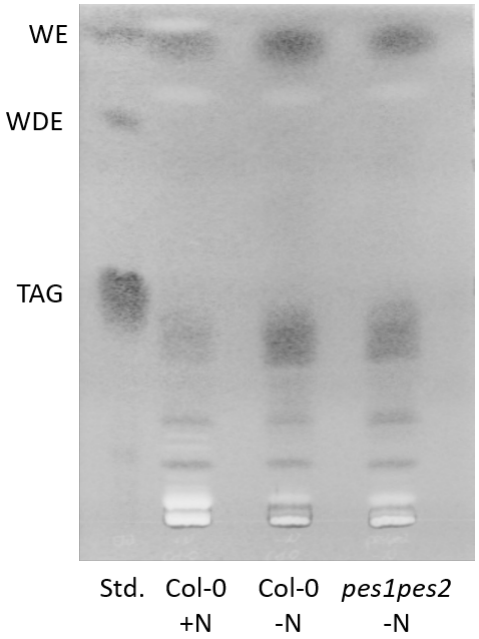

Figure 3.23 – Screening for WDEs in *A. thaliana* Col-0 and *pes1pes2* leaves. Plants were grown on synthetic medium containing nitrogen (+N) or devoid of nitrogen (-N). Non-polar lipids were separated by TLC with 90:10:1 (v/v/v) hexane/diethyl ether/acetic acid, stained with primuline and visualised under UV-light. Std. - standard containing Birkenöl and di12:0-1,16-hexadecanediol.

was detectable in oePES2 plants (Figure 3.24).

3.2.3 Heterologous Expression of PES2 in Sf9 cells

The expression of tpPES2 in *N. benthamiana* resulted in an active protein that is able to synthesise FAPEs. The attempt to use this protein in *in vitro* assays was not successful. Therefore, a change of the expression system was needed. The expression of proteins in insect cells with the help of the baculovirus expression system is an alternative strategy for eukaryotic proteins whose expression is problematic in a prokaryote such as *E. coli*. Therefore, PES2oTP (without chloroplast targeting signal, but harbouring an N-terminal His tag) was cloned into the pFastBac1 vector and introduced into DH10Bac *E. coli* cells to generate recombinant PES2oTP bacmid. Sf9 cells were transfected with the PES2oTP bacmid to produce a P1 baculovirus stock. The P1 baculovirus stock was used for the expression of PES2oTP with a MOI of 0.1. Cells were incubated until the viability was below 30%. The expression was confirmed by SDS-PAGE and immunoblotting (Figure 3.25). The SDS-PAGE shows an additional band in PES2oTP that is absent in the control sample and that migrates between 58 and 80 kDa. The corresponding band in the immunoblot detected with the His-detector kit gives a high signal intensity. A band that migrates at the same height is visible in the immunoblot of the empty cell control but with a much lower intensity. Hence, this might be unspecific signal background and the high intensity band depicts the expression of PES2oTP.

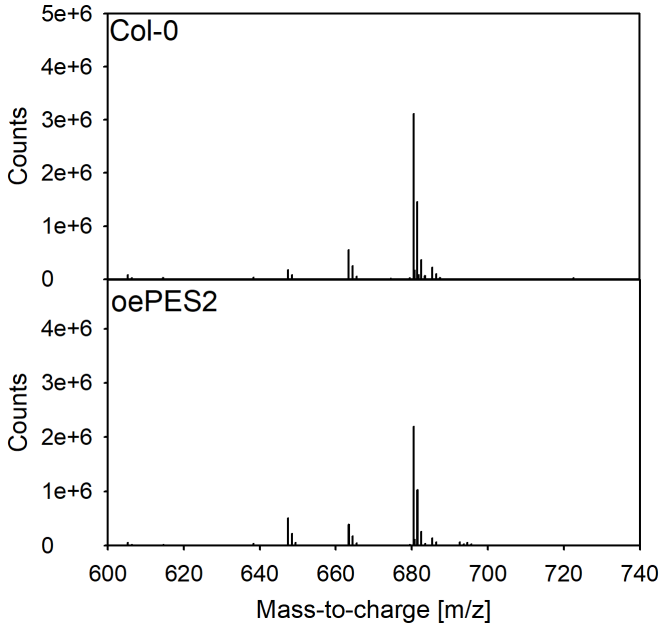

Figure 3.24 – Screening of WDEs in leaves of *A. thaliana* Col-0 plants that overexpress PES2. Lipids were isolated, purified by SPE and analysed by Q-TOF MS. Depicted is the range of the total ion chromatogram where WDEs would be expected.

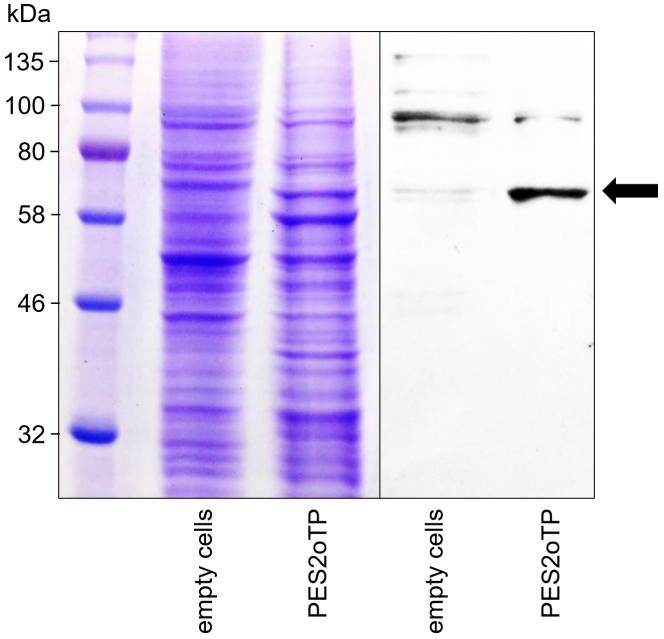

Figure 3.25 – The expression of PES2oTP in insect cells (Sf9) was confirmed by SDS-PAGE (left) and immunoblotting (right). The total protein was extracted from insect cells, which are not infected (empty cells) or infected with baculovirus expressing PES2oTP, and was used for SDS-PAGE and Coomassie staining. The proteins were blotted and detected using the His-detector kit. The western blot band at ~65 kDa (arrow) corresponds to the size of PES2oTP carrying an N-terminal His tag (69 kDa). The western blot band at 100 kDa represents a non-specific protein which cross reacted with the His-detector kit.

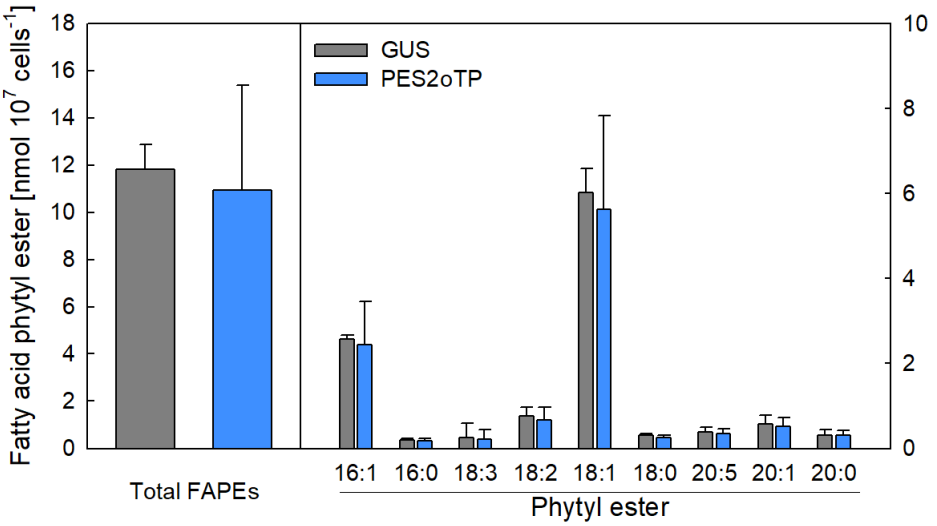

Figure 3.26 – Sf9 cells infected with PES2oTP or GUS baculovirus stock were incubated with phytol for 24 h. GUS expressing cells were used as a negative control. Cells were harvested, lipids extracted, FAPEs were purified by SPE and analysed by Q-TOF MS/MS. The total FAPE content was calculated (left) as well as the fatty acid distribution of FAPEs (right). Bars represent the means of 4–5 replicates with error bars indicating the SD.

The activity of the protein was tested in a phytol feeding assay. Sf9 cells were infected with P2 PES2oTP baculovirus stock for 24 h and incubated with phytol for additional 24 h. Insect cells harbouring a GUS expressing baculovirus construct were used as a negative control. After the 24 h feeding experiment, 100% of the cells were dead. Cells were harvested, lipids extracted, FAPEs purified by SPE and analysed by Q-TOF MS/MS. The feeding of phytol leads to an accumulation of FAPEs in the two cell strains, but without a difference between GUS and PES2oTP expressing cells (Figure 3.26). The FAPEs detected contain mainly 16:1 and 18:1 fatty acids. No differences in the fatty acid composition of FAPEs from GUS and PES2oTP lines can be observed.

3.2.4 Overexpression of PES2 in *A. thaliana*

Another way to examine the function of an enzyme is the overexpression of the protein in the homologous organism, which in this case is *A. thaliana*. To this end, Col-0 plants were transformed with PES2 overexpression constructs including the putative chloroplast signal peptide (oePES2) by floral dipping. The construct was designed in a way that PES2 is under the control of an 35S promoter for ubiquitous gene expression and that DsRed is expressed as a reporter. As a consequence, positive transformed seeds could be identified by their red fluorescence. The DsRed seeds were selected and grown on MS plates containing hygromycin for additional selection. Plants from the T2 generation were screened for overexpression of PES2. To this end, total RNA was extracted, cDNA was synthesised and subjected to qPCR with gene specific primers for *Actin2* and *PES2*. The fold change in gene expression was calculated with the $2^{-\Delta\Delta C_T}$ method (Livak and

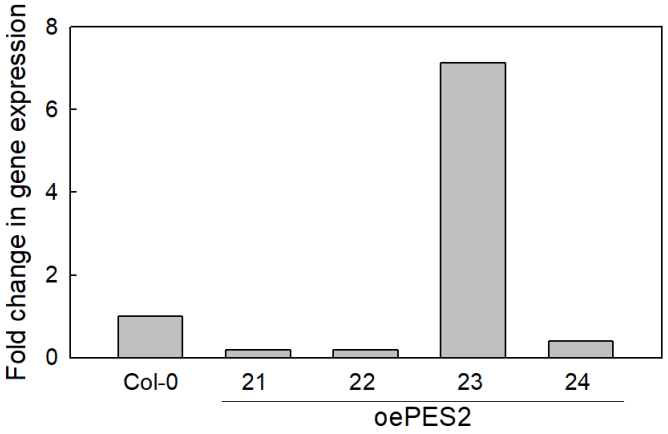

Figure 3.27 – Expression analysis of PES2 overexpression plants (oePES2). Total RNA was isolated from leaves of soil grown plants, cDNA was synthesised and subjected to qPCR using gene specific primers for *Actin2* and *PES2*. The fold change in gene expression was calculated with the $2^{-\Delta\Delta C_T}$ method (Livak and Schmittgen, 2001). Bars represent the means of three technical replicates of a single RNA isolation.

Schmittgen, 2001). One plant was identified that showed a seven-fold higher expression of PES2 in comparison to the control (#23, Figure 3.27).

The seeds of plant #23 were screened for red fluorescence and selected seeds were sown on soil. Before lipid extraction, plants were double checked for red fluorescence. Lipids were extracted from leaves of five individual plants of the progeny, FAPEs and TAGs were purified by SPE and analysed by Q-TOF MS/MS. Neither FAPEs (Figure 3.28-A) nor TAGs (Figure 3.28-B) or WDEs (*data not shown*) accumulated in leaves of the daughter plants of oePES2 plant #23.

3.3 FAPE Content under Drought Stress in *A. thaliana*

Previously it had been shown that FAPEs accumulated in *A. thaliana* under different conditions that cause chlorotic stress such as senescence or nitrogen deprivation (Ischebeck et al., 2006; Gaude et al., 2007). Anderson et al. (1984) demonstrated, that FAPEs accumulate in bean under drought stress and that the drought tolerant bean species *Phaseolus acutifolius* accumulates more FAPEs than the less drought tolerant species *Phaseolus vulgaris*. One part of this project is the investigation, if *A. thaliana* also accumulates FAPEs under drought stress. Therefore, plants were grown on MS/2% sucrose medium on plates containing 10% or 20% PEG or without PEG as control. FAPEs accumulate in *A. thaliana* upon drought stress (Figure 3.29). With 10% PEG, FAPEs accumulate 3.7-fold higher than in comparison to the control. Plants grown on 20% PEG have six times more FAPEs than control plants. The fatty acid composition of FAPEs is comparable to the composition under nitrogen deprivation with 16:3-phytol as the main FAPE species. Therefore, drought stress causes a general increase in FAPEs, but does not change the FAPE composition.

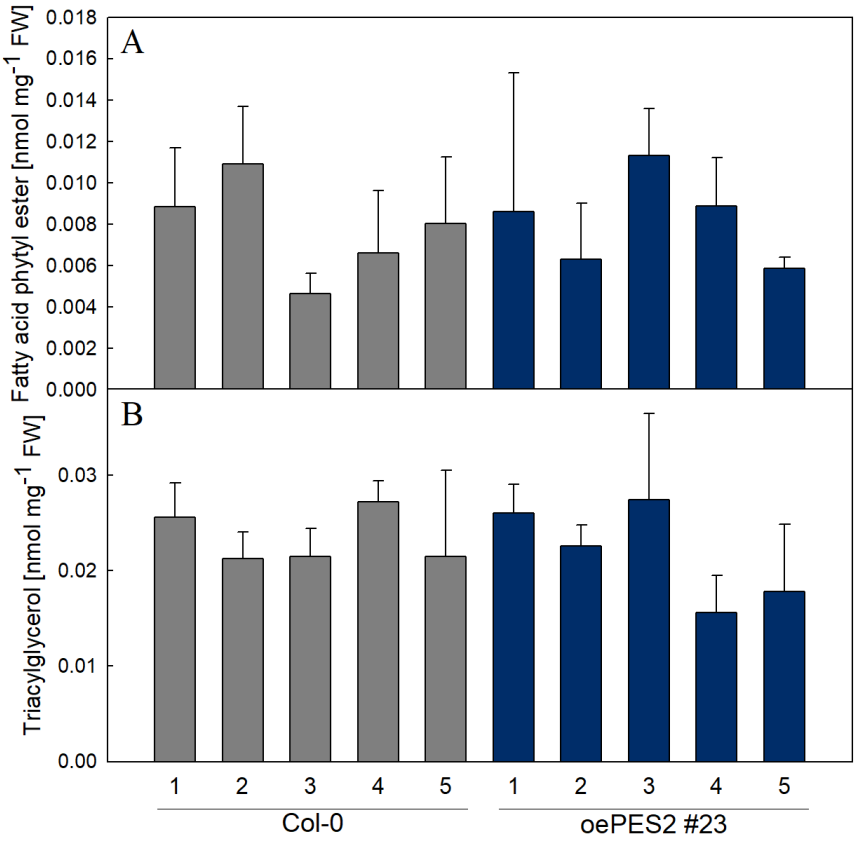

Figure 3.28 – Lipid analysis of PES2 overexpression plants. Lipids were extracted from five individual plants that are offspring of plant #23. FAPEs and TAGs were purified by SPE and analysed by Q-TOF MS/MS. Bars represent the means of 4–5 replicates with error bars indicating the SD.

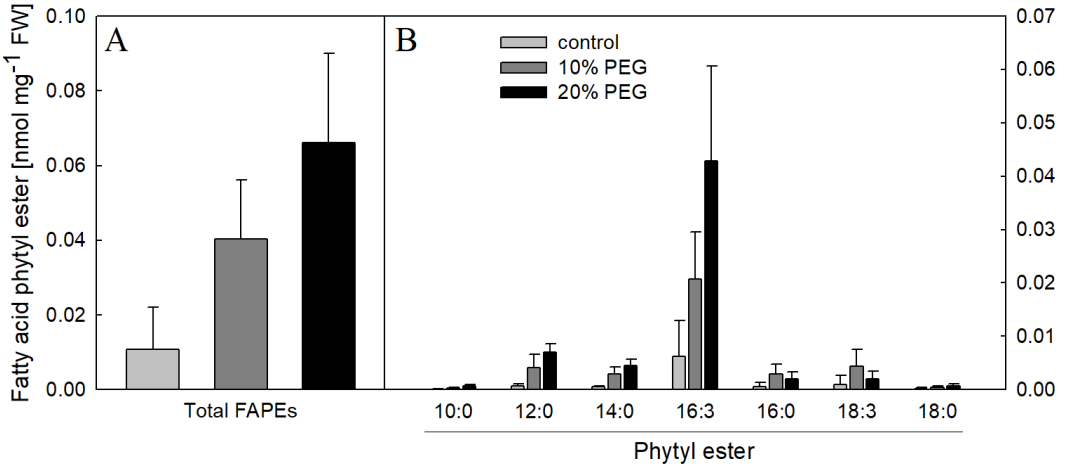

Figure 3.29 – Analysis of FAPEs under drought stress in *A. thaliana*. Col-0 plants were grown on plates without (control) or with 10% or 20% PEG. Lipids were extracted, FAPEs purified by SPE and analysed by Q-TOF MS-MS. The total FAPE content was calculated (left) as well as the fatty acid composition of FAPEs (right). Bars represent the means of 4–5 replicates with error bars indicating the SD.

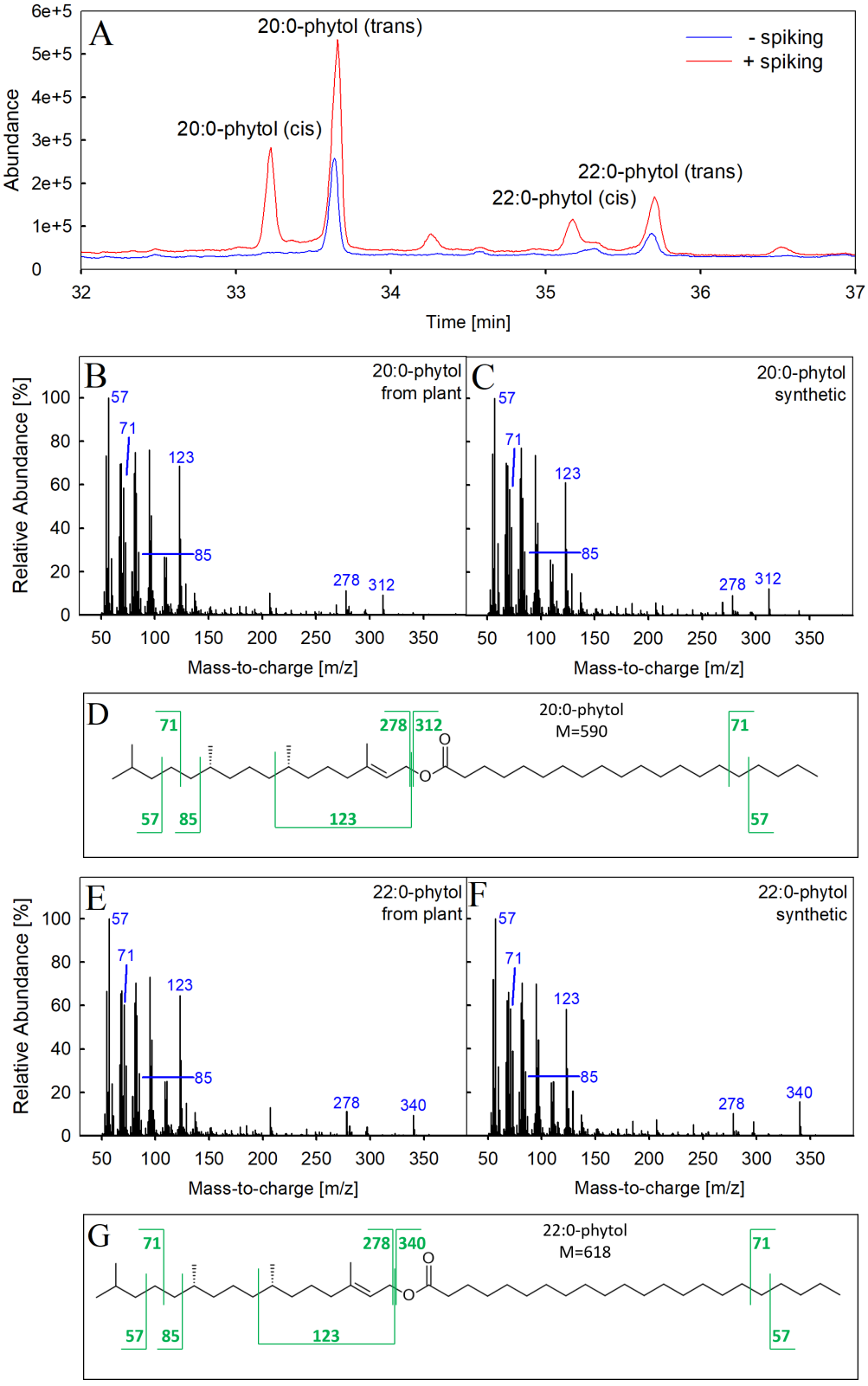

Figure 3.30 – Identification of VLC-FAPEs in senescent *N. benthamiana* leaves. A purified FAPE extract from senescent leaves was spiked with synthesised 20:0- and 22:0-phytol and intact FAPEs analysed by GC-MS. A – Overlay of total ion chromatograms with (+spiking) or without spiking (-spiking). B – GC-MS mass spectrum of plant 20:0-phytol (peak at 33.694 min of -spiking chromatogram). C – GC-MS mass spectrum of synthetic 20:0-phytol standard. D – Fragmentation of 20:0-phytol. E – Mass spectrum of plant 22:0-phytol (peak at (35.845 min of -spiking chromatogram). C – GC-MS mass spectrum of synthetic 22:0-phytol standard. D – Fragmentation of 22:0-phytol.

3.4 Very Long-Chain Fatty Acid Phytyl Ester

During the experiment of heterologous expression of PES2 in *N. benthamiana*, FAPEs were also quantified in senescent *N. benthamiana* leaves by Q-TOF MS/MS. Contrary to expectations, FAPEs are observed that contain fatty acids with chain lengths longer than C18, mainly 20:0- and 22:0-phytol. To date, only FAPEs with fatty acids up to C18 were identified in plants. Therefore it was questionable, if these new long-chain and very long-chain FAPEs are indeed FAPEs or different compounds that have the same masses of parental and fragment ions and thus cannot be distinguished by Q-TOF MS/MS.

In the following, FAPEs with fatty acids up to C18 are referred to as long-chain FAPES and FAPEs with fatty acids longer than C18 are designated as very-long-chain (VLC) FAPEs (VLC-FAPEs).

3.4.1 Identification of VLC-FAPEs

To prove the identity of 20:0- and 22:0-phytol, standards were chemically synthesised and their retention time and mass spectra analysed by GC-MS. Spiking experiments were performed by adding chemically synthesised 20:0- and 22:0-phytol to lipid extracts purified from senescent *N.benthamiana* leaves, followed by GC-MS analysis. The GC-MS chromatogram of the spiked sample shows two peaks that exactly comigrate with peaks in the non-spiked control sample (Figure 3.30-A). Two additional peaks are found in the spiked sample that are absent in the non-spiked control and that elute at an earlier retention time than the two above mentioned peaks. The commercially available phytol used for chemical FAPE synthesis was composed of a mixture of *cis* and *trans* isomers (Sigma-Aldrich, phytol data sheet), while the naturally occurring phytol contains exclusively the *trans* configuration. Therefore, the peaks present in both samples, are the naturally occurring *trans* isomers of 20:0- and 22:0-phytol, while the other two peaks, that are absent from the control, reflect the *cis* isomers of the synthesised 20:0- and 22:0-phytol standards.

Mass spectra of 20:0-phytol and 22:0-phytol from senescent *N. benthamiana* leaves (Figure 3.30-B and -E, respectively) are compared to mass spectra from synthesised 20:0-phytol and 22:0-phytol standards (Figure 3.30-C and -D, respectively). The mass spectra of the plant FAPEs and their corresponding synthesised esters are almost identical. Characteristic fragments of phytol are m/z 123 and m/z 278 (Figure 3.30-D and -G) and can be found in all four mass spectra, proving the existence phytol moiety of the compounds. The fragments m/z 312 for 20:0 and m/z 340 for 22:0 in plant derived and synthetic esters correspond to the fatty acid moiety.

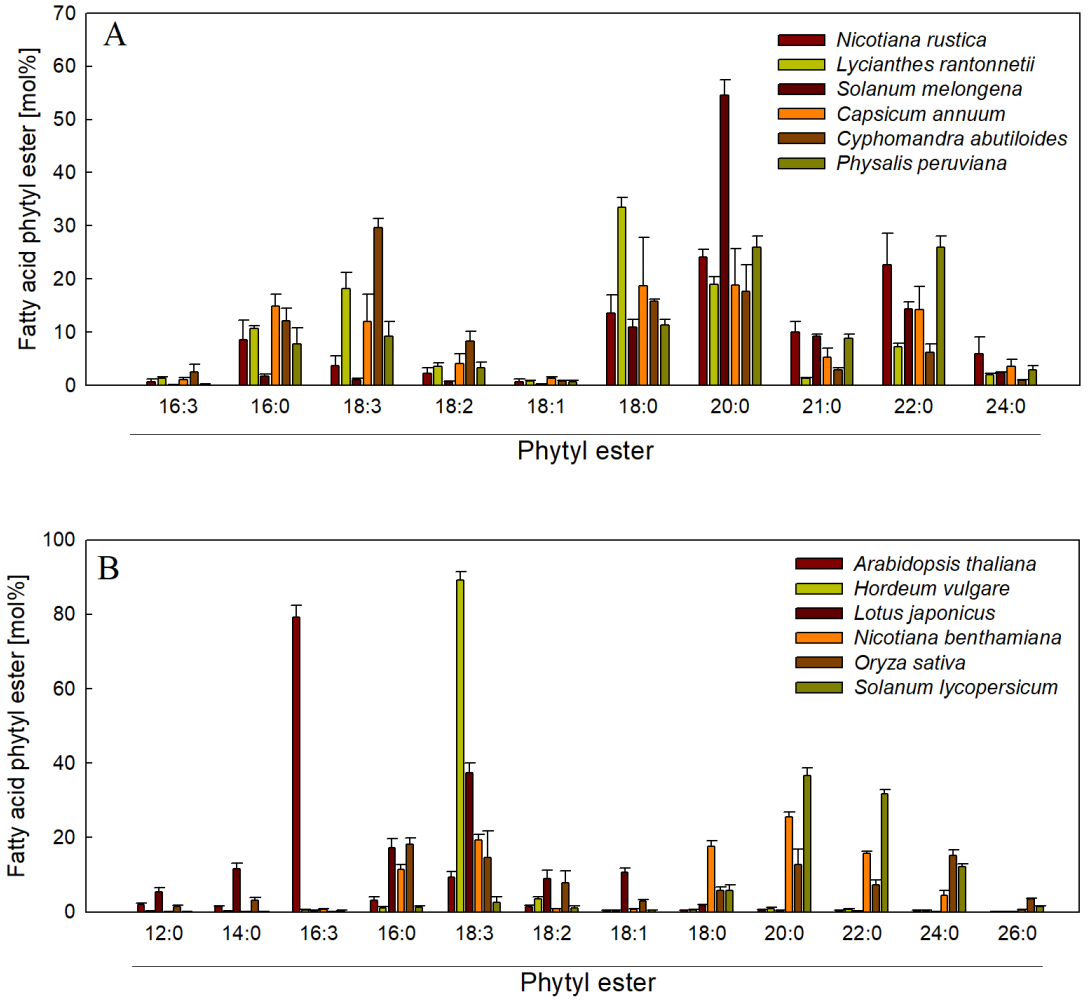

Figure 3.31 – The FAPE composition in senescent leaves from plants of the Solanaceae family (A) and from model plant species (B) was determined by Q-TOF MS/MS. Data show the relative molar fatty acid composition of FAPEs. Bars represent the means of 4–5 replicates with error bars indicating the SD.

3.4.2 Screening of Different Plant Species for VLC-FAPEs

The data shown in Figure 3.31-A show that senescent leaves of *N. benthamiana* contain FAPEs with fatty acids longer than C18. In contrast, FAPEs from *A. thaliana* only contain fatty acids with chain lengths up to C18. To investigate if the occurrence of VLC-FAPEs is only true for *N. benthamiana* or for all members of the Solanaceae family, or if these VLC-FAPEs also occur in other plant families, the fatty acid compositions of FAPEs from several Solanaceae species and different plant model organisms were examined. Plants were collected from the Botanical Gardens in Bonn in autumn 2014. Lipids were isolated from freeze-dried senescent (yellow) leaves, FAPEs were purified by SPE and quantified by Q-TOF MS/MS.

All Solanaceae species analysed contain FAPEs with C20, C22 and C24 fatty acids (Figure 3.31-A). In *Lycianthes rantonnetii*, 20:0-phytol is the most abundant FAPE species with 55 mol%. In the remaining five Solanaceae species analysed, 20:0-phytol amounts to 20–30 mol%. In *Capsicum annuum* and *Cyphomandra abutiloides*, the relative amounts of 20:0- and 22:0-phytol are approximately the same. In *Nicotiana rustica*, *Lycianthes rantonnetii* and *Physalis peruviana*, the amount of 22:0-phytol is less than the amount of 20:0-phytol. The relative amount of 24:0-phytol is lower in all Solanaceae species as compared to 20:0- or 22:0-phytol. *Lycianthes rantonnetii* only contains FAPEs with saturated C18 to C24 fatty acids. The other five Solanaceae species also contain shorter fatty acids with 16:0 and unsaturated fatty acids such as 18:3 and 18:2.

Species from different plant families, that serve as model organisms for research, were also investigated regarding their fatty acid composition in FAPEs. *Nicotiana benthamiana* and *Solanum lycopersicum* are also representatives of the Solanaceae family and also contain 20:0-, 22:0- and 24:0-phytol comparable to *Nicotiana rustica* as described above (Figure 3.31-B). In *A. thaliana* (Brassicaceae) and *Lotus japonicus* (Fabaceae), no FAPEs with fatty acids longer than C18 are observed. The main FAPE of *A. thaliana* is 16:3-phytol which counts up to 80 mol%. *Lotus japonicus* has a broader distribution of fatty acids from C12 to C18 with higher relative amounts of 18:3 (37 mol%). *Oryza sativa*, a member of the Poaceae, contains also very long-chain FAPEs with fatty acids up to C26. The relative composition of fatty acids is approximately even distributed between 16:0, 18:3, 18:2, 18:0, 20:0, 22:0 and 24:0. In contrast, *Hordeum vulgare*, which is also a Poaceae, only contains FAPEs with fatty acids up to C18. The major FAPE species is 18:3-phytol with 90 mol%.

3.4.3 Localisation of VLC-FAPEs

The previous experiment demonstrated the existence of FAPEs with fatty acid chain lengths longer than C18 in senescent *N. benthamiana* leaves. Up to now, only FAPEs with fatty acid chain lengths up to C18 were identified and characterised. The medium and long chain FAPEs are localised in

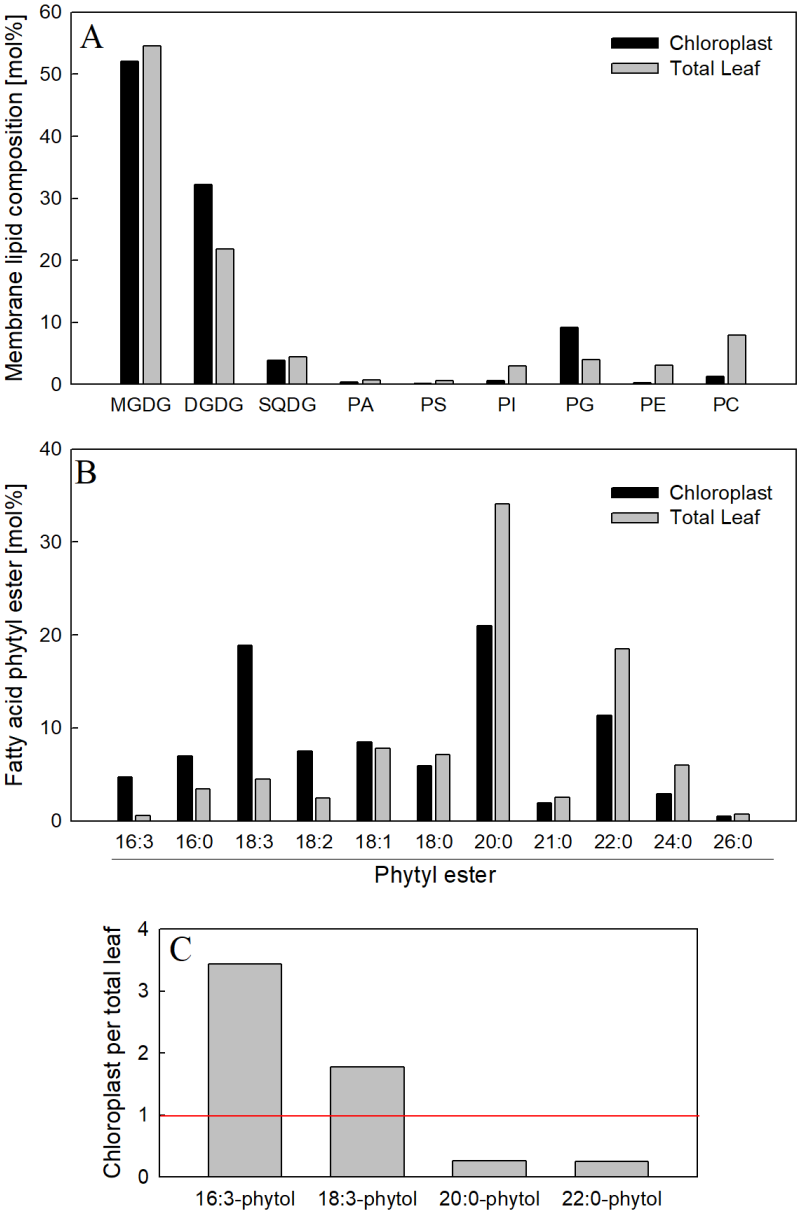

Figure 3.32 – Lipids from isolated intact chloroplasts of *S. lycopersicum* leaves were analysed in comparison to lipids that were extracted from total leaf samples. Lipids were isolated as described before and FAPEs were purified by SPE. FAPEs, phospho- and galactolipids were quantified by Q-TOF MS/MS. A – Molar composition of phospho- and galactolipids. B – Molar composition of FAPEs. C – The FAPE amount was related to the total amount of phospho- and galactolipids. The ratio of amounts in isolated chloroplasts and total leaf was calculated and depicted in the bar chart. Bars represent the values of a single replicate.

the plastoglobules of chloroplasts (Gaude et al., 2007). In plants, fatty acid biosynthesis takes place in the plastids. Fatty acids are synthesised up to a chain length of C18 and then exported to the ER where they are elongated to very long chain fatty acids. Because of this fact, it is questionable, whether the VLC-FAPEs identified in *N. benthamiana* are synthesised and localised in the chloroplast. To study the localisation of VLC-FAPEs in the plant cell, intact chloroplasts of senescent *S. lycopersicum* leaves were isolated. Lipids were extracted and FAPEs were purified by SPE. FAPEs, phospho- and galactolipids were quantified by Q-TOF MS/MS. The analysis was done as described in Chapter 3.2.2.7. The relative composition of membrane lipids was assessed (Figure 3.32-A). The chloroplast extract showed an enrichment in DGDG and PG and a high decrease of PI and PE compared to the total leaf extract. This indicates a successful isolation of intact chloroplasts without contamination.

FAPEs were quantified and the molar composition was compared between chloroplast and total leaf lipid extracts. The main FAPE species in the total leaf extract is 20:0- and 22:0-phytol with 34 and 19 mol%, respectively (Figure 3.32-B). In contrast to that, the main FAPE species in the chloroplast extract are 18:3- (19 mol%), 20:0- (21 mol%) and 22:0-phytol (11 mol%).

FAPE amounts were related to the total amount of phospho- and galactolipids and the ratio of these values in chloroplasts to total leaf lipids was calculated (Figure 3.32-C). The ratio for 18:3-phytol is larger than one, indicating that it might be localised to the chloroplasts. In contrast, the ratio for 20:0- and 22:0-phytol is below one, pointing towards a localisation outside of the chloroplast.

3.5 Biochemical Characterisation of *S. lycopersicum pale yellow petal 1* Mutant Plants

3.5.1 Analysis of FAPEs in Different Tomato Tissues

Orthologous gene sequences of the *ELT* genes can be found in all chlorophyll-containing organisms including plants, algae and cyanobacteria. Recently, a mutant population of *S. lycopersicum* was screened and two mutant plants were isolated that show a pale yellow petal (PYP) phenotype (Ariizumi et al., 2014). Through next generation sequencing and map-based cloning, the two mutations were found to be allelic, because they localise to a single gene, *Solyc01g098110*. Therefore, the two mutants were designated as *pyp1-1* and *pyp1-2*. The disruption of the PYP1 locus resulted in the loss of fatty acid xanthophyll esters in the petals of tomato flowers indicating that PYP1 is a xanthophyll ester synthase. PYP1 shows 73% sequence similarity on polypeptide level to *A. thaliana* PES1. In addition, the PYP1 sequence revealed an α/β hydrolase-fold like domain and an acyltransferase like domain as they are also present in the ELT sequences. Because of these

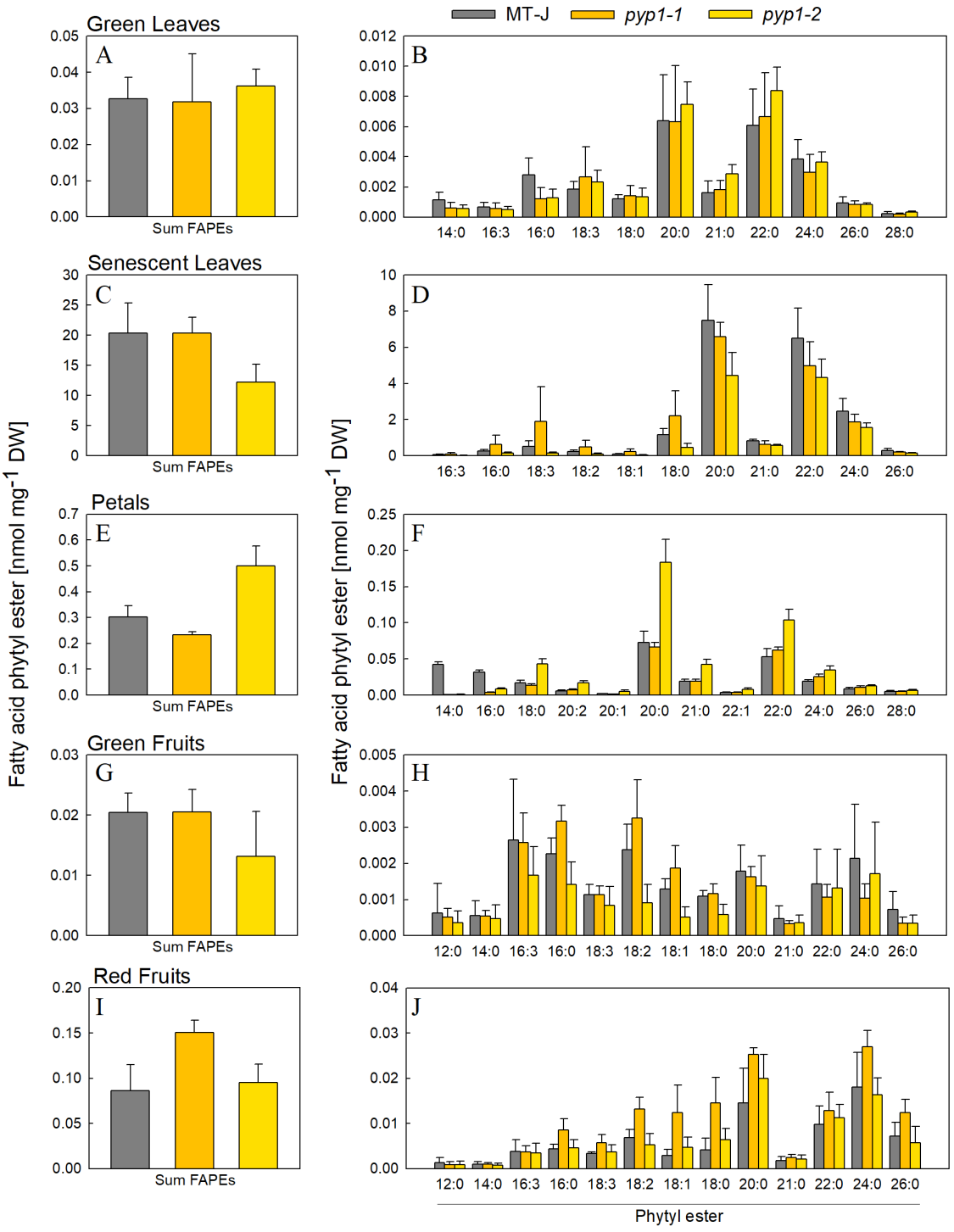

Figure 3.33 – Analysis of the FAPE content and composition in different tissues of *S. lycopersicum* MT-J and the mutants *pyp1-1* and *pyp1-2*. Lipids were isolated, FAPEs were purified by SPE and quantified by Q-TOF MS/MS. Bar diagrams on the left side show the total FAPE amounts while bar diagrams on the right side show the fatty acid distribution in FAPEs. FAPEs were quantified in green leaves (A, B), senescent leaves (C, D), petals (E, F), green fruits (G, H) and red fruits (I, J). Bars represent the means of 4–5 replicates with error bars indicating the SD.

similarities, the question was raised, whether PYP1 might also have phytyl ester synthase activity, and whether PES/PES2 in *A. thaliana* might be involved in FAXE synthesis.

To address this question, FAPEs were isolated and purified from freeze-dried wild type tomato tissues and quantified by Q-TOF MS/MS. The highest amount of FAPEs is found in senescent tomato leaves with 20.3 nmol $mg^{-}1$ DW, followed by petals with 0.3 nmol $mg^{-}1$ DW (Figure 3.33-C and -E). FAPEs are very low abundant in green leaves and green fruits (Figure 3.33-A and -G). After fruit ripening, the FAPE content is four times higher in red fruits as compared to green fruits (Figure 3.33-G and -I). In comparison, the FAPE content in senescent leaves is 700 times higher than in green leaves.

The fatty acid composition of FAPEs is comparable in all measured tissues with minor differences. In general, fatty acids in FAPEs of *S. lycopersicum* are mainly saturated with chain lengths of C14 up to C26. The main FAPE fatty acids in senescent leaves, petals and red fruits are 20:0 and 22:0 (Figure 3.33-D, -F and -J). In addition, 18:0 and 24:0 are found in FAPEs of senescent leaves (Figure 3.33-D). Flowers also have FAPEs with 14:0, 16:0 and 24:0 (Figure 3.33-F). FAPEs in red fruits contain mainly VLC fatty acids with 20:0 up to 26:0 (Figure 3.33-J). Because of the low abundance of FAPEs in green leaves and green fruits, it is difficult to accurately quantify the FAPE species compared to background signals (Figure 3.33-B and -H). This also results to the high standard deviations.

The FAPE content of the *pyp1-1* and *pyp1-2* mutants were compared to the wild type cultivar MT-J. No differences are observed in the total FAPE amount in green leaves and green fruits (Figure 3.33-A and -G). In senescent leaves, the FAPE amount in *pyp1-1* is comparable to MT-J, but in *pyp1-2* decreased by half (Figure 3.33-C). The decrease in *pyp1-2* is reflected in all FAPE species (Figure 3.33-D), as there is no significant difference in the relative fatty acid composition (*data not shown*). The FAPE content in petals is slightly decreased in *pyp1-1* and 1.5 times increased in *pyp1-2* (Figure 3.33-E). Interestingly, the slight reduction in *pyp1-1* is due to the absence of 14:0- and 16:0-phytol (Figure 3.33-E). Although *pyp1-2* showed an increase in total FAPE amount, the amount of 14:0- and 16:0-phytol in *pyp1-2* is also drastically decreased. The total increase is mainly due to a high increase in 20:0- and 22:0-phytol. In contrast, the FAPE amount in red fruits of *pyp1-2* is comparable to that of MT-J, but 1.7 times higher in *pyp1-1* (Figure 3.33-I). The higher FAPE amount in red fruits of *pyp1-1* is observed in all FAPE species (Figure 3.33-J).

3.5.2 Analysis of Fatty Acid Xanthophyll Esters in Tomato Flowers

HPLC analysis of petals of *pyp1* mutant plants by Ariizumi et al. (2014) revealed that the disruption of PYP1 leads to the loss of fatty acid xanthophyll mono- and diesters (FAXmEs and FAXdEs, respectively). These esters mainly consist of saturated 14:0 and 16:0 fatty acids esterified to neox-

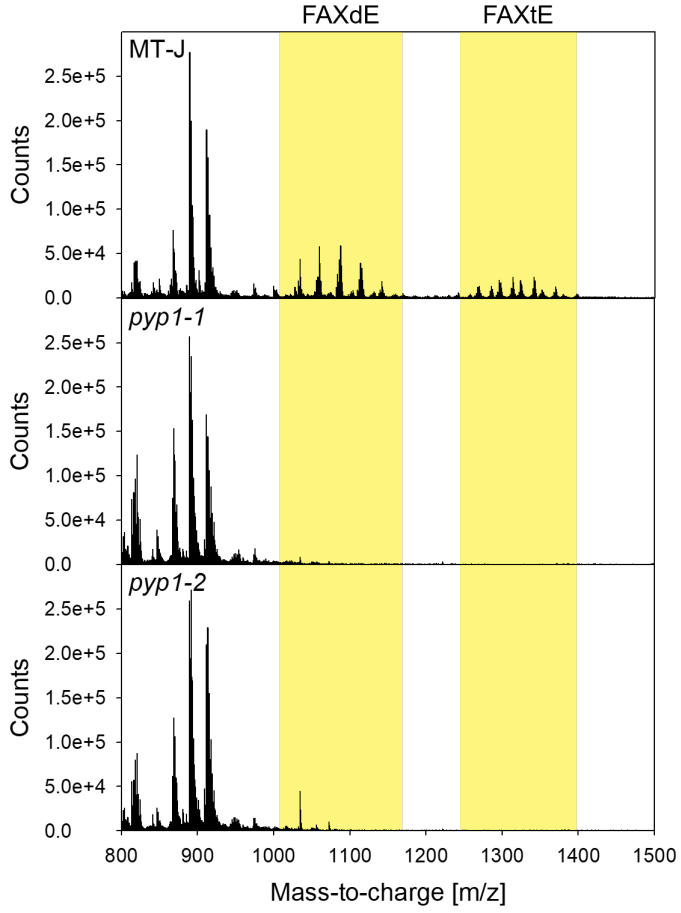

Figure 3.34 – Total non-polar lipids from petals of *S. lycopersicum pyp1* mutant lines were analysed by Q-TOF MS. The total ion chromatograms show two series of lipids in wild type MT-J that are absent in *pyp1-1* and *pyp1-2* (highlighted in yellow).

anthin or violaxanthin. To further investigate these lipids, non-polar lipids from petals were isolated and analysed by Q-TOF MS. The total ion chromatogram of tomato wild type MT-J petals shows two series of masses absent from *pyp1-1* and *pyp1-2* petals (Figure 3.34). The masses of the first series range from m/z ~ 1000 to m/z ~ 1130. The theoretical masses of FAXdEs with neoxanthin/violaxanthin or lutein/zeaxanthin containing saturated fatty acids were calculated as ammonium adducts $[M + NH_4]^+$ and as proton adducts $[M + H]^+$. Because neoxanthin/violaxanthin as well as lutein/zeaxanthin, respectively, are isomers, these molecules are isobaric and the isomers as well as the corresponding esters cannot be differentiated by direct infusion Q-TOF MS. The masses of the first series correlate to the masses of the neoxanthin/violaxanthin ammonium adducts indicating that the first series are FAXdEs containing neoxanthin/violaxanthin.

The second series of lipids that are absent in the *pyp1* mutants, are found in a mass range of m/z ~ 1200 to m/z ~ 1350. Among the xanthophylls that occur in the petals of *S. lycopersicum*, neoxanthin is the only one that contains three hydroxyl groups and thus can possibly form fatty acid xanthophyll triesters (FAXtEs). Theoretical masses for these FAXtEs were again calculated

as ammonium adducts $[M + NH_4]^+$ and as proton adducts $[M + H]^+$. The calculated masses of the ammonium adducts fit to the masses of the second series which indicates that *S. lycopersicum* petals contain an additional group of xanthophyll esters which are neoxanthin triesters. The two *pyp1* mutant lines are devoid of neoxanthin triesters.

Previously it was shown that *pyp1-1* and *pyp1-2* are also devoid of monoesters containing neoxanthin or violaxanthin (Ariizumi et al., 2014). The calculated masses for the corresponding ammonium and proton adducts are in the range of m/z ~ 801 to m/z 885 and m/z 783 to m/z ~ 867, respectively. Corresponding peaks in the total ion chromatogram of MT-J could not be detected. TAGs are also non-polar lipids and their masses are in the same range as the calculated masses for FAXmEs. As this analysis was conducted with total non-polar lipid extracts, it is possible that TAGs are more abundant than FAXmEs and therefore suppress the FAXmEs during ionisation in Q-TOF MS analysis.

To overcome the problem of the suppression of FAXmEs in total non-polar lipid extracts, purification of lipid extracts by TLC was carried out. The routinely used mobile phase for the analysis of non-polar lipids by TLC is hexane/diethyl ether/acetic acid. The composition needs to be adjusted to the polarity of the analytes. For WEs, a composition of 90:10:1 (v/v/v) is used while TAGs are analysed with 70:30:1 (v/v/v). These solvent combinations were tested with non-polar lipids of petals but none of them resulted in a satisfactory separation. Further solvent compositions were tested and in the end the use of hexane/diethyl ether/acetic acid 50:50:1 (v/v/v) resulted in a better separation. Directly after taking out the TLC from the developing tank, yellow bands in MT-J lipid extracts were visible. Routinely, TLC plates are stained with primuline and visualised under UV-light. When this staining was applied to TLC plates containing petal lipids, only a few lipid bands could be detected that were much less in number and intensity than observed before the staining. In addition, during the staining process, the yellow bands first became lighter and finally vanished completely. TLC analysis was repeated and because most of the petal lipids are already visible by eye due to their yellow colour, TLC plates were not stained but further processed for scanning. During this procedure, the yellow bands again vanished. Therefore, the yellow bands disappear in ambient air within 5–10 min after taking out the TLC plate from the developing tank. Therefore, processing of TLC plates had to be done fast.

Non-polar lipids from petals of MT-J and *pyp1-1* were isolated and separated by TLC (Figure 3.35-A). In the lane of wild type MT-J, several yellow bands are visible that are absent from the lane of *pyp1-1*. The three bright yellow bands in MT-J were isolated from the TLC plate, lipids were extracted from the silica material and analysed by Q-TOF MS (Figure 3.35-B). The extracted band with the highest retention factor contains FAXtEs while the band with the middle retention factor contains FAXdEs. The series of FAXtEs and FAXdEs reveal the same masses as seen before

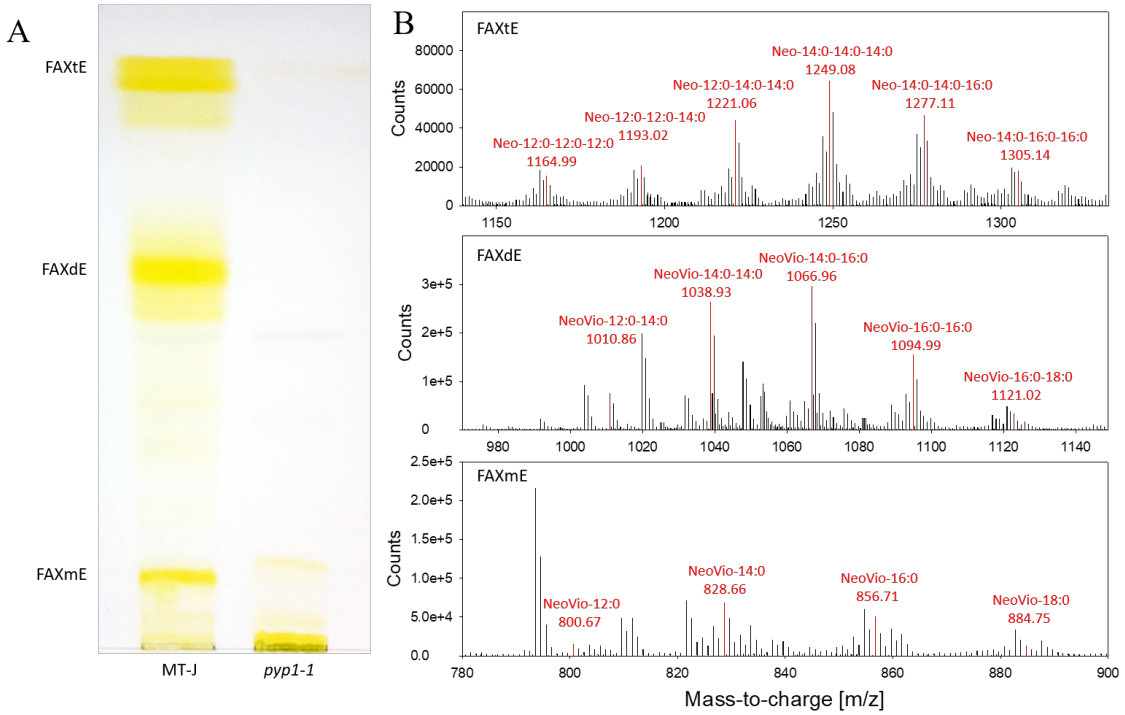

Figure 3.35 – Analysis of FAXEs from *S. lycopersicum* MT-J petals. A – Non-polar lipids from petals of MT-J and *pyp1-1* were isolated and purified by TLC. The plate was not stained, but shows the authentic colours of FAXEs. B – FAXE spots were isolated from the TLC plate, lipids were extracted from the silica material and analysed by direct infusion Q-TOF MS. Because neoxanthin and violaxanthin have the exact same mass, mono- and diesters of these xanthophylls cannot be distinguished by direct infusion mass spectrometry and are therefore labelled as *NeoVio* esters. Tagged peaks are coloured in red.

in the to total non-polar lipid extracts. In the third band, masses corresponding to ammonium adducts of FAXmEs with neoxanthin/violaxanthin are detected. Therefore the separation with hexane/diethyl ether/acetic acid 50:50:1 (v/v/v) was successful.

Taking a closer look at the total ion chromatogram, it can be observed that every FAXE peak is in the middle of a groups of peaks with successive masses. Peaks with a higher mass are isotopic peaks that contain one or more ^{13}C atoms. Peaks with masses that are reduced by 2, 4 or 6 mass units indicate unsaturated bonds while masses in between represent isotopes of the unsaturated molecules. The results indicate that FAXEs can also contain unsaturated fatty acids.

3.5.3 Screening for FAXEs in *Camelina sativa* and *A. thaliana*

The occurrence of FAXEs has been demonstrated for petals of *S. lycopersicum* (Ariizumi et al., 2014), for senescent leaves of *Fagus sylvatica* (Tevini and Steinmüller, 1985) and for several fruits, e.g. chilli, pepper, blood orange, clementine, mango, papaya and pumpkin (Breithaupt and Bamedi, 2001). In the present study, the existence of FAXEs was further investigated in the model plants *Camelina sativa* and *A. thaliana*. *Camelina sativa* also possesses yellow flowers as

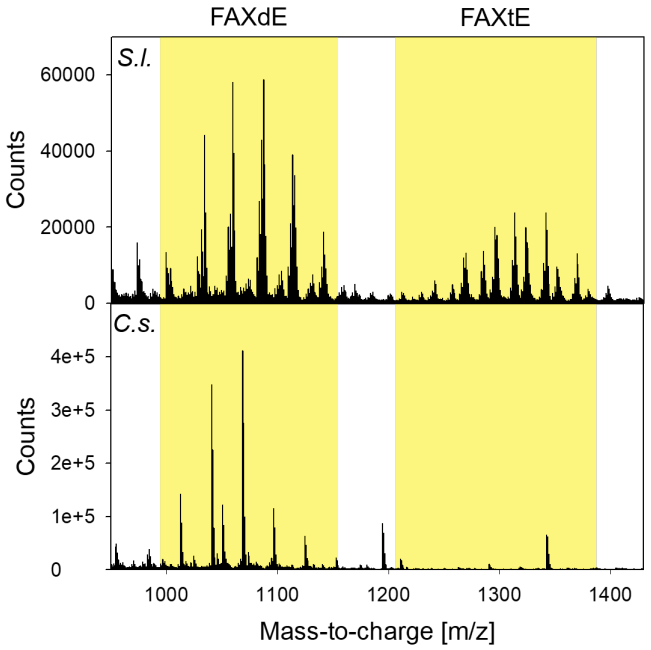

Figure 3.36 – Analysis of FAXEs from *Camelina sativa* (*C.s.*) petals in comparison to *S. lycopersicum* (*S.l.*) petals. Non-polar lipids were isolated from petals and analysed by Q-TOF MS. Masses observed in *Camelina sativa* do not correspond to masses of FAXEs and are therefore unknown lipids or contaminants.

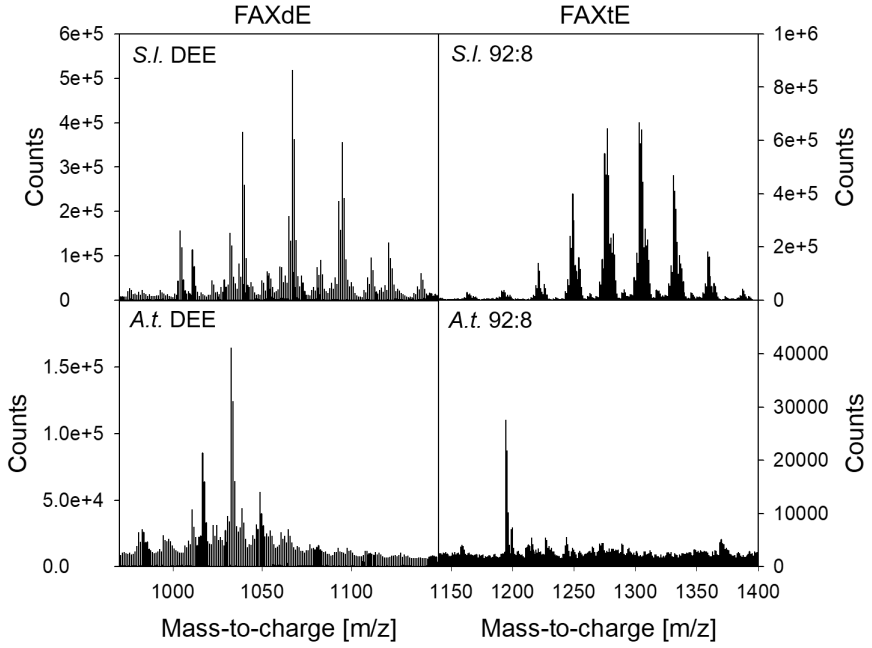

Figure 3.37 – Screening for FAXEs in senescent leaves of *A. thaliana* (*A.t.*) in comparison to FAXEs from *S. lycopersicum* (*S.l.*) petals. Non-polar lipids were isolated, FAXEs were purified by SPE and analysed by Q-TOF MS. Masses observed in *A. thaliana* do not correspond to masses of FAXEs and are therefore unknown lipids or contaminants.

it is the case for *S. lycopersicum* while *A. thaliana* petals are white. Therefore, non-polar lipids of *Camelina sativa* petals were extracted and analysed by Q-TOF MS. Total ion chromatograms of *S. lycopersicum* and *Camelina sativa* petal extracts were compared (Figure 3.36). The TIC of *Camelina sativa* shows no series of lipids in the characteristic mass range of FAXdEs or FAXtEs.

In contrast to *S. lycopersicum* and *Camelina sativa*, *A. thaliana* has no yellow coloured flowers. Because FAXEs also accumulate under senescence, lipids were extracted from senescent *A. thaliana* leaves and purified by SPE. FAXtEs were eluted with 92:8 (v/v) hexane/diethyl ether and FAXdEs were eluted with diethyl ether. Purified FAXEs were analysed by Q-TOF MS. Lipids from *A. thaliana* were compared to purified lipids from *S. lycopersicum* petals. Neither the masses of FAXdEs, nor the masses of FAXtEs can be found in senescent *A. thaliana* leaves (Figure 3.37).

4 Discussion

Chlorophyll is the most abundant pigment in the biosphere. The degradation of chlorophyll leads to the release of large amounts of chlorophyll breakdown products. In this process, the phytol side chain is hydrolysed from the chlorophyll molecule. The hydrolysis is catalysed by the pheophytinase or the chlorophyll dephytylase (Schelbert et al., 2009; Lin et al., 2016). Only a small fraction of the released phytol is degraded, the main fraction is further processed (Peisker et al., 1989). Phytol can be incorporated into fatty acid phytyl esters (FAPEs), tocopherols, chlorophyll and phylloquinone (Ischebeck et al., 2006). The esterification of phytol into FAPEs is catalysed by phytyl ester synthases. In *A. thaliana* two enzymes, PES1 and PES2, have been characterised which are expressed under senescence and which have phytyl ester synthase activity (Lippold et al., 2012). PES1 and PES2 belong to a family of six esterase/lipase/thioesterase (ELT) like proteins, and the remaining four ELT enzymes have not been characterised yet. The ELT proteins have in common a similar protein structure with predictions for a hydrolase and an acyltransferase domain. In this work, the further characterisation of PES2 is presented as well as the characterisation of ELT3, ELT4, ELT5 and ELT6. In addition, mutants of the xanthophyll ester synthase PYP1 from *S. lycopersicum* were analysed regarding a putative phytyl ester synthase activity.

4.1 Members of the ELT Family are Involved in Seed FAPE Production

For the characterisation of the ELT family members, the gene expression in *A. thaliana* wild type plants and the lipid composition of *elt* mutant plants were investigated. The expression of *PES1*, *PES2*, *ELT3* and *ELT4* is highly increased during developmental leaf senescence and under nitrogen deprivation. Furthermore, *PES1*, *ELT4*, *ELT5* and *ELT6* show elevated expression levels in the inflorescences. The lipid analysis of the *ELT* single insertion mutant lines and the newly generated double mutant *elt4elt6* revealed no differences in FAPE content and composition compared to wild type under nitrogen deprivation. In contrast, the double mutant *pes1pes2* showed a strong reduction in FAPE content under nitrogen deprivation compared to wild type as shown by

Lippold et al. (2012). The addition of a third mutation in the newly generated *pes1pes2elt4* triple mutant does not lead to a further decrease in FAPE accumulation as compared to *pes1pes2*. These results demonstrate that although the expression of *ELT3* and *ELT4* is increased under nitrogen deprivation, they do not play a major role in FAPE accumulation under this condition. ELT4 was shown to be part of the plastoglobule proteome (Lundquist et al., 2012). Therefore, ELT4 might be responsible for the esterification of other non-polar lipids such as triacylglycerol or not yet identified non-polar lipids in the plastoglobules. The thylakoid membranes contain, besides membrane lipids and chlorophyll, numerous other components required for photosynthesis, e.g. other pigments. During senescence, the thylakoid membranes are disintegrated and concomitantly the photosynthetic apparatus as well. Therefore, ELT4 might be involved in processing other breakdown products.

The *pes1pes2* double mutant is not completely devoid of FAPEs and Lippold et al. (2012) suggested, that the residual FAPEs are produced by other ELT enzymes. The results presented here show that the four remaining ELT enzymes are individually not essential for FAPE synthesis under nitrogen deprivation. This leads to the conclusion that the ELT enzymes either are no phytyl ester synthases, or have redundant functions, or are active under different conditions than nitrogen deprivation. To address the question of redundant functions, it would be necessary to produce further multiple mutants besides *pes1pes2elt4*. A broader experiment with different conditions to induce chlorotic stress would be helpful to screen for a situation under which the ELT enzymes are active.

Although it has been known for a long time that chlorophyll is degraded during seed maturation, there are only few studies dealing with the mechanisms and regulations of chlorophyll degradation and the fate of the breakdown products in maturing seeds. For the first time, Kanwischer (2007) has shown that during seed maturation FAPEs accumulate. The *pao1* mutant is impaired in chlorophyll breakdown which results in a stay-green phenotype and a high seed abortion rate (Pružinská et al., 2003). In addition, the *pao1* mutant shows a decreased seed FAPE content in comparison to wild type seeds (vom Dorp, 2015). This result indicates that the chlorophyll-derived phytol is an important but not the only source for the production of FAPEs in seeds as the *pao1* seeds still contain some FAPEs. However, other than this, nothing more is known about the mechanisms or enzymes that are involved in seed FAPE production. Therefore, the seed FAPE analysis presented in this study gives a first hint to answer the question which enzymes are involved in this process. The total FAPE content is decreased in *elt4elt6* and *pes1pes2elt4* mutant seeds, with minor changes in *pes1pes2* seeds. The relative amount of FAPEs related to the total FA amount is decreased in the seeds of all three mutants, with the highest decrease in *pes1pes2elt4* and smaller decreases in *elt4elt6* and *pes1pes2* as compared to wild type. These results demonstrate that some of the ELT enzymes are involved in seed FAPE production. *PES1*, *ELT4* and *ELT6* are highly expressed in

inflorescences, and therefore, these might be the responsible enzymes. To identify the responsible enzyme, it would be helpful to analyse the seed FAPE content of single mutant lines.

The leaf and seed results together indicate that in different tissues, different enzymes are responsible for the synthesis of FAPEs. In addition, different conditions might also activate different enzymes for FAPE synthesis. Therefore, the ELT enzymes might be involved in the FAPE production under not-yet investigated conditions such as drought stress, dark induced senescence or other abiotic or biotic stresses.

The feeding of wild type, *elt4elt6*, *pes1pes2* and *pes1pes2elt4* plantlets with different alcohols was conducted to test additional ester synthase activities of the ELT enzymes. Upon feeding of phytol, 18:0ol, farnesol and 1,16-16:0diol, the respective esters accumulated in the wild type. The mutants showed no differences in ester accumulation compared to wild type after feeding of phytol and farnesol. However, the feeding of 18:0ol and 1,16-16:0diol to *pes1pes2* and *pes1pes2elt4* caused a reduced accumulation of 18:0ol ester and 1,16-16:0diol diester compared to wild type. These results will be discussed in Chapter 4.6. The feeding of phytol to *pes1pes2* was previously performed by Lippold et al. (2012) who observed a reduced accumulation of FAPEs, different from the results presented here. The difference in the experimental procedure was that in the present work, Tween-20 was used as a detergent to help solubilisation of substrates. Because Tween-20 contains fatty acids in ester linkage (Kerwin, 2008), extra amounts of fatty acids were introduced into the experiment which can also be used as substrates for esterification. Probably the excess in alcohol and fatty acid substrates led to the activity of unspecific acyltransferases, maybe at the ER, and therefore, the loss of activity of PES1 and PES2 was compensated. To overcome this problem, other detergents could be tested that do not introduce fatty acids.

4.2 The Fatty Acid Preference of Heterologously Expressed *A. thaliana* PES2 is in Agreement with Its *In Vivo* Specificity

One part of this project was the further characterisation of PES2, especially with regard to substrate specificity. To this end, PES2oTP was expressed in *E. coli* cells. After feeding of phytol, an accumulation of FAPEs was observed which was higher under expression of PES2oTP in comparison to an empty vector control. These results confirmed that PES2 carries phytyl ester synthase activity. The fatty acid composition of FAPEs produced by PES2oTP reflected the fatty acid composition of *E. coli* total lipids. To test the substrate specificity of PES2, purified enzyme or crude enzyme extracts would be required. Unfortunately, it was not possible to purify or extract PES2oTP protein from *E. coli* cells in an active state.

In a second attempt, the baculovirus system was used for heterologous expression of proteins in

Sf9 insect cells. The successful expression of PES2oTP was confirmed by immunoblotting. The feeding of phytol to baculovirus infected insect cells led to the accumulation of FAPEs. However, there were no differences in FAPE accumulation between the expression of PES2oTP and the GUS expressing negative control. The fatty acid composition of these FAPEs was similar to the fatty acid composition of total lipids from Sf9 cells analysed by Marheineke et al. (1998), although the relative amount of 18:0-phytol was low in comparison to the amount of 18:0 in total lipids. At this point the question arises, if the protein has no activity or if the background activity derived from endogenous acyltransferases of the insect cells is too high so that the activity of PES2oTP cannot be distinguished from background. To overcome this problem, two reaction parameters could be adjusted. First, the feeding could be stopped earlier with the result that only the highly specific PES2 utilises the phytol for FAPE production and not rather unspecific endogenous acyltransferases. Second, the feeding could be conducted with a lower concentration of phytol for the same reason as before that only the highly specific PES2 uses the phytol and that an excess of phytol is not used by unspecific acyltransferases. Ultimately, a protein extract should be prepared from PES2oTP expressing insect cells and used for *in vitro* enzyme assays. To this end, one could also isolate microsomal proteins given that PES2oTP most likely binds to the membranes because it has one transmembrane domain, as all ELT proteins.

In a third attempt, PES2 was transiently overexpressed in leaves of *N. benthamiana*. Only the expression of the full length ORF of PES2 including a putative N-terminal chloroplast targeting signal led to the production of FAPEs in leaves of *N. benthamiana* and thus confirmed its phytyl ester synthase activity. Upon expression in chloroplasts of *N. benthamiana* mesophyll cells, PES2 produces FAPEs but no TAGs, WEs, or SEs. In contrast, Aslan et al. (2014) reported the accumulation of WEs upon expression of PES2 in leaves of *N. benthamiana* in combination with expression of a FAR. The accumulated WEs contained mainly 12:0 and 14:0, two fatty acids which are typically utilised by PES2. However, in the experiments by Aslan et al. (2014) PES2 was always co-expressed with a FAR. Therefore, it can be concluded that PES2 alone is not able to produce WEs above the background levels because of a lack of long-chain alcohols in the chloroplasts.

FAPEs that accumulate upon expression of PES2 in leaves of *N. benthamiana* contained mainly 12:0, 14:0 and 16:3 fatty acids. In contrast, *N. benthamiana* leaves accumulate mainly 16:0-, 18:0-, 18:3-, 20:0- and 22:0-phytol during senescence. Therefore, the substrate specificities of the endogenous *N. benthamiana* phytyl ester synthases differ from that of *A. thaliana* PES2. In fact, the fatty acid distribution of the FAPEs produced by PES2 in *N. benthamiana* leaves is similar to the fatty acid preference of PES2 in *A. thaliana* as deduced from by the double mutant *pes1pes2* which is devoid of 12:0-, 14:0- and 16:3-phytol.

In addition to the expression in *N. benthamiana* leaves, PES2 was stably overexpressed in

A. thaliana under control of the 35S promoter. One plant was identified that showed an increased expression of PES2, but no accumulation of FAPEs in green leaves could be observed in comparison to wild type. This result could be explained by the fact that under normal conditions, phytol is mainly bound in chlorophyll and therefore, phytol might not be available for FAPE synthesis by PES2 in green leaves. To overcome this problem, PES2 overexpressing plants could be fed with phytol. However, the expression analysis was conducted with only technical replicates, because only a single transgenic PES2 overexpression plant could be selected by RT-PCR. Therefore the validity of this experiment remains unclear. It might be advantageous to screen more transgenic plants by RT-PCR to obtain independent overexpressing lines and to quantify the expression with biological replicates.

4.3 PES2 Produces WDEs After Expression in Leaves of *N. benthamiana*

In addition to FAPEs, a further band became visible in TLC plates of lipid extracts of PES2 expressing *N. benthamiana* leaves that contains a series of lipids which were absent from the control. Two successive masses of this series have a difference of m/z 28 which indicates that the lipids contain aliphatic chains with different lengths. This result was confirmed by targeted MS/MS experiments, which demonstrated that the additional band on the TLC plate consists of WDEs that contain saturated fatty acids ranging from C10 to C16, with 12:0 and 14:0 being the most abundant fatty acids, esterified to a hexadecanediol backbone. Again, the fatty acid composition in the WDEs correlates to the fatty acid preference of PES2 in *A. thaliana*, although it is striking that no 16:3 was incorporated into the WDEs. Probably PES2 is only able to esterify saturated fatty acids when hexadecanediol serves as substrate. On the other hand, the fatty acid species could be indicative for the source of the fatty acids. Lippold et al. (2012) proposed that 16:3 employed for FAPE synthesis is derived from the breakdown of MGDG during senescence, while 10:0-, 12:0-, and 14:0-phytol might be derived from their respective ACP thioesters which are intermediates of the fatty acid *de novo* synthesis in the plastids. Since after infiltration PES2 was expressed in green *N. benthamiana* leaves, it is likely that the fatty acids for the synthesis of WDEs originate from the fatty acid *de novo* synthesis rather than from breakdown of membrane lipids.

Besides fatty acids, WDEs contain an alkanediol backbone. During the first investigations by Q-TOF MS/MS, only hexadecanediol could be identified as an alkanediol backbone in the WDEs produced by PES2. In-source fragmentation was employed to specifically select monoester product ions with the quadrupole. Each monoester ion had only one specific fatty acid product ion and all monoesters contained the same hexadecanediol product ion. In conclusion, the series of

WDEs presented here contain one unique backbone i.e. hexadecanediol. The dissociation of ions during Q-TOF MS/MS analysis does not always allow conclusions about the structure of a molecule. Therefore, it can be helpful to compare the dissociation pattern to those of standards. To this end, WDEs were synthesised with commercially available 1,2-hexadecanediol and 1,16-hexadecanediol. The Q-TOF MS/MS analysis showed that the dissociation patterns of synthesised WDEs and plant derived WDEs are different. Hence, the backbone of the WDEs produced by PES2 is neither 1,2-hexadecanediol nor 1,16-hexadecanediol.

For the elucidation of the hexadecanediol structure, NMR and GC-MS analyses were employed. The results obtained by these two methods showed that the diol backbone is 1,6-hexadecanediol. Usually, WDEs or free alkanediols are constituents of the plant cuticle. Components of the plant cuticle and their structures were elucidated in numerous studies (see Jetter et al. (2006) for an overview). However, fatty alcohols or alkanediols did not show up as components in a screening of the leaf wax composition of different *Nicotiana* species (Heemann et al., 1983). Furthermore, the analysis of the leaf cuticular wax of *Nicotiana glauca* revealed the occurrence of C24, C26 and C28 fatty alcohols but no occurrence of alkanediols was reported (Cameron et al., 2006). On the other side, up to 15% of the total wax load of *Nicotiana glauca* leaves were composed of unidentified compounds. The identification of these compounds was not possible because of their low abundances (Cameron et al., 2006). Therefore it cannot be excluded that *Nicotiana glauca* contains alkanediols in its leaf cuticular waxes. Chang and Grunwald (1976b) identified duvatrienediols as a major component of the cuticular wax of *Nicotiana tabacum* leaves. In addition to duvatrienediols, the cuticular wax contains alkanes and fatty acids, but no fatty alcohols or alkanediols (Chang and Grunwald, 1976a). Since *N. benthamiana* has not been analysed by Heemann et al. (1983) or someone else, it would be interesting to investigate the composition of cuticular waxes and of the cutin polymer of *N. benthamiana* leaves.

4.4 WDEs Might be Synthesised and Stored in Different Organelles

Cuticle monomers are believed to be exclusively synthesised in the ER of epidermis cells and transported to the leaf surface. The WDEs reported here are produced by PES2 which is only active when it is expressed as the full length ORF with an N-terminal targeting signal directing the protein to the chloroplasts. The isolation of chloroplasts of PES2-expressing *N. benthamiana* leaves revealed that the chloroplasts contain WDEs although, related to total leaf lipid content, the amount of WDEs decreased during chloroplast isolation. Therefore, the WDEs are synthesised in the chloroplasts in the first place and are therefore found in the chloroplast lipid extracts. Subsequently, WDEs are presumably exported from the chloroplast and stored in a different site. During

chloroplast isolation, the abundance of all non-plastidic material is depleted which would give rise to the decrease in relative amounts of WDEs in isolated chloroplasts. It was tested if the WDEs are exported to the leaf surface of PES2-expressing *N. benthamiana* plants and end up in the cuticular waxes by dipping of infiltrated leaves in chloroform. The result was negative as the chloroform extract was devoid of WDEs. In fact, this results was expected since the infiltration of *N. benthamiana* leaves with *A. tumefaciens* leads to an infection and genetic transformation of mainly mesophyll cells. In contrast, the components of cuticular waxes are synthesised in and exported from epidermal cells. In the end, the results presented here indicate that WDEs in the PES2-expressing mesophyll cells are produced in the chloroplasts, then exported out of the chloroplasts, but it remained unclear in which compartment the WDEs finally accumulated.

Inside the chloroplasts, non-polar lipids, such as FAPEs, FAXEs or tocopherols, are stored in the plastoglobules. Furthermore, PES2 was found as part of the plastoglobule proteome which indicates that it is localised to the plastoglobules of chloroplasts (Vidi et al., 2006; Ytterberg et al., 2006). Therefore, it is likely that WDEs are produced in the plastoglobules of the chloroplasts. A further fractionation of membranes from isolated chloroplasts would be needed as a proof. To this end, first a large amount of pure and intact chloroplasts needs to be isolated. The chloroplast isolation itself requires a high amount of healthy, non-stressed leaf material. However, the amount of PES2-expressing leaf material is limited. Second, the infiltration of *N. benthamiana* leaves with *A. tumefaciens* cells harbouring the PES2 constructs inevitable leads to plant stress. This can be observed with an increasing leaf senescence during incubation. On the other side, an incubation over a couple of days is needed for the establishment of PES2 expression and the subsequent accumulation of WDEs. Therefore it is probably impossible to determine the suborganellar localisation of WDEs in the PES2-expressing leaves.

4.5 A Possible Pathway for Synthesis of 1,6-Hexadecanediol in *N. benthamiana* and *A. thaliana*

The results presented here show that WDEs are produced by PES2 in the chloroplasts by esterification of fatty acids to 1,6-hexadecanediol. As medium-chain fatty acids which accumulate in the WDE fraction, are intermediates of the *de novo* fatty acid synthesis in the plastids of plants, the origin of the fatty acids can be easily explained. On the other side, alkanediols have not been observed in chloroplasts. Alcohols, which might be precursors for the synthesis of alkanediols, are known to be produced in the ER as monomers of the cuticle and suberin. Primary alcohols are synthesised by reduction of acyl-CoA or acyl-ACP to alcohols catalysed by FARs. Since PES2 is an *A. thaliana* enzyme and *A. thaliana* is a convenient model organism in terms of mutant availability and plant

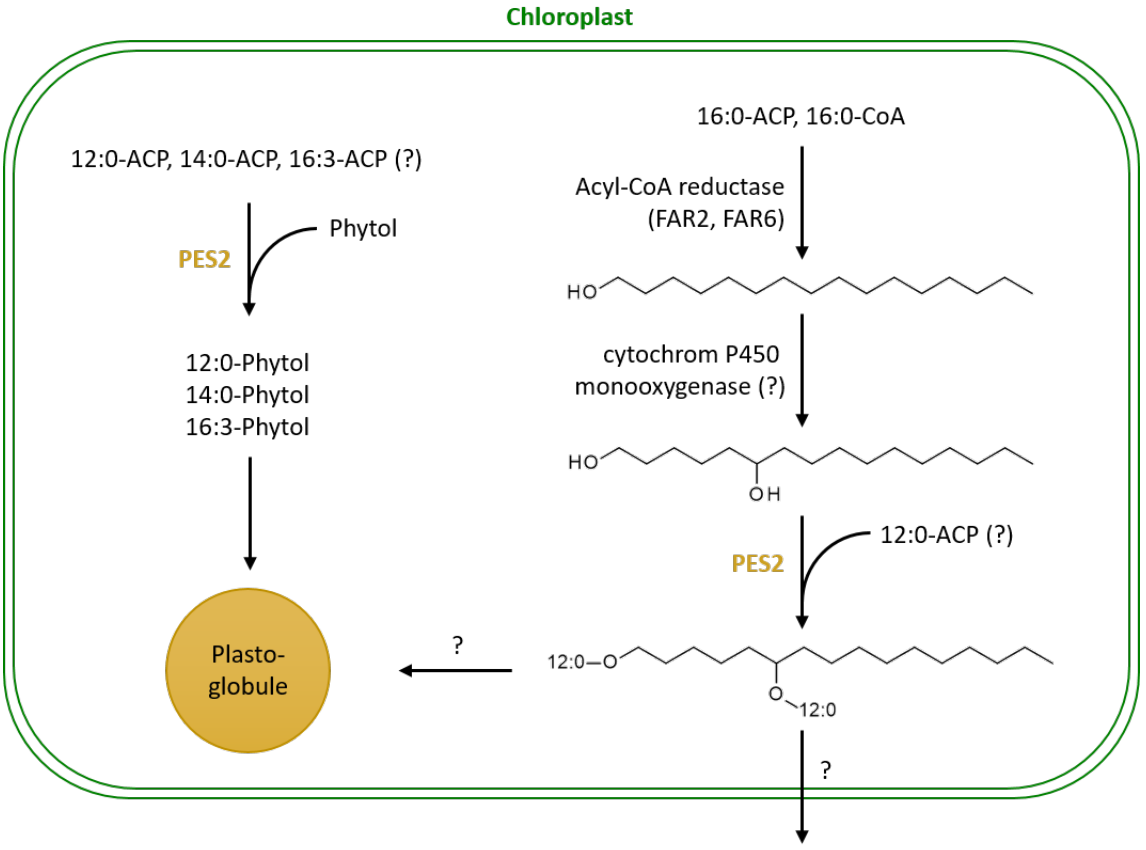

Figure 4.1 – Involvement of PES2 in the synthesis of FAPEs and WDEs in the chloroplasts. Putative paths/substrates/enzymes are marked with a question mark. ACP – acyl carrier protein, CoA – coenzyme A, FAR – fatty acid reductase, PES – phytyl ester synthase.

cultivation, it might be helpful to use *A. thaliana* to investigate the putative pathway for the production of 1,6-hexadecanediol assuming that *A. thaliana* is able to produce 1,6-hexadecanediol. *A. thaliana* contains a family of eight characterised FARs, six of which are localised to the ER (see Rowland and Domergue (2012) for an overview). Interestingly, the remaining two, FAR2 (synonymous: MS2) and FAR6, are localised to the plastids and show a substrate specificity for palmitoyl-ACP (hexadecanoyl-ACP, 16:0-ACP) (Chen et al., 2011; Doan et al., 2012). Thus, the action of these two enzymes presumably leads to the production of hexadecanol in the chloroplasts, which might be further processed to the secondary alcohol 1,6-hexadecanediol (Figure 4.1).

Secondary alcohols can be synthesised by hydroxylases via mid chain hydroxylation of alkanes. In *A. thaliana*, the midchain alkane hydroxylase 1 (MAH1) has been identified that is responsible for the production of secondary alcohols as components of stem cuticular wax (Greer et al., 2007; Wen and Jetter, 2009). The identification of MAH1 followed a reverse-genetic approach (Greer et al., 2007), which will be shortly described in the following. The *A. thaliana* genome contains 272 cytochrome P450 genes (including pseudogenes) (Bak et al., 2011). The search for candidate genes was narrowed down to the *CYP86* clan including its subfamilies *CYP86*, *CYP94*, *CYP96*

and *CYP704*, because some of its members are involved in the hydroxylation of fatty-acyl derived compounds (Greer et al., 2007). The *A. thaliana* genome contains 33 sequences that belong to the *CYP86* clan. Finally, the gene *CYP96A15* from the *CYP86* clan was selected as a candidate based on expression data and then identified as *MAH1* (Greer et al., 2007).

The in-chain hydroxylation of hexadecanol yielding 1,6-hexadecanediol would need a chloroplast localised homologue of MAH1. As there are numerous unidentified members of the cytochrome P450 enzyme family, it is possible that there is an enzyme which is a not yet known chloroplast localised alcohol in-chain hydroxylase. For the identification of candidate genes, a similar approach as the one leading to the identification of MAH1 could be contemplated. Besides the different localisation, the major differences between MAH1 and a hydroxylase involved in 1,6-hexadecanediol synthesis would be the regiospecificity. MAH1 catalyses the single or multiple hydroxylation of vicinal CH_2 groups located near the centre of the aliphatic chain, which has a length of C27 up to C31, leading to functional groups between C-13 and C-15 (Wen and Jetter, 2009). This regiospecificity would not lead to the formation of 1,6-hexadecanediol.

The search for candidate genes for a hydroxylase involved in 1,6-hexadecanediol synthesis within the cytochrome P450 enzyme family might therefore be limited to members of the CYP86 clan, and to proteins harbouring a chloroplast targeting sequence. The *A. thaliana* genome contains 33 genes that belong to the *CYP86* clan. The Aramemnon database (Schwacke et al., 2003) was used to scan the entire cytochrome P450 enzyme family for proteins that are predicted to be chloroplast localised. The localisation is indicated by a consensus prediction score of several prediction tools where a score above 12 indicates a high prediction for chloroplast localisation and a score below 12 but above 5 indicates a low prediction. Proteins with a score below five are considered not to be chloroplast localised. The *A. thaliana* genome contains five cytochrome P450 proteins that have a chloroplast prediction with a high score and 51 cytochrome P450 genes with a low score. The combination of the list of proteins which belong to the CYP86 clan (33 proteins) and the list of chloroplast localised cytochrome P450 enzymes (5 + 51 proteins) results in a list of 86 candidate genes (Appendix Table 7.12) because three candidate proteins belong to both groups, i.e. CYP86C1, CYP94B2 and CYP86B2, which are CYP86 clan members and predicted to localise to the chloroplast. From the five proteins that have a prediction score for chloroplast localisation above 12, four have already been characterised: CYP97A3, CYP97C1 and CYP97B3 are hydroxylases involved in the xanthophyll biosynthesis (Kim and DellaPenna, 2006; Tian et al., 2004; Kim et al., 2010) and are found as members of the chloroplast proteome (Zybailov et al., 2008). CYP77A6 is an in-chain fatty acid hydroxylase that produces 10,16-hydroxy hexadecanoic acid from 16-hydroxy hexadecanoic acid for the synthesis of cutin in flowers (Li-Beisson et al., 2009). There is currently no experimental evidence for a chloroplast or an ER localisation of

CYP77A6, but in general, the synthesis of cutin monomers is localised to the ER. The fifth enzyme, CYP706A1, is not yet characterised and therefore a candidate for an in-chain hydroxylase. A complete list of all 86 candidate genes is given in Appendix Table 7.12. A shortened version of the list comprising candidate genes with unknown function and which have the highest chloroplast localisation scores is given in Table 4.1. Interestingly, none of these genes belongs to the *CYP86* clan as the members of this group have rather low predictions for chloroplast localisation.

Table 4.1 – Cytochrome P450 candidate genes for an in-chain hydroxylase that produces 1,6-hexadecanediol. The AramLocCon values are taken from aramemnon (Schwacke et al., 2003) and represent consensus prediction values for the chloroplast localisation of the enzyme calculated on a method based on Schwacke et al. (2007). Values above 12 indicate a high prediction, values below 12 and above five indicate a low prediction and proteins with values below five are considered not to be chloroplast localised.

Gene Number	Systematic Designation	Chloroplast Localisation Score
At4g22690	*CYP706A1*	17.7
At1g13080	*CYP71B2*	11.8
At5g06905	*CYP712A2*	11.5
At3g48320	*CYP71A21*	9.4
At1g74110	*CYP78A10*	8.3
At1g11610	*CYP71A18*	7.7
At5g25140	*CYP71B13*	7.5
At4g37340	*CYP81D3*	7.3
At4g12300	*CYP706A4*	7.2
At3g48310	*CYP71A22*	7.2
At3g26230	*CYP71B24*	7.1
At3g48290	*CYP71A24*	7.0
At3g20940	*CYP705A30*	7.0

The mechanism of alkane or alcohol in-chain hydroxylation (as e.g. catalysed by MAH1) has been proposed for plants in which both, substrates and products, have the same chain lengths, e.g. *Pisum sativum*. The cuticular waxes of pea leaves contain alkanes and secondary alcohols with the same chain lengths (Wen et al., 2006). However, in some plant species, wax components were identified that have functional groups only on every other C-atom (β-substituted) and the chain lengths of substances, which could be substrate-product-related, differ. In this case, another mechanism was suggested where functional groups are introduced during acyl chain elongation (von Wettstein-Knowles, 1995). Fatty acid elongation is a four-step cycle comprising condensation, reduction, dehydration and a second reduction. In each cycle, a keto group is introduced into the acyl chain by condensation of malonyl-ACP and acyl-ACP. Subsequently, the keto group is removed in the following three steps. Polyketide synthases use the intermediates of the elongation cycle for a further condensation of malonyl-ACP giving rise to compounds that contain either two keto groups, a keto plus an hydroxyl group or a keto group plus an unsaturated C-C bond.

Malonyl-ACP is a C3 compound elongating the acyl chain by two carbon atoms, because CO_2 is lost during the elongation reaction. Therefore, this mechanism would result in a pattern where two functional groups are separated by an odd number of bridging methylene groups, i.e. a 1,3-, 1,5-, 1,7-, 1,9-substitution pattern. Accordingly, the production of 1,6-hexadecanediol would not be possible by this mechanism. Therefore it is more likely that 1,6-hexadecanediol is produced by in-chain hydroxylation by the action of a not yet identified cytochrome P450 monooxygenase.

Furthermore, it should be noted that the FAR and MAH enzymes that have been identified, are *A. thaliana* genes, whereas the identified WDEs are produced in leaves of *N. benthamiana*. Although they are produced by the *A. thaliana* PES2 enzyme, the substrate 1,6-hexadecanediol is produced by *N. benthamiana* enzymes. Thus, it has to be taken into account that the *N. benthamiana* genome might contain genes that are not present in the *A. thaliana* genome and that *A. thaliana* might not have enzymes that are able to produce 1,6-hexadecanediol.

4.6 PES2 is the First Plant Enzyme with Wax Diester Synthase Activity

Although WDEs have been identified as components of the cuticular leaf wax of some plant species, up to now, no plant enzyme has been characterised that shows *in vivo* or *in vitro* wax diester synthase activity. So far, enzymes with wax diester synthase activity were characterised in the bacterium *Acinetobacter calcoaceticus*, in the mouse and in the protozoon *Tetrahymena thermophila*. The bifunctional wax ester synthase/acyl-CoA:diacylglycerol acyltransferase ADP1 from *Acinetobacter calcoaceticus* was heterologously expressed in *E. coli* and upon feeding the cells with 1,16-hexadecanediol, WDEs accumulated (Kalscheuer et al., 2003). In addition, the feeding of *Acinetobacter calcoaceticus* cells with 1,16-hexadecanediol results in WDE accumulation and the fatty acid composition of the produced WDEs was similar as the fatty acid profile of whole cells. The mouse acyl-CoA:diacylglycerol acyltransferase DGAT1 was characterised by studying lipid metabolism in DGAT1-deficient mice (Smith et al., 2000). Unexpectedly, the $Dgat^{-/-}$ mice showed atrophic sebaceous glands and abnormal fur with changes in the fur lipid composition and functional defects of the fur (Chen et al., 2002). The fur lipid phenotype is caused by a loss of WDEs which are the main lipid on the of skin surface of mice. DGAT1 was heterologously expressed in insect cells and *in vitro* tests with insect cell membranes and 1,2-hexadecanediol as substrate demonstrated that DGAT1 harbours wax diester synthase activity (Yen et al., 2005). In *Tetrahymena thermophila*, four DGAT2-related enzymes have been identified that have wax ester synthase (WS) activity (Biester et al., 2012). After heterologous expression in yeast, *in vitro* tests were conducted by incubating yeast membranes with 1,2-dodecanediol or

1,12-dodecanediol. Only TtWS2 utilised the two dodecanediol substrates revealing that it has wax diester synthase activity.

Results obtained in present work demonstrate that PES2 possesses wax diester synthase activity: (i) The heterologous expression of PES2 in leaves of *N. benthamiana* leads to the accumulation of 1,6-hexadecanediol diesters. (ii) feeding of 1,16-hexadecanediol to *A. thaliana* wild type plants results in the production of WDEs while the accumulation of WDE was reduced in the *pes1pes2* double mutant. The latter result indicates that a certain proportion of the WDEs are produced by PES1 or PES2. However, no WDEs were so far found in *A. thaliana* leaf waxes. In contrast to ADP1 from *Acinetobacter calcoaceticus*, the fatty acid composition of the WDEs produced by PES2 in *N. benthamiana* leaves does not represent the fatty acid profile of *N. benthamiana* leaves but rather the substrate preference of PES2. Therefore, PES2 seems to have considerable specificity for the acyl chain of the acyl donor substrate. On the other hand, these results demonstrate that PES2 presumably is a promiscuous acyltransferase with respect to the acyl acceptor (alcohol) where it shows broad substrate specificity.

4.7 The Occurrence of VLC-FAPEs Suggests that an Additional Site for FAPE Synthesis Might Exist

FAPEs were also measured in non-infiltrated senescent leaves of *N. benthamiana* to compare the fatty acid compositions of endogenous FAPEs and PES2-derived FAPEs. Besides the known 16:0-, 18:3-, and 18:0-phytol esters, senescent leaves of *N. benthamiana* contain unusual FAPEs that were identified by GC-MS analysis as 20:0- and 22:0-phytol. Because the acyl moiety in these FAPE species contains VLC-FAs, they are designated as VLC-FAPEs. The investigation of lipids in senescent leaves of different plant species showed that VLC-FAPEs are found in all analysed Solanaceae species including *S. lycopersicum* and also in the Poaceae *Oryza sativa* but not in the Poaceae *Hordeum vulgare*, nor in the Brassicaceae *A. thaliana* nor in the Fabaceae *Lotus japonicus*. Therefore, the appearance of VLC-FAPEs in senescent leaves is rather species dependent than characteristic for a whole plant family.

The presence of VLC-FAPEs in senescent leaves was unexpected because previous studies indicated an exclusive localisation for the synthesis and storage of FAPEs to the chloroplast. This hypothesis was supported by three findings. First, the occurrence of medium chain fatty acids with a length of C10 up to C14 in FAPEs implies that the fatty acids are derived from the plastidial fatty acid *de novo* synthesis (Ischebeck et al., 2006; Gaude et al., 2007). Second, FAPEs are localised to the plastoglobules in isolated chloroplasts (Gaude et al., 2007). And finally PES1 and PES2, the main phytyl ester synthases of *A. thaliana*, localise to the chloroplasts and were identified as

members of the plastoglobule proteome (Lippold et al., 2012; Vidi et al., 2006; Ytterberg et al., 2006). These three observations strongly indicate the localisation of FAPEs to the chloroplasts. On the other side, these findings neither exclude the occurrence of FAPEs outside of the chloroplast nor the existence of further enzymes with phytyl ester synthase activity.

The occurrence of VLC-FAPEs has been reported before, as components of the cuticular wax of flowers (Griffiths et al., 1999) and from whole leaves (Pereira et al., 2002). Sunflower and olive oil contain a certain amount of WEs beside the major component TAG. The WEs fractions of sunflower and olive oils contain phytol esterified to 18:0, 18:1, 20:0, 20:1, 22:0 and 24:0 (Reiter and Lorbeer, 2001; Biedermann et al., 2008). Reiter and Lorbeer (2001) also measured fatty acid geranylgeranyl esters (FAGGEs) in different types of sunflower oils and found that the amount of FAGGEs is negatively correlated to the amount of FAPEs. Geranylgeraniol is a diterpene alcohol structurally similar to phytol, but carrying four double bonds instead of only one. It was proposed that the composition of isoprenoid esters depends on the maturation stage of sunflower seeds (Reiter and Lorbeer, 2001). This would indicate a connection between the synthesis of FAPEs and FAGGEs, although it has never been shown that free geranylgeraniol or the geranylgeranyl moiety of FAGGEs can be reduced to phytol. On the other hand, Keller et al. (1998) demonstrated that GGPP can be reduced to phytol-PP by GGR, and that chlorophyll can be produced from geranylgeranylated chlorophyll by GGR. Therefore, it might also be possible that the geranylgeranyl moiety of FAGGEs is reduced to phytyl yielding the corresponding FAPEs. Thus, there are two potential scenarios for the production of FAPEs in sunflower seeds: (i) FAGGEs are derived from the cytosolic geranylgeraniol pool or from the breakdown of geranylgeranylated chlorophyll in the chloroplast and are then converted to FAPEs by the action of GGR in the chloroplast or (ii) FAGGEs and FAPEs are produced independently with precursors derived from chlorophyll breakdown. However, as these FAPEs are detected in seeds and the VLC-FAPEs reported here are produced in senescent leaves, they might be derived from different biosynthetic pathways.

Griffiths et al. (1999) analysed the epicuticular waxes from flowers of *Vicia faba* (faba bean) and identified FAPEs as 7% of the total wax content. The analysis of the fatty acid composition revealed that phytol is mainly esterified to 20:0 and 22:0 and to a lower extent to 18:0 and 24:0. Furthermore, FAPEs were identified as minor compounds of the waxes of the Amazonian tree *Simaruba amara* leaves with fatty acids ranging from C12 to C25 with mostly 16:0, 18:0, 20:0, 22:0 and 24:0 groups (Pereira et al., 2002). The authors claimed that these FAPEs are components of the epicuticular waxes. However, wax lipid extracts were prepared with minced leaves that were extracted several times (for a total of 30 min) in dichloromethane with ultrasonic agitation. Using this method, it is very likely that the lipid extract contained many intracellular lipids, possibly even derived from the chloroplasts. For this reason lipid extracts that are used for the analysis of epicu-

ticular waxes are normally prepared by dipping leaves for only 5–30 sec in chloroform. Therefore, the VLC-FAPEs identified in *Simaruba amara* leaves could also derive from intracellular lipids and not from the epicuticular wax. Unfortunately, Griffiths et al. (1999) and Pereira et al. (2002) give no explanation for the origin, synthesis, or transport of these unusual FAPEs. In general, WEs that are components of the epicuticular wax are synthesised in the ER and transported to the plasma membrane by unknown mechanisms and exported to the leaf surface by ABC transporters (Li-Beisson et al., 2013). While it is clear that *Vicia faba* flowers contain FAPEs in their flower epicuticular waxes, FAPEs from *Simaruba amara* were isolated from whole leaves and it remains unclear whether they are localised intracellular or to the leaf surface. Thus, FAPEs might be synthesised in the ER as well, where they might be processed by the same enzymes and enter the same transport pathway as it is the case for WEs.

The occurrence of VLC-FAPEs in senescent leaves of *N. benthamiana* identified in the present study cannot be explained with an exclusively chloroplast-localised synthesis and storage of FAPEs during leaf senescence. 20:0 and 22:0 fatty acids are not synthesised in the plastidial *de novo* synthesis. In general, VLC-FAs and their derivatives occur as components of the cuticular wax, suberin, phosphatidylserine (PS), sphingolipids or storage lipids, i.e. TAGs, and are synthesised in the ER. 16:0-ACP, 18:0-ACP and 18:1-ACP are synthesised *de novo* in the plastids and 16:0, 18:0 and 18:1 are exported to the ER where they undergo several cycles of acyl chain elongation yielding in VLC-FA-CoAs. The existence of FAPEs as part of cuticular waxes demonstrate a connection between FAPE production and the biosynthesis and assembly of leaf waxes. However, in general the existence of FAPEs as part of the cuticular wax is intriguing because phytol is synthesised in the chloroplasts and the most typical condition of FAPE production is connected to chlorophyll degradation which is also located to the chloroplasts.

Leaves of *N. benthamiana* contain small amounts of 20:0 and 22:0 (Kosma et al., 2014). Therefore it is likely that the VLC-FAs for VLC-FAPE synthesis derive from the fatty acid elongation pathway in the ER. At this point the question arises about where the phytol "meets" the VLC-FAs or in other words, if the phytol is exported from the chloroplast to the ER or if the VLC-FAs are transported into the chloroplasts after their elongation at the ER. To address this question, chloroplasts of senescent leaves from *S. lycopersicum* were isolated since they also contain VLC-FAPEs. The FAPE analysis revealed that 16:3- and 18:3-phytol are enriched while 20:0- and 22:0-phytol are depleted by chloroplast isolation and are only found in traces in isolated chloroplasts which could be due to contaminations occurring during chloroplast isolation. These results show that VLC-FAPEs do not accumulate in the chloroplasts as it is the case for FAPEs with a chain length up to C18. This observation can be seen as an indication for the synthesis of VLC-FAPEs in the ER.

The main question in this context is how phytol gets into the ER. In general, there are two possibilities: phytol is either transported to the ER or it is synthesised in the cytosol or the ER. Previously, it was shown that phytol-PP is produced by GGR that is localised to the chloroplast (Keller et al., 1998; Tanaka et al., 1999). If this phytol-PP or chlorophyll-derived phytol is used for the production of VLC-FAPEs in the ER, the transport of phytol from the chloroplast to the ER would be necessary. Thus, phytol would need to cross the inner and outer membrane of the chloroplast and to be transferred to the ER membrane. Another non-polar lipid that is synthesised and stored in the chloroplast is tocopherol. Therefore, the anti-oxidative function of tocopherol would be exclusively localised to the chloroplasts. In contrast, tocopherol-deficiency affects ER synthesised lipids although tocopherol is synthesised and stored in the chloroplast (Maeda et al., 2008; Song et al., 2010). On the basis of transorganellar complementation tests and microscopical evidence for physical chloroplast/ER contact sides, Mehrshahi et al. (2013) proposed a model for contact sides at which the bilayers of the plastidial outer membrane and the ER membrane form hemifused bilayers. By that, nonpolar compounds localised to the chloroplast would be accessible to ER localised enzymes (Mehrshahi et al., 2013). This model would explain how phytol or other lipids get into contact with ER-localised enzymes of the leaf wax biosynthesis.

Another mechanism could be the export of phytol from the chloroplasts by transporters. Phytanoyl-CoA 2-hydroxylase (PAHX) mutants of *A. thaliana* were characterised that are impaired in the α-oxidation of phytanoyl-CoA to pristanal and consequently accumulate phytanoyl-CoA under dark induced senescence (Araújo et al., 2011). Phytanoyl-CoA was suggested as a downstream product of phytol degradation. The mammal PAHX is localised to the peroxisomes (Jansen et al., 1999). Therefore it is likely that the degradation of phytol during senescence is localised to the peroxisomes. This scenario would require a re-localisation of phytol from chloroplasts to peroxisomes. However, currently it is unknown whether phytol can be exported from the chloroplasts.

The second possibility comprises the synthesis of phytol or phytol-PP in the cytosol or directly in the ER. A precursor for the synthesis of phytol-PP is GGPP which is generated from condensation of four isoprene units. Protein prenylation is an example for post-translational modifications. Prenylation is the addition of a farnesyl or geranylgeranyl moiety to the cysteine residue of a protein catalysed by transferases which are localised to the cytosol (Wang and Casey, 2016). The required substrates FPP or GGPP are synthesised by condensation of cytosolic IPP which is derived from the mevalonate pathway. Therefore, a cytosolic GGPP pool exits that could act as precursor for the synthesis of phytol-PP, although there are no reports about the presence of a cytosolic GGR. Phosphorylated derivatives of farnesol, geranylgeraniol or phytol have a higher polarity and might diffuse from the cytosol to the ER.

Taken together, it can be hypothesised that the FAPEs found in epicuticular waxes and the

VLC-FAPEs in senescent leaves are synthesised by the same biosynthetic pathway which would be localised to the ER. To further develop this hypothesis, the next question would be about which enzymes are involved in the ER localised FAPE synthesis. Prior to the identification of PES1 and PES2, Ischebeck et al. (2006) already suggested that wax ester synthases might be involved in FAPE production. In general, wax ester synthases are known to have a broader range of substrates, e.g. as demonstrated for ADP1 from *Acinetobacter calcoaceticus* and the wax ester synthases from *Tetrahymena thermophila* (Kalscheuer et al., 2003; Kalscheuer and Steinbüchel, 2003; Biester et al., 2012).

As described above, PES1 and PES2 are the main enzymes in *A. thaliana* that are responsible for FAPE synthesis during senescence. The *pes1pes2* double mutant shows a highly reduced FAPE content in senescent leaves and lacks nearly all FAPEs except for 16:0- and 18:3-phytol. The analysis of nitrogen deprived *elt* mutants did not lead to the identification of additional phytyl ester synthases. Therefore it is still unclear which enzymes are responsible for the production of 16:0- and 18:3-phytol. In the light of FAPEs that are localised outside of the chloroplasts, it is questionable if these missing enzymes belong to the ELT family and are localised to the chloroplast. Alternatively, acyltransferases of other enzyme families localised to the ER could be involved in phytyl ester synthesis. Probably not only the enzymes responsible for the production of 16:0- and 18:3-phytol are located to the ER, but also these two FAPE species are located outside of the chloroplast. Concerning the localisation of FAPEs, Gaude et al. (2007) isolated chloroplasts, fractionated the different membranes and analysed their FAPE content. By that, FAPEs were localised to the plastoglobules. However, firstly, this result does not exclude the occurrence of FAPEs outside of the chloroplasts; secondly, there was no fatty acid composition of the analysed FAPEs presented leaving it unclear if 16:0- and 18:3-phytol are localised to the chloroplasts; and finally, there was no comparison of FAPE composition between isolated chloroplasts and whole leaf extracts. Therefore, it might still be possible that 16:0- and 18:3-phytol are localised outside of the chloroplast. A new chloroplast isolation with a total leaf control would be helpful to gain new insights or to reject this theory. If the model plant *A. thaliana* also contains FAPEs that are localised to the ER, this would facilitate the search, characterisation and identification of candidate genes. In *A. thaliana*, *WSD1* has been identified and characterised as a member of the bifunctional wax ester synthase/diacylglycerol acyltransferase (WS/DGAT) gene family and which is localised to the ER (Li et al., 2008). Besides *WSD1*, the family contains ten genes that are annotated as WS/DGAT enzymes but which are not yet characterised. Therefore, these genes are candidates for an acyltransferase that is responsible for the production of FAPEs in the ER. It would be interesting to see, if *wsd* mutants show any difference in the FAPE content in comparison to wild type.

4.8 *A. thaliana* Accumulates FAPEs Under Osmotically Induced Drought Stress

The most prominent situation in which the accumulation of FAPEs was observed and investigated is during leaf senescence. However, basically every developmental program or stress that leads to chlorophyll degradation could potentially lead to the accumulation of FAPEs. In general, chlorophyll is degraded during seed maturation and germination, flowering, fruit ripening and during leaf senescence which can occur seasonally or prior to the death of the plant (Hendry et al., 1987) and also during steady-state turnover (Lin et al., 2016). Besides, chlorophyll is broken down in response to abiotic stresses such as heat, cold, UV and γ-irradiation, high light, darkness, or deficiency in nutrients and to biotic stresses such as viral, bacterial and fungal pathogen attacks (Hendry et al., 1987; Thomas and Stoddart, 1980). Although this is known for a long time, only a few studies were focused on the synthesis of FAPEs under different chlorotic stresses so far. Upon frost damage, Gellerman et al. (1975) observed an increase of phytol in the WEs of the grass *Phleum pratense* but no change in the fatty acid composition in comparison to healthy plants.

To induce chlorotic stress, a plant cultivation system with plants growing on nitrogen deprived medium in petri dishes in a defined environment has been established to ensure reproducibility. To study FAPE accumulation during alternative stress situations, drought has been chosen because it is an important factor for agriculture as it can severely affect crop production. For drought, a similar system was established with PEG-8000 containing medium. PEG-8000 changes the osmotic potential of the medium and thus induces a controlled water deficit in the plant.

The analysis of *A. thaliana* wild type plants grown on PEG containing medium revealed that FAPEs accumulate under osmotically induced drought stress. The amount of FAPEs is positively correlated with the PEG content. Drought derived FAPEs have the same fatty acid composition as nitrogen deprivation derived FAPEs, and also the degree of drought stress has no impact on the fatty acid composition. The results are in accordance with previous observations by Anderson et al. (1984). These authors analysed the FAPE content under drought stress in mature bean leaves and found a 10–20 fold increase in FAPEs. A comparison of the drought resistant bean species *Phaseolus acutifolius* with the less resistant species *Phaseolus vulgaris* demonstrated that *Phaseolus acutifolius* accumulates 2-fold more FAPEs than *Phaseolus vulgaris*.

In conclusion, it is likely that FAPEs produced under nitrogen deprivation and under drought stress have the same biosynthetic origin and that the same enzymes are involved. However, it is still questionable if there are other phytyl ester synthases involved in FAPE production under different stresses, especially in the light of the unknown functions of the ELT enzymes.

4.9 PYP1 is Involved in FAPE Synthesis in *S. lycopersicum* Petals

Recently, the xanthophyll ester synthase PYP1 from *S. lycopersicum* was identified which shows highest sequence similarity to the phytyl ester synthase PES1 from *A. thaliana* (Ariizumi et al., 2014). The two enzymes share the same protein domain structure with an α/β hydrolase-fold like domain and an acyltransferase like domain. Because of the similarities, it was proposed that PYP1 might also have phytyl ester synthase activity. To test this hypothesis, the FAPE content in different plant organs from wild type MT-J, *pyp1-1* and *pyp1-2* plants was analysed.

The highest FAPE amounts were found in senescent leaves, 70-fold less in petals and 200-fold less in red fruits. The amounts of FAPEs in green leaves and fruits were very low and hardly distinguishable from the background. FAPEs typically accumulate when chlorophyll is degraded e.g. when green leaves turn yellow during leaf senescence or when green fruits turn red during fruit ripening. This scenario is in agreement with the observations of an increase of FAPEs in senescent leaves and red fruits of *S. lycopersicum* in comparison to the corresponding green tissues.

The main fatty acids of FAPEs in *S. lycopersicum* are 20:0, 22:0 and 24:0 in petals, senescent leaves and ripe fruits. Interestingly, in addition to the above described occurrence of VLC-FAPEs in senescent leaves, *S. lycopersicum* also contains VLC-FAPEs in other organs like petals or fruits. VLC-FAPEs have been previously reported in petals of *Vicia faba* where they are part of the epicuticular wax layer (Griffiths et al., 1999). Therefore, the VLC-FAPEs determined in the present study might also be components of the cuticular wax of *S. lycopersicum* petals. The data generated here originate from total lipid extracts which prevents any conclusion about the localisation of VLC-FAPEs in *S. lycopersicum* petals. It would be helpful to extract and analyse only the cuticular waxes to draw a conclusion about the localisation of VLC-FAPEs.

In addition, petals contain considerable amounts of 14:0- and 16:0-phytol. These two FAPE species are drastically reduced in *pyp1-1* and *pyp1-2* which demonstrates that PYP1 has phytyl ester synthase activity and that PYP1 is responsible for the synthesis of 14:0- and 16:0-phytol in petals. *pyp1-1* and *pyp1-2* have been previously characterised by a complete loss of neoxanthin and violaxanthin mono- and diesters in the petals. These FAXmEs and FAXdEs mainly contain 14:0 and 16:0 fatty acids. Therefore it is intriguing that the corresponding FAPE species are also nearly absent from the petals of *pyp1-1* and *pyp1-2*. These results certainly show that PYP1 has phytyl ester synthase activity and that PYP1 has a high specificity for 14:0 and 16:0.

Additional changes in the total FAPE amount in comparison to wild type can be observed: the amount of FAPEs is decreased in senescent leaves of *pyp1-2*, it is increased in petals of *pyp1-2*, and it is increased in red fruits of *pyp1-1*. However, since these changes are restricted to only one mutant allele, respectively, while the other mutant allele shows no change, it is difficult to relate the lipid changes to changes in the activity of PYP1.

4.10 Petals from *S. lycopersicum* Contain Neoxanthin Triesters Produced by PYP1

Previously, *pyp1-1* and *pyp1-2* from *S. lycopersicum* have been described which are devoid of FAXmEs and FAXdEs consisting of neoxanthin or violaxanthin (Ariizumi et al., 2014). Besides these two series of FAXEs, a third series of yellow lipids can be observed by TLC that is absent from *pyp1-1* and *pyp1-2*. Analysis by Q-TOF MS/MS revealed that these lipids are neoxanthin triesters. Neoxanthin and violaxanthin are isomers but since violaxanthin only contains two hydroxyl groups it can only form mono- and diesters. In contrast, neoxanthin contains three hydroxyl groups which allows the formation of triesters. Until now, the existence of neoxanthin triesters was only reported for leaves of apple trees (Cardini, 1982). Interestingly, leaves of young apple trees contain only free neoxanthin and with the age of the tree the amount of esterified neoxanthin increases but neoxanthin mono- or diester were not detected at all (Cardini, 1983). In contrast, petals of *S. lycopersicum* contain all three types of neoxanthin esters with neoxanthin triesters identified in this study and neoxanthin mono- and diesters distinguished from violaxanthin mono- and diesters by Ariizumi et al. (2014).

The masses of the highest abundant neoxanthin triesters peaks correspond to the calculated masses of neoxanthin triesters with 12:0, 14:0 and 16:0 fatty acids. However, the fatty acid composition has not been analysed in detail yet. Neighbouring peaks indicate the occurrence of further unsaturated fatty acids, also in the range of C12 and C14, which is quite unexpected as desaturation in plants normally occurs from C16 on. Cardini (1982) analysed the fatty acid composition of neoxanthin triesters in leaves of apple trees and found mainly 16:0, 16:1, 18:0 and 18:1 esterified to neoxanthin and lower amounts of 12:0, 14:0, 18:2 and 20:0. In addition, they found traces of fatty acids which they could not identify by GC-MS, but based on retention time they presumed that these fatty acids are 12:1, 12:2, 12:3, 14:1, 14:2, 14:3 16:2 and 16:3 in neoxanthin triesters. Taken together, these results indicate that neoxanthin triesters might contain unusual medium- and long-chain unsaturated fatty acids. It would be helpful to conduct a detailed analysis of the fatty acid composition of purified neoxanthin triesters with an identification of the fatty acid species.

In conclusion these result show that petals of *S. lycopersicum* contain neoxanthin triesters and that in addition to the synthesis of FAXmEs and FAXdEs, PYP1 is also responsible for the synthesis of neoxanthin triesters. Besides the three bright yellow bands of FAXEs visible in lipid extracts of the *S. lycopersicum* wild type MT-J (Figure 3.35-A), there are several more bands in different shades of yellow visible in the lane of MT-J that are absent from *pyp1-1*. This implicates that PYP1 might be responsible for the synthesis of further, not yet identified compounds.

4.11 Senescent *A. thaliana* leaves and *Camelina sativa* Petals are Devoid of FAXEs

FAXEs are typically found in coloured tissues such as flowers or fruits e.g. in petals of *S. lycopersicum* or in fruits of *Capsicum annuum* (Ariizumi et al., 2014; Hornero-Méndez and Mínguez-Mosquera, 2000). In addition, FAXEs are synthesised during senescence of beech leaves (Tevini and Steinmüller, 1985). Up to now, FAXEs were not reported for the two model plants *Camelina sativa* and *A. thaliana*. The results obtained here confirmed that senescent leaves of *A. thaliana* and yellow flowers of *Camelina sativa* are devoid of FAXEs.

A. thaliana seeds are normally devoid of FAXEs, but the overexpression of the *β-carotene oxygenase* gene from *Haematococcus pluvialis* in *A. thaliana* seeds leads to the accumulation of free and esterified ketocarotenoids (Stålberg et al., 2003). The results demonstrate that *A. thaliana* contains acyltransferases which are able to synthesise FAXEs. Since the ELT enzymes are homologous to the xanthophyll ester synthase PYP1, they might be capable of producing FAXEs. To address this question, the *β-carotene oxygenase* gene from *Haematococcus pluvialis* could be overexpressed in the *elt* mutants. If the accumulation of FAXEs is decreased or absent in one of the mutants, that would indicate an involvement of the respective gene in FAXE accumulation in *β-carotene oxygenase* overexpressing *A. thaliana* seeds.

5 Summary

Chlorophyll is the most abundant pigment in the biosphere, and its degradation leads to the release of large amounts of chlorophyll breakdown products, i.e. pheophorbide and phytol. Only a minor fraction of the released phytol is degraded. Phytol can be further processed by incorporation into fatty acid phytyl esters (FAPEs) or tocopherols. In *A. thaliana*, two phytyl ester synthases, PES1 and PES2, have been characterised which are expressed under senescence and which catalyse the esterification of chlorophyll-derived phytol and fatty acids. PES1 and PES2 belong to a family of six esterase/lipase/thioesterase (ELT) like proteins in *A.thaliana*. In this work, the analysis of PES2 as well as the characterisation of the remaining four ELT enzymes, ELT3, ELT4, ELT5, and ELT6, were presented. In addition, mutants of the closely related xanthophyll ester synthase PYP1 from *Solanum lycopersicum* were investigated.

Expression analysis of the *ELT* genes revealed that, similar to PES1 and PES2, the expression of *ELT3* and *ELT4* was increased under senescence. Furthermore, *PES1*, *ELT4*, *ELT5*, and *ELT6* showed elevated expression levels in inflorescences. The FAPE analysis of *elt* single mutants and the newly generated double mutant *elt4elt6* showed no differences compared to wild type under nitrogen deprivation induced senescence. Previous results revealed that the double mutant *pes1pes2* contains decreased FAPE amounts under nitrogen deprivation compared to wild type. The introduction of a third mutation in the newly generated triple mutant *pes1pes2elt4* did not lead to a further decrease in FAPE content. The analysis of the seed FAPE content of the multiple mutants revealed a decrease in FAPEs in *elt4elt6* and *pes1pes2elt4* demonstrating the involvement of ELT enzymes in seed FAPE production. FAPE accumulation under drought stress was investigated to study different stress conditions under which chlorophyll is degraded. Upon osmotically induced drought stress, *A. thaliana* accumulates FAPEs with the same fatty acid distribution as observed under nitrogen deprivation.

The heterologous expression of PES2 in *E. coli* cells and in leaves of *N. benthamiana* resulted in an increased accumulation of FAPEs compared to controls. The fatty acid distribution of FAPEs in PES2-expressing *N. benthamiana* leaves reflected the fatty acid preference of PES2 observed in *A. thaliana*. In addition to FAPEs, PES2 produced wax diesters (WDEs) when expressed in the chloroplasts of *N. benthamiana* leaves. These WDEs contained two fatty acids esterified to

hexadecanediol as shown by Q-TOF MS/MS experiments. The backbone was identified by GC-MS and NMR as 1,6-hexadecanediol. This results represents the first report of 1,6-hexadecanediol in plants, and the first report of an alkanediol in chloroplasts. The fatty acid moieties in the WDEs were identified as mainly 12:0 and 14:0. The lipid analysis of isolated chloroplasts of infiltrated *N. benthamiana* leaves indicated that WDEs are first synthesised in the chloroplasts and then exported. Taken together these results unveil PES2 as the first plant enzyme that harbours wax diester synthase activity.

Screening of the FAPE composition of different plant species under senescence revealed the accumulation of unusual very long-chain FAPEs (VLC-FAPEs) which contain fatty acids with chain lengths longer than C20. These VLC-FAPEs were identified in different plant species from several families. The occurrence of VLC fatty acids is not typical for the chloroplast. Therefore, VLC-FAPE are presumably produced outside of chloroplasts, deduced from FAPE measurements of chloroplast isolated from senescent *S. lycopersicum* leaves.

PYP1 from *S. lycopersicum*, an ortholog of PES1 and PES2, has previously been identified as a xanthophyll ester synthase which is responsible for the synthesis of xanthophyll esters in petals of *S. lycopersicum*. Because PYP1 is closely related to phytyl ester synthases, the accumulation of FAPEs in different organs of *S. lycopersicum* was analysed. 14:0- and 16:0-phytol were strongly reduced in petals of *pyp1* mutant plants indicating the involvement of PYP1 in FAPE synthesis in petals of *S. lycopersicum*. The fatty acid moieties of the decreased FAPE species reflects the fatty acid preference of PYP1 in xanthophyll ester synthesis as PYP1 mainly produces neoxanthin and violaxanthin esters with 14:0 and 16:0 fatty acids.

The further analysis of xanthophyll esters in petals of *S. lycopersicum* revealed the occurrence of a third group of xanthophyll esters besides mono- and diesters, e.g. neoxanthin triesters which have only been reported before for leaves of apple trees. The study of *pyp1-1* petals showed that PYP1 is also responsible for the synthesis of neoxanthin triesters. In contrast to *S. lycopersicum*, the yellow petals of *Camelina sativa* and the senescent leaves of *A. thaliana* are devoid of xanthophyll esters.

In conclusion it could be shown that ELT enzymes are quite promiscuous regarding the acyl acceptors such as phytol, alcanediols and xanthophylls. On the other side, individual ELT enzymes are specific for certain fatty acid chain lengths.

6 References

Addlesee, H. A., Gibson, L. C., Jensen, P. E., and Hunter, C. N. (1996). Cloning, sequencing and functional assignment of the chlorophyll biosynthesis gene, *chlP*, of *Synechocystis* sp. PCC 6803. *FEBS Letters*, 389(2):126–130.

Addlesee, H. A. and Hunter, C. N. (1999). Physical mapping and functional assignment of the geranylgeranyl-bacteriochlorophyll reductase gene, *bchP*, of *Rhodobacter sphaeroides*. *Journal of Bacteriology*, 181(23):7248–7255.

Agranoff, B. W., Eggerer, H., Henning, U., and Lynen, F. (1959). Isopentenol pyrophosphate isomerase. *Journal of the American Chemical Society*, 81(5):1254–1255.

Anderson, W. H., Gellerman, J. L., and Schlenk, H. (1984). Effect of drought on phytyl wax esters in *Phaseolus* leaves. *Phytochemistry*, 23(11):2695–2696.

Araújo, W. L., Ishizaki, K., Nunes-Nesi, A., Tohge, T., Larson, T. R., Krahnert, I., Balbo, I., Witt, S., Dörmann, P., Graham, I. A., Leaver, C. J., and Fernie, A. R. (2011). Analysis of a range of catabolic mutants provides evidence that phytanoyl-coenzyme A does not act as a substrate of the electron-transfer flavoprotein/electron-transfer flavoprotein:ubiquinone oxidoreductase complex in *Arabidopsis* during dark-induced senescence. *Plant Physiology*, 157(1):55–69.

Ariizumi, T., Kishimoto, S., Kakami, R., Maoka, T., Hirakawa, H., Suzuki, Y., Ozeki, Y., Shirasawa, K., Bernillon, S., Okabe, Y., Moing, A., Asamizu, E., Rothan, C., Ohmiya, A., and Ezura, H. (2014). Identification of the carotenoid modifying gene *PALE YELLOW PETAL 1* as an essential factor in xanthophyll esterification and yellow flower pigmentation in tomato (*Solanum lycopersicum*). *Plant Journal*, 79(3):453–465.

Armstrong, G. A. (1994). Eubacteria show their true colors: genetics of carotenoid pigment biosynthesis from microbes to plants. *Journal of Bacteriology*, 176(16):4795–4802.

Aslan, S., Sun, C., Leonova, S., Dutta, P., Dörmann, P., Domergue, F., Stymne, S., and Hofvander, P. (2014). Wax esters of different compositions produced via engineering of leaf chloroplast metabolism in *Nicotiana benthamiana*. *Metabolic Engineering*, 25:103–112.

Austin, J. R., Frost, E., Vidi, P. A., Kessler, F., and Staehelin, L. A. (2006). Plastoglobules are lipoprotein subcompartments of the chloroplast that are permanently coupled to thylakoid membranes and contain biosynthetic enzymes. *Plant Cell*, 18(7):1693–1703.

Bak, S., Beisson, F., Bishop, G., Hamberger, B., Höfer, R., Paquette, S., and Werck-Reichhart, D. (2011). Cytochromes P450. *The Arabidopsis Book*, 9:e0144.

Bartoli, C. G., Simontacchi, M., Tambussi, E., Beltrano, J., Montaldi, E., and Puntarulo, S. (1999). Drought and watering-dependent oxidative stress: effect on antioxidant content in *Triticum aestivum* L. leaves. *Journal of Experimental Botany*, 50(332):375–383.

Bednarek, P., Pislewska-Bednarek, M., Svatos, A., Schneider, B., Doubsky, J., Mansurova, M., Humphry, M., Consonni, C., Panstruga, R., Sanchez-Vallet, A., Molina, A., and Schulze-Lefert, P. (2009). A glucosinolate metabolism pathway in living plant cells mediates broad-spectrum antifungal defense. *Science*, 323(5910):101–106.

Beisel, K. G., Jahnke, S., Hofmann, D., Köppchen, S., Schurr, U., and Matsubara, S. (2010). Continuous turnover of carotenes and chlorophyll a in mature leaves of *Arabidopsis* revealed by $^{14}CO_2$ pulse-chase labeling. *Plant Physiology*, 152(4):2188–2199.

Beytia, E., Dorsey, J. K., Marr, J., Cleland, W. W., and Porter, J. W. (1970). Purification and mechanism of action of hog liver mevalonic kinase. *Journal of Biological Chemistry*, 245(20):5450–5458.

Biedermann, M., Haase-Aschoff, P., and Grob, K. (2008). Wax ester fraction of edible oils: analysis by on-line LC-GC-MS and GC×GC-FID. *European Journal of Lipid Science and Technology*, 110(12):1084–1094.

Biester, E.-M., Hellenbrand, J., and Frentzen, M. (2012). Multifunctional acyltransferases from *Tetrahymena thermophila*. *Lipids*, 47(4):371–381.

Biswal, B. (1995). Carotenoid catabolism during leaf senescence and its control by light. *Journal of Photochemistry and Photobiology B*, 30(1):3–13.

Bligh, E. G. and Dyer, W. J. (1959). A rapid method of total lipid extraction and purification. *Canadian Journal of Biochemistry and Physiology*, 37(8):911–917.

Bloch, K., Chayking, S., Phillips, A. H., and de Waard, A. (1959). Mevalonic acid pyrophosphate and isopentenylpyrophosphate. *Journal of Biological Chemistry*, 234:2595–2604.

Böttcher, C., Westphal, L., Schmotz, C., Prade, E., Scheel, D., and Glawischnig, E. (2009). The multifunctional enzyme CYP71B15 (PHYTOALEXIN DEFICIENT3) converts cysteine-indole-3-acetonitrile to camalexin in the indole-3-acetonitrile metabolic network of *Arabidopsis thaliana*. *Plant Cell*, 21(6):1830–1845.

Bouvier, F., Rahier, A., and Camara, B. (2005). Biogenesis, molecular regulation and function of plant isoprenoids. *Progress in Lipid Research*, 44(6):357–429.

Breithaupt, D. E. and Bamedi, A. (2001). Carotenoid esters in vegetables and fruits: a screening with emphasis on β-cryptoxanthin esters. *Journal of Agricultural and Food Chemistry*, 49(4):2064–2070.

Britton, G. (1998). Overview of carotenoid biosynthesis. In Britton, G., Liaaen-Jensen, S., and Pfander, H., editors, *3. Biosynthesis and Metabolism*, Carotenoids, pages 13–147. Birkhäuser, Basel.

Browse, J., McCourt, P. J., and Somerville, C. R. (1986). Fatty acid composition of leaf lipids determined after combined digestion and fatty acid methyl ester formation from fresh tissue. *Analytical Biochemistry*, 152(1):141–145.

Buchanan, M. S., Hashimoto, T., and Asakawa, Y. (1996). Phytyl esters and phaeophytins from the hornwort *Megaceros flagellaris*. *Phytochemistry*, 41(5):1373–1376.

Buchanan-Wollaston, V. (1997). The molecular biology of leaf senescence. *Journal of Experimental Botany*, 48(2):181–199.

Bunea, A., Socaciu, C., and Pintea, A. (2014). Xanthophyll esters in fruits and vegetables. *Notulae Botanicae Horti Agrobotanici Cluj-Napoca*, 42(2):310–324.

Camara, B. and Monéger, R. (1978). Free and esterified carotenoids in green and red fruits of *Capsicum annuum*. *Phytochemistry*, 17(1):91–93.

Cameron, K. D., Teece, M. A., and Smart, L. B. (2006). Increased accumulation of cuticular wax and expression of lipid transfer protein in response to periodic drying events in leaves of tree tobacco. *Plant Physiology*, 140(1):176–183.

Cardini, F. (1982). Carotenoids in ripe green and in autumn senescing leaves of apple tree: I - Qualitative composition of free carotenoids, xanthophyll esters and fatty acids of esters. *Giornale Botanico Italiano*, 116(3-4):97–115.

Cardini, F. (1983). Carotenoids in ripe green and in autumn senescing leaves of apple tree: II - Seasonal changes of free carotenoids and xanthophyll esters and relationship between their content and senescing stage. *Giornale Botanico Italiano*, 117(1-2):75–97.

Cazzonelli, C. I. and Pogson, B. J. (2010). Source to sink: regulation of carotenoid biosynthesis in plants. *Trends in Plant Science*, 15(5):266–274.

Chang, S. Y. and Grunwald, C. (1976a). Duvatrienediol, alkanes, and fatty acids in cuticular wax of tobacco leaves of various physiological maturity. *Phytochemistry*, 15(6):961–963.

Chang, S. Y. and Grunwald, C. (1976b). Duvatrienediols in cuticular wax of Burley tobacco leaves. *Journal of Lipid Research*, 17(1):7–11.

Chappell, J. (1995). Biochemistry and molecular biology of the isoprenoid biosynthetic pathway in plants. *Annual Review of Plant Physiology and Plant Molecular Biology*, 46(1):521–547.

Charrier, B., Champion, A., Henry, Y., and Kreis, M. (2002). Expression profiling of the whole *Arabidopsis* Shaggy-like kinase multigene family by real-time reverse transcriptase-polymerase chain reaction. *Plant Physiology*, 130(2):577–590.

Chen, A., Dale Poulter, C., and Kroon, P. A. (1994). Isoprenyl diphosphate synthases: Protein sequence comparisons, a phylogenetic tree, and predictions of secondary structure. *Protein Science*, 3(4):600–607.

Chen, H. C., Smith, S. J., Tow, B., Elias, P. M., and Farese, R. V. (2002). Leptin modulates the effects of acyl CoA:diacylglycerol acyltransferase deficiency on murine fur and sebaceous glands. *Journal of Clinical Investigation*, 109(2):175–181.

Chen, W., Yu, X.-H., Zhang, K., Shi, J., de Oliveira, S., Schreiber, L., Shanklin, J., and Zhang, D. (2011). *Male Sterile2* encodes a plastid-localized fatty acyl carrier protein reductase required for pollen exine development in *Arabidopsis*. *Plant Physiology*, 157(2):842–853.

Collakova, E. and DellaPenna, D. (2001). Isolation and functional analysis of homogentisate phytyltransferase from *Synechocystis* sp PCC 6803 and *Arabidopsis*. *Plant Physiology*, 127(3):1113–1124.

Compagnon, V., Diehl, P., Benveniste, I., Meyer, D., Schaller, H., Schreiber, L., Franke, R., and Pinot, F. (2009). CYP86B1 is required for very long chain ω-hydroxyacid and α,ω-dicarboxylic acid synthesis in root and seed suberin polyester. *Plant Physiology*, 150(4):1831–1843.

Corpet, F. (1988). Multiple sequence alignment with hierarchical clustering. *Nucleic Acids Research*, 16(22):10881–10890.

Cranwell, A., Jaworski, G., and Bickley, H. M. (1990). Hydrocarbons, sterols, esters and fatty acids in six freshwater chlorophytes. *Phytochemistry*, 29(1):145–151.

Cranwell, P. A., Robinson, N., and Eglinton, G. (1985). Esterified lipids of the freshwater dinoflagellate *Peridinium lomnickii*. *Lipids*, 20(10):645–651.

Csupor, L. (1970). Das Phytol in vergilbten Blättern. *Planta Medica*, 18(05):37–41.

Cunningham, F. X. and Gantt, E. (1998). Genes and enzymes of carotenoid biosynthesis in plants. *Annual Review of Plant Physiology and Plant Molecular Biology*, 49:557–583.

Cunningham, F. X., Lafond, T. P., and Gantt, E. (2000). Evidence of a role for LytB in the nonmevalonate pathway of isoprenoid biosynthesis. *Journal of Bacteriology*, 182(20):5841–5848.

Dalgarn, D., Miller, P., Bricker, T., Speer, N., Jaworski, J. G., and Newman, D. W. (1979). Galactosyl transferase activity of chloroplast envelopes from senescent soybean cotyledons. *Plant Science Letters*, 14(1):1–5.

D'Ambrosio, C., Stigliani, A. L., and Giorio, G. (2011). Overexpression of *CrtR-b2* (carotene beta hydroxylase 2) from *S. lycopersicum* L. differentially affects xanthophyll synthesis and accumulation in transgenic tomato plants. *Transgenic Research*, 20(1):47–60.

Dhindsa, R. S., Plumb-Dhindsa, P., and Thorpe, T. A. (1981). Leaf senescence: correlated with increased levels of membrane permeability and lipid peroxidation, and decreased levels of superoxide dismutase and catalase. *Journal of Experimental Botany*, 32(1):93–101.

Doan, T. T. P., Domergue, F., Fournier, A. E., Vishwanath, S. J., Rowland, O., Moreau, P., Wood, C. C., Carlsson, A. S., Hamberg, M., and Hofvander, P. (2012). Biochemical characterization of a chloroplast localized fatty acid reductase from *Arabidopsis thaliana*. *Biochimica et Biophysica Acta*, 1821(9):1244–1255.

Dodge, J. D. (1970). Changes in chloroplast fine structure during the autumnal senescence of betula leaves. *Annals of Botany*, 34(4):817–824.

Durr, I. F. and Rudney, H. (1960). The reduction of beta-hydroxy-beta-methyl-glutaryl coenzyme A to mevalonic acid. *Journal of Biological Chemistry*, 235:2572–2578.

Ebel, P., Imgrund, S., vom Dorp, K., Hofmann, K., Maier, H., Drake, H., Degen, J., Dörmann, P., Eckhardt, M., Franz, T., and Willecke, K. (2014). Ceramide synthase 4 deficiency in mice causes lipid alterations in sebum and results in alopecia. *Biochemical Journal*, 461(1):147–158.

Eichenberger, W. and Grob, E. C. (1962). Beiträge zur Biochemie der pflanzlichen Plastiden. 2. Mitteilung. Über die Herbstcarotinoide von *Acer platanoides* (L.). *Helvetica Chimica Acta*, 45(5):1556–1563.

Eichenberger, W. and Grob, E. C. (1963). Beiträge zur Chemie der pflanzlichen Plastiden. 3. Mitteilung. Über das Vorkommen von Lutein-3-linolenat in gelben Herbstblättern von *Acer platanoides* (L.). *Helvetica Chimica Acta*, 46(6):2411–2417.

Eisenreich, W., Schwarz, M., Cartayrade, A., Arigoni, D., Zenk, M. H., and Bacher, A. (1998). The deoxyxylulose phosphate pathway of terpenoid biosynthesis in plants and microorganisms. *Chemistry and Biology*, 5(9):221–233.

Ellinger, D., Stingl, N., Kubigsteltig, I. I., Bals, T., Juenger, M., Pollmann, S., Berger, S., Schuenemann, D., and Mueller, M. J. (2010). DONGLE and DEFECTIVE IN ANTHER DEHISCENCE1 lipases are not essential for wound- and pathogen-induced jasmonate biosynthesis: redundant lipases contribute to jasmonate formation. *Plant Physiology*, 153(1):114–127.

Emanuelsson, O., Nielsen, H., and Heijne, G. (1999). ChloroP, a neural network-based method for predicting chloroplast transit peptides and their cleavage sites. *Protein Science*, 8:978–984.

Eriksson, S., Stransfeld, L., Adamski, N. M., Breuninger, H., and Lenhard, M. (2010). KLUH/CYP78A5-dependent growth signaling coordinates floral organ growth in *Arabidopsis*. *Current Biology*, 20(6):527–532.

Estelle, M. A. and Somerville, C. (1987). Auxin-resistant mutants of *Arabidopsis thaliana* with an altered morphology. *Molecular and General Genetics*, 206:200–206.

Fang, W., Wang, Z., Cui, R., Li, J., and Li, Y. (2012). Maternal control of seed size by *EOD3/CYP78A6* in *Arabidopsis thaliana*. *Plant Journal*, 70(6):929–939.

Ferguson, C. H. R. and Simon, E. W. (1973). Membrane lipids in senescing green tissues. *Journal of Experimental Botany*, 24(2):307–316.

Ferguson, J. J. and Rudney, H. (1959). The biosynthesis of β-hydroxy-β-methylglutaryl coenzyme A in yeast. I. Identification and purification of the hydroxymethylglutaryl coenzymecondensing enzyme. *Journal of Biological Chemistry*, 234(5):1072–1075.

Finn, R. D., Coggill, P., Eberhardt, R. Y., Eddy, S. R., Mistry, J., Mitchell, A. L., Potter, S. C., Punta, M., Qureshi, M., Sangrador-Vegas, A., Salazar, G. A., Tate, J., and Bateman, A. (2016). The Pfam protein families database: towards a more sustainable future. *Nucleic Acids Research*, 44(D1):D279–85.

Franich, R. A., Gowar, A. P., and Volkman, J. K. (1979). Secondary diols of *Pinus radiata* needle epicuticular wax. *Phytochemistry*, 18(9):1563–1564.

Furuya, T., Yoshikawa, T., Kimura, T., and Kaneko, H. (1987). Production of tocopherols by cell culture of safflower. *Phytochemistry*, 26(10):2741–2747.

Galpaz, N., Ronen, G., Khalfa, Z., Zamir, D., and Hirschberg, J. (2006). A chromoplast-specific carotenoid biosynthesis pathway is revealed by cloning of the tomato white-flower locus. *Plant Cell*, 18(8):1947–1960.

Gan, S. and Amasino, R. M. (1997). Making sense of senescence (molecular genetic regulation and manipulation of leaf senescence). *Plant Physiology*, 113(2):313–319.

Gau, W., Ploschke, H.-J., and Wünsche, C. (1983). Mass spectrometric identification of xanthophyll fatty acid esters from marigold flowers (*Tagetes erecta*) obtained by high performances liquid chromatography and craig counter-current distribution. *Journal of Chromatography*, 262:277–284.

Gaude, N., Bréhélin, C., Tischendorf, G., Kessler, F., and Dörmann, P. (2007). Nitrogen deficiency in *Arabidopsis* affects galactolipid composition and gene expression and results in accumulation of fatty acid phytyl esters. *Plant Journal*, 49(4):729–739.

Gellerman, J. L., Anderson, W. H., and Schlenk, H. (1975). Synthesis and analysis of phytyl and phytenoyl wax esters. *Lipids*, 10(11):656–661.

Gepstein, S. (1988). Photosynthesis. In Noodén, L. D., editor, *Senescence and aging in plants*, American Society of Plant Physiologists monograph series, pages 85–109. Acad. Pr, San Diego, Calif.

Gepstein, S., Sabehi, G., Carp, M.-J., Hajouj, T., Nesher, M. F. O., Yariv, I., Dor, C., and Bassani, M. (2003). Large-scale identification of leaf senescence-associated genes. *Plant Journal*, 36(5):629–642.

Goffman, F. D., Velasco, L., and Becker, H. C. (1999). Tocopherols accumulation in developing seeds and pods of rapeseed (*Brassica napus* L.). *European Journal of Lipid Science and Technology*, 101(10):400–403.

Goodwin, T. W. (1958). Studies in carotenogenesis. 24. The changes in carotenoid and chlorophyll pigments in the leaves of deciduous trees during autumn necrosis. *Biochemical Journal*, 68(3):503–511.

Goodwin, T. W. (1980). Carotenoids in higher plants. In Goodwin, T. W., editor, *The Biochemistry of the Carotenoids*, pages 143–203. Springer Netherlands, Dordrecht.

Gray, J. C. (1988). Control of isoprenoid biosynthesis in higher plants. *Advances in Botanical Research*, (14):25–91.

Greene, R. A. and Foster, E. O. (1933). The liquid wax of seeds of *Simmondsia californica*. *Botanical Gazette*, 94(4):826–828.

Greer, S., Wen, M., Bird, D., Wu, X., Samuels, L., Kunst, L., and Jetter, R. (2007). The cytochrome P450 enzyme CYP96A15 is the midchain alkane hydroxylase responsible for formation of secondary alcohols and ketones in stem cuticular wax of *Arabidopsis*. *Plant Physiology*, 145(3):653–667.

Griffiths, D., Robertson, G. W., Shepherd, T., and Ramsay, G. (1999). Epicuticular waxes and volatiles from faba bean (*Vicia faba*) flowers. *Phytochemistry*, 52(4):607–612.

Grob, E. C. and Csupor, L. (1967). Zur Kenntnis der Blattlipide von *Acer platanoides* L. während der herbstlichen Vergilbung. *Experientia*, 23(12):1004–1005.

Gross, J. and Flügel, M. (1982). Pigment changes in peel of the ripening banana (*Musa cavendishi*). *Die Gartenbauwissenschaft*, 47(2):62–64.

Guyer, L., Hofstetter, S. S., Christ, B., Lira, B. S., Rossi, M., and Hörtensteiner, S. (2014). Different mechanisms are responsible for chlorophyll dephytylation during fruit ripening and leaf senescence in tomato. *Plant Physiology*, 166(1):44–56.

Hahn, F. M., Hurlburt, A. P., and Poulter, C. D. (1999). *Escherichia coli* open reading frame 696 is *idi*, a nonessential gene encoding isopentenyl diphosphate isomerase. *Journal of Bacteriology*, 181(15):4499–4504.

Harrison, S. J., Mott, E. K., Parsley, K., Aspinall, S., Gray, J. C., and Cottage, A. (2006). A rapid and robust method of identifying transformed *Arabidopsis thaliana* seedlings following floral dip transformation. *Plant Methods*, 2(1):19.

Harwood, J. L., Jones, Anne V. H. M., and Thomas, H. (1982). Leaf senescence in a non-yellowing mutant of *Festuca pratensis*. *Planta*, 156(2):152–157.

Hecht, S., Eisenreich, W., Adam, P., Amslinger, S., Kis, K., Bacher, A., Arigoni, D., and Rohdich, F. (2001). Studies on the nonmevalonate pathway to terpenes: the role of the GcpE (IspG) protein. *Proceedings of the National Academy of Sciences of the United States of America*, 98(26):14837–14842.

Heemann, V., Brümmer, U., Paulsen, C., and Seehofer, F. (1983). Composition of the leaf surface gum of some *Nicotiana* species and *Nicotiana tabacum* cultivars. *Phytochemistry*, 22(1):133–135.

Heitz, T., Widemann, E., Lugan, R., Miesch, L., Ullmann, P., Désaubry, L., Holder, E., Grausem, B., Kandel, S., Miesch, M., Werck-Reichhart, D., and Pinot, F. (2012). Cytochromes P450 CYP94C1 and CYP94B3 catalyze two successive oxidation steps of plant hormone jasmonoyl-isoleucine for catabolic turnover. *Journal of Biological Chemistry*, 287(9):6296–6306.

Hendry, G. A. F., Houghton, J. D., and Brown, S. B. (1987). The degradation of chlorophyll — a biological enigma. *New Phytologist*, 107(2):255–302.

Herz, S., Wungsintaweekul, J., Schuhr, C. A., Hecht, S., Luttgen, H., Sagner, S., Fellermeier, M., Eisenreich, W., Zenk, M. H., Bacher, A., and Rohdich, F. (2000). Biosynthesis of terpenoids: YgbB protein converts 4-diphosphocytidyl-2C-methyl-D-erythritol 2-phosphate to 2C-methyl-D-erythritol 2,4-cyclodiphosphate. *Proceedings of the National Academy of Sciences of the United States of America*, 97(6):2486–2490.

Hiltbrunner, A., Bauer, J., Vidi, P.-A., Infanger, S., Weibel, P., Hohwy, M., and Kessler, F. (2001). Targeting of an abundant cytosolic form of the protein import receptor at Toc159 to the outer chloroplast membrane. *Journal of Cell Biology*, 154(2):309–316.

Höfer, R., Briesen, I., Beck, M., Pinot, F., Schreiber, L., and Franke, R. (2008). The *Arabidopsis* cytochrome P450 *CYP86A1* encodes a fatty acid ω-hydroxylase involved in suberin monomer biosynthesis. *Journal of Experimental Botany*, 59(9):2347–2360.

Horie, Y., Ito, H., Kusaba, M., Tanaka, R., and Tanaka, A. (2009). Participation of chlorophyll b reductase in the initial step of the degradation of light-harvesting chlorophyll a/b-protein complexes in *Arabidopsis*. *Journal of Biological Chemistry*, 284(26):17449–17456.

Hornero-Méndez, D. and Mínguez-Mosquera, M. I. (2000). Xanthophyll esterification accompanying carotenoid overaccumulation in chromoplast of *Capsicum annuum* ripening fruits is a constitutive process and useful for ripeness index. *Journal of Agricultural and Food Chemistry*, 48(5):1617–1622.

Hörtensteiner, S. (2013). Update on the biochemistry of chlorophyll breakdown. *Plant Molecular Biology*, 82(6):505–517.

Hörtensteiner, S. and Kräutler, B. (2011). Chlorophyll breakdown in higher plants. *Biochimica et Biophysica Acta*, 1807(8):977–988.

Hörtensteiner, S., Wüthrich, K. L., Matile, P., Ongania, K.-H., and Kräutler, B. (1998). The key step in chlorophyll breakdown in higher plants. *Journal of Biological Chemistry*, 273(25):15335–15339.

Howitt, C. A. and Pogson, B. J. (2006). Carotenoid accumulation and function in seeds and non-green tissues. *Plant, Cell and Environment*, 29(3):435–445.

Howitt, C. A., Pogson, B. J., Cuttriss, A. J., and Mimica, J. L. (2007). Carotenoids. In Wise, R. R. and Hoober, J. K., editors, *The structure and function of plastids*, Advances in Photosynthesis and Respiration, pages 315–334. Springer, Dordrecht.

Hull, A. K., Vij, R., and Celenza, J. L. (2000). *Arabidopsis* cytochrome P450s that catalyze the first step of tryptophan-dependent indole-3-acetic acid biosynthesis. *Proceedings of the National Academy of Sciences of the United States of America*, 97(5):2379–2384.

Hung, C.-Y., Aspesi, P., Hunter, M. R., Lomax, A. W., and Perera, I. Y. (2014). Phosphoinositide-signaling is one component of a robust plant defense response. *Frontiers in Plant Science*, 5:267.

Ischebeck, T., Zbierzak, A. M., Kanwischer, M., and Dörmann, P. (2006). A salvage pathway for phytol metabolism in *Arabidopsis*. *Journal of Biological Chemistry*, 281(5):2470–2477.

Jalink, H., van der Schoor, R., Frandas, A., van Pijlen, J. G., and Bino, R. J. (1998). Chlorophyll fluorescence of *Brassica oleracea* seeds as a non-destructive marker for seed maturity and seed performance. *Seed Science Research*, 8(04):10.

Janick-Buckner, D., Hammock, D. J., Johnson, J. M., Osborn, J. M., and Buckner, B. (1999). Biochemical and ultrastructural analysis of the *y10* mutant of maize. *Journal of Heredity*, 90(5):507–513.

Jansen, G. A., Verhoeven, N. M., Denis, S., Romeijn, G.-J., Jakobs, C., ten Brink, H. J., and Wanders, R. J. (1999). Phytanic acid α-oxidation: identification of 2-hydroxyphytanoyl-CoA lyase in rat liver and its localisation in peroxisomes. *Biochimica et Biophysica Acta*, 1440(2–3):176–182.

Jetter, R. (2000). Long-chain alkanediols from *Myricaria germanica* leaf cuticular waxes. *Phytochemistry*, 55(2):169–176.

Jetter, R., Kunst, L., and Samuels, A. L. (2006). Composition of plant cuticular waxes. In Riederer, M. and Müller, C., editors, *Biology of the plant cuticle*, volume 23 of *Annual plant reviews*, pages 145–181. Blackwell, Oxford.

Jetter, R. and Riederer, M. (1999). Long-chain alkanediols, ketoaldehydes, ketoalcohols and ketoalkyl esters in the cuticular waxes of *Osmunda regalis* fronds. *Phytochemistry*, 52(5):907–915.

Jetter, R., Riederer, M., Seyer, A., and Mioskowski, C. (1996). Homologous long-chain alkanediols from *Papaver* leaf cuticular waxes. *Phytochemistry*, 42(6):1617–1620.

Kalscheuer, R. and Steinbüchel, A. (2003). A novel bifunctional wax ester synthase/acyl-CoA diacylglycerol acyltransferase mediates wax ester and triacylglycerol biosynthesis in *Acinetobacter calcoaceticus* ADP1. *Journal of Biological Chemistry*, 278(10):8075–8082.

Kalscheuer, R., Uthoff, S., Luftmann, H., and Steinbüchel, A. (2003). In vitro and in vivo biosynthesis of wax diesters by an unspecific bifunctional wax ester synthase/acyl-CoA diacylglycerol acyltransferase from *Acinetobacter calcoaceticus* ADP1. *European Journal of Lipid Science and Technology*, 105(10):578–584.

Kanda, P. and Wells, M. A. (1981). Facile acylation of glycerophosphocholine catalyzed by trifluoroacetic anhydride. *Journal of Lipid Research*, 22(5):877–879.

Kanwischer, M. (2007). *Phytol aus dem Chlorophyllabbau ist limitierend für die Tocopherol (Vitamin E)-Synthese*. PhD thesis, Universität Potsdam, Potsdam.

Kanwischer, M., Porfirova, S., Bergmüller, E., and Dörmann, P. (2005). Alterations in tocopherol cyclase activity in transgenic and mutant plants of *Arabidopsis* affect tocopherol content, tocopherol composition, and oxidative stress. *Plant Physiology*, 137(2):713–723.

Katz, J. J. and Norris, J. R. (1973). Chlorophyll and light energy transduction in photosynthesis. *Current Topics in Bioenergetics*, (5):41–75.

Kaup, M. T., Froese, C. D., and Thompson, J. E. (2002). A role for diacylglycerol acyltransferase during leaf senescence. *Plant Physiology*, 129(4):1616–1626.

Keller, Y., Bouvier, F., D'Harlingue, A., and Camara, B. (1998). Metabolic compartmentation of plastid prenyllipid biosynthesis. Evidence for the involvement of a multifunctional geranylgeranyl reductase. *European Journal of Biochemistry*, 164(2):555–569.

Kerwin, B. A. (2008). Polysorbates 20 and 80 used in the formulation of protein biotherapeutics: structure and degradation pathways. *Journal of Pharmaceutical Sciences*, 97(8):2924–2935.

Keskitalo, J., Bergquist, G., Gardeström, P., and Jansson, S. (2005). A cellular timetable of autumn senescence. *Plant Physiology*, 139(4):1635–1648.

Kim, H., Choi, D., and Suh, M. C. (2017). Cuticle ultrastructure, cuticular lipid composition, and gene expression in hypoxia-stressed *Arabidopsis* stems and leaves. *Plant Cell Reports*, 36(6):815–827.

Kim, J. and DellaPenna, D. (2006). Defining the primary route for lutein synthesis in plants: the role of *Arabidopsis* carotenoid β-ring hydroxylase CYP97A3. *Proceedings of the National Academy of Sciences of the United States of America*, 103(9):3474–3479.

Kim, J.-E., Cheng, K. M., Craft, N. E., Hamberger, B., and Douglas, C. J. (2010). Over-expression of *Arabidopsis thaliana* carotenoid hydroxylases individually and in combination with a beta-carotene ketolase provides insight into in vivo functions. *Phytochemistry*, 71(2-3):168–178.

Kitaoka, N., Matsubara, T., Sato, M., Takahashi, K., Wakuta, S., Kawaide, H., Matsui, H., Nabeta, K., and Matsuura, H. (2011). *Arabidopsis CYP94B3* encodes jasmonyl-L-isoleucine 12-hydroxylase, a key enzyme in the oxidative catabolism of jasmonate. *Plant and Cell Physiology*, 52(10):1757–1765.

Knee, M. (1972). Anthocyanin, carotenoid, and chlorophyll changes in the peel of cox's orange pippin apples during ripening on and off the tree. *Journal of Experimental Botany*, 23(1):184–196.

Knee, M. (1988). Carotenol esters in developing apple fruits. *Phytochemistry*, 27(4):1005–1009.

Koiwai, A., Matsuzaki, T., Suzuki, F., and Kawashima, N. (1981). Changes in total and polar lipids and their fatty acid composition in tobacco leaves during growth and senescence. *Plant and Cell Physiology*, 22(6):1059–1065.

Koo, A. J., Thireault, C., Zemelis, S., Poudel, A. N., Zhang, T., Kitaoka, N., Brandizzi, F., Matsuura, H., and Howe, G. A. (2014). Endoplasmic reticulum-associated inactivation of the hormone jasmonoyl-L-isoleucine by multiple members of the cytochrome P450 94 family in *Arabidopsis*. *Journal of Biological Chemistry*, 289(43):29728–29738.

Kosma, D. K., Murmu, J., Razeq, F. M., Santos, P., Bourgault, R., Molina, I., and Rowland, O. (2014). AtMYB41 activates ectopic suberin synthesis and assembly in multiple plant species and cell types. *Plant Journal*, 80(2):216–229.

Köster, J., Thurow, C., Kruse, K., Meier, A., Iven, T., Feussner, I., and Gatz, C. (2012). Xenobiotic- and jasmonic acid-inducible signal transduction pathways have become interdependent at the *Arabidopsis CYP81D11* promoter. *Plant Physiology*, 159(1):391–402.

Kuhn, R. and Wiegand, W. (1929). Über konjugierte Doppelbindungen IX. Der Farbstoff der Judenkirschen (*Physalis alkekengi* und *Physalis franchetti*). *Helvetica Chimica Acta*, 12(1):499–506.

Kuhn, R., Winterstein, A., and Kaufmann, W. (1930). Zur Kenntnis des Physalis-Farbstoffes (Über konjugierte Doppelbindungen, XII). *Berichte der Deutschen Chemischen Gesellschaft (A and B Series)*, 63(6):1489–1497.

Kumagai, M. H., Keller, Y., Bouvier, F., Clary, D., and Camara, B. (1998). Functional integration of non-native carotenoids into chloroplasts by viral-derived expression of capsanthin-capsorubin synthase in *Nicotiana benthamiana*. *Plant Journal*, 14(3):305–315.

Kunst, L., Browse, J., and Somerville, C. (1988). Altered regulation of lipid biosynthesis in a mutant of *Arabidopsis* deficient in chloroplast glycerol-3-phosphate acyltransferase activity. *Proceedings of the National Academy of Sciences of the United States of America*, 85:4143–4147.

Kuzuyama, T., Takagi, M., Kaneda, K., Watanabe, H., Dairi, T., and Seto, H. (2000). Studies on the nonmevalonate pathway: Conversion of 4-(cytidine 5'-diphospho)-2-C-methyl-d-erythritol to its 2-phospho derivative by 4-(cytidine 5'-diphospho)-2-C-methyl-d-erythritol kinase. *Tetrahedron Letters*, 41(16):2925–2928.

Laemmli, U. K. (1970). Cleavage of structural proteins during the assembly of the head of bacteriophage T4. *Nature*, 227:680–685.

Lai, C., Kunst, L., and Jetter, R. (2007). Composition of alkyl esters in the cuticular wax on inflorescence stems of *Arabidopsis thaliana cer* mutants. *Plant Journal*, 50(2):189–196.

Langmeier, M., Ginsburg, S., and Matile, P. (1993). Chlorophyll breakdown in senescent leaves: demonstration of Mg-dechelatase activity. *Physiologia Plantarum*, 89(2):347–353.

Lennox, E. S. (1955). Transduction of linked genetic characters of the host by bacteriophage P1. *Virology*, 1(2):190–206.

Li, F., Wu, X., Lam, P., Bird, D., Zheng, H., Samuels, L., Jetter, R., and Kunst, L. (2008). Identification of the wax ester synthase/acyl-coenzyme A:diacylglycerol acyltransferase WSD1 required for stem wax ester biosynthesis in *Arabidopsis*. *Plant Physiology*, 148(1):97–107.

Li-Beisson, Y., Pollard, M., Sauveplane, V., Pinot, F., Ohlrogge, J., and Beisson, F. (2009). Nanoridges that characterize the surface morphology of flowers require the synthesis of cutin polyester. *Proceedings of the National Academy of Sciences of the United States of America*, 106(51):22008–22013.

Li-Beisson, Y., Shorrosh, B., Beisson, F., Andersson, M. X., Arondel, V., Bates, P. D., Baud, S., Bird, D., Debono, A., Durrett, T. P., Franke, R. B., Graham, I. A., Katayama, K., Kelly, A. A., Larson, T., Markham, J. E., Miquel, M., Molina, I., Nishida, I., Rowland, O., Samuels, L.,

Schmid, K. M., Wada, H., Welti, R., Xu, C., Zallot, R., and Ohlrogge, J. (2013). Acyl-lipid metabolism. *The Arabidopsis Book*, 11:e0161.

Lichtenthaler, H. K. (1968). Plastoglobuli and the fine structure of plastids. *Endeavour*, 27:144–149.

Lichtenthaler, H. K. (1970). Die Lokalisation der Plastidenchinone und Carotinoide in den Chromoplasten der Petalen von *Sarothamnus scoparius* (L.) Wimm ex Koch. *Planta*, 90(2):142–152.

Lichtenthaler, H. K., Rohmer, M., and Schwender, J. (1997a). Two independent biochemical pathways for isopentenyl diphosphate and isoprenoid biosynthesis in higher plants. *Physiologia Plantarum*, 101(3):643–652.

Lichtenthaler, H. K., Schwender, J., Disch, A., and Rohmer, M. (1997b). Biosynthesis of isoprenoids in higher plant chloroplasts proceeds via a mevalonate-independent pathway. *FEBS Letters*, 400(3):271–274.

Lim, P. O., Kim, H. J., and Nam, H. G. (2007). Leaf senescence. *Annual Review of Plant Biology*, 58:115–136.

Lin, Y.-P., Wu, M.-C., and Charng, Y.-y. (2016). Identification of a chlorophyll dephytylase involved in chlorophyll turnover in *Arabidopsis*. *Plant Cell*, 28(12):2974–2990.

Lippold, F., vom Dorp, K., Abraham, M., Hölzl, G., Wewer, V., Lindberg Yilmaz, J., Lager, I., Montandon, C., Besagni, C., Kessler, F., Stymne, S., and Dörmann, P. (2012). Fatty acid phytyl ester synthesis in chloroplasts of *Arabidopsis*. *Plant Cell*, 24(5):2001–2014.

Liu, W., Xie, Y., Ma, J., Luo, X., Nie, P., Zuo, Z., Lahrmann, U., Zhao, Q., Zheng, Y., Zhao, Y., Xue, Y., and Ren, J. (2015). IBS: an illustrator for the presentation and visualization of biological sequences. *Bioinformatics*, 31(20):3359–3361.

Livak, K. J. and Schmittgen, T. D. (2001). Analysis of relative gene expression data using real-time quantitative PCR and the $2^{-\Delta\Delta C}{}_{T}$ method. *Methods*, 25(4):402–408.

Loesecke, H. v. (1929). Quantitative changes in the chloroplast pigments in the peel of bananas during ripening. *Journal of the American Chemical Society*, 51(8):2439–2443.

Lundquist, P. K., Poliakov, A., Bhuiyan, N. H., Zybailov, B., Sun, Q., and van Wijk, K. J. (2012). The functional network of the *Arabidopsis* plastoglobule proteome based on quantitative proteomics and genome-wide coexpression analysis. *Plant Physiology*, 158(3):1172–1192.

Luttgen, H., Rohdich, F., Herz, S., Wungsintaweekul, J., Hecht, S., Schuhr, C. A., Fellermeier, M., Sagner, S., Zenk, M. H., Bacher, A., and Eisenreich, W. (2000). Biosynthesis of terpenoids: YchB protein of *Escherichia coli* phosphorylates the 2-hydroxy group of 4-diphosphocytidyl-2C-methyl-D-erythritol. *Proceedings of the National Academy of Sciences of the United States of America*, 97(3):1062–1067.

Maeda, H., Sage, T. L., Isaac, G., Welti, R., and DellaPenna, D. (2008). Tocopherols modulate extraplastidic polyunsaturated fatty acid metabolism in *Arabidopsis* at low temperature. *Plant Cell*, 20(2):452–470.

Marheineke, K., Grünewald, S., Christie, W., and Reiländer, H. (1998). Lipid composition of *Spodoptera frugiperda* (Sf9) and *Trichoplusia ni* (Tn) insect cells used for baculovirus infection. *FEBS Letters*, 441(1):49–52.

Marshall, P. S., Morris, S. R., and Threlfall, D. R. (1985). Biosynthesis of tocopherols: A re-examination of the biosynthesis and metabolism of 2-methyl-6-phytyl-1,4-benzoquinol. *Phytochemistry*, 24(8):1705–1711.

Matile, P., Hörtensteiner, S., Thomas, H., and Krautler, B. (1996). Chlorophyll breakdown in senescent leaves. *Plant Physiology*, 112(4):1403–1409.

Meguro, M., Ito, H., Takabayashi, A., Tanaka, R., and Tanaka, A. (2011). Identification of the 7-hydroxymethyl chlorophyll a reductase of the chlorophyll cycle in *Arabidopsis*. *Plant Cell*, 23(9):3442–3453.

Mehrshahi, P., Stefano, G., Andaloro, J. M., Brandizzi, F., Froehlich, J. E., and DellaPenna, D. (2013). Transorganellar complementation redefines the biochemical continuity of endoplasmic reticulum and chloroplasts. *Proceedings of the National Academy of Sciences of the United States of America*, 110(29):12126–12131.

Mellado-Ortega, E. and Hornero-Méndez, D. (2015). Carotenoid profiling of *Hordeum chilense* grains: The parental proof for the origin of the high carotenoid content and esterification pattern of tritordeum. *Journal of Cereal Science*, 62:15–21.

Molina, I., Bonaventure, G., Ohlrogge, J., and Pollard, M. (2006). The lipid polyester composition of *Arabidopsis thaliana* and *Brassica napus* seeds. *Phytochemistry*, 67(23):2597–2610.

Munné-Bosch, S. and Alegre, L. (2000). Changes in carotenoids, tocopherols and diterpenes during drought and recovery, and the biological significance of chlorophyll loss in *Rosmarinus officinalis* plants. *Planta*, 210(6):925–931.

Murashige, T. and Skoog, F. (1962). A revised medium for rapid growth and bio assays with tobacco tissue cultures. *Physiologia Plantarum*, 15(3):473–497.

Nakajima, S., Ito, H., Tanaka, R., and Tanaka, A. (2012). Chlorophyll b reductase plays an essential role in maturation and storability of *Arabidopsis* seeds. *Plant Physiology*, 160(1):261–273.

Nilsson, A. K., Fahlberg, P., Johansson, O. N., Hamberg, M., Andersson, M. X., and Ellerström, M. (2016). The activity of HYDROPEROXIDE LYASE 1 regulates accumulation of galactolipids containing 12-oxo-phytodienoic acid in *Arabidopsis*. *Journal of Experimental Botany*, 67(17):5133–5144.

Nisar, N., Li, L., Lu, S., Khin, N. C., and Pogson, B. J. (2015). Carotenoid metabolism in plants. *Molecular Plant*, 8(1):68–82.

Patterson, G. W., Hugly, S., and Harrison, D. (1993). Sterols and phytyl esters of *Arabidopsis thaliana* under normal and chilling temperatures. *Phytochemistry*, 33:1381–1383.

Paznocht, L., Kotíková, Z., Šulc, M., Lachman, J., Orsák, M., Eliášová, M., and Martinek, P. (2018). Free and esterified carotenoids in pigmented wheat, tritordeum and barley grains. *Food Chemistry*, 240:670–678.

Peisker, C., Düggelin, T., Rentsch, D., and Matile, P. (1989). Phytol and the breakdown of chlorophyll in senescent leaves. *Journal of Plant Physiology*, 135(4):428–432.

Pereira, A. S., Siqueira, D. S., Elias, V. O., Simoneit, B. R., Cabral, J. A., and Aquino Neto, F. R. (2002). Three series of high molecular weight alkanoates found in Amazonian plants. *Phytochemistry*, 61(6):711–719.

Pott, I., Breithaupt, D. E., and Carle, R. (2003). Detection of unusual carotenoid esters in fresh mango (*Mangifera indica* L. cv. 'Kent'). *Phytochemistry*, 64(4):825–829.

Pružinská, A., Tanner, G., Anders, I., Roca, M., and Hörtensteiner, S. (2003). Chlorophyll breakdown: Pheophorbide a oxygenase is a Rieske-type iron-sulfur protein, encoded by the *accelerated cell death 1* gene. *Proceedings of the National Academy of Sciences of the United States of America*, 100:15259–15264.

Reiter, B. and Lorbeer, E. (2001). Analysis of the wax ester fraction of olive oil and sunflower oil by gas chromatography and gas chromatography-mass spectrometry. *Journal of the American Oil Chemists' Society*, 78:881–888.

Richter, W. J. and Burlingame, A. L. (1968). New evidence for the electron-impact induced migration of trimethylsilyl substituents. *Chemical Communications*, (19):1158–1160.

Riederer, M. and Schreiber, L. (2001). Protecting against water loss: Analysis of the barrier properties of plant cuticles. *Journal of Experimental Botany*, 52(363):2023–2032.

Rise, M., Cojocaru, M., Gottlieb, H. E., and Goldschmidt, E. E. (1989). Accumulation of α-tocopherol in senescing organs as related to chlorophyll degradation. *Plant Physiology*, 89(4):1028–1030.

Rivas, J. D. (1991). Reversed-phase high-performance liquid chromatographic separation of lutein and lutein fatty acid esters from marigold flower petal powder. *Journal of Chromatography*, 464:442–447.

Roessner, U., Wagner, C., Kopka, J., Trethewey, R. N., and Willmitzer, L. (2000). Simultaneous analysis of metabolites in potato tuber by gas chromatography-mass spectrometry. *Plant Journal*, 23(1):131–142.

Rohdich, F., Hecht, S., Gärtner, K., Adam, P., Krieger, C., Amslinger, S., Arigoni, D., Bacher, A., and Eisenreich, W. (2002). Studies on the nonmevalonate terpene biosynthetic pathway: metabolic role of IspH (LytB) protein. *Proceedings of the National Academy of Sciences of the United States of America*, 99(3):1158–1163.

Rohdich, F., Kis, K., Bacher, A., and Eisenreich, W. (2001). The non-mevalonate pathway of isoprenoids: genes, enzymes and intermediates. *Current Opinion in Chemical Biology*, 5(5):535–540.

Rohdich, F., Wungsintaweekul, J., Eisenreich, W., Richter, G., Schuhr, C. A., Hecht, S., Zenk, M. H., and Bacher, A. (2000). Biosynthesis of terpenoids: 4-diphosphocytidyl-2C-methyl-D-erythritol synthase of *Arabidopsis thaliana*. *Proceedings of the National Academy of Sciences of the United States of America*, 97(12):6451–6456.

Rohdich, F., Wungsintaweekul, J., Fellermeier, M., Sagner, S., Herz, S., Kis, K., Eisenreich, W., Bacher, A., and Zenk, M. H. (1999). Cytidine 5'-triphosphate-dependent biosynthesis of isoprenoids: YgbP protein of *Escherichia coli* catalyzes the formation of 4-diphosphocytidyl-2-C-methylerythritol. *Proceedings of the National Academy of Sciences of the United States of America*, 96(21):11758–11763.

Rohmer, M., Knani, M., Simonin, P., Sutter, B., and Sahm, H. (1993). Isoprenoid biosynthesis in bacteria: A novel pathway for the early steps leading to isopentenyl diphosphate. *Biochemical Journal*, 295(2):517–524.

Rohmer, M., Seemann, M., Horbach, S., Bringer-Meyer, S., and Sahm, H. (1996). Glyceraldehyde 3-phosphate and pyruvate as precursors of isoprenic units in an alternative non-mevalonate pathway for terpenoid biosynthesis. *Journal of the American Chemical Society*, 118(11):2564–2566.

Rontani, J.-F., Bonin, P. C., and Volkman, J. K. (1999). Production of wax esters during aerobic growth of marine bacteria on isoprenoid compounds. *Applied and Environmental Microbiology*, 65(1):221–230.

Roughan, P. G., Slack, C. R., and Holland, R. (1978). Generation of phospholipid artefacts during extraction of developing soybean seeds with methanolic solvents. *Lipids*, 13(7):497–503.

Rowland, O. and Domergue, F. (2012). Plant fatty acyl reductases: enzymes generating fatty alcohols for protective layers with potential for industrial applications. *Plant Science*, 193-194:28–38.

Rupasinghe, S. G., Duan, H., and Schuler, M. A. (2007). Molecular definitions of fatty acid hydroxylases in *Arabidopsis thaliana*. *Proteins*, 68(1):279–293.

Sánchez, M., Nicholls, D. G., and Brindley, D. N. (1973). The relationship between palmitoyl-coenzyme A synthetase activity and esterification of sn-glycerol 3-phosphate in rat liver mitochondria. *Biochemical Journal*, 132(4):697–706.

Sanger, J. E. (1971). Quantitative investigations of leaf pigments from their inception in buds through autumn coloration to decomposition in falling leaves. *Ecology*, 52(6):1075–1089.

Sato, Y., Morita, R., Katsuma, S., Nishimura, M., Tanaka, A., and Kusaba, M. (2009). Two short-chain dehydrogenase/reductases, NON-YELLOW COLORING 1 and NYC1-LIKE, are required for chlorophyll b and light-harvesting complex II degradation during senescence in rice. *Plant Journal*, 57(1):120–131.

Sattler, S. E., Gilliland, L. U., Magallanes-Lundback, M., Pollard, M., and DellaPenna, D. (2004). Vitamin E is essential for seed longevity and for preventing lipid peroxidation during germination. *Plant Cell*, 16(6):1419–1432.

Schelbert, S., Aubry, S., Burla, B., Agne, B., Kessler, F., Krupinska, K., and Hörtensteiner, S. (2009). Pheophytin pheophorbide hydrolase (pheophytinase) is involved in chlorophyll breakdown during leaf senescence in *Arabidopsis*. *Plant Cell*, 21(3):767–785.

Schippers, J. H. M., Schmidt, R., Wagstaff, C., and Jing, H.-C. (2015). Living to die and dying to live: the survival strategy behind leaf senescence. *Plant Physiology*, 169(2):914–930.

Schmidt, A. and Gershenzon, J. (2007). Cloning and characterization of isoprenyl diphosphate synthases with farnesyl diphosphate and geranylgeranyl diphosphate synthase activity from Norway spruce (*Picea abies*) and their relation to induced oleoresin formation. *Phytochemistry*, 68(21):2649–2659.

Schoefs, B., Rmiki, N.-E., Rachadi, J., and Lemoine, Y. (2001). Astaxanthin accumulation in *Haematococcus* requires a cytochrome P450 hydroxylase and an active synthesis of fatty acids. *FEBS Letters*, 500(3):125–128.

Schwacke, R., Fischer, K., Ketelsen, B., Krupinska, K., and Krause, K. (2007). Comparative survey of plastid and mitochondrial targeting properties of transcription factors in *Arabidopsis* and rice. *Molecular Genetics and Genomics*, 277(6):631–646.

Schwacke, R., Schneider, A., van der Graaff, E., Fischer, K., Catoni, E., Desimone, M., Frommer, W. B., Flügge, U.-I., and Kunze, R. (2003). ARAMEMNON, a novel database for *Arabidopsis* integral membrane proteins. *Plant Physiology*, 131:16–26.

Schwender, J., Zeidler, J., Gröner, R., Müller, C., Focke, M., Braun, S., Lichtenthaler, F. W., and Lichtenthaler, H. K. (1997). Incorporation of 1-deoxy-D-xylulose into isoprene and phytol by higher plants and algae. *FEBS Letters*, 414(1):129–134.

Shimoda, Y., Ito, H., and Tanaka, A. (2016). *Arabidopsis STAY-GREEN*, Mendel's green cotyledon gene, encodes magnesium-dechelatase. *Plant Cell*, 28(9):2147–2160.

Smith, S. J., Cases, S., Jensen, D. R., Chen, H. C., Sande, E., Tow, B., Sanan, D. A., Raber, J., Eckel, R. H., and Farese, R. V. (2000). Obesity resistance and multiple mechanisms of triglyceride synthesis in mice lacking Dgat. *Nature Genetics*, 25(1):87–90.

Soll, J., Kemmerling, M., and Schultz, G. (1980). Tocopherol and plastoquinone synthesis in spinach chloroplasts subfractions. *Archives of Biochemistry and Biophysics*, 204(2):544–550.

Song, W., Maeda, H., and DellaPenna, D. (2010). Mutations of the ER to plastid lipid transporters *TGD1, 2, 3 and 4* and the ER oleate desaturase *FAD2* suppress the low temperature-induced phenotype of *Arabidopsis* tocopherol-deficient mutant *vte2*. *Plant Journal*, 62(6):1004–1018.

Sotelo-Silveira, M., Cucinotta, M., Chauvin, A.-L., Chávez Montes, R. A., Colombo, L., Marsch-Martínez, N., and de Folter, S. (2013). Cytochrome P450 CYP78A9 is involved in *Arabidopsis* reproductive development. *Plant Physiology*, 162(2):779–799.

Stålberg, K., Lindgren, O., Ek, B., and Höglund, A.-S. (2003). Synthesis of ketocarotenoids in the seed of *Arabidopsis thaliana*. *Plant Journal*, 36(6):771–779.

Steinmüller, D. and Tevini, M. (1985). Composition and function of plastoglobuli. I. Isolation and purification from chloroplasts and chromoplasts. *Planta*, 163(2):201–207.

Stoddart, J. L. and Thomas, H. (1982). Leaf senescence. In Boulter, D. and Parthier, B., editors, *Nucleic Acids and Proteins in Plants I*, Encyclopedia of Plant Physiology, pages 592–636. Springer, Berlin, Heidelberg.

Streb, P., Shang, W., Feierabend, J., and Bligny, R. (1998). Divergent strategies of photoprotection in high-mountain plants. *Planta*, 207(2):313–324.

Takagi, M., Kuzuyama, T., Kaneda, K., Watanabe, H., Dairi, T., and Seto, H. (2000). Studies on the nonmevalonate pathway: Formation of 2-C-methyl-d-erythritol 2,4-cyclodiphosphate from 2-phospho-4-(cytidine 5'-diphospho)-2-C-methyl-d-erythritol. *Tetrahedron Letters*, 41(18):3395–3398.

Takahashi, S., Kuzuyama, T., Watanabe, H., and Seto, H. (1998). A 1-deoxy-D-xylulose 5-phosphate reductoisomerase catalyzing the formation of 2-C-methyl-D-erythritol 4-phosphate in an alternative nonmevalonate pathway for terpenoid biosynthesis. *Proceedings of the National Academy of Sciences of the United States of America*, 95(17):9879–9884.

Tanaka, R., Hirashima, M., Satoh, S., and Tanaka, A. (2003). The *Arabidopsis-accelerated cell death* Gene ACD1 is involved in oxygenation of pheophorbide a. *Plant and Cell Physiology*, 44(12):1266–1274.

Tanaka, R., Oster, U., Kruse, E., Rüdiger, W., and Grimm, B. (1999). Reduced activity of geranylgeranyl reductase leads to loss of chlorophyll and tocopherol and to partially geranylgeranylated chlorophyll in transgenic tobacco plants expressing antisense RNA for geranylgeranyl reductase. *Plant Physiology*, 120(3):695–704.

Tchen, T. T. (1958). Mevalonic kinase: purification and properties. *Journal of Biological Chemistry*, 233(5):1100–1103.

Tevini, M. and Steinmüller, D. (1985). Composition and function of plastoglobuli: II. Lipid composition of leaves and plastoglobuli during beech leaf senescence. *Planta*, 163(1):91–96.

Thomas, H. (2013). Senescence, ageing and death of the whole plant. *New Phytologist*, 197(3):696–711.

Thomas, H. and Stoddart, J. L. (1980). Leaf senescence. *Annual Review of Plant Physiology*, 31(1):83–111.

Tian, L., Musetti, V., Kim, J., Magallanes-Lundback, M., and DellaPenna, D. (2004). The *Arabidopsis* LUT1 locus encodes a member of the cytochrome P450 family that is required for carotenoid ε-ring hydroxylation activity. *Proceedings of the National Academy of Sciences of the United States of America*, 101(1):402–407.

Towbin, H., Staehelin, T., and Gordon, J. (1979). Electrophoretic transfer of proteins from polyacrylamide gels to nitrocellulose sheets: procedure and some applications. *Proceedings of the National Academy of Sciences of the United States of America*, 76(9):4350–4354.

Tulloch, A. P. (1971). Diesters of diols in wheat leaf wax. *Lipids*, 6(9):641–644.

Tulloch, A. P. (1973). Composition of leaf surface waxes of *Triticum* species: Variation with age and tissue. *Phytochemistry*, 12(9):2225–2232.

Tulloch, A. P. and Hoffman, L. L. (1974). Epicuticular waxes of *Secale cereale* and *Triticale* hexaploide leaves. *Phytochemistry*, 13(11):2535–2540.

Valentin, H. E., Lincoln, K., Moshiri, F., Jensen, P. K., Qi, Q., Venkatesh, T. V., Karunanandaa, B., Baszis, S. R., Norris, S. R., Savidge, B., Gruys, K. J., and Last, R. L. (2006). The *Arabidopsis vitamin E pathway gene5-1* mutant reveals a critical role for phytol kinase in seed tocopherol biosynthesis. *Plant Cell*, 18(1):212–224.

van Wijk, K. J. and Kessler, F. (2017). Plastoglobuli: Plastid microcompartments with integrated functions in metabolism, plastid developmental transitions, and environmental adaptation. *Annual Review of Plant Biology*, 68:253–289.

Vicentini, F., Hortensteiner, S., Schellenberg, M., Thomas, H., and Matile, P. (1995). Chlorophyll breakdown in senescent leaves identification of the biochemical lesion in a stay-green genotype of *Festuca pratensis* Huds. *New Phytologist*, 129(2):247–252.

Vidi, P. A., Kanwischer, M., Baginsky, S., Austin, J. R., Csucs, G., Dörmann, P., Kessler, F., and Bréhélin, C. (2006). Tocopherol cyclase (VTE1) localization and vitamin E accumulation in chloroplast plastoglobule lipoprotein particles. *Journal of Biological Chemistry*, 281(16):11225–11234.

vom Dorp, K. (2015). *Phytol and tocopherol metabolism in Arabidopsis thaliana*. PhD thesis, Rheinische Friedrich-Wilhelms-Universität Bonn, Bonn.

vom Dorp, K., Dombrink, I., and Dörmann, P. (2013). Quantification of diacylglycerol by mass spectrometry. *Methods in Molecular Biology*, 1009:43–54.

vom Dorp, K., Hölzl, G., Plohmann, C., Eisenhut, M., Abraham, M., Weber, A. P. M., Hanson, A. D., and Dörmann, P. (2015). Remobilization of phytol from chlorophyll degradation is essential for tocopherol synthesis and growth of *Arabidopsis*. *Plant Cell*, 27(10):2846–2859.

von Wettstein-Knowles, P. (1995). Biosynthesis and genetics of waxes. In Hamilton, R. J., editor, *Waxes: Chemistry, Molecular Biology and Functions*, volume 6 of *The Oily Press lipid library*, pages 91–120. The Oily Press, Dundee.

Wanders, R. J., Jansen, G. A., and Lloyd, M. D. (2003). Phytanic acid alpha-oxidation, new insights into an old problem: a review. *Biochimica et Biophysica Acta*, 1631(2):119–135.

Wang, K. C. and Ohnuma, S.-I. (2000). Isoprenyl diphosphate synthases. *Biochimica et Biophysica Acta*, 1529(1–3):33–48.

Wang, M. and Casey, P. J. (2016). Protein prenylation: unique fats make their mark on biology. *Nature Reviews Molecular Cell Biology*, 17(2):110–122.

Wellesen, K., Durst, F., Pinot, F., Benveniste, I., Nettesheim, K., Wisman, E., Steiner-Lange, S., Saedler, H., and Yephremov, A. (2001). Functional analysis of the *LACERATA* gene of *Arabidopsis* provides evidence for different roles of fatty acid ω-hydroxylation in development. *Proceedings of the National Academy of Sciences of the United States of America*, 98(17):9694–9699.

Wen, M., Au, J., Gniwotta, F., and Jetter, R. (2006). Very-long-chain secondary alcohols and alkanediols in cuticular waxes of *Pisum sativum* leaves. *Phytochemistry*, 67(22):2494–2502.

Wen, M. and Jetter, R. (2009). Composition of secondary alcohols, ketones, alkanediols, and ketols in *Arabidopsis thaliana* cuticular waxes. *Journal of Experimental Botany*, 60(6):1811–1821.

White, T., Bursten, S., Federighi, D., Lewis, R. A., and Nudelman, E. (1998). High-resolution separation and quantification of neutral lipid and phospholipid species in mammalian cells and sera by multi-one-dimensional thin-layer chromatography. *Analytical Biochemistry*, 258(1):109–117.

Wildi, B. and Lütz, C. (1996). Antioxidant composition of selected high alpine plant species from different altitudes. *Plant, Cell and Environment*, 19(2):138–146.

Wood, C. C., Petrie, J. R., Shrestha, P., Mansour, M. P., Nichols, P. D., Green, A. G., and Singh, S. P. (2009). A leaf-based assay using interchangeable design principles to rapidly assemble multistep recombinant pathways. *Plant Biotechnology Journal*, 7(9):914–924.

Wright, L. D. (1961). Biosynthesis of isoprenoid compounds. *Annual Review of Biochemistry*, 30(1):525–548.

Wuthrich, K. L., Bovet, L., Hunziker, P. E., Donnison, I. S., and Hortensteiner, S. (2000). Molecular cloning, functional expression and characterisation of RCC reductase involved in chlorophyll catabolism. *Plant Journal*, 21(2):189–198.

Xiao, F., Goodwin, S. M., Xiao, Y., Sun, Z., Baker, D., Tang, X., Jenks, M. A., and Zhou, J.-M. (2004). *Arabidopsis CYP86A2* represses *Pseudomonas syringae* type III genes and is required for cuticle development. *EMBO Journal*, 23(14):2903–2913.

Yasumoto, S., Fukushima, E. O., Seki, H., and Muranaka, T. (2016). Novel triterpene oxidizing activity of *Arabidopsis thaliana* CYP716A subfamily enzymes. *FEBS Letters*, 590(4):533–540.

Yeats, T. H. and Rose, J. K. C. (2013). The formation and function of plant cuticles. *Plant Physiology*, 163(1):5–20.

Yen, C.-L. E., Monetti, M., Burri, B. J., and Farese, R. V. (2005). The triacylglycerol synthesis enzyme DGAT1 also catalyzes the synthesis of diacylglycerols, waxes, and retinyl esters. *Journal of Lipid Research*, 46(7):1502–1511.

Young, A. J., Wellings, R., and Britton, G. (1991). The fate of chloroplast pigments during senescence of primary leaves of *Hordeum vulgare* and *Avena sativum*. *Journal of Plant Physiology*, 137(6):701–705.

Ytterberg, A. J., Peltier, J. B., and van Wijk, K. J. (2006). Protein profiling of plastoglobules in chloroplasts and chromoplasts. A surprising site for differential accumulation of metabolic enzymes. *Plant Physiology*, 140(3):984–997.

Zhang, W., Liu, T., Ren, G., Hörtensteiner, S., Zhou, Y., Cahoon, E. B., and Zhang, C. (2014). Chlorophyll degradation: the tocopherol biosynthesis-related phytol hydrolase in *Arabidopsis* seeds is still missing. *Plant Physiology*, 166(1):70–79.

Zhu, X., Suzuki, K., Saito, T., Okada, K., Tanaka, K., Nakagawa, T., Matsuda, H., and Kawamukai, M. (1997). Geranylgeranyl pyrophosphate synthase encoded by the newly isolated gene GGPS6 from *Arabidopsis thaliana* is localized in mitochondria. *Plant Molecular Biology*, 35(3):331–341.

Zybailov, B., Rutschow, H., Friso, G., Rudella, A., Emanuelsson, O., Sun, Q., and van Wijk, K. J. (2008). Sorting signals, N-terminal modifications and abundance of the chloroplast proteome. *PLoS One*, 3(4):e1994.

7 Appendix

7.1 Targeted Lists for Q-TOF MS/MS Analysis

Table 7.1 – Targeted list for the Q-TOF MS/MS analysis of fatty acid phytyl esters. In positive ion mode, fatty acid phytyl esters formed ammonium adducts $[M + NH_4]^+$ and were measured by neutral loss scanning of the phytol-H_2O fragment of 278.2974. The collision energy was set to 5 V.

Fatty Acid Phytyl Esters	Formula [M]	Parental Ion $[M + NH_4]^+$	Neutral Loss [Phytol – H_2O]
6:0-phytol	$C_{26}H_{50}O_2$	412.4155	278.2974
8:0-phytol	$C_{28}H_{54}O_2$	440.4468	
9:0-phytol	$C_{29}H_{56}O_2$	454.4624	
10:0-phytol	$C_{30}H_{58}O_2$	468.4781	
11:0-phytol	$C_{31}H_{60}O_2$	482.4937	
12:0-phytol	$C_{32}H_{62}O_2$	496.5094	
13:0-phytol	$C_{33}H_{64}O_2$	510.5250	
14:0-phytol	$C_{34}H_{66}O_2$	524.5407	
15:0-phytol	$C_{35}H_{68}O_2$	538.5563	
16:4-phytol	$C_{36}H_{62}O_2$	544.5094	
16:3-phytol	$C_{36}H_{64}O_2$	546.5250	
16:2-phytol	$C_{36}H_{66}O_2$	548.5407	
16:1-phytol	$C_{36}H_{68}O_2$	550.5563	
16:0-phytol	$C_{36}H_{70}O_2$	552.5720	
17:0-phytol (I.S.)	$C_{37}H_{72}O_2$	566.5876	
18:4-phytol	$C_{38}H_{66}O_2$	572.5407	
18:3-phytol	$C_{38}H_{68}O_2$	574.5563	
18:2-phytol	$C_{38}H_{70}O_2$	576.5720	
18:1-phytol	$C_{38}H_{72}O_2$	578.5876	
18:0-phytol	$C_{38}H_{74}O_2$	580.6033	
20:5-phytol	$C_{40}H_{68}O_2$	598.5563	
20:4-phytol	$C_{40}H_{70}O_2$	600.5720	
20:3-phytol	$C_{40}H_{72}O_2$	602.5876	
20:2-phytol	$C_{40}H_{74}O_2$	604.6033	
20:1-phytol	$C_{40}H_{76}O_2$	606.6189	
20:0-phytol	$C_{40}H_{78}O_2$	608.6346	
22:1-phytol	$C_{42}H_{80}O_2$	634.6502	
22:0-phytol	$C_{42}H_{82}O_2$	636.6659	
24:0-phytol	$C_{44}H_{86}O_2$	664.6972	
26:0-phytol	$C_{46}H_{90}O_2$	692.7285	
28:0-phytol	$C_{48}H_{94}O_2$	720.7598	
30:0-phytol	$C_{50}H_{98}O_2$	748.7911	

Table 7.2 – Targeted list for the Q-TOF MS/MS analysis of wax esters. In positive ion mode, wax esters formed ammonium adducts $[M + NH_4]^+$ (left table) and were measured by product ion scanning of the proton adduct ion of the fatty acid fragment $[FA + H]^+$ (right table). The mass of the respective alcohol moiety was calculated from the difference between the mass of the parental ion and the mass of the product ion. This difference represents the neutral loss of the alcohol $[Alc - H_2O + NH_3]$. The collision energy was set to 15 V.

Parental Ions

Formula [M]	$[M + NH_4]^+$
$C_{22}H_{44}O_2$	358.3680
$C_{24}H_{48}O_2$	386.3993
$C_{26}H_{52}O_2$	414.4306
$C_{28}H_{56}O_2$	442.4619
$C_{30}H_{60}O_2$	470.4932
$C_{32}H_{64}O_2$	498.5245
$C_{34}H_{68}O_2$	526.5558
$C_{35}H_{70}O_2$ (I.S.)	540.5714
$C_{36}H_{72}O_2$	553.5871
$C_{38}H_{76}O_2$	582.6184
$C_{40}H_{80}O_2$	609.6497
$C_{42}H_{84}O_2$	638.6810
$C_{44}H_{88}O_2$	666.7123
$C_{46}H_{92}O_2$	694.7436
$C_{48}H_{96}O_2$	722.7749

Product Ions

Fatty Acid	Formula [FA]	$[FA + H]^+$
12:0	$C_{12}H_{24}O_2$	217.2041
14:0	$C_{14}H_{28}O_2$	245.2354
16:0	$C_{16}H_{32}O_2$	273.2667
17:0	$C_{17}H_{34}O_2$	271.2632
18:0	$C_{18}H_{36}O_2$	301.2980
20:0	$C_{20}H_{40}O_2$	313.3101
22:0	$C_{22}H_{44}O_2$	341.3414
24:0	$C_{24}H_{48}O_2$	369.3727

Table 7.3 – Targeted list for the Q-TOF MS/MS analysis of wax diesters of hexadecanediol. In positive ion mode, wax diesters formed ammonium adducts $[M + NH_4]^+$ (left table) and were measured by neutral loss scanning of the fatty acid fragment $[FA - H_2O + NH_3]$ (right table). The identity of the second esterified fatty acid in the wax diesters was concluded by subtracting the masses of neutral loss and hexadecanediol from the parental ion mass. The collision energy was set to 20 V for 1,16-hexadecanediol diesters. For the analysis of 1,6-hexadecanediol diesters the same targeted list was applied, but the collision energy was adjusted to 10 V.

Parental Ions

Formula [M]	$[M + NH_4]^+$
$C_{32}H_{62}O_4$	528.4992
$C_{34}H_{66}O_4$	556.5305
$C_{36}H_{70}O_4$	584.5618
$C_{38}H_{74}O_4$	612.5931
$C_{40}H_{78}O_4$	640.6244
$C_{42}H_{82}O_4$	668.6557
$C_{44}H_{80}O_4$	690.6400
$C_{44}H_{82}O_4$	692.6557
$C_{44}H_{84}O_4$	694.6713
$C_{44}H_{86}O_4$	696.6870
$C_{46}H_{84}O_4$	718.6713
$C_{46}H_{86}O_4$	720.6870
$C_{46}H_{88}O_4$	722.7026
$C_{46}H_{90}O_4$	724.7183
$C_{48}H_{88}O_4$	746.7026
$C_{48}H_{90}O_4$	748.7183
$C_{48}H_{92}O_4$	750.7339
$C_{48}H_{94}O_4$	752.7496
$C_{50}H_{98}O_4$	780.7809

Neutral Loss

Fatty Acid	Formula [FA]	$[FA - H_2O + NH_3]$
8:0	$C_8H_{18}O_2$	143.1310
10:0	$C_{10}H_{20}O_2$	171.1623
12:0	$C_{12}H_{24}O_2$	199.1936
14:0	$C_{14}H_{28}O_2$	227.2249
16:3	$C_{16}H_{26}O_2$	249.2093
16:2	$C_{16}H_{28}O_2$	251.2249
16:1	$C_{16}H_{30}O_2$	253.2406
16:0	$C_{16}H_{32}O_2$	255.2562
18:3	$C_{18}H_{30}O_2$	277.2406
18:2	$C_{18}H_{32}O_2$	279.2562
18:1	$C_{18}H_{34}O_2$	281.2719
18:0	$C_{18}H_{36}O_2$	283.2875

Table 7.4 – Targeted list for the Q-TOF MS/MS analysis of sterol esters. In positive ion mode, sterol esters formed ammonium adducts $[M + NH_4]^+$ and were measured by product ion scanning of the sterol backbone $[SE + H]^+$. The collision energy was set to 13 V.

Sterol Esters	Formula [M]	Parental Ion $[M + NH_4]^+$	Product Ion $[SE + H]^+$
12:0-Cholesterol	$C_{39}H_{68}O_2$	586.5558	369.3505
12:0-Campesterol	$C_{40}H_{70}O_2$	600.5714	383.3662
12:0-Stigmasterol	$C_{41}H_{70}O_2$	612.5714	395.3662
12:0-Sitosterol	$C_{41}H_{72}O_2$	614.5871	397.3818
14:0-Cholesterol	$C_{41}H_{72}O_2$	614.5871	369.3505
14:0-Campesterol	$C_{42}H_{74}O_2$	628.6027	383.3662
16:3-Cholesterol	$C_{43}H_{70}O_2$	636.5714	369.3505
16:2-Cholesterol	$C_{43}H_{72}O_2$	638.5871	369.3505
14:0-Stigmasterol	$C_{43}H_{74}O_2$	640.6027	395.3662
16:1-Cholesterol (I.S.)	$C_{43}H_{74}O_2$	640.6027	369.3505
14:0-Sitosterol	$C_{43}H_{76}O_2$	642.6184	397.3818
16:0-Cholesterol (I.S.)	$C_{43}H_{76}O_2$	642.6184	369.3505
16:3-Campesterol	$C_{44}H_{72}O_2$	650.5871	383.3662
16:2-Campesterol	$C_{44}H_{74}O_2$	652.6027	383.3662
16:1-Campesterol	$C_{44}H_{76}O_2$	654.6184	383.3662
16:0-Campesterol	$C_{44}H_{78}O_2$	656.6340	383.3662

Table 7.4 - Targeted list of sterol esters continued.

16:3-Stigmasterol	$C_{45}H_{72}O_2$	662.5871	395.3662
16:2-Stigmasterol	$C_{45}H_{74}O_2$	664.6027	395.3662
16:3-Sitosterol	$C_{45}H_{74}O_2$	664.6027	397.3818
18:3-Cholesterol	$C_{45}H_{74}O_2$	664.6027	369.3505
16:1-Stigmasterol	$C_{45}H_{76}O_2$	666.6184	395.3662
16:2-Sitosterol	$C_{45}H_{76}O_2$	666.6184	397.3818
18:2-Cholesterol	$C_{45}H_{76}O_2$	666.6184	369.3505
16:0-Stigmasterol	$C_{45}H_{78}O_2$	668.6340	395.3662
16:1-Sitosterol	$C_{45}H_{78}O_2$	668.6340	397.3818
18:1-Cholesterol (I.S.)	$C_{45}H_{78}O_2$	668.6340	369.3505
16:0-Sitosterol	$C_{45}H_{80}O_2$	670.6497	397.3818
18:0-Cholesterol (I.S.)	$C_{45}H_{80}O_2$	670.6497	369.3505
18:3-Campesterol	$C_{46}H_{76}O_2$	678.6184	383.3662
18:2-Campesterol	$C_{46}H_{78}O_2$	680.6340	383.3662
18:1-Campesterol	$C_{46}H_{80}O_2$	682.6497	383.3662
18:0-Campesterol	$C_{46}H_{82}O_2$	684.6653	383.3662
18:3-Stigmasterol	$C_{47}H_{76}O_2$	690.6184	395.3662
18:3-Sitosterol	$C_{47}H_{78}O_2$	692.6340	397.3818
18:2-Stigmasterol	$C_{47}H_{78}O_2$	692.6340	395.3662
20:3-Cholesterol	$C_{47}H_{78}O_2$	692.6340	369.3505
18:2-Sitosterol	$C_{47}H_{80}O_2$	694.6497	397.3818
18:1-Stigmasterol	$C_{47}H_{80}O_2$	694.6497	395.3662
20:2-Cholesterol	$C_{47}H_{80}O_2$	694.6497	369.3505
18:0-Stigmasterol	$C_{47}H_{82}O_2$	696.6653	395.3662
18:1-Sitosterol	$C_{47}H_{82}O_2$	696.6653	397.3818
20:1-Cholesterol	$C_{47}H_{82}O_2$	696.6653	369.3505
18:0-Sitosterol	$C_{47}H_{84}O_2$	698.6810	397.3818
20:0-Cholesterol	$C_{47}H_{84}O_2$	698.6810	369.3505
20:3-Campesterol	$C_{48}H_{80}O_2$	706.6497	383.3662
20:2-Campesterol	$C_{48}H_{82}O_2$	708.6653	383.3662
20:1-Campesterol	$C_{48}H_{84}O_2$	710.6810	383.3662
20:0-Campesterol	$C_{48}H_{86}O_2$	712.6966	383.3662
20:3-Stigmasterol	$C_{49}H_{80}O_2$	718.6497	395.3662
22:3-Cholesterol	$C_{49}H_{82}O_2$	720.5245	369.3505
20:2-Stigmasterol	$C_{49}H_{82}O_2$	720.6653	395.3662
20:3-Sitosterol	$C_{49}H_{82}O_2$	720.6653	397.3818
20:1-Stigmasterol	$C_{49}H_{84}O_2$	722.6810	395.3662
20:2-Sitosterol	$C_{49}H_{84}O_2$	722.6810	397.3818
22:2-Cholesterol	$C_{49}H_{84}O_2$	722.6810	369.3505
20:0-Stigmasterol	$C_{49}H_{86}O_2$	724.6966	395.3662
20:1-Sitosterol	$C_{49}H_{86}O_2$	724.6966	397.3818
22:1-Cholesterol	$C_{49}H_{86}O_2$	724.6966	369.3505
20:0-Sitosterol	$C_{49}H_{88}O_2$	726.7123	397.3818
22:0-Cholesterol	$C_{49}H_{88}O_2$	726.7123	369.3505
22:3-Campesterol	$C_{50}H_{84}O_2$	734.5401	383.3662
22:2-Campesterol	$C_{50}H_{86}O_2$	736.6966	383.3662
22:1-Campesterol	$C_{50}H_{88}O_2$	738.7123	383.3662
22:0-Campesterol	$C_{50}H_{90}O_2$	740.7279	383.3662
22:3-Stigmasterol	$C_{51}H_{84}O_2$	746.5401	395.3662
22:3-Sitosterol	$C_{51}H_{86}O_2$	748.5558	397.3818
22:2-Stigmasterol	$C_{51}H_{86}O_2$	748.6966	395.3662
22:1-Stigmasterol	$C_{51}H_{88}O_2$	750.7123	395.3662
22:2-Sitosterol	$C_{51}H_{88}O_2$	750.7123	397.3818

Table 7.4 - Targeted list of sterol esters continued.

22:0-Stigmasterol	$C_{51}H_{90}O_2$	752.7279	395.3662
22:1-Sitosterol	$C_{51}H_{90}O_2$	752.7279	397.3818
22:0-Sitosterol	$C_{51}H_{92}O_2$	754.7436	397.3818

Table 7.5 – Targeted list for the Q-TOF MS/MS analysis of TAG. In positive ion mode, TAG formed ammonium adducts $[M + NH_4]^+$ (left table) and were measured by neutral loss scanning of a fatty acid fragment $[FA + NH_3]$ (right table). The collision energy was set to 20 V.

Parental Ions

TAG	Formula [M]	$[M + NH_4]^+$
30:0 (I.S.)	$C_{33}H_{62}O_6$	572.4890
33:3 (I.S.)	$C_{36}H_{62}O_6$	608.4890
36:0	$C_{39}H_{74}O_6$	656.5829
38:0	$C_{41}H_{78}O_6$	684.6142
40:3	$C_{43}H_{76}O_6$	706.5986
40:0	$C_{43}H_{82}O_6$	712.6455
42:3	$C_{45}H_{80}O_6$	734.6299
42:2	$C_{45}H_{82}O_6$	736.6455
42:1	$C_{45}H_{84}O_6$	738.6612
42:0	$C_{45}H_{86}O_6$	740.6768
44:6	$C_{47}H_{80}O_6$	758.6299
44:3	$C_{47}H_{82}O_6$	760.6455
44:2	$C_{47}H_{84}O_6$	762.6612
44:1	$C_{47}H_{86}O_6$	764.6768
44:0	$C_{47}H_{90}O_6$	768.7081
46:6	$C_{49}H_{82}O_6$	784.6455
46:5	$C_{49}H_{84}O_6$	786.6612
46:4	$C_{49}H_{86}O_6$	788.6768
46:3	$C_{49}H_{88}O_6$	790.6925
46:2	$C_{49}H_{90}O_6$	792.7081
46:1	$C_{49}H_{92}O_6$	794.7238
46:0	$C_{49}H_{94}O_6$	796.7394
48:9	$C_{51}H_{80}O_6$	806.6299
48:6	$C_{51}H_{86}O_6$	812.6768
48:5	$C_{51}H_{88}O_6$	814.6925
48:4	$C_{51}H_{90}O_6$	816.7081
48:3	$C_{51}H_{92}O_6$	818.7238
48:2	$C_{51}H_{94}O_6$	820.7394
48:1	$C_{51}H_{96}O_6$	822.7551
48:0	$C_{51}H_{98}O_6$	824.7707
50:6	$C_{53}H_{90}O_6$	840.7081
50:5	$C_{53}H_{92}O_6$	842.7238
50:4	$C_{53}H_{94}O_6$	844.7394
50:3	$C_{53}H_{96}O_6$	846.7551
50:2	$C_{53}H_{98}O_6$	848.7707
50:1	$C_{53}H_{100}O_6$	850.7864
50:0	$C_{53}H_{102}O_6$	852.8020
52:9	$C_{55}H_{88}O_6$	862.6925
52:8	$C_{55}H_{90}O_6$	864.7081
52:7	$C_{55}H_{92}O_6$	866.7238

Neutral Loss

Fatty Acid	Formula [FA]	$[FA + NH_3]$
10:0	$C_{10}H_{20}O_2$	189.1728
11:1	$C_{11}H_{20}O_2$	201.1728
12:0	$C_{12}H_{24}O_2$	217.2041
14:0	$C_{14}H_{28}O_2$	245.2354
16:3	$C_{16}H_{26}O_2$	267.2198
16:0	$C_{16}H_{32}O_2$	273.2667
18:3	$C_{18}H_{30}O_2$	295.2511
18:2	$C_{18}H_{32}O_2$	297.2667
18:1	$C_{18}H_{34}O_2$	299.2824
18:0	$C_{18}H_{36}O_2$	301.2980

Table 7.5 - Targeted list of TAG continued.

52:6	$C_{55}H_{94}O_6$	868.7394
52:5	$C_{55}H_{96}O_6$	870.7551
52:4	$C_{55}H_{98}O_6$	872.7707
52:3	$C_{55}H_{100}O_6$	874.7864
52:2	$C_{55}H_{102}O_6$	876.8020
52:1	$C_{55}H_{104}O_6$	878.8177
52:0	$C_{55}H_{106}O_6$	880.8333
54:9	$C_{57}H_{92}O_6$	890.7238
54:8	$C_{57}H_{94}O_6$	892.7394
54:7	$C_{57}H_{96}O_6$	894.7551
54:6	$C_{57}H_{98}O_6$	896.7707
54:5	$C_{57}H_{100}O_6$	898.7864
54:4	$C_{57}H_{102}O_6$	900.8020
54:3	$C_{57}H_{104}O_6$	902.8177
54:2	$C_{57}H_{106}O_6$	904.8333

Table 7.6 – Targeted list for the Q-TOF MS/MS analysis of fatty acid farnesyl esters. In positive ion mode, fatty acid farnesyl esters formed ammonium adducts $[M + NH_4]^+$ and were measured by neutral loss scanning of the farnesyl-H_2O fragment 204.1878. The collision energy was set to 5 V.

Fatty Acid Farnesyl Esters	Formula [M]	Parental Ion $[M + NH_4]^+$	Neutral Loss [Farnesol – H_2O]
8:0-Farnesol	$C_{23}H_{40}O_2$	366.3372	204.1878
10:0-Farnesol	$C_{25}H_{44}O_2$	394.3685	
12:0-Farnesol	$C_{27}H_{48}O_2$	422.3998	
14:0-Farnesol	$C_{29}H_{52}O_2$	450.4311	
15:0-Farnesol	$C_{30}H_{54}O_2$	464.4468	
16:0-Farnesol	$C_{31}H_{56}O_2$	478.4624	
16:3-Farnesol	$C_{31}H_{50}O_2$	472.4155	
17:0-Farnesol	$C_{32}H_{58}O_2$	492.4781	
18:0-Farnesol	$C_{33}H_{60}O_2$	506.4937	
18:1-Farnesol	$C_{33}H_{58}O_2$	504.4781	
18:2-Farnesol	$C_{33}H_{56}O_2$	502.4624	
18:3-Farnesol	$C_{33}H_{54}O_2$	500.4468	
20:0-Farnesol	$C_{35}H_{64}O_2$	534.5250	
22:0-Farnesol	$C_{37}H_{68}O_2$	562.5563	

Table 7.7 – Targeted list for the Q-TOF MS/MS analysis of fatty acid xanthophyll ester with neoxanthin and violaxanthin. Because neoxanthin and violaxanthin have the exact same mass, mono- and diesters of these xanthophylls cannot be distinguished by MS/MS experiments. Thus they are referred as *NeoVio* esters. Violaxanthin harbours only two hydroxy groups and can therefore only form mono- and diesters. Neoxanthin harbours three hydroxy groups and can form triesters. Each NeoVio diester and neoxanthin triester sum formula can stand for several fatty acid compositions. In the following table one possible combination is given exemplarily. In positive ion mode, xanthophyll esters formed ammonium adducts $[M + NH_4]^+$. The collision energy was set to 15 V for NeoVio mono- and diesters and adjusted to 25 V for neoxanthin triesters.

Fatty Acid Xanthophyll Ester	Formula [M]	Parental Ion $[M + NH_4]^+$
Neoxanthin/Violaxanthin Monoester		
12:0-NeoVio	$C_{52}H_{78}O_5$	800.6193
14:1-NeoVio	$C_{54}H_{80}O_5$	826.6349
14:0-NeoVio	$C_{54}H_{82}O_5$	828.6506
16:3-NeoVio	$C_{56}H_{80}O_5$	850.6349
16:2-NeoVio	$C_{56}H_{82}O_5$	852.6506
16:1-NeoVio	$C_{56}H_{84}O_5$	854.6662
16:0-NeoVio	$C_{56}H_{86}O_5$	856.6819
18:3-NeoVio	$C_{58}H_{84}O_5$	878.6662
18:2-NeoVio	$C_{58}H_{86}O_5$	880.6819
18:1-NeoVio	$C_{58}H_{88}O_5$	882.6975
18:0-NeoVio	$C_{58}H_{90}O_5$	884.7132
20:1-NeoVio	$C_{60}H_{92}O_5$	910.7288
20:0-NeoVio	$C_{60}H_{94}O_5$	912.7445
Neoxanthin/Violaxanthin Diester		
12:0-12:0-NeoVio	$C_{64}H_{100}O_6$	982.7864
12:0-14:0-NeoVio	$C_{66}H_{104}O_6$	1010.8177
14:0-14:1-NeoVio	$C_{68}H_{106}O_6$	1036.8333
14:0-14:0-NeoVio	$C_{68}H_{108}O_6$	1038.8490
14:0-16:3-NeoVio	$C_{70}H_{106}O_6$	1060.8333
14:0-16:2-NeoVio	$C_{70}H_{108}O_6$	1062.8490
14:0-16:1-NeoVio	$C_{70}H_{110}O_6$	1064.8646
14:0-16:0-NeoVio	$C_{70}H_{112}O_6$	1066.8803
16:0-16:3-NeoVio	$C_{72}H_{110}O_6$	1088.8646
16:0-16:2-NeoVio	$C_{72}H_{112}O_6$	1090.8803
16:0-16:1-NeoVio	$C_{72}H_{114}O_6$	1092.8959
16:0-16:0-NeoVio	$C_{72}H_{116}O_6$	1094.9116
16:3-18:0-NeoVio	$C_{74}H_{114}O_6$	1116.8959
16:2-18:0-NeoVio	$C_{74}H_{116}O_6$	1118.9116
16:1-18:0-NeoVio	$C_{74}H_{118}O_6$	1120.9272
16:0-18:0-NeoVio	$C_{74}H_{120}O_6$	1122.9429
18:0-18:0-NeoVio	$C_{76}H_{124}O_6$	1150.9742
Neoxanthin Triester		
12:0-12:0-12:0-Neo	$C_{76}H_{122}O_7$	1164.9534
12:0-12:0-14:0-Neo	$C_{78}H_{126}O_7$	1192.9847
12:0-14:0-14:1-Neo	$C_{80}H_{128}O_7$	1219.0004
12:0-14:0-14:0-Neo	$C_{80}H_{130}O_7$	1221.0160
12:0-14:0-16:2-Neo	$C_{82}H_{130}O_7$	1245.0160
12:0-14:0-16:1-Neo	$C_{82}H_{132}O_7$	1247.0317
12:0-14:0-16:0-Neo	$C_{82}H_{134}O_7$	1249.0473
14:0-14:0-16:3-Neo	$C_{84}H_{132}O_7$	1271.0317
14:0-14:0-16:2-Neo	$C_{84}H_{134}O_7$	1273.0473

Table 7.7 - Targeted list of xanthophyll esters continued.

14:0-14:0-16:1-Neo	$C_{84}H_{136}O_7$	1275.0630
14:0-14:0-16:0-Neo	$C_{84}H_{138}O_7$	1277.0786
14:0-16:0-16:3-Neo	$C_{86}H_{136}O_7$	1299.0630
14:0-16:0-16:2-Neo	$C_{86}H_{138}O_7$	1301.0786
14:0-16:0-16:1-Neo	$C_{86}H_{140}O_7$	1303.0943
14:0-16:0-16:0-Neo	$C_{86}H_{142}O_7$	1305.1099
16:0-16:0-16:3-Neo	$C_{88}H_{140}O_7$	1327.0943
16:0-16:0-16:2-Neo	$C_{88}H_{142}O_7$	1329.1099
16:0-16:0-16:1-Neo	$C_{88}H_{144}O_7$	1331.1256
16:0-16:0-16:0-Neo	$C_{88}H_{146}O_7$	1333.1412
16:0-16:3-18:0-Neo	$C_{90}H_{144}O_7$	1355.1256
16:0-16:2-18:0-Neo	$C_{90}H_{146}O_7$	1357.1412
16:0-16:1-18:0-Neo	$C_{90}H_{148}O_7$	1359.1569
16:0-16:0-18:0-Neo	$C_{90}H_{150}O_7$	1361.1725
16:1-18:0-18:0-Neo	$C_{92}H_{152}O_7$	1387.1882
16:0-18:0-18:0-Neo	$C_{92}H_{154}O_7$	1389.2038
18:0-18:0-18:0-Neo	$C_{94}H_{158}O_7$	1417.2351

Table 7.8 – MS parameters for the Q-TOF MS/MS analysis of phospho- and galactolipids for the quantification in positive ion mode.

Lipid Class	Parental Ion	Collision Energy [V]	Neutral Loss [u]	Product Ion [m/z]
MGDG	$[M + NH_4]^+$	12	179.0556	
DGDG	$[M + NH_4]^+$	17	341.1084	
SQDG	$[M + NH_4]^+$	19	261.0518	
PA	$[M + NH_4]^+$	20	115.0034	
PS	$[M + H]^+$	22	185.0089	
PI	$[M + NH_4]^+$	20	277.0563	
PE	$[M + H]^+$	20	141.0191	
PG	$[M + NH_4]^+$	20	189.0402	
PC	$[M + H]^+$	35		184.0739

Table 7.9 – Targeted list for the Q-TOF MS/MS analysis of phospho- and galactolipids for the quantification in positive ion mode.

Lipid	Mass [m/z]	Lipid	Mass [m/z]	Lipid	Mass [m/z]
	$[M + NH_4]^+$		$[M + NH_4]^+$		$[M + H]^+$
34:6 MGDG	764.5307	28:0 PA (I.S.)	610.4448	28:0 PE (I.S.)	636.4604
34:5 MGDG	766.5463	34:6 PA	682.4442	34:4 PE	712.4912
34:4 MGDG	768.5620	34:5 PA	684.4462	34:3 PE	714.5069
34:3 MGDG	770.5776	34:4 PA	686.4755	34:2 PE	716.5225
34:2 MGDG	772.5933	34:3 PA	688.4912	34:1 PE	718.5382
34:1 MGDG	774.6089	34:2 PA	690.5068	36:6 PE	736.4912
34:0 MGDG (I.S.)	776.6246	34:1 PA	692.5225	36:5 PE	738.5069
36:6 MGDG	792.5620	36:6 PA	710.4755	36:4 PE	740.5225
36:5 MGDG	794.5776	36:5 PA	712.4912	36:3 PE	742.5382
36:4 MGDG	796.5933	36:4 PA	714.5068	36:2 PE	744.5538
36:3 MGDG	798.6089	36:3 PA	716.5225	36:1 PE	746.5695
36:2 MGDG	800.6246	36:2 PA	718.5381	38:6 PE	764.5225
36:1 MGDG	802.6402	40:0 PA (I.S.)	778.6326	38:5 PE	766.5382
36:0 MGDG (I.S.)	804.6559		$[M + H]^+$	38:4 PE	768.5538
38:6 MGDG	820.5933	28:0 PS (I.S.)	680.4503	38:3 PE	770.5695
38:5 MGDG	822.6089	34:4 PS	756.4810	38:2 PE	772.5851
38:4 MGDG	824.6246	34:3 PS	758.4967	40:3 PE	798.6008
38:3 MGDG	826.6402	34:2 PS	760.5123	40:2 PE	800.6164
	$[M + NH_4]^+$	34:1 PS	762.5280	40:0 PE (I.S.)	804.6477
34:6 DGDG	926.5835	36:5 PS	782.4967	42:3 PE	826.6321
34:5 DGDG	928.5992	36:4 PS	784.5123	42:2 PE	828.6477
34:4 DGDG	930.6148	36:3 PS	786.5280		$[M + NH_4]^+$
34:3 DGDG	932.6305	36:2 PS	788.5436	28:0 PG (I.S.)	684.4816
34:2 DGDG	934.6461	36:1 PS	790.5593	32:1 PG	738.5279
34:1 DGDG	936.6618	38:6 PS	808.5123	32:0 PG	740.5436
34:0 DGDG (I.S.)	938.6775	38:5 PS	810.5280	34:4 PG	760.5123
36:6 DGDG	954.6148	38:4 PS	812.5436	34:3 PG	762.5279
36:5 DGDG	956.6305	38:3 PS	814.5593	34:2 PG	764.5436
36:4 DGDG	958.6461	38:2 PS	816.5749	34:1 PG	766.5592
36:3 DGDG	960.6618	38:1 PS	818.5906	34:0 PG	768.5749
36:2 DGDG	962.6774	40:4 PS	840.5749	40:0 PG (I.S.)	852.6694
36:1 DGDG	964.6931	40:3 PS	842.5906		$[M + H]^+$
36:0 DGDG (I.S.)	966.7087	40:2 PS	844.6062	28:0 PC (I.S.)	678.5074
38:6 DGDG	982.6461	40:1 PS	846.6219	32:0 PC	734.5695
38:5 DGDG	984.6618	40:0 PS (I.S.)	848.6375	34:4 PC	754.5382
38:4 DGDG	986.6774	42:4 PS	868.6062	34:3 PC	756.5538
38:3 DGDG	988.6931	42:3 PS	870.6219	34:2 PC	758.5695
	$[M + NH_4]^+$	42:2 PS	872.6375	34:1 PC	760.5851
34:6 SQDG	828.4926	42:1 PS	874.6532	36:6 PC	778.5382
34:5 SQDG	830.5082	44:3 PS	898.6532	36:5 PC	780.5538
34:4 SQDG	832.5239	44:2 PS	900.6688	36:4 PC	782.5695
34:3 SQDG	834.5395		$[M + NH_4]^+$	36:3 PC	784.5851
34:2 SQDG	836.5552	34:4 PI	848.5283	36:2 PC	786.6008
34:1 SQDG	838.5708	34:3 PI	850.5440	36:1 PC	788.6164
34:0 SQDG (I.S.)	840.5865	34:2 PI	852.5597	38:6 PC	806.5695
36:6 SQDG	856.5239	34:1 PI	854.5753	38:5 PC	808.5851
36:5 SQDG	858.5395	34:0 PI (I.S.)	856.5910	38:4 PC	810.6008
36:4 SQDG	860.5552	36:6 PI	872.5283	38:3 PC	812.6164
36:3 SQDG	862.5708	36:5 PI	874.5440	38:2 PC	814.6321
36:2 SQDG	864.5865	36:4 PI	876.5596	40:5 PC	836.6164
36:1 SQDG	866.6022	36:3 PI	878.5753	40:4 PC	838.6321
36:0 SQDG (I.S.)	868.6178	36:2 PI	880.5909	40:3 PC	840.6477
		36:1 PI	882.6066	40:2 PC	842.6634
		36:0 PI (I.S.)	884.6223	40:0 PC (I.S.)	846.6952

7.2 NMR data

Table 7.10 – NMR data of 1,6-Di-*O*-acyl-hexadecane-1,6-diol. ^{1}H, ^{13}C, [700.43 MHz/176.12 MHz, $CDCl_3$, 300 K]: ^{13}C assignments based on ^{1}H, ^{13}C-HSQC, ^{1}H, ^{13}C-HSQC-TOCSY and ^{1}H, ^{13}C-HMBC. All chemical shifts are referenced on the residual solvent signal (δ_H=7.26; δ_C=77.16).

^{1}H NMR data Chemical shift / Coupling constances		^{13}C NMR data Chemical shift	
Proton (signal form)	δ (ppm) / J (Hz)	Carbon	δ (ppm)
1,6-hexadecanediol			
1-H (t)	4.04 / 6.7	C-1	64.2
2-H (m)	1.64–1.59	C-2	28.6
3-H (m)	1.36–1.29	C-3	25
4-H (m)	1.39–1.32	C-4	25.8
5-H (m)	1.55–1.50	C-5	34
6-H (m)	4.89–4.84	C-6	73.9
7-H (m)	1.53–1.47	C-7	34
8-H (m)	1.31–1.24	C-8	25.3
9-H (m)	1.28–1.24	C-9	29.2
Ester-bound fatty acids			
		CO	173.9^{O-1}, 173.6^{O-6}
α-H @ O-1 (t)	2.28 / 7.5	C-α^{O-1}	34.6
α-H @ O-6 (t)	2.27 / 7.4	C-α^{O-6}	34.8
β-H (m)	1.65–1.59	C-β	25.1
γ-H (m)	1.33–1.29	C-γ	29.2
Further aliphatic signals			
CH_2-groups	1.31–1.24[a]	CH_2-groups	$29.9 \cdots 29.3$[a]
$CH_3-CH_2-\underline{CH_2}$ (m)	1.28–1.23	$CH_3-CH_2-\underline{C}H_2$	31.9
$CH_3-\underline{CH_2}$ (m)	1.33–1.26	$CH_3-\underline{C}H_2$	22.6
$\underline{CH_3}-CH_2$ (t)	0.88 / 7.1	$\underline{C}H_2-CH_2$	14.2

[a] no specified assignment possible due to overlapping of too much signals

7.3 Vector Maps

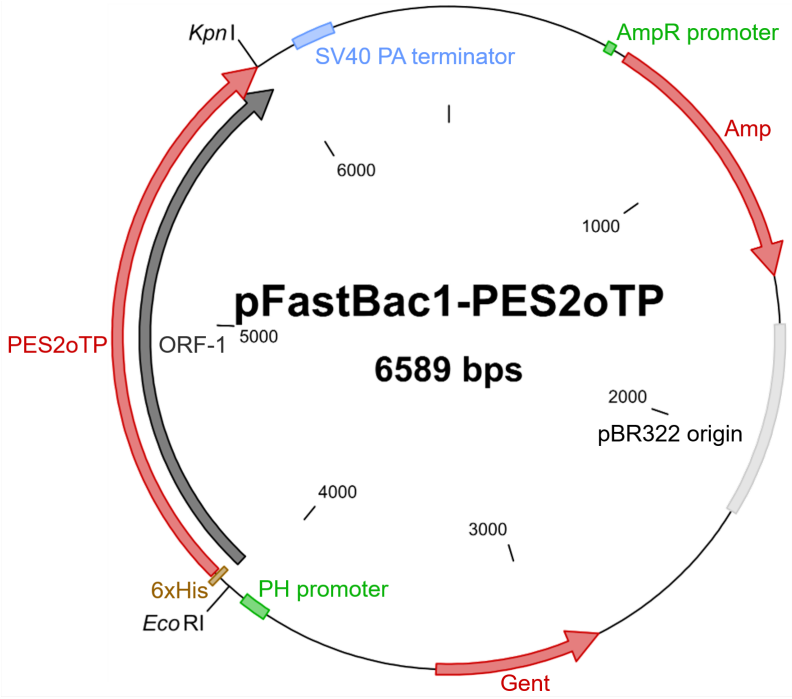

Figure 7.1 – Vector map of pFastBac1-PES2oTP.

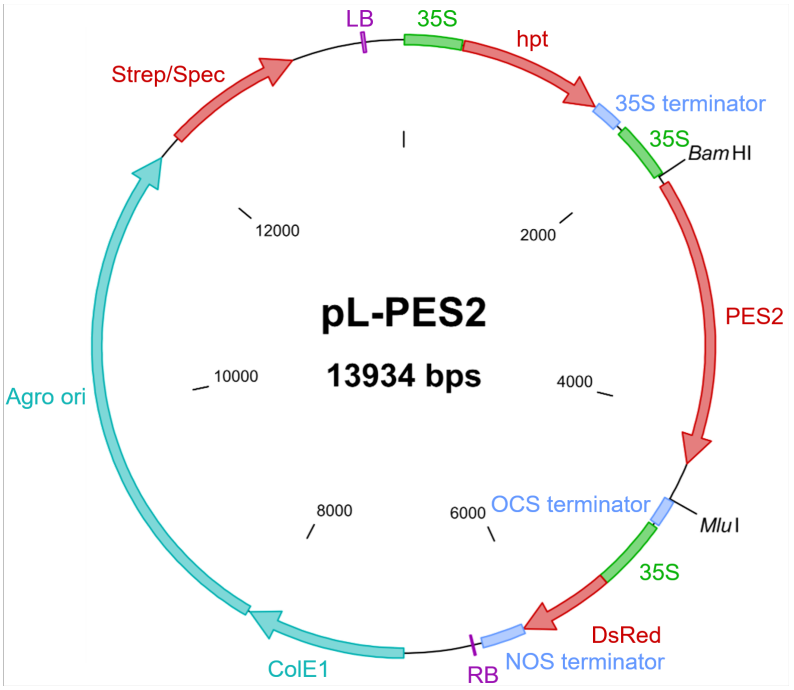

Figure 7.2 – Vector map of pL-PES2.

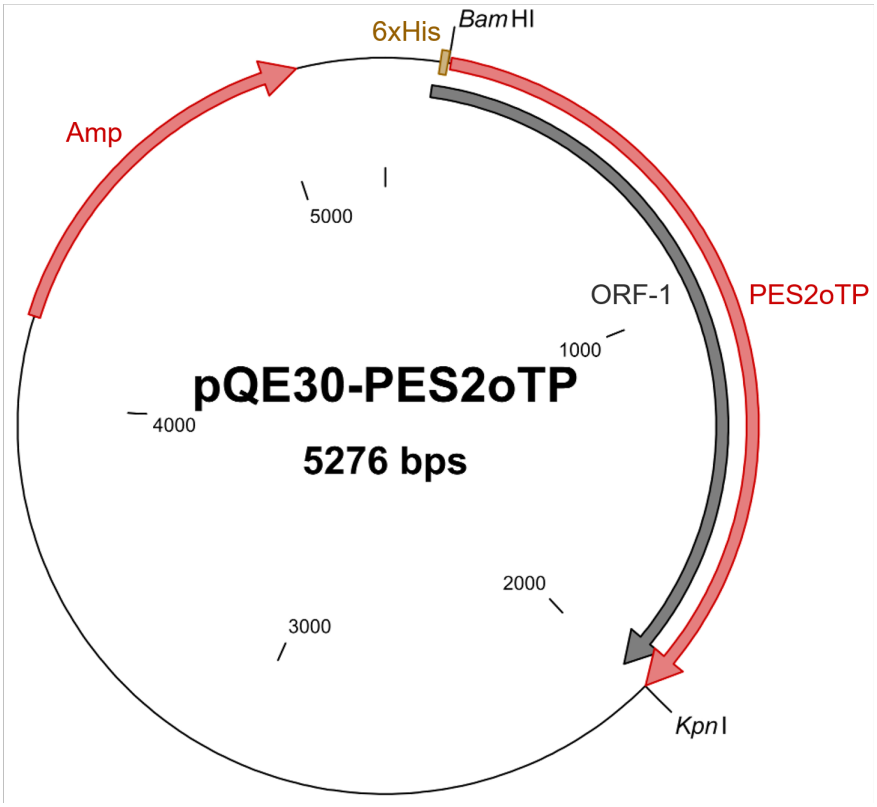

Figure 7.3 – Vector map of pQE30-PES2oTP.

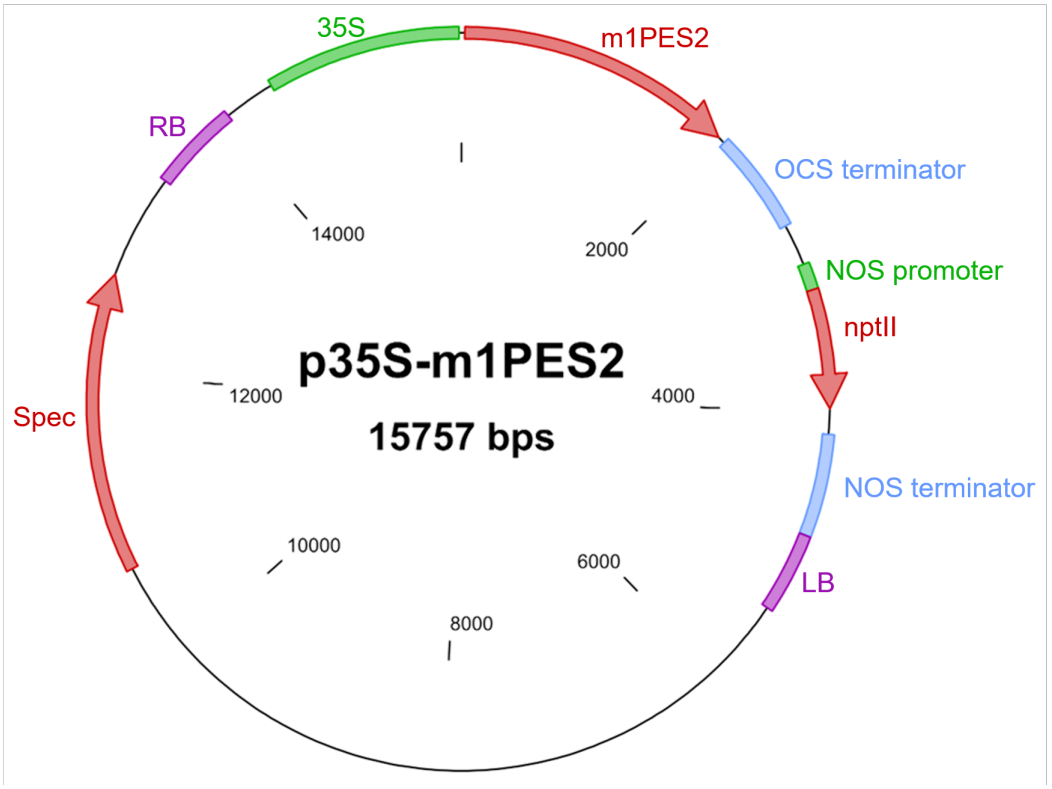

Figure 7.4 – Vector map of p35S-m1PES2.

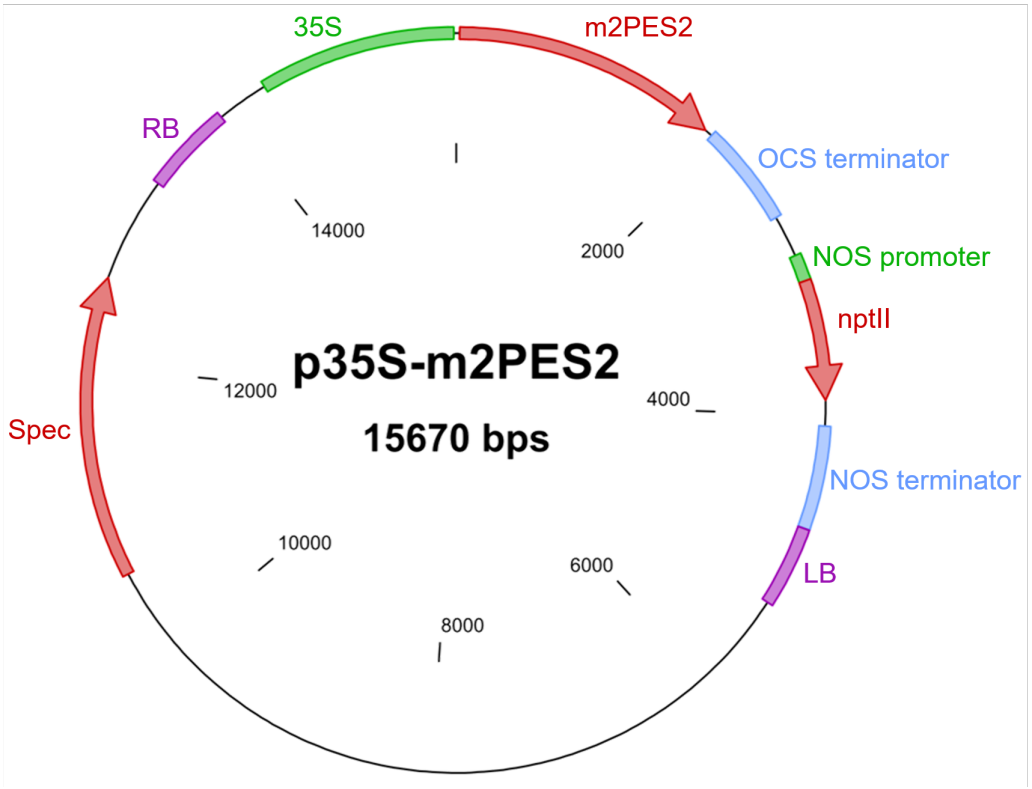

Figure 7.5 – Vector map of p35S-m2PES2.

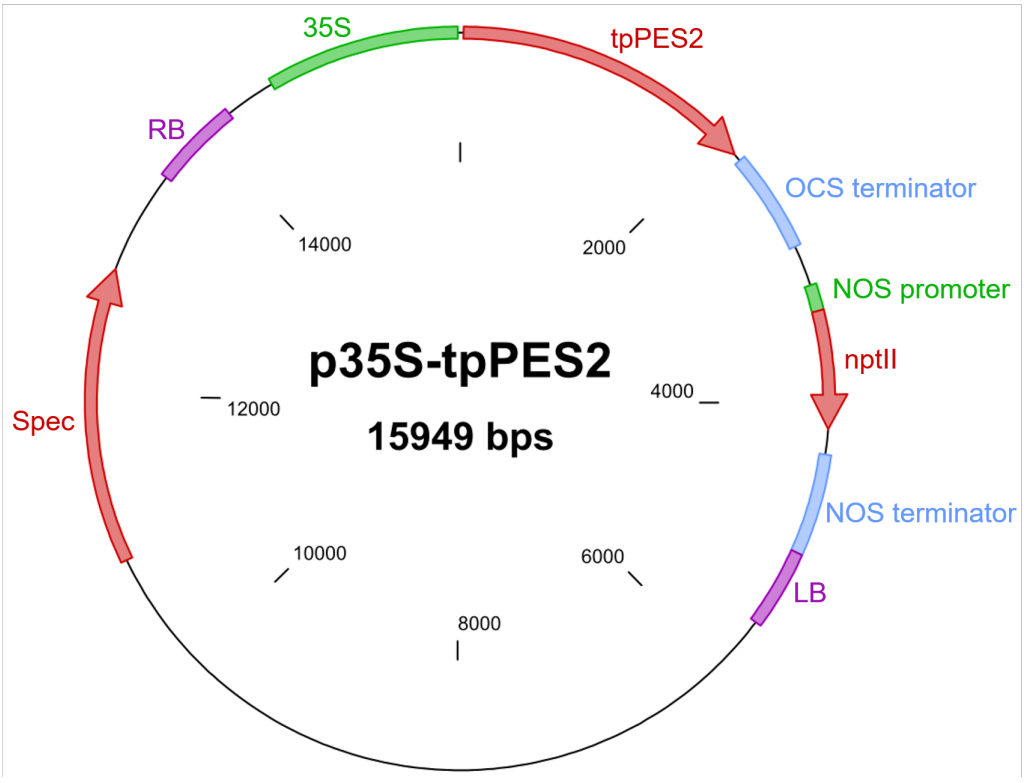

Figure 7.6 – Vector map of p35S-tpPES2.

7.4 Sequences of PES2 Constructs

Figure 7.7 – For the expression of PES2 in plants,constructs with different peptide lengths were used. tpPES2 was the full length ORF including its putative N-terminal chloroplast targeting sequence. m1PES2 and m2PES2 were truncated ORFs lacking the first 64 and 93 N-terminal amino acids, respectively, according to different predictions. Sequences were aligned with MultAlin (Corpet, 1988).

7.5 Synthetic Oligonucleotides

Table 7.11 – List of synthetic oligonucleotides. [1]Zhang et al. (2014), [2]Charrier et al. (2002), [3]Thermo Fisher Scientific, Braunschweig (DE), [4]Qiagen, Hilden (DE)

Target	Primer	Sequence	Product [bp]
Genotyping			
SALK_034549	PD706	TAGTCGAAGATGTTTTGAGGCAG	1275
	PD707	GTAAGCAAGTTCTCCCTTACTTG	
SALK_071769	PD708	CACATGTGACATGTCCAATATCG	1284
	PD709	CCAATAGCGTTGGAAGACCATC	
SALK_139280C	bn1460	ATGCATTGTTCGACCTCAGAC	1265
	bn1461	TACTGAATGGAATATTCCGCG	
pst20507	bn1712	CTCAATCTTCGGTCTCTGTGC	1146
	bn1713	ATTGGTCTATTTGGGAAACGG	
SALK_107487C	bn2057	TTATCGCCGTGGGAAGTCAC	1143
	bn2058	ACCTCAAGTTAACAGAGTCTTGTGT	
GK-319C08	bn2181	AATGGGTCTATTTGGGAAACG	1210
	bn2182	TTGAAGCCTTGAAGGTTTGTG	
SALK_112407	bn1469	TTCCAGTCACTGATCGTACCC	1198
	bn1468	ATCGCGTCCACTGCAATATAC	
SALK_005682	bn1831	TCCATATACGTACACGGAGGC	1258
	bn1830	ACATTGCTGCAAACGGATAAC	
SALK_071625C	bn1470	CGCTGATTTTGGAACTCTGAC	1137
	bn1471	TCACCACTTTCCCATCTTCTG	
SAIL_1160_D05	bn1472	CAATCGCTCTTCTTTCACAGG	952
	bn1473	ATGTGCATTGGCAAAAATAGC	
T-DNA (SALK)	bn78	ATTTTGCCGATTTCGGAAC	
T-DNA (SAIL)	bn1474	GCCTTTTCAGAAATGGATAAATAGCCTTGCTTCC	
T-DNA (GABI-Kat)	bn1920	ATAATAACGCTGCGGACATCTACATTTT	
Transposon (RIKEN)	bn126	TACCTCGGGTTCGAAATC	
Expression analysis			
At1g54570 (PES1)	bn1256	CCTGTCACCGCAACCAATC	480
	bn1257	CTCTACCTCCGCCTTTACCTC	
At3g26840 (PES2)	bn1258	GAACGGTCCGAGTTTGTG	247
	bn1259	ACCGCCCTGGAATCTTAG	
At3g26820 (ELT3)	bn2018	CCGCGAAGCTTTGCATAGAA	408
	bn2019	TGTTCGACCTCAGACTTTGCT	
At5g41120 (ELT4)	bn1916	TGCACAGAAAGGGTGAAG	500
	bn1917	GGTTGGGATTTGGGAAGAG	
At5g41120 (ELT4)	bn2860	TGGAACCTCTCCCACCTTCT	344
	bn2861	GGCGAATGAGCCCTAATCCA	
At5g41130 (ELT5)	bn1918	TGCACAGAAAGGGTGAAG	342
	bn1919	CATTTAGCTCGTCCTCTC	
At3g02030 (ELT6)	bn1881	GGCCAGAGAAAGCAGAGTTTG	344
	bn1882	CTTCTTCACGTCTGCGTACAC	
At3g18780 (ACT2)	bn1854	GCCATCCAAGCTGTTCTCTC	629
	bn1855	GAACCACCGATCCAGACACT	
At3g26840 (PES2)[1]	bn2948	CTGCGAAATTGTCCTGGATT	107
	bn2949	TCTCATCGCCTTCCCTTATG	
At3g18780 (ACT2)[2]	bn2141	GGTAACATTGTGCTCAGTGGTGG	108
	bn2142	AACGACCTTAATCTTCATGCTGC	

Sequencing			
pJET1.2 vector[3]	bn2633	CGACTCACTATAGGGAGAGCGGC	
	bn2634	AAGAACATCGATTTTCCATGGCAG	
pQE vector[4]	bn2638	CGGATAACAATTTCACACAG	
	bn2639	GTTCTGAGGTCATTACTGG	
Cloning			
*Bam*HI-PES2oTP-*Kpn*I	bn189	GGATCCATGAGAGAGTTCGTCGGAGATGGAG	1839
	bn190	GGTACCTTAGAGATCAAACGTTGGAATTTCAGA	
*Bam*HI-ND1-*Avr*II	PD809	GGATCCATGGTAAAGGAAACTCTAATTCC	1029
	PD854	ACCTAGGATCTCAGGCTTCACAAAATCAGTC	
*Bam*HI-PES2oTP-*Kpn*I	PD855	ATCCTAGGTATGAATGGTGTTGAAGCTGATCGGC	1220
	PD796	ACGCGTTAGGCAGTGCAAGAGAGTTGAG	

7.6 List of Cytochrome P450 Candidate Genes for In-Chain Hydroxylation

Table 7.12 – List of cytochrome P450 candidate genes for the in-chain hydroxylation of 1-hexadecanol to produce 1,6-hexadecanediol in chloroplasts. The score gives the consensus prediction value for chloroplast localisation of the respective protein. Values are taken from aramemnon (Schwacke et al., 2003) and their calculation is based on a method described in Schwacke et al. (2007). Values above 12 indicate a high prediction, values below 12 and above five indicate a low prediction and proteins with values below five are considered not to be chloroplast localised. Genes marked with an asterisk belong to the *CYP86* clan.

Gene Number	Systematic Designation	Chloroplast Localisation Score	Reference
At1g31800	*CYP97A3*	28.0	LUT5, β-ring hydroxylase (Kim and DellaPenna, 2006)
At3g53130	*CYP97C1*	26.8	LUT1, ε-ring hydroxylase (Tian et al., 2004)
At4g22690	*CYP706A1*	17.7	
At4g15110	*CYP97B3*	15.4	hydroxylation of β-ring of β-carotene (Kim et al., 2010)
At3g10570	*CYP77A6*	13.4	in-chain fatty acid hydroxylase, production of dihydroxypalmitates from 16-hydroxypalmitate for cutin synthesis (Li-Beisson et al., 2009)
At1g13080	*CYP71B2*	11.8	
At5g06905	*CYP712A2*	11.5	
At3g48320	*CYP71A21*	9.4	
At2g22330	*CYP79B3*	8.8	converts tryptophan to indole-3-acetaldoxime (Hull et al., 2000)
At1g13710	*CYP78A5*	8.7	KLUH, involved in signalling to promote organ growth (Eriksson et al., 2010)
At4g39950	*CYP79B2*	8.5	converts tryptophan to indole-3-acetaldoxime (Hull et al., 2000)

At1g74110	*CYP78A10*	8.3	
At3g61880	*CYP78A9*	8.2	involved in reproduction (Sotelo-Silveira et al., 2013)
At5g23190	*CYP86B1* *	8.1	RALPH, very long chain fatty acid hydroxylase (Compagnon et al., 2009)
At4g15440	*CYP74B2*	7.8	HPL1, hydroperoxide lyase 1, located in chloroplast envelopes (Nilsson et al., 2016)
At1g11610	*CYP71A18*	7.7	
At5g25140	*CYP71B13*	7.5	
At5g36110	*CYP716A1*	7.3	Oxidation of α-amyrin, β-amyrin, and lupeol (Yasumoto et al., 2016)
At4g37340	*CYP81D3*	7.3	
At4g12300	*CYP706A4*	7.2	
At3g48310	*CYP71A22*	7.2	
At3g26230	*CYP71B24*	7.1	
At3g48290	*CYP71A24*	7.0	
At3g20940	*CYP705A30*	7.0	
At3g48270	*CYP71A26*	6.6	
At3g10560	*CYP77A7*	6.6	
At4g37330	*CYP81D4*	6.5	
At4g15360	*CYP705A3*	6.4	
At5g25120	*CYP71B11*	6.4	
At4g37430	*CYP81F1*	6.3	
At1g33730	*CYP76C5*	6.2	
At3g28740	*CYP81D11*	6.1	involved in detoxification and insect pest defense (Köster et al., 2012)
At2g45550	*CYP76C4*	6.0	
At3g53280	*CYP71B5*	5.9	
At5g04660	*CYP77A4*	5.9	
At4g20235	*CYP71A28*	5.9	
At2g46660	*CYP78A6*	5.8	EOD3, controls seed size (Fang et al., 2012)
At1g79370	*CYP79C1*	5.8	
At5g25130	*CYP71B12*	5.7	
At5g63450	*CYP94B1* *	5.7	converts jasmonoyl-l-isoleucine to 12-hydroxy-jasmonoyl-l-isoleucine (Koo et al., 2014)
At5g08250	*CYP86B2* *	5.6	
At4g37370	*CYP81D8*	5.6	
At3g26830	*CYP71B15*	5.4	PAD3, converts cysterine-indole-3-acetonitrile to camalexin (Böttcher et al., 2009)
At5g57220	*CYP81F2*	5.4	essential for pathogen-induced 4-methoxyindol-3-ylmethylglucosinolate accumulation (Bednarek et al., 2009)
At4g37410	*CYP81F4*	5.4	
At2g05180	*CYP705A6*	5.4	
At2g45580	*CYP76C3*	5.4	
At3g48280	*CYP71A25*	5.4	
At3g44250	*CYP71B38*	5.3	

At3g26170	*CYP71B19*	5.3	
At1g58260	*CYP79C2*	5.2	
At3g48520	*CYP94B3*	5.2	jasmonyl-L-isoleucine 12-hydroxylase (Kitaoka et al., 2011)
At4g13310	*CYP71A20*	5.1	
At3g61035	*CYP76C8P*	5.1	
At1g73340	*CYP720A1*	5.1	
At1g64900	*CYP89A2*	5.1	
At1g24540	*CYP86C1* *	5.0	
At1g13110	*CYP71B7*	5.0	
At3g01900	*CYP94B2* *	5.0	
At5g52320	*CYP96A4* *	3.6	predicted midchain alkane hydroxylase (Kim et al., 2017)
At4g39480	*CYP96A9* *	3.5	
At1g65340	*CYP96A3* *	3.2	
At1g69500	*CYP704B1* *	3.1	
At1g34540	*CYP94D1* *	2.8	
At4g00360	*CYP86A2* *	2.4	ATT1, catalyses fatty acid oxidation (Xiao et al., 2004)
At3g56630	*CYP94D2* *	2.4	
At4g32170	*CYP96A2* *	2.2	
At2g44890	*CYP704A1* *	1.9	
At1g01600	*CYP86A4* *	1.9	fatty acid ω-hydroxylase (Li-Beisson et al., 2009)
At5g58860	*CYP86A1* *	1.8	HORST, fatty acid ω-hydroxylase involved in suberin biosynthesis (Höfer et al., 2008)
At2g21910	*CYP96A5* *	1.6	
At2g23180	*CYP96A1* *	1.5	
At1g63710	*CYP86A7* *	1.3	fatty acid hydroxylase (Rupasinghe et al., 2007)
At4g39510	*CYP96A12* *	1.2	
At2g45510	*CYP704A2* *	0.5	
At1g13140	*CYP86C3* *	0.5	
At4g39490	*CYP96A10* *	0.5	
At1g57750	*CYP96A15* *	0.5	MAH1, midchain alkane hydroxylase (Greer et al., 2007)
At1g47620	*CYP96A8* *	0.4	
At1g13150	*CYP86C4* *	0.0	
At2g27690	*CYP94C1* *	-0.1	carboxylates jasmonoyl-l-isoleucine to 12-carboxy-jasmonoyl-l-isoleucine (Heitz et al., 2012)
At2g45970	*CYP86A8* *	-0.5	LCR, fatty acid ω-hydroxylation (Wellesen et al., 2001)
At5g02900	*CYP96A13* *	-0.9	
At3g26125	*CYP86C2* *	-1.0	
At4g39500	*CYP96A11* *	-1.3	
At1g47630	*CYP96A7* *	-	